

University of Alberta

**SEDIMENTOLOGY, ICHNOLOGY, AND SEQUENCE STRATIGRAPHY
OF THE MIDDLE – UPPER EOCENE SUCCESSION IN THE
FAYUM DEPRESSION, EGYPT**

by

Zaki Ali Abdel-Fattah

A thesis submitted to the Faculty of Graduate Studies and Research
in partial fulfillment of the requirements for the degree of

Doctor of Philosophy

Department of Earth and Atmospheric Sciences

©Zaki Ali Abdel-Fattah

Fall 2009

Edmonton, Alberta

Permission is hereby granted to the University of Alberta Libraries to reproduce single copies of this thesis and to lend or sell such copies for private, scholarly or scientific research purposes only. Where the thesis is converted to, or otherwise made available in digital form, the University of Alberta will advise potential users of the thesis of these terms.

The author reserves all other publication and other rights in association with the copyright in the thesis and, except as herein before provided, neither the thesis nor any substantial portion thereof may be printed or otherwise reproduced in any material form whatsoever without the author's prior written permission.

Examining Committee

Dr. S. George Pemberton, Department of Earth and Atmospheric Sciences
(Supervisor)

Dr. Murray K. Gingras, Department of Earth and Atmospheric Sciences
(Supervisor)

Dr. Michael W. Caldwell, Department of Earth and Atmospheric Sciences

Dr. John-Paul Zonneveld, Department of Earth and Atmospheric Sciences

Dr. Mark V. H. Wilson, Department of Biological Sciences

Dr. James A. MacEachern, Department of Earth Sciences, University of Simon Fraser

Dedication

I dedicate this thesis to the soul of my father, to my beloved mother,
to my marvelous wife (Hadeer) and to my sweetie daughter (Mennah).

ABSTRACT

Middle-Upper Eocene successions were studied in the Fayum Depression in order to establish depositional and paleoenvironmental models that link the ichnological and sedimentologic data to relative sea-level changes in a sequence stratigraphic framework. Five facies associations (FA1- FA5) are identified. The facies depositional models show overall progradation from quiescent open-marine bay (FA1-2: Gehannam and Birket Qarun formations) to lagoon/distributary channel/estuary sedimentary environments (FA3-5: Qasr El-Sagha Formation). The facies successions and their stratigraphic evolution are controlled by a regional, second-order cycle associated with the northward regression of the Tethys, which is overprinted by subordinate third- and higher-order cycles.

Whale-bearing FA1 and FA2 are subdivided into five sedimentary facies. Seventeen ichnospecies belonging to thirteen ichnogenera, as well as rhizoliths are observed within these facies. Facies Association 1 accumulated in a low-energy fully-marine bay, whereas FA 2 represents a bay margin / supratidal paleoenvironments. Clastic point-sources are dominantly hypopycnal although eolian sand may represent an important source locally. The quiescent marine bay is a typical environment and biome for the Eocene whales. Preservation of these fossil whales must occur in association with rapid sedimentation rates, but sufficiently that bioturbation eradicates the physical sedimentary structures.

Unusual, large-sized sedimentary structures are examined along the parasequence-bounding surfaces of the Birket Qarun Sandstone. Ichnological data, petrography and stable-isotope analysis are integrated to propose a bio-sedimentologic/diagenetic model, interpreting the origin of these structures as concretion growths around ichnofossils. The marine pore-water carbon was influenced by organic carbon and mixing of meteoric

groundwater under eodiagenetic conditions. These conditions led to the precipitation of pervasive authigenic calcite-dominated cement in and around the burrows.

More than twenty-five *Glossifungites* Ichnofacies–demarcated discontinuities are examined in the study area. These surfaces are grouped into those of autocyclic and those of allocyclic origin. Occurrences of the allocyclically significant *Glossifungites* Ichnofacies can be classified into sequence-bounding, systems tract-bounding and parasequence-bounding surfaces. Sequence-bounding *Glossifungites* Ichnofacies–demarcated surfaces divide the studied successions into four third-order sequences. Systems tract-bounding and parasequence-bounding *Glossifungites* Ichnofacies–demarcated surfaces display higher-order cycles, overprinting the third-order cycles.

ACKNOWLEDGEMENTS

First and foremost, I would like to express my deepest gratitude to my dear supervisors; Dr. Murray K. Gingras and Dr. S. George Pemberton who strongly influence my academic career. I am heartily thanking them for their contributions of time, patience, encouragement, support, and for giving me the opportunities to attend international conferences. I would like to express my sincere gratitude to Dr. Murray Gingras for his leading and discussion in the field, for his critical reading of the manuscript, and for his friendly guidance during the course of the thesis work. I am deeply indebted to Dr. S. George Pemberton for suggesting the study area, his kind supervision, guidance, continual encouragement, reading the manuscript, and for his fruitful discussion.

I would like to thank the Mission Department and Culture Affairs Sector (Higher Education and Scientific Research Ministry, Egyptian Government) for the four-year scholarship and funding support. I thank Dr. Ahmed Khairy and Dr. Hesham El-Asmar for facilitating the scientific mission to Fayum. Thanks to Dr. Mohamed S. Khalil, Dr. Moustafa Fouda and Wahid Salama of the Egyptian Environmental Affairs Agency (EEAA) for assistance in obtaining fieldwork permits. I extend special thanks to the executives and rangers of the Nature Protective Sector (NCS) of the Fayum area (Hossam Kamel, Gebeli Abou-Alkhair, Wed Abdel Latif and Mohamed Sameh) for their continual help during the course of our field excursions. I am appreciating the fieldwork assistance and reading the manuscripts of chapters 2 and 3 provided by Dr. Michael Caldwell (University of Alberta). Deep thanks to the fieldwork assistance provided by Dr. Hesham El-Asmar and Mohamed Sarhan (Faculty of Science - Damietta), and Gebeli Abou-Alkhair (EEAA). Thanks to Hilary Corlett (University of Alberta) for her assistance in stable-isotope analysis.

Special thanks are extended to Dr. James MacEachern who was both the external examiner of my defense and the reviewer of the published (online) paper (Chapter 2). His recommendations and comments are greatly improved the thesis. Thanks are also extended to Dr. Philip Gingerich and Dr. Shannan Peters for their reviewing of the manuscript of the published paper (Chapter 2). I would like to thank my defense committee members Dr. Mark V.H. Wilson and Dr. J.P. Zonneveld. Thanks to NSERC Discovery Grants to Dr. S. George Pemberton and Dr. Murray K. Gingras funded aspects of the fieldwork and laboratory analyses. Finally, I heartily thank all my colleagues of the Ichnology Research Group (IRG) at University of Alberta for their continual help and fruitful discussions. To those of you I have failed to mention or those of you my language can not express my true feelings and appreciations- thank you!

TABLE OF CONTENTS

CHAPTER 1: INTRODUCTION	1
GEOGRAPHY, ACCESSIBILITY AND STUDY AREA LOCATIONS	2
GEOLOGIC SETTING AND PREVIOUS WORK	4
<i>Tectonic Setting</i>	4
<i>Stratigraphy</i>	6
<i>Sedimentology</i>	9
SEQUENCE STRATIGRAPHY: AN OVERVIEW OF CONCEPTS AND NOMENCLATURES ...	9
AIMS AND THESIS ORGANIZATION	12
REFERENCES	15
 CHAPTER 2: SEDIMENTARY ENVIRONMENTS AND DEPOSITIONAL CHARACTERS OF THE MIDDLE-UPPER EOCENE WHALE- BEARING SUCCESSION IN THE FAYUM DEPRESSION, EGYPT	 25
INTRODUCTION	25
GEOLOGIC SETTING AND STUDY AREA	26
REPORTED TRACE FOSSILS	30
REPORTED FACIES ASSOCIATIONS	35
INTERPRETATION	54
GEHANNAM FORMATION	54
BIRKET QARUN FORMATION	57
QASR EL-SAGHA FORMATION	58
<i>Umm Rigl and Temple Members</i>	59

Table of Contents (continued)

<i>Dir Abu Lifa Member</i>	60
SEA-LEVEL HISTORY	64
DISCUSSION	65
PALEOENVIRONMENT AND DISTRIBUTION OF THE EOCENE WHALES IN THE FAYUM DEPRESSION	67
OCCURENCES OF EOCENE WHALES	68
CONCLUSIONS	69
REFERENCES	71
 CHAPTER 3: MIDDLE - UPPER EOCENE FACIES ARCHITECTURE AND TRACE FOSSILS INTERPRETING THE PALEOENVIRONMENT AND SEDIMENTOLOGIC SETTING OF THE WHALE-BEARING GEHANNAM AND BIRKET QARUN FORMATIONS, WADI EL-HITAN, FAYUM-EGYPT	79
INTRODUCTION	79
STUDY AREA LOCATIONS	80
METHODS	80
GEOLOGIC AND STRATIGRAPHIC SETTING	82
FACIES ARCHITECTURE	83
FACIES ASSOCIATION 1: OPEN-MARINE BAY DEPOSITS	83
<i>Facies 1 (F1): Fine- to Very Fine-Grained Bioturbated Sandstones</i>	83
<i>Facies 2 (F2): Medium- to Fine-Grained Bioturbated Sandstones</i>	88
FACIES ASSOCIATION 2: BAY-MARGIN / COASTAL DEPOSITS	90

Table of Contents (continued)

<i>Facies 3 (F3): Laminated Sandy Shale</i>	90
<i>Facies 4 (F4): Sandy Siltstone</i>	90
<i>Facies 5 (F5): Fine-Grained Sandstone</i>	92
 BIOGENIC SEDIMENTARY STRUCTURES	92
INVERTEBRATE TRACE FOSSILS	92
PLANT-ROOT FOSSILS (RHIZOLITHS)	98
<i>Type 1 Rhizoliths</i>	98
<i>Type 2 Rhizoliths</i>	98
 PALEOENVIRONMENTAL AND SEDIMENTOLOGIC SETTING	100
INTERPRETATION OF FACIES ASSOCIATION 1	100
INTERPRETATION OF FACIES ASSOCIATION 2	102
 DISCUSSION	104
SOURCE OF SEDIMENTS IN FACIES ASSOCIATION 1	104
PALEOENVIRONMENT AND PALEO GEOGRAPHIC DISTRIBUTION OF THE FAYUM	
EOCENE WHALES	107
PRESERVATION OF THE FOSSIL-WHALE BONES	108
 SUMMARY	109
 REFERENCES	111

CHAPTER 4: SIGNIFICANCE OF HYPOBURROW NODULE	
FORMATION ASSOCIATED WITH LARGE BIOGENIC	
SEDIMENTARY STRUCTURES IN THE UPPER EOCENE BIRKET	
QARUN FORMATION, WADI EL-HITAN, FAYUM-EGYPT	119

Table of Contents (continued)

INTRODUCTION	119
GEOLOGIC SETTING AND STUDY AREA	120
METHODOLOGY	122
LARGE SEDIMENTARY STRUCTURES	123
MORPHOLOGY AND SIZE	123
ICHOLOGICAL TEXTURE AND CHARACTERS	129
PETROGRAPHY AND DIAGENESIS	130
DEPOSITIONAL UNIT I (HOST SANDSTONE)	130
DEPOSITIONAL UNIT II (OVERLYING SANDSTONE / COQUINA)	133
LARGE SEDIMENTARY STRUCTURES	136
STABLE ISOTOPE GEOCHEMISTRY	140
ISOTOPIC SIGNATURE	140
INTERPRETATION OF BULK CALCITE AND BULK DOLOMITE ISOTOPIC SIGNATURE	142
<i>Bulk Calcite Isotopic Signature</i>	142
<i>Bulk Dolomite Isotopic Signature</i>	144
ORIGIN OF THE LARGE SEDIMENTARY STRUCTURES	145
STAGE A	145
STAGE B	146
STAGE C	146
STAGE D	148
STAGE E	149
DISCUSSION AND IMPLICATIONS	149

Table of Contents (continued)

BIOTURBATION AND DIAGENESIS	149
SEDIMENTOLOGIC AND SEQUENCE STRATIGRAPHIC IMPLICATIONS	151
<i>Sedimentary Environment</i>	151
<i>Sequence Stratigraphy</i>	152
CONCLUSIONS	153
REFERENCES	155
 CHAPTER 5: THE <i>GLOSSIFUNGITES</i> ICHNOFACIES AND SEQUENCE STRATIGRAPHIC ANALYSIS: A CASE STUDY FROM THE MIDDLE- UPPER EOCENE SUCCESSION, FAYUM DEPRESSION, EGYPT	 162
INTRODUCTION	162
GEOLOGIC SETTING	163
DEFINED FACIES ASSOCIATIONS	166
<i>GLOSSIFUNGITES</i> ICHNOFACIES AND DISCONTINUITIES	171
<i>GLOSSIFUNGITES</i> ICHNOFACIES— DEMARCATED SURFACES	173
AUTOCYCLIC <i>GLOSSIFUNGITES</i> ICHNOFACIES- DEMARCATED SURFACES.....	177
<i>Deltaic Distributary Channels: Autocyclic Glossifungites Ichnofacies- Demarcated Surfaces (AuGS1)</i>	177
<i>Estuarine Channels: Autocyclic Glossifungites Ichnofacies- Demarcated Surfaces (AuGS2)</i>	178
ALLOCYCLIC <i>GLOSSIFUNGITES</i> ICHNOFACIES- DEMARCATED SURFACES	180
<i>Sequence-Bounding Glossifungites Ichnofacies-Demarcated Surfaces</i>	180

Table of Contents (continued)

FS/SB1-GS- <i>Glossifungites</i> Ichnofacies- demarcated surface	181
FS/SB2-GS- <i>Glossifungites</i> Ichnofacies- demarcated surface	181
SB3- sequence boundary surface	182
<i>Systems Tract-Bounding Glossifungites Ichnofacies- Demarcated Surfaces</i>	185
Maximum flooding- <i>Glossifungites</i> Ichnofacies-demarcated surface (MFS-GS).....	185
Transgressive- <i>Glossifungites</i> Ichnofacies-demarcated surface (MFS-GS)	186
<i>Parasequence-Bounding Surfaces (Flooding Surfaces FS)</i>	188
Parasequence flooding (wave ravinement) surfaces (S3-FSs-GS) ...	188
Parasequence flooding (wave and/or tidal ravinement) surfaces (S3-FSs-GS and S4-FSs-GS)	189
 SEQUENCE STRATIGRAPHY AND SEA-LEVEL HISTORY	192
MIDDLE EOCENE (LATE BARTONIAN) SEQUENCE 1	193
LATE EOCENE (EARLY PRIABONIAN) SEQUENCE 2	193
LATE EOCENE (PRIABONIAN) SEQUENCE 3	195
LATE EOCENE (LATE PRIABONIAN) SEQUENCE 4	196
 DISCUSSION AND CONCLUSIONS	196
<i>GLOSSIFUNGITES</i> ICHNOFACIES- DEMARCATED SURFACES	196
SEQUENCES' HIERARCHY	199
 REFERENCES	201
 CHAPTER 6: SUMMARY AND CONCLUSIONS	213

Table of Contents (continued)

APPENDIX	220
Description of the stratigraphic, sedimentologic and ichnological field data, collected through detailed outcrop logging in the measured sections of the Middle-Upper Eocene succession in the areas of Wadi El-Hitan and Qasr El-Sagha, Fayum-Egypt	220
1. Minqar El-Hut Composite Section (Wadi El-Hitan)	220
2. Sandouk El-Borneta Section (Wadi El-Hitan)	223
3. Qasr El-Sagha Temple Section (Qasr El Sagha)	225
4. Wadi Efreet-Dir Abu Lifa Section (Qasr El-Sagha)	228
5. Upper Part of Dir Abu Lifa Member (Qasr El-Sagha Fm) in the Four Measured Sections Between Dir Abu Lifa and West Wadi Efreet (Qasr El-Sagha).....	231

LIST OF TABLES

TABLE 1.1. Correlation chart of the lithostratigraphic classifications of the Middle Eocene – Oligocene succession of the Fayum area and its vicinities.	7
TABLE 1.2. Biostratigraphic classifications of the Middle - Upper Eocene succession in the Fayum area.	8
TABLE 2.1. The lithostratigraphic classifications of the Middle Eocene – Oligocene succession of the Fayum area and its vicinities.	29
TABLE 2.2. Description of the trace fossils reported from the Middle - Upper Eocene succession studied.	32
TABLE 2.3. Summary of the characteristics of the identified facies associations and their depositional characters.	36
TABLE 2.4. Summary of the characteristics of transgressively emplaced erosional discontinuities.	41
TABLE 3.1. Summary of the characteristics of the facies associations (FA1 and FA2) and their identified sedimentary facies (F1- F5).	84
TABLE 3.2. Type ichnospecies, short diagnoses, ethologies, trophic behaviors, and possible trace-maker organisms of the Middle - Upper Eocene ichnogenera in the area of Wadi El-Hitan.	93
TABLE 3.3. Description of the ichnospecies identified in the whale-bearing Gehannam and Birket Qarun formations, Wadi El-Hitan area.	94
TABLE 4.1. Summary of the characteristics and depositional affinities of the structure-associated depositional units.	124
TABLE 4.2. Morphometric measurements of six large amphora-like sedimentary structures in the Old Camp site, Wadi El-Hitan area.	128
TABLE 4.3. Carbon and oxygen stable-isotope data of the bulk calcite cement (microcrystalline, prismatic, mosaic and coarse crystalline calcite \pm bioclasts) and the bulk dolomite cement (microcrystalline and zoned rhombs \pm dolomitized bioclasts).	141

List of Tables (continued)

TABLE 5.1. Summary of the stratigraphic, sedimentologic and depositional characters of the identified facies associations (FA1 – FA5). 167

TABLE 5.2. Examples of occurrences of the *Glossifungites* Ichnofacies through time and space in the rock record. 172

TABLE 5.3. The diagnostic characters of the identified key-stratigraphic surfaces in the study area. 174

LIST OF FIGURES

FIGURE 1.1. A- Location map of the study area. B- Geologic map of the Fayum depression, Egypt.	3
FIGURE 1.2. Tectonic setting of the Fayum (Gindi) Basin.	5
FIGURE 1.3. Schematic diagram of the idealized architecture of a third-order sequence, showing systems tracts and the key-stratigraphic surfaces.	11
FIGURE 2.1. A- Location map of the Fayum depression, Egypt. B- Geological map of the Fayum and its adjacent area.	27
FIGURE 2.2. Legend and key to symbols used in figures and illustrations.	31
FIGURE 2.3. Trace fossils and rhizoliths found in the Middle-Upper Eocene succession, Fayum area.	34
FIGURE 2.4. Correlation chart of the Middle-Upper Eocene succession in Minqar El-Hut and Sandouk El-Borneta sections in the area of Wadi El-Hitan (Whale Valley), SW Fayum.	42
FIGURE 2.5. Selected photographs of FA1 from Gehannam and Birket Qarun formations in the area of Wadi El-Hitan.	43
FIGURE 2.6. Selected lithofacies and ichnofacies of the bay-margin settings of FA2 from the Gehannam Formation in the area of Wadi El-Hitan.	45
FIGURE 2.7. Correlation chart of the Upper Eocene Qasr El-Sagha Formation for the two composite sections; Qasr El-Sagha Temple and Dir Abu Lifa – Wadi Efreet in the area of Qasr El-Sagha, NE Fayum.	46
FIGURE 2.8. Selected lithofacies, ichnofacies and sedimentary structures of FA3 from the Temple Member, in the area of Qasr El-Sagha.	47
FIGURE 2.9. Lithofacies, ichnofacies and sedimentary structures of the deltaic distributary channels of FA4, Dir Abu Lifa Member in the area of Qasr El-Sagha.	49
FIGURE 2.10. Correlation chart of the upper part of Dir Abu Lifa Member (Qasr El-Sagha Formation) exposed in the area between West Wadi Efreet and East Dir Abu Lifa (not to scale horizontally).	51

List of Figures (continued)

FIGURE 2.11. Selected lithofacies, biofacies, ichnofacies and sedimentary structures of the estuarine channels (FA 5) forming the upper part of Dir Abu Lifa Member in the area of Qasr El-Sagha.	52
FIGURE 2.12. Schematic SW-NE compiled cross-section of the succession of stacked facies associations, the key stratigraphic surfaces, and the main sedimentary environments of the Middle-Upper Eocene succession at Wadi El-Hitan and Qasr El-Sagha areas in the Fayum depression (not to scale).	55
FIGURE 2.13. Correlation chart of the lithostratigraphy, the identified sequences and sequence boundaries of the compiled Middle-Upper Eocene succession in the study area, with the regional sequences of Hardenbol et al. (1998) and the global eustatic sea-level curve of Haq et al. (1987).	65
FIGURE 3.1. A- Location map of the Fayum depression, Egypt. B- Geological map of the Fayum depression and the studied sections in the area of Wadi El-Hitan.	81
FIGURE 3.2. Legend and key to symbols used in figures and illustrations.	85
FIGURE 3.3. Correlation chart of the Middle-Upper Eocene succession in the composite section of Minqar El-Hut and Sandouk El-Borneta section in the area of Wadi El-Hitan.	86
FIGURE 3.4. Selected photographs, showing the characteristics of Facies 1 (FA1).	87
FIGURE 3.5. Selected photographs, showing the characteristics of Facies 2 (FA1).	89
FIGURE 3.6. Selected photographs, showing the characteristics of Facies 3 through Facies 5 (FA2).	91
FIGURE 3.7. Invertebrate trace fossils.	95
FIGURE 3.8. Invertebrate trace fossils.	97
FIGURE 3.9. Type 1 and Type 2 rhizoliths.	99

List of Figures (continued)

FIGURE 3.10. A- Schematic block diagram, showing the depositional settings and paleoenvironments of the whale-bearing open-bay sandstones (FA1) and the bay-margin deposits (FA2) in the area of Wadi El-Hitan. B- Trace-fossil suites, attributed to the <i>Cruziana</i> Ichnofacies, dominating F1 and F2 of FA1 in a low-energy open-marine bay setting. C- Ichnological succession and ichnocoenosis in the genetically related F3, F4, and F5 FA2.	101
FIGURE 3.11. Generalized sedimentary depositional models of northern Egypt, comprising Fayum area, during Middle Eocene (A) and Late Eocene (B).	105
FIGURE 4.1. A- Location map of the study area. B- Geological map of the Fayum depression and the studied sections in the area of Wadi El-Hitan.	121
FIGURE 4.2. Correlation of the Upper Eocene Birket Qarun Formation at the composite Minqar El-Hut and Old Camp site section with Sandouk El-Borneta section, in the area of Wadi El-Hitan, SW Fayum.	125
FIGURE 4.3. Large-sized sedimentary structures and their associated depositional units.	126
FIGURE 4.4. A- Columnar chart, showing the relationship between the maximum height (H) and the maximum diameter (D) for the six morphometric measurements illustrated in Table 1. B- Drop-line chart representing the distribution of the diameter/height (D / H) ratios of the six morphometric measurements illustrated in Table 1.	129
FIGURE 4.5. Large longitudinal (B) and cross-sectional (C) polished slabs were cut through a large sedimentary structure (A).	130
FIGURE 4.6. Optical (crossed nicols) photomicrographs and SEM images of the quartz arenite microfacies (depositional unit I).	131
FIGURE 4.7. Optical (crossed nicols) photomicrographs and SEM images of the depositional unit II.....	135
FIGURE 4.8. Plain-light and crossed-nicols photomicrographs of the large sedimentary structures.	136

List of Figures (continued)

FIGURE 4.9. Optical photomicrographs (crossed nicols) and SEM images of the different structure zones.	138
FIGURE 4.10. A cross plot of $\delta^{13}\text{C}_{\text{PDB}}$ versus $\delta^{18}\text{O}_{\text{PDB}}$ of the bulk calcite and bulk dolomite.	142
FIGURE 4.11. SEM photograph showing well-preserved long and dark organic material (Org) in the structure-adjacent hosting-sandstone zone (Qz is quartz and Ca is calcite).	143
FIGURE 4.12. A- Range of temperature and the calculated $\delta^{18}\text{O}_{\text{SMOW}}$ value of pore fluids constructed for the analyzed $\delta^{18}\text{O}_{\text{PDB}}$ range of the bulk calcite (-4.63 to -7.22‰) using the calcite-water fractionation equation of Friedman and O'Neil (1977). The bulk calcite field marks the calculated temperature, assuming that the $\delta^{18}\text{O}_{\text{SMOW}}$ value of pore fluids lies between -2 and -4‰. B- Range of temperature and the calculated $\delta^{18}\text{O}_{\text{SMOW}}$ value of pore fluids constructed for the analyzed $\delta^{18}\text{O}_{\text{PDB}}$ range of the bulk dolomite (-1.41 to -11.20‰), using the dolomite-water fractionation equation of Land (1983). The bulk-dolomite field marks the calculated temperature, assuming that the $\delta^{18}\text{O}_{\text{SMOW}}$ value of the pore fluids was between -2 and -4‰.	145
FIGURE 4.13. Schematic diagrams of the four stages of the bio-sedimentological model, summarizing the development of the parasequence-constrained, large-sized sedimentary structures in the upper part of the Birket Qarun Formation. ...	147
FIGURE 4.14. Detailed chart of the integrated stratigraphic, sedimentological and ichnological data, summarizing the sedimentary environment and sequence stratigraphic architecture of the structure-associated depositional units in the Birket Qarun Formation.	153
FIGURE 5.1. A- Location map of the Fayum depression. B- Geological map of the Fayum and its adjacent area (Nile Valley and northward to the Greater Cairo), compiled and modified after Beadnell (1905), Said (1962), GSE (1981, 1983), and Gingerich (1992).	164
FIGURE 5.2. Legend and key to symbols used in figures and illustrations.	165
FIGURE 5.3. Selected photographs showing the ichnological/sedimentological characters of the identified facies associations (FA1 - FA5).	169

List of Figures (continued)

FIGURE 5.4. Schematic diagram, showing the development of a <i>Glossifungites</i> -Ichnofacies demarcated discontinuity.	171
FIGURE 5.5. Correlation of the Middle-Upper Eocene succession in the Minqar El-Hut composite section with the Sandouk El-Borneta section, Wadi El-Hitan area, SW Fayum.	175
FIGURE 5.6. Correlation of the Upper Eocene succession of Qasr El-Sagha Temple section with Dir Abu Lifa – Wadi Efrete composite section, in the area of Qasr El-Sagha area, NE Fayum.	176
FIGURE 5.7. Autocyclic <i>Glossifungites</i> Ichnofacies-demarcated surfaces (Au-GS).	179
FIGURE 5.8. Sequence-bounding <i>Glossifungites</i> Ichnofacies-demarcated surfaces (SB-GS).	183
FIGURE 5.9. Systems tract-bounding <i>Glossifungites</i> Ichnofacies-demarcated surfaces (MFS-GS and TS-GS).	187
FIGURE 5.10. Parasequence-bounding <i>Glossifungites</i> Ichnofacies-demarcated surfaces (FSs-GS).	190
FIGURE 5.11. SW-NE diagrammatic cross-section, showing the sequence stratigraphic framework, sedimentology and lithostratigraphy of the compiled Middle-Upper Eocene succession in the Wadi El-Hitan and Qasr El-Sagha study areas.	194
FIGURE 5.12. Correlation chart of the identified sequences and key-stratigraphic surfaces of the Middle-Upper Eocene succession in the study area with the regional sequences in European basins of Hardenbol et al. (1998) and the global eustatic sea-level curve of Haq et al. (1987). The age is calibrated after the global Eocene chronostratigraphic time scale (Gradstein et al., 2004), the planktonic foraminifera zonation of (1) Berggren et al. (1995) and (2) Haggag and Bolli (1996), and the nannoplanktonic zonation of (3) Martini (1971) and (4) Zalat (1995).	200

CHAPTER 1: INTRODUCTION

The Eocene and Oligocene strata present at the Fayum oasis in Egypt display unique and spectacularly preserved marine-vertebrate skeletons (e.g., some of the oldest whales discovered) and terrestrial-vertebrate bones. Recently, the districts of the Fayum depression have become protected areas that are managed by Nature Conservation Sectors (NCS) of the Egyptian Environmental Affairs Agency (EEAA). Wadi El-Hitan (Whale Valley) was added to UNESCO's World Heritage list in 2005 because of its remarkable marine-vertebrate fossils, notably due to the abundant fossil whale skeletons located there.

The present study aims to integrate ichnological, sedimentologic and stratigraphic analyses to identify depositional characteristics, sedimentary environments and the sequence stratigraphy / sea-level history of the Middle-Upper Eocene strata in the Fayum area. The current study is important for many reasons. Firstly, addition of the Wadi El-Hitan area to UNESCO's World Heritage list has led to growing international interest in the geology of the Fayum area. Secondly, previous sedimentologic and sequence stratigraphic work (described below) is exceedingly inadequate and incomplete. Finally, none of the previous studies considered the ichnological data present in the study area and its application in sedimentology, paleoenvironmental analysis and sequence stratigraphy.

Ichnology has been proven to provide invaluable paleoenvironmental information (e.g., Ekdale et al., 1984; Savrda and Bottjer, 1989; Pemberton et al., 1992; Bromley, 1996; Gingras et al., 1998, 2002a; McIlroy, 2004; Buatois et al., 2005; MacEachern et al., 2005, 2007; Nesbitt and Campbell, 2006; Hembree and Hasiotis, 2007; MacEachern and Gingras, 2007). Moreover, trace fossils are known to have genetic-stratigraphic significance (e.g., MacEachern et al., 1992, 2007; Pemberton and MacEachern, 1995; Gingras et al., 2000, 2002b; Savrda et al., 2001; Holz, 2003; Pemberton et al., 2004; Morris et al., 2006). Finally, ichnological data can provide detailed sedimentological data,

such as rate of sedimentation and evidence of event deposition (Seilacher, 1982; Frey and Goldring, 1992; Pemberton and MacEachern, 1997; MacEachern et al., 2005; Gingras et al., 1999, 2002a,b, 2007).

GEOGRAPHY, ACCESSIBILITY AND STUDY AREA LOCATIONS

The name Fayum is from the Coptic word ‘phiom’ or ‘pa-yom’, meaning lake or sea. The Fayum depression is the nearest Western Desert depression to the Nile Valley and Cairo. The Fayum is an important province of Egypt. The Fayum oasis is accessible along several well-paved highways and via the railroad. It can be approached by three main roads (Fig. 1.1A): 1- the Cairo-Fayum highway, entering Fayum at Kom Aushim, along the eastern edge of the depression; 2- Cairo-Assuit desert road; and 3- Wasta-Fayum road.

The present work focuses on the Middle-Upper Eocene succession in two areas: Wadi El-Hitan (Whale Valley) and Qasr El-Sagha (El-Sagha Temple) in the vicinity of the Fayum depression (Fig. 1.1). Two sections were studied in the area of Wadi El-Hitan, SE of the Fayum depression (Fig. 1.1). The first composite section is collected from and around Minqar El-Hut (between N 29° 15' 48" - E 30° 02' 47" and N 29° 16' 02" - E 30° 03' 51") and the Old Camp site (N 29° 15' 55" - E 30° 01' 24"). The second section is measured entirely from Sandouk El-Borneta (N 29° 17' 00" - E 30° 03' 00").

The second area “Qasr El-Sagha”—named after the small incomplete old temple—is located to the northwestern side of Birket Qarun. Two sections (Fig. 1.1) are studied: Qasr El-Sagha Temple section (N 29° 35' 42" - E 30° 40' 41") and the composite section between Dir Abu Lifa and Wadi Efreet (lies between N 29° 36' 11" - E 30° 41' 46" and N 29° 37' 06" - E 30° 41' 44"). The upper part of Dir Abu Lifa Member is collected from the southwestern side of Wadi Efreet (N 29° 36' 38" - E 30° 40' 05"), the north western side of Wadi Efreet (N 29° 37' 08" - E 30° 40' 32"), the eastern side of Wadi Efreet (N 29° 36' 40" - E 30° 40' 42"), and from the northeast of Dir Abu Lifa (N 29° 37' 20" - E 30° 41' 45").

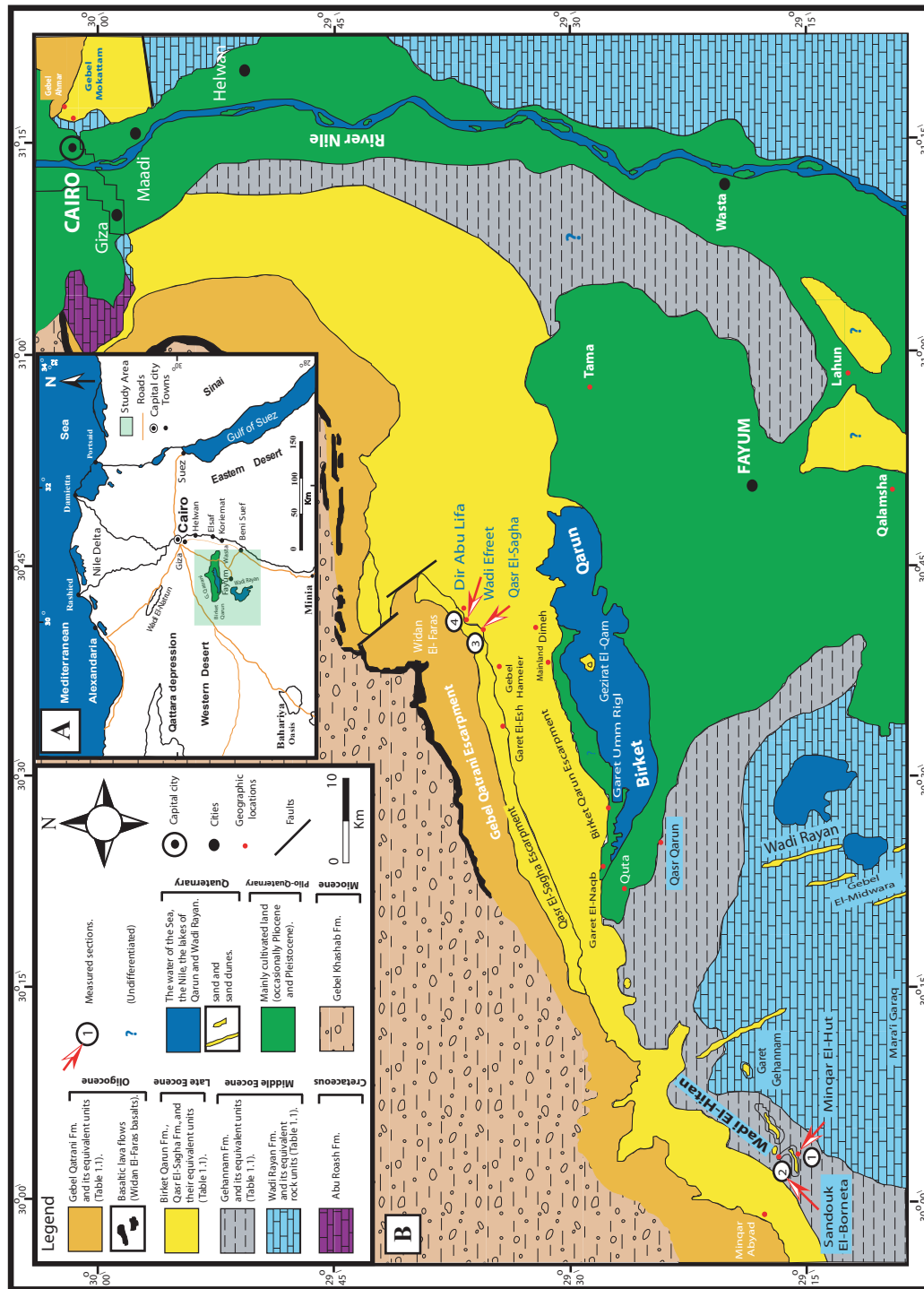


FIGURE 1.1. A- Location map of the study area. **B-** Geologic map of the Fayum depression, Egypt. Compiled and modified after Beadnell (1905), Said (1962), GSE (1981, 1983) and Gingerich (1992).

GEOLOGIC SETTING AND PREVIOUS WORK

The Fayum depression (Fig. 1.1) has a triangular shape and occupies an area of 17,000 km². The Fayum area can be classified (e.g., Beadnell, 1905) into the following three physiographic provinces the depressions (Fayum and Wadi Rayan), the northern escarpments, and the surrounding desert region (Fig. 1.1). Geological investigations of the Fayum area date back to eighteenth century. Interest in geology of Fayum was provoked by Schweinfurth's (1877) discovery of fossil bones that were identified later by Dames (1894) as remains of the extinct cetacean genus *Zeuglodon* (now placed in the genus *Basilosaurus*). These earlier works were devoted mainly to paleontology, general geology, and stratigraphy with brief notes on the sedimentary environments (e.g., Blanckenhorn, 1903; Beadnell, 1905; Hume, 1911; Cu viller, 1930).

Tectonic setting

The Fayum basin is one of the northern pericratonic (intra-continental) sag basins, located in the unstable shelf of the African cratonic margin (El Hawat, 1997) (Figs. 1.2A and B). The Fayum sag basin developed during Jurassic rifting events concurrent with the opening of the Tethys Sea. These were associated with continual extension and strike-slip sinistral tectonics between Africa and Eurasia (Smith, 1971) (Fig. 1.2C). The advent of the Late Cretaceous was marked by a new period of compressional tectonics, associated with strike-slip dextral shearing tectonics (Fig. 1.2C) between Africa and Eurasia (Guiraud et al., 2005). The Fayum basin was uplifted during the Late Cretaceous Syrian Arc activity. Consequently, this basin was effectively subdivided into two major Paleocene-Eocene depocentres: the northern Tiba basin and the southern Gindi or the lower Nile basin (El Zarka, 1983).

In Middle Eocene, the southern Gindi (lower Nile) basin attained N-S orientation and became the main depocentre between Assiut and Cairo. Since the Middle Eocene, the margins of Egypt have been dominated by vertical movements, associated with a gradual

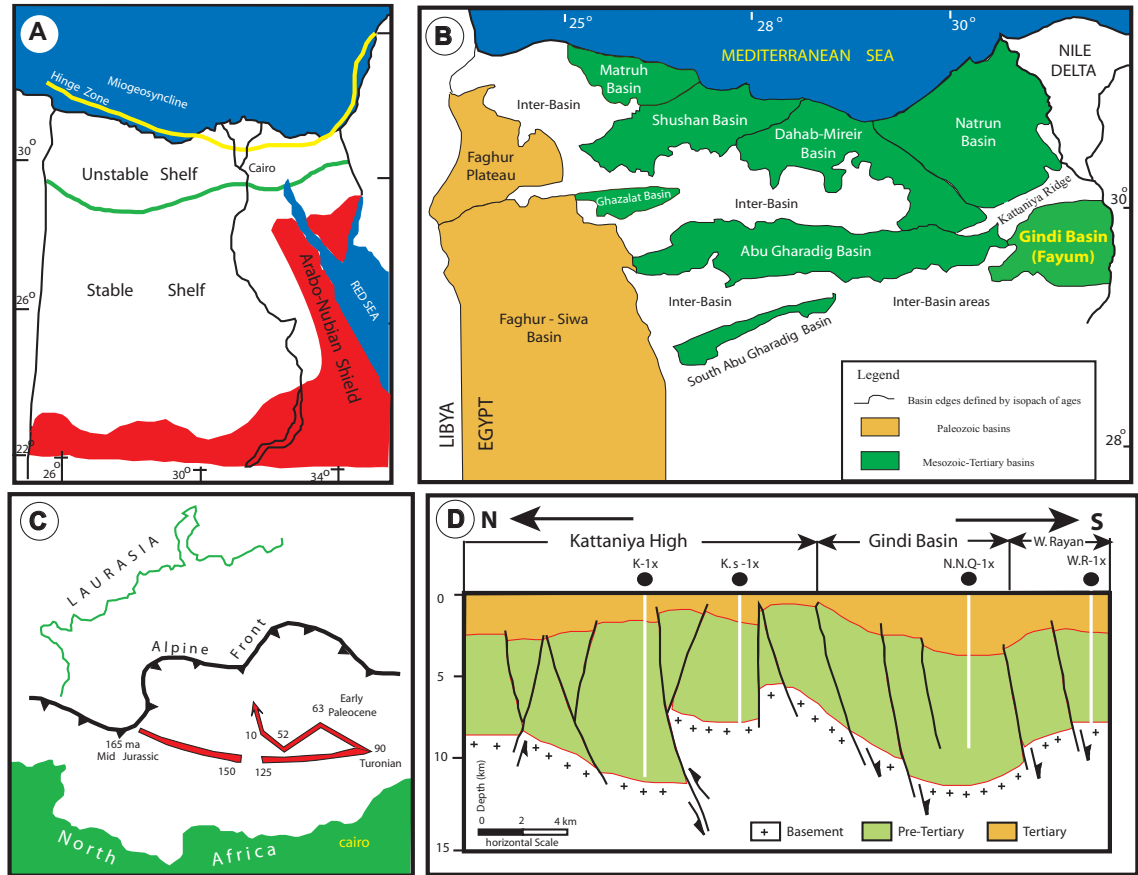


FIGURE 1.2. Tectonic setting of the Fayum (Gindi) Basin. **A-** The unstable shelf (including northern Western Desert intra-cratonic basins) in relation to the main tectonic framework of Egypt (map redwan after Said, 1990). **B-** Gindi (Fayum) basin lies to the SE of the the northern Western Desert sag basins, (map Redrwan and simplified after EGPC, 1992). **C-** Jurassic (Callovian) to Recent motion of North Africa relative to Europe (modified after Robertson Research Intl., 1982). **D-** N-S cross section showing the tectonic relation between the Kattaniya high and Gindi Basin (Data from the four composite logs: Kattanyia-1x, Kattanyia South-1x, Qarun-1x and Wadi Rayan- 1x, in addition to the seismic profile) modified and simplified after Younes (2003).

sinking of the Mediterranean Sea and an opening of the Red Sea (Sestini, 1984). The advent of the Late Eocene witnessed a continuous lowering of the sea level, progressive emergence, and erosion of the structural highs that provided clastic sediments to the Late Eocene basins of the northern Egypt (Salem, 1976). The Oligocene was a time of uplift, regression, volcanicity and continental sedimentation (Said, 1990).

The Fayum or Gindi basin is part of the unstable shelf belt (Fig. 1.2A), characterized by a complex subsurface structural framework. Faults and folds, inherited from the Syrian Arc Orogeny, are masked by the relatively simple surface geology of the Eocene-Oligocene succession in the Fayum depression (Fig. 1.2D). This sedimentary succession forms almost horizontal and blanket-like strata that dip gently toward the north, averaging between 2° and 3°. There are small localized faults, which occur in different parts of the Fayum depression (Fig. 1.1).

Stratigraphy

The present work follows with some modifications the lithostratigraphic classification of Beadnell (1905) and the emendation of Said (1962) as illustrated in Table 1.1. The Umm Rigl Member of Gingerich (1992) is used herein to define the lowermost strata of the Qasr El-Sagha Formation in the area of Wadi El-Hitan. Upwards, Bown and Kraus' (1988) lithostratigraphic subdivision of the Upper Eocene Qasr El-Sagha Formation in the vicinity of Qasr El-Sagha into the lower Temple Member and the upper Dir Abu Lifa Member is adopted.

Outcrop stratigraphy is represented mainly by Middle Eocene limestone, shale and sandstone changing to Upper Eocene clastics, followed by the continental Oligocene and continental to marginal marine Miocene sedimentary packages. Five rock units are recognized as follows from the base to the top: the Middle Eocene Wadi Rayan and Gehannam formations, the Upper Eocene Birket Qarun and Qasr El-Sagha formations, and the Oligocene Gebel Qatrani Formation (Fig. 1.1, Table 1.1). The age is assigned to these rock units (Table 1.2) in accordance with previous biostratigraphic studies (e.g., Ansary, 1955; Abdou and Abdelkireem, 1975; Strougo, 1979; Bassiouni et al., 1984; Strougo and Haggag, 1984; Haggag, 1990; Zalat, 1995; Haggag and Bolli, 1995, 1996; Elewa et al., 1998; Morsi et al., 2003; Seiffert et al., 2008).

TABLE 1.1. Correlation chart of the lithostratigraphic classifications of the Middle Eocene – Oligocene succession of the Fayum area and its vicinities.

E O C E N E					
PRESENT WORK	Oligocene				
	Gebel Qatrani Formation	Late (Priabonian)	Middle (Bartonian)		
		Qasr El Sagha Formation	Birket Qarun Formation	Gehannan Formation	Wadi Rayan Formation
SWEDAN (1992)	Gebel Qatrani Formation	Qasr El Sagha Formation	Birket Qarun Formation	Mokattam Formation	Qazzun Formation Rayan Formation Samalut Formation
	Oligocene	Late Eocene		Middle Eocene	
SAID (1990)	Gebel Qatrani Formation	Qasr El Sagha Formation		Gehannan Formation	Gharag Formation Sath El-Hadid Formation Midawara Formation Muweilih Fm Samalut Fm
	Oligocene	Late Eocene		Middle Eocene	
BASSIOUNI et al., (1984)	El Qatrani Formation	Qasr El Sagha Formation	Birket Qarun Formation	Gehannan Formation	El Midawarah Formation El Mishgigah member Wadi Rayan Formation Muweilih member
	Oligocene	Late Eocene		Middle Eocene	
ISMAIL and ABDEL-KAREEM (1971)	Gebel Qatrani Formation	Qasr El Sagha Formation	Gehannan shale member	Gehannan marl member	El-Mishgigah member Wadi Rayan Formation El-Masakeet member
		Late Eocene		Middle Eocene	
BISHAY (1966) Nile Valley (between wasta and Samalut)		Fayum Formation	Beni Suef Formation	El-Fashn Formation	Qarara Fm Maghaghia Fm Samalut Fm
		Late Eocene		Middle Eocene	
SAID (1962)	Qatrani Formation	Qasr El Sagha Formation	Birket Qarun Formation	Gehannan Formation	Wadi Rayan Formation
	Oligocene	Late Eocene		Middle Eocene	
ISKANDAR (1943)	Gebel Qatrani Formation	Qasr El Sagha member	Birket Qarun member	Ravine beds member	El Gharag Formation Sath El-Hadid Formation Midawara Formation Muweilih Formation
	Oligocene	Late Eocene		Middle Eocene	
		Gehannam Formation		Wadi Rayan Group	
BEADNELL (1905)	Fluvio-marine series	The Qasr El Sagha series	The Birket Qarun series	The Ravine beds	The Wadi Rayan series
	Oligocene	Middle			

TABLE 1.2. Biostratigraphic classifications of the Middle – Upper Eocene succession in the Fayum area.

ROCK UNITS	Beadnell (1905)		Abdou and Abdel-Kireem (1975)	Strougo and Haggag (1984)	Haggag (1990)	Zalat (1995)	Haggag and Bolli (1996)	Elewa et al. (1998)		
	Middle Eocene									
Gehannan Formation	Fish - scale beds		Gobigerapsis semimolatus (P15-P16)	Middle Eocene		Middle Eocene		Middle Eocene		
Birket Qarun Formation	Operculina - Nummulites beds			Late Eocene		Late Eocene				
Qasr El Sagha Formation	Carolia beds		Planktonic Forams Zones	Planktonic Forams Zones		Late Eocene				
				Middle Eocene		Middle Eocene		Late Eocene		
				Gobigerina pseudompliapertura (P15 ?)		Discaster saipanensis (NP17)				
				Truncorotaloides rohrri (P14)		Chiasmolithus oamaruensis (NP18)		Middle Eocene		
				Gobigerina theka semimolata (P15-P16)		Isthmolithus recurvus (NP19)				
				Truncorotaloides rohrri (P14)		Gobigerina theka semimolata (P15-P16)		Lutetian		
				Globigerina theka semimolata (P15-P16)		Truncorotaloides rohrri				
				Globigerina theka semimolata (P15-P16)		Globigerina theka semimolata (P15-P16)		Bartonian		
				Globigerina theka semimolata (P15-P16)		Globigerina theka semimolata (P15-P16)				
				Globigerina theka semimolata (P15-P16)		Globigerina theka semimolata (P15-P16)		Planktonic Forams		
				Globigerina theka semimolata (P15-P16)		Globigerina theka semimolata (P15-P16)				
				Globigerina theka semimolata (P15-P16)		Globigerina theka semimolata (P15-P16)		Ostracoda		
				Globigerina theka semimolata (P15-P16)		Globigerina theka semimolata (P15-P16)				
				Globigerina theka semimolata (P15-P16)		Globigerina theka semimolata (P15-P16)		Benthonic Forams		
				Globigerina theka semimolata (P15-P16)		Globigerina theka semimolata (P15-P16)				

Sedimentology

The first detailed facies analyses of the succession were those of Vondra (1974) and Bown and Kraus (1988). Vondra (1974) focused mainly on the Upper Eocene Qasr El-Sagha Formation in the area of Qasr El-Sagha NE Fayum. Bown and Kraus (1988) worked out the stratigraphy and paleoenvironmental implications of the Upper Eocene Qasr El-Sagha Formation, focusing on the Dir Abu Lifa Member and the Oligocene sequence. A dynamic stratigraphic model was developed by Gingerich (1992), who related the Middle-Upper Eocene sedimentary formations and facies in Fayum to sea-level changes. Salem (1976) analyzed the sedimentological data from sixty subsurface wells in northern Egypt to establish a sedimentation pattern and model of the Tertiary system that included the Fayum area. A study of microfacies associations with some geochemical analysis of samples had been done by Blondeau et al. (1984). El-Anbaawy et al. (1984) discussed the distribution of clay-mineral content in the Gehannam and Birket Qarun formations.

Aref and Morsy (2000) recognized and interpreted polygonal shrinkage cracks filled with gypsum along the upper surface of two mudstone layers in the Upper Eocene Qasr El Sagha Formation. The sedimentary characters of the Eocene sequences were studied by Ahmed (2001). Eocene and Oligocene paleoecology and paleogeography in the Fayum basin were discussed by Dolson et al. (2002). Recently, the concretions of the Birket Qarun Sandstone have been studied by Wanas (2008). More recently, Peters et al. (2009) have related the distribution and preservation of the fossil-whale skeletons in the area of Wadi El-Hitan to the relative sea level changes and sequence stratigraphy.

SEQUENCE STRATIGRAPHY: AN OVERVIEW OF CONCEPTS AND NOMENCLATURE

A concise summary of the basic sequence stratigraphic concepts and nomenclature is warranted. The current study is based on excellent outcrop data of the Middle-Upper Eocene clastic succession in the Fayum sag basin, all within the range of high-resolution

sequence stratigraphy. The sequence stratigraphy is the study of genetically related facies within a framework of chronostratigraphically significant surfaces (Van Wagoner et al., 1990). The sequence stratigraphic paradigm accommodates the interplay of relative sea-level changes, basin physiography and sediment flux or supply. These variables determine the accommodation space and the character of key bounding surfaces, as well as the stratal architecture within sequences and systems tracts (see Van Wagoner et al., 1990; Posamentier and Allen, 1999; Catuneanu et al., 2009).

The sequence is the fundamental unit in sequence stratigraphic analysis. The term “sequence” was originally defined by Mitchum et al. (1977) as “a stratigraphic unit composed of a relatively conformable succession of genetically related strata bounded at its top and base by unconformities or their correlative conformities.” The term “unconformity” was defined later by Van Wagoner et al. (1988) as “a surface separating younger from older strata along which there is evidence of subaerial erosion and truncation (and in some areas correlative submarine erosion) and subaerial exposure, and along which a significant hiatus is indicated” (Fig. 1.3).

Parasequences constitute the building blocks of the sequence. A parasequence is a conformable, genetically related succession of beds or bedsets, bounded by marine-flooding surfaces or their correlative surfaces (Van Wagoner et al., 1988).

The term “systems tract” was first defined by Brown and Fisher (1977) as “a linkage of contemporaneous depositional systems, where a depositional system is a three-dimensional assemblage of lithofacies genetically linked by active (modern) or inferred (ancient) processes and environments”. Within a relative sea-level cycle, three main systems tracts representing different parts of the relative sea-level cycle are typically developed (Fig. 1.3). The lowstand systems tract (LST) is the basal systems tract deposited during an interval of relative sea-level fall at the offlap break, and accumulates during slow rates of fall and/or subsequent relative slow sea-level rise. The transgressive systems tract (TST) is deposited during relative sea-level rise, with successions

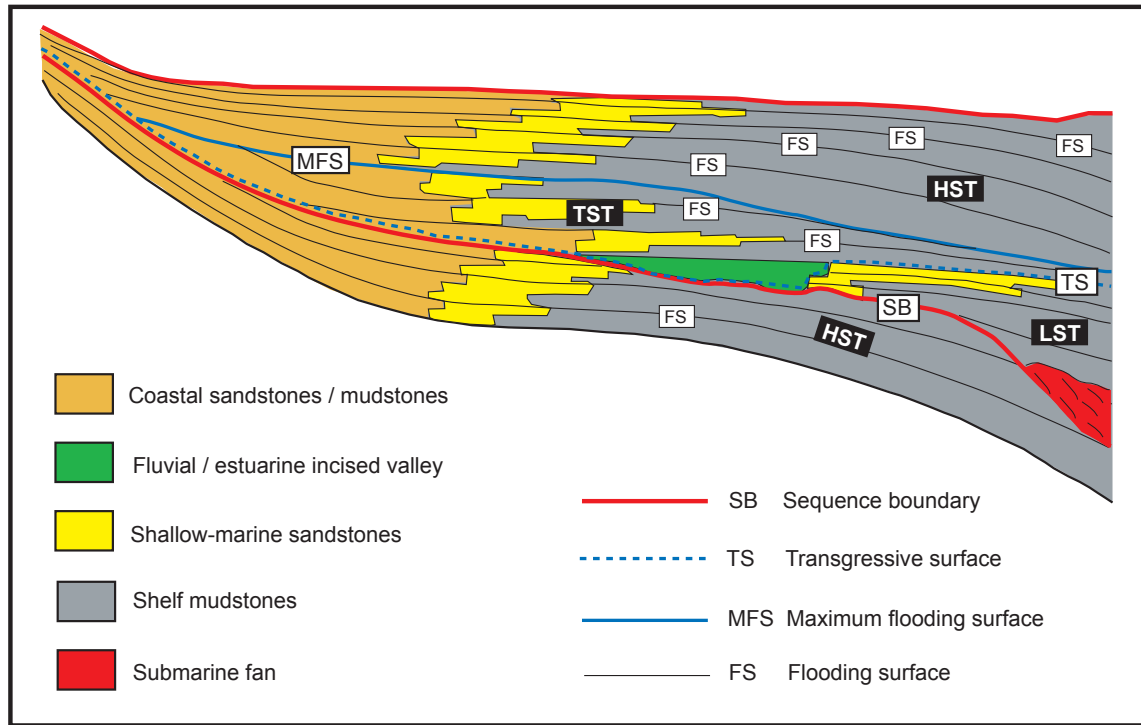


FIGURE 1.3. Schematic diagram of the idealized architecture of a third-order sequence, showing systems tracts, and the key-stratigraphic surfaces. Modified after Van Wagoner et al. (1990).

displaying retrogradational to aggradational stratal stacking pattern. The transgressive systems tract is succeeded by the highstand systems tract (HST), which is produced by a decelerating rate of relative sea-level rise through time, resulting in initial aggradational and later progradational architecture.

Four types of flooding surfaces, which herald minor breaks within a sequence can be identified (Fig. 1.3). Marine flooding surfaces (FS) are surfaces separating older from younger rock, marked by deeper-water strata resting on shallower-water strata (Van Wagoner et al., 1988, 1990). Transgressive surfaces (TS) are flooding surfaces, marking the onset of significant marine flooding, which overlies lowstand or highstand regressive sections (e.g., Posamentier and Allen, 1999). Ravinement surfaces or transgressive surfaces of erosion (TSE) are scoured by tides and/or waves during the landward shift of the shoreline (Catuneanu et al., 2009). Finally, the maximum flooding surface (MFS)

represents the surface that exists at the time of maximum transgression of the shelf, and separates the TST from the overlying HST (e.g., Posamentier and Allen, 1999).

AIMS AND THESIS ORGANIZATION

The thesis is divided into six chapters, which cover the sedimentology, ichnology and sequence stratigraphy of the Middle-Upper Eocene succession in the Fayum depression, Egypt. The data and results are organized into fifteen tables and fifty-three figures, in addition to the appendix. The introductory chapter introduces the geography, accessibility and study area locations, the geologic setting and previous work in the study area, and the aims and thesis organization. The concluding chapter “Summary and Conclusions” summarizes the results and broader contributions of the thesis work.

Chapter 2 integrates sedimentologic (facies associations) and ichnological (ichnofossils and ichnofacies) data into key-stratigraphic surfaces, in order to establish paleodepositional and paleoenvironmental models of the studied Eocene strata. These models link the depositional affinities to the relative sea-level history within a sequence stratigraphic framework during the deposition of the compiled Middle-Upper Eocene strata in the Fayum depression. The reported trace fossils—mostly invertebrate trace fossils, local rhizoliths, and very rare continental traces—are briefly described, illustrated and tabulated. Five facies associations (FA1 - FA5) are identified and described. The pertinent data are then combined to interpret and discuss the sedimentary environments of the Middle Eocene Gehannam Formation and the Upper Eocene Birket Qarun Formation, as well as the three members (Umm Rigl, Temple and Dir Abu Lifa) of the Upper Eocene Qasr El-Sagha Formation. Transgressive surfaces of erosion (TSE) have been differentiated into wave ravinement (Type 1 TSE) and wave/tidal ravinement (Type 2 TSE) surfaces. Some of these transgressive surfaces of erosion are either merged with sequence boundaries (SB) or coincide with maximum flooding surfaces (MFS) and transgressive surfaces (TS) or represent parasequence-bounding flooding surfaces (FS).

The refined depositional models stand to: (1) provide excellent analogues for offshore-to marginal marine strata at other locales; (2) produce well-developed facies models of various facies occurrences; (3) display many unusual ichnological-sedimentological associations in the study intervals, which may serve to interpret the stratigraphic record elsewhere; and, (4) help to interpret the occurrence of the well-preserved fossil-whale skeletons.

Chapter 3 focuses on the facies architecture, trace-fossil distributions, and ichnofacies types in order to interpret the paleoenvironment and sedimentologic setting of the whale-bearing Gehannam and Birket Qarun formations in the area of Wadi El-Hitan. Based on sedimentologic field data, petrography and scanning electron microscope investigations, along with ichnological/paleontological data, five facies (F1-F5) belonging to two main facies associations (FA1 and FA2) are identified and described. Seventeen ichnospecies belonging to thirteen ichnogenera are identified within these facies. Additionally, fossil-plant roots (rhizoliths) occur at predictable stratigraphic levels. Biological and sedimentological characteristics of the facies associations are used to interpret the paleoenvironments of FA1 and FA2, and to suggest a depositional model for the whale-bearing succession. The source and transport mechanisms of the highly thoroughly whale-bearing sandstones (FA1) are discussed. Moreover, this chapter discusses the relationship between the quiescent marine bay paleoenvironment covering the area of Wadi El-Hitan and the distribution, paleogeography and preservation of the fossil-whale skeletons.

Chapter 4 describes and interprets the origin and sedimentologic/sequence stratigraphic implications of unusual large-sized sedimentary structures in the whale-bearing sandstones of the Upper Eocene Birket Qarun Formation, in the area of Wadi El-Hitan. The sedimentologic and ichnological characters of the structures-associated depositional unit I (hosting sandstone) and depositional unit II (overlying and burrow fills sandstone/lag/coquina deposits) are investigated. Field data and measurements are used

to describe the various structures' sizes and morphologies, as well as their ichnological characters. Examination of polished longitudinal and cross-sectional slabs demonstrates complex ichnological texture and characters. Microfacies and petrographic study of the standard petrographic thin sections examined, SEM investigations, and carbon / oxygen stable-isotopic analyses are integrated to elucidate the diagenetic history of these structures and their associated depositional units. A bio-sedimentological model is suggested to interpret the origin of these unusual large sedimentary structures. The origin of the reported large sedimentary structures and its relation to bioturbation, diagenesis, and stable isotopic signatures are discussed. The sedimentological and sequence stratigraphic implications of these structures and their associated depositional units are emphasized.

Chapter 5 deals with the occurrences of the *Glossifungites* Ichnofacies and sequence stratigraphic analysis. The compiled Middle-Upper Eocene succession in the Fayum depression introduces unusual occurrences and outstanding outcrop exposures of the suites of the *Glossifungites* Ichnofacies. Facies analysis and softground ichnofacies are used to identify the depositional environments of the reported facies associations and their corresponding rock units. The relationship of the *Glossifungites* Ichnofacies and associated discontinuities are discussed, with a brief summary of their worldwide stratigraphic and paleogeographic distribution in the rock record. A genetic classification of more than twenty-five *Glossifungites*–Ichnofacies demarcated surfaces recorded from the study area is suggested. This approach is based mainly on: (1) the origin (autogenic or allogenic) of discontinuity surfaces; (2) the stratigraphic setting and relation of the allocyclically originated surfaces to the key sequence stratigraphic surfaces (SB, FS/SB, MFS, TS and FS); (3) surface-associated sedimentological characters; and, (4) ichnological criteria, such as substrate types, trace-fossil suites, bioturbation densities, ichnogenera diversities, maximum burrow diameters, and burrow-penetration depths. The recognized *Glossifungites*–Ichnofacies demarcated surfaces associated with key

sequence stratigraphic-bounding discontinuities, are used in the sequence stratigraphic architecture of the Middle-Upper Eocene succession in the Fayum depression. Moreover, regional extrapolation of the reported sequence boundaries (FS/SB1, FS/SB2 and SB3), and hierarchy of the reported sequences and relative sea-level fluctuations are discussed through correlations with more regional and global Eocene data.

REFERENCES

- Abdou, H.F. and Abdel-Kireem, M.R., 1975, Planktonic foraminiferal zonation of the middle and upper Eocene rocks of Fayum province, Egypt: *Revista Española de Micropaleontología*, v. 7, p. 15-64.
- Ahmed, S.M., 2001, Contribution to sedimentary nature of Eocene sequence, Fayum, Egypt: *Sedimentology of Egypt*, v. 9, p. 27-41.
- Ansary, S. E., 1955, Report on the foraminiferal fauna from the upper Eocene of Egypt: *Desert Bulletin Institute, Egypt*, v. 6, 160 pp.
- Aref, M.A.M. and Morsy, M.A., 2000, Polygonal shrinkage cracks filled with gypsum in the upper Eocene, Fayum, Egypt: *Sedimentology of Egypt*, v. 8, p. 89-103.
- Bassiouni, M., Boukhary, M., Shama, K. and Blondeau, A., 1984, Middle Eocene Ostracodes from Fayoum, Egypt: *Géologie Méditerranéenne*, v. 11, p. 181-192.
- Beadnell, H.J.L., 1905, The topography and geology of the Fayum Province of Egypt: *Egyptian Survey Department, Cairo*, 101 pp.
- Bishay, Y., 1966, Studies on the larger foraminifera of the Eocene of the Nile Valley between Assiut, Cairo and SW Sinai: Unpublished Ph.D. Thesis, Alexandria University, 244 pp.
- Blanckenhorn, M., 1903, Neue geologisch-stratigraphische Beobachtungen in Aegypten: *Sitzungsberichte der Mathematisch-physikalischen Classe der Königlichen Bayerischen Akademie der Wissenschaften*, v. 32, p. 353-433.

- Blondeau, A., Boukhary, M. and Shamah, K., 1984, Les microfacies de l'Eocene et de l'Oligocene de la Province du Fayoum, Egypte : *Revue de Paléobiologie*, v. 3, p. 243-267.
- Bown, T.M. and Kraus, M.J., 1988, Geology and paleoenvironment of the Oligocene Jebel Qatrani Formation and adjacent rocks, Fayum depression, Egypt: United States Geological Survey Professional Paper, v. 1452, p. 1-60.
- Bromley, R.G., 1996, Trace Fossils: Biology, Taphonomy and Applications. 2nd edition: Chapman and Hall, London, 361 pp.
- Brown, L.F. and Fisher, W.L., 1977, Seismic-stratigraphic interpretation of depositional systems: Examples from Brazilian rift and pull-apart basins, in Payton, C.E., ed., *Seismic Stratigraphy-Applications to hydrocarbon exploration*: American Association of Petroleum Geologists Memoir, v. 26, p. 213-248.
- Buatois, L.A., Gingras, M.K., MacEachern, J., Mángano, M.G., Zonneveld, J-P., Pemberton, S.G., Netto, R.G. and Martin, A., 2005, Colonization of brackish-water systems through time: Evidence from the trace-fossil record: *Palaaios*, v. 20, p. 321-347.
- Catuneanu, O., Abreu, V., Bhattacharya, J.P., Blum, M.D., Dalrymple, R.W., Eriksson, P.G., Fielding, C.R., Fisher, W.L., Galloway, W.E., Gibling, M.R., Giles, K.A., Holbrook, J.M., Jordan, R., Kendall, C.G.St.C., Macurda, B., Martinsen, O.J., Miall, A.D., Neal, J.E., Nummedal, D., Pomar, L., Posamentier, H.W., Pratt, B.R., Sarg, J.F., Shanley, K.W., Steel, R.J., Strasser, A., Tucker, M.E. and Winker, C., 2009, Towards the standardization of sequence stratigraphy: *Earth-Science Reviews*, v. 92, p. 1-33.
- Cuvillier, J., 1930, Révision du nummulitique Egyptein: *Mémoires Institut d'Egypte*, v. 16, p. 1-371.

- Dames, W.B., 1894, Über Zeuglodonten aus Aegypten und die Beziehungen der archaeoceten zu den übrigen Cetaceen: Géologique und Paläontologische Abhandlungen, Jena, v. 5, p. 189-222.
- Dolson, J., El Barkooky, A., Gingerich, P.D., Prochazka, N. and Shann, M., 2002, The Eocene and Oligocene Paleo-Ecology and Paleo-Geography of Whale Valley and the Fayum Basins: Implications for Hydrocarbon Exploration in the Nile Delta and Eco-Tourism in the Greater Fayum Basin: AAPG, Search Discovery Article # 10030: <http://www.searchanddiscovery.com/documents/cairo/index.htm>.
- EGPC, 1992, Western Desert, oil and gas fields (A comprehensive overview): The Egyptian General Petroleum Corporation, Cairo, 431 pp.
- Ekdale, A.A., Bromley, R.G. and Pemberton, S.G., 1984, Ichnology: The use of trace fossils in sedimentology and stratigraphy: Society of Economic Paleontologists and Mineralogists Short Course Note, v. 15, 317 pp.
- El-Anbaawy, M.I.; Dardir, A.A. and Meabed, E.E., 1984, Lithostratigraphy and clay mineralogy of some bentonitic clays in area east of the El-Fayoum depression, Egypt: Annals of the Geological Survey of Egypt, v. 14, p. 151-164.
- Elewa, A.M.T, Omar, A.A. and Dakrory, A.M., 1998, Biostratigraphical and paleoenvironmental studies on some Eocene ostracodes and foraminifers from the Fayoum depression, Western Desert, Egypt: Egyptian Journal of Geology, v. 42, p. 439-469.
- El Hawat, A.S., 1997, Sedimentary basins of Egypt: An Overview of Dynamic Stratigraphy, in Selly, R.C., ed., African basins, in Hsü, K.J., Ser. ed., Sedimentary Basin of the World: Elsevier, Amsterdam, v. 3, p. 39-85.
- El Zarka, M.H., 1983, Mode of hydrocarbon generation and prospects of the northern part of the Western Desert, Egypt: Journal of African Earth Sciences, v. 1, p. 295-304.
- Frey, R.W. and Goldring, R., 1992, Marine event beds and recolonization surfaces as revealed by trace fossil analysis: Geological Magazine, v. 129, p. 325–335.

- Geological Survey of Egypt 'GSE', 1981, Geological Map of Egypt, scale 1: 2,000,000: Egyptian Geological Survey and Mining Authority, Ministry of Industry and Mineral Resources, Cairo, 1 sheet.
- Geological Survey of Egypt 'GSE', 1983, Geological Map of Greater Cairo Area, scale 1: 100,000: Egyptian Geological Survey and Mining Authority, Ministry of Industry and Mineral Resources, Cairo, 1 sheet.
- Gibert, J.M. de and Goldring, R., 2007, An ichnofabric approach to the depositional interpretation of the intensely burrowed Bateig Limestone, Miocene, SE Spain: *Sedimentary Geology*, v. 194, p. 1-16.
- Gingerich, P.D., 1992, Marine mammals (Cetacea and Sirenia) from the Eocene of Gebel Mokattam and Fayum, Egypt; stratigraphy, age and paleoenvironments: *University of Michigan Papers in Paleontology*, v. 30, p. 1-84.
- Gingras, M.K., Bann, K.L., MacEachern, J.A., Waldron, J. and Pemberton, S.G., 2007, A conceptual framework for the application of trace fossils, in MacEachern, J.A., Bann, K.L., Gingras, M.K. and Pemberton, S. G., eds., *Applied Ichnology: Society of Economic Paleontologists and Mineralogists Short Course Notes*, v. 52, p. 1-25.
- Gingras, M.K., MacEachern, J.A. and Pemberton, S.G., 1998, A comparative analysis of the ichnology of wave and river-dominated allomembers of the Upper Cretaceous Dunvegan Formation: *Bulletin of Canadian Petroleum Geology*, v. 46, p. 51-73.
- Gingras, M.K., Pemberton, S.G. and Saunders, T., 2000, Firmness profiles associated with tidal-creek deposits: The temporal significance of Glossifungites assemblages: *Journal of Sedimentary Research*, v. 70, p. 1017-1025.
- Gingras, M.K., Pemberton, S.G., Saunders, T. and Clifton, H.E., 1999, The ichnology of modern and Pleistocene brackish-water deposits at Willapa Bay, Washington; variability in estuarine settings: *Palaios*, v. 14, p. 352-374.

- Gingras, M.K., Räsänen, M.E., Pemberton, S.G. and Romero, L.P., 2002a, Ichnology and sedimentology reveal depositional characteristics of bay-margin parasequences in Miocene Amazonian foreland basin: *Journal of Sedimentary Research*, v. 72, p. 871–883.
- Gingras, M.K., Räsänen, M. and Ranzi, A., 2002b, The significance of bioturbated inclined heterolithic stratification in the southern part of the Miocene Solimões Formation, Rio Acre, Amazonia Brazil: *Palaios*, v. 17, p. 591–601.
- Guiraud, R., Bosworth, W., Thierry, J. and Delplanque, A., 2005, Phanerozoic geological evolution of Northern and Central Africa: An overview: *Journal of African Earth Sciences*, v. 43, p. 83-143.
- Haggag, M.A., 1990, *Globigerina pseudoampliapertura* Zone, a new Late Eocene planktonic foraminiferal zone (Fayoum area, Egypt): *Neues Jahrbuch für Geologie und Paläontologie Monatshefte*, v. 5, p. 295-307.
- Haggag, M.A. and Bolli, H.M., 1995, *Globigerinatheka index aegyptiaca*, a new late Eocene planktonic foraminiferal subspecies from Fayoum, Egypt: *Revista Española de Micropaleontología*, v. 27, p. 143-147.
- Haggag, M.A. and Bolli, H.M., 1996, The origin of *Globigerinatheka semiinvoluta* (Keijzer), Upper Eocene, Fayoum area, Egypt: *Neues Jb. Neues Jahrbuch für Geologie und Paläontologie Monatshefte*, v. 6, p. 365-374.
- Hembree, D.I. and Hasiotis, S.T., 2007, Paleosols and ichnofossils of the White River Formation of Colorado: Insight into soil ecosystems of the North American mid-continent during the Eocene-Oligocene transition: *Palaios*, v. 22, p. 123-142.
- Holz, M., 2003, Sequence stratigraphy of a lagoonal estuarine system- an example from the lower Permian Rio Bonito Formation, Paraná Basin, Brazil: *Sedimentary Geology*, v. 162, p. 305-331.
- Hume, W.F., 1911, The effects of secular oscillation in Egypt during the Cretaceous and Eocene periods: *Quarterly Journal Geological Society of London*, v. 67, p. 118-148.

- Iskandar, F., 1943, Geological survey of the Gharaq El Sultani Sheet No. 68/54: The Standard Oil Company of Egypt. S. A., Report No. 57, 36 pp.
- Ismail, M.M. and Abdel-Kireem, M.R., 1971, Contributions to the stratigraphy of the Fayoum Province: Bulletin Faculty of Science Alexandria University, v. 11, p. 57-63.
- MacEachern, J.A., Bann, K.L., Bhattacharya, J.P. and Howell, C.D., 2005, Ichnology of deltas: organism responses to the dynamic interplay of rivers, waves, storms and tides, in Bhattacharya, B.P. and Giosan, L., eds., River Deltas: Concepts, Models and Examples: Society of Economic Paleontologists and Mineralogists Special Publication, v. 83, p. 49-85.
- MacEachern, J.A., Bann, K.L., Gingras, M.K. and Pemberton, S.G., 2007, The Ichnofacies Paradigm: High-resolution Paleoenvironmental Interpretation of the Rock Record, in MacEachern, J.A., Bann, K.L., Gingras, M.K. and Pemberton, S. G., eds., Applied Ichnology: Society of Economic Paleontologists and Mineralogists Short Course Notes, v. 52, p. 26-63.
- MacEachern, J.A. and Gingras, M.K., 2007, Recognition of brackish-water trace fossil suites in the Cretaceous Western Interior Seaway of Alberta, in Bromley, R.G., Buatois, L.A., Mángano, M.G., Genise, J.F. and Melchor, R.N., eds., Sediment–Organism Interactions: a Multifaceted Ichnology: Society of Economic Paleontologists and Mineralogists Special Publication, v. 88, p. 147–192.
- MacEachern, J.A., Raychaudhuri, I. and Pemberton, S.G., 1992, Stratigraphic applications of the Glossifungites ichnofacies: delineating discontinuities in the rock record, in Pemberton, S.G., ed., Applications of Ichnology to Petroleum Exploration, A Core Workshop: Society of Economic Paleontologists and Mineralogists Core Workshop Note, v. 17, p. 169-198.

- McIlroy, D., 2004, The Application of Ichnology to palaeoenvironmental and Stratigraphic Analysis: Geological Society London Special Publication, v. 288, 490 pp.
- Mitchum, R.M., Vail, P.R. and Thompson, S., 1977, Seismic stratigraphy and global changes of sea level, Part 2: The depositional sequence as a basic unit for stratigraphic analysis, in Payton, C.E., ed., Seismic stratigraphy-Applications to hydrocarbon exploration: American Association of Petroleum Geologists Memoir, v. 26, p. 53-62.
- Morris, J.E., Hampson, G.J. and Johnson, H.D., 2006, A sequence stratigraphic model for an intensely bioturbated shallow-marine sandstone: the Bridport Sand Formation, Wessex Basin, UK: Sedimentology, v. 53, p. 1229-1263.
- Morsi, A.M., Boukhary, M. and Strougo, A., 2003, Middle-upper Eocene ostracods and Nummulites from Gebel Na'alun, southeastern Fayum, Egypt: Revue de Micropaléontologie, v. 46, p. 143-160.
- Nesbitt, E.A. and Campbell, K.A., 2006, The paleoenvironmental significance of Psilonichnus: Palaios, v. 21, p. 187-196.
- Pemberton, S.G. and MacEachern, J.A., 1995, The sequence stratigraphic significance of trace fossils: examples from the Cretaceous foreland basin of Alberta, Canada, in Van Wagoner, J.C. and Bertram, G., eds., Sequence Stratigraphy of Foreland Basins Deposits: Outcrops and Subsurface Examples from the Cretaceous of North America: American Association of Petroleum Geologists Memoir, v. 64, p. 429-475.
- Pemberton, S.G. and MacEachern, J.A., 1997, The ichnological signature of storm deposits: the use of trace fossils in event stratigraphy, in Brett, C.E., ed., Palaeontological Event Horizons Ecological and Evolutionary Implications: Columbia University Press, p. 73-109.

- Pemberton, S.G., MacEachern, J.A. and Ranger, M.J., 1992, Ichnology and event stratigraphy: the use of trace fossils in recognizing tempestites. in Pemberton, S.G., ed., Applications of Ichnology to Petroleum Exploration, A Core Workshop: Society of Economic Paleontologists and Mineralogists Core Workshop Note, v. 17, p. 85–117.
- Pemberton, S.G., MacEachern, J. A. and Saunders, T., 2004, Stratigraphic applications of substrate-specific ichnofacies: delineating discontinuities in the rock record, in MacIlory, D., ed., The Application of Ichnology to Palaeoenvironmental and Stratigraphic Analysis: Geological Society of London Special Publication, v. 288, p. 29-62.
- Peters, S.E., Antar, M.S.M., Zalmout, I.S. and Gingerich, P.D., 2009, Sequence stratigraphic control on preservation of late Eocene whales and other vertebrates at Wadi Al-Hitan, Egypt: *Palaios*, v. 24, p. 290–302.
- Posamentier, H.W. and Allen, G.P., 1999, Siliciclastic sequence stratigraphy- concepts and applications: Society of Economic Paleontologists and Mineralogists, Concepts in Sedimentology and Paleontology, v. 7, 210 pp.
- Robertson Research International (RRI), Associated Research consultants in association with Scott Pickford, Associates Limited & ERC Energy Resource Consultants Limited (1982): Petroleum potential evaluation, Western Desert, ARE: Report prepared for Egyptian General Petroleum Corporation (EGPC), Cairo, 8 volumes.
- Said, R., 1962, The geology of Egypt: Elsevier, Amsterdam and New York, 377 pp.
- Said, R., 1990, The geology of Egypt: A. A. Balkema, Rotterdam, 734 pp.
- Salem, R., 1976, Evolution of Eocene-Miocene sedimentation patterns in parts of northern Egypt: American Association of Petroleum Geologists Bulletin, v. 60, p. 34-64.

- Savrda, C.E. and Bottjer, D.J., 1989, Trace fossil models for reconstructing oxygenation histories of ancient marine bottom waters: application to Upper Cretaceous Niobrara Formation, Colorado: *Palaeogeography, Palaeoclimatology, Palaeoecology*, v. 74, p. 49-74.
- Savrda, C.E., Browning, J.V., Krawinkle, H. and Hesselbo, S.P., 2001, Firmground ichnofabrics in deep-water sequence stratigraphy, Tertiary clinoform-toe deposits, New Jersey slope: *Palaaios*, v. 16, p. 294-305.
- Schweinfurth, G., 1877, Reise die Wüste von Heluan bis Qeneh, 24 Marz bis 18 Mai 1877: *Petermanns Geographische Mitteilungen (Gotha)*, v. 23, p. 387-389.
- Seiffert, E.R., Bown, T.M., Clyde, W.C. and Simons, E.L., 2008, Geology, paleoenvironment, and age of Birket Qarun locality 2 (BQ-2), Fayum Depression, Egypt, in Fleagle, J.G. and Gilbert, C.C., eds., Elwyn L. Simons: A Search for Origins: Springer-Verlag, New York, p. 71-86.
- Seilacher, A., 1982, Distinctive features of sandy tempestites, in Einsele, G. and Seilacher, A., eds., *Cyclic and Event Stratification*: Springer-Verlag, Berlin, p. 333-349.
- Sestini, G., 1984, Tectonic and sedimentary history of NE African margin (Egypt/Libya), in Dixon, J.E. and Robertson, A.H.F., eds., *The geological evolution of the eastern Mediterranean*: Geological Society of London Special Publication, v. 17, p. 161-175.
- Smith, A.G., 1971, Alpine deformation and the oceanic areas of Tethys, Mediterranean and Atlantic: *Geological Society of American Bulletin*, v. 82, p. 2039-2070.
- Strougo, A., 1979, The Middle Eocene-Upper Eocene boundary in Egypt: *Annals of the Geological Survey of Egypt*, v. 9, p. 455-470.
- Strougo, A. and Haggag, M.A.Y., 1984, Contribution to the age determination of the Gehannam Formation in the Fayum Province, Egypt: *Neues Jb. Neues Jahrbuch für Geologie und Paläontologie Monatshefte*, v. 1, p. 46-52.

- Swedan, A.H., 1992, Stratigraphy of the Eocene sediments in the Fayum area: *Annals of the Geological Survey of Egypt*, v. 18, p. 157-166.
- Van Wagoner, J.C., Mitchum, R.M., Campion, K.M. and Rahmanian, V.D., 1990, Siliciclastic sequence stratigraphy in well logs, cores, and outcrops: Concepts for high-resolution correlation of time and facies: *American Association of Petroleum Geologists, Methods in Exploration Series*, v.7, p. 1-55.
- Van Wagoner, J.C., Posamentier, H.W., Mitchum, R.M., Vail, P.R., Sarg, J.F., Loutit, T.S. and Hardenbol, J., 1988, An overview of the fundamentals of sequence stratigraphy and key definitions, in Wilgus, C.K., Hastings, B.S., Kendall, C.G.St. C., Posamentier, H.W., Ross, C.A. and Van Wagoner, J.C., eds., *Sea-level changes-an integrated approach: Society of Economic Paleontologists and Mineralogists, Special publication*, v. 42, p. 39-45.
- Vondra, C.F., 1974, Upper Eocene transitional and near-shore marine Qasr el Sagha Formation, Fayum Depression, Egypt: *Annals of the Geological Survey of Egypt*, v. 4, p. 79-94.
- Wanas, H.A., 2008, Calcite-cemented concretions in shallow marine and fluvial sandstones of the Birket Qarun Formation (Late Eocene), El-Faiyum depression, Egypt: Field, petrographic and geochemical studies: Implications for formation conditions: *Sedimentary Geology*, v. 212, p. 40-48.
- Younes, M.A., 2003, Geochemical fingerprints of crude oils and related source rock potentials in the Gindi basin, northern Western Desert of Egypt: *Oil Gas European Magazine*, v. 29, p. 200-205.
- Zalat, A.A., 1995, Calcareous nanoplankton and diatoms from the Eocene / Pliocene sediments, Fayoum depression, Egypt: *Journal of African Earth Sciences*, v. 20, p. 227-244.

CHAPTER 2: SEDIMENTARY ENVIRONMENTS AND DEPOSITIONAL CHARACTERS OF THE MIDDLE-UPPER EOCENE WHALE-BEARING SUCCESSION IN THE FAYUM DEPRESSION, EGYPT *

INTRODUCTION

The Fayum area is an oasis in the Western Desert, Egypt characterized by excellent exposure of extremely fossiliferous Eocene strata (Fig. 2.1). The current study is important for three reasons. First, because Wadi El-Hitan area, SE Fayum, was added to UNESCO's World Heritage list in 2005, there is growing international interest in the geology of Fayum area. Secondly, previous sedimentologic and sequence stratigraphic reports do not adequately assess the depositional character of the Fayum-Eocene strata (e.g., Vondra, 1974; Bown and Kraus, 1988, Gingerich, 1992; Ahmed, 2001; Dolson et al., 2002). Finally, none of the aforementioned studies considered the ichnological data present in the marine units of the Eocene succession and their application in paleoecology, sedimentology and sequence stratigraphy.

Despite excellent exposure of Eocene strata in the area, a refined depositional model relating the depositional affinities of the Middle - Upper Eocene strata to relative sea-level history has not yet been established. Owing to the presence of outstanding outcrop exposure, a local sedimentologic / stratigraphic characterization stands to: (1) provide excellent analogues for offshore- to marginal-marine strata at other locales; (2) produce well-developed facies models of various facies occurrences; and (3) establish paleoenvironmental models to interpret the occurrence of the well-preserved fossil-whale skeletons. Given the strengths of the studied dataset, this chapter's primary aim is to provide a depositional interpretation of the area's Eocene sedimentary record. As discussed below, many of the intervals display unusual ichnological-sedimentological

* A version of this chapter has been published online (September 15th, 2009) in *SEDIMENTOLOGY* journal as "Sedimentary environments and depositional characteristics of the Middle to Upper Eocene whale-bearing succession in the Fayum depression, Egypt", by: Zaki A. Abdel-Fattah , Murray, K. Gingras, Michael. W. Caldwell and S. George Pemberton. doi: 10.1111/j.1365-3091.2009.01091.x.

associations that may serve to interpret the stratigraphic record elsewhere. Moreover, the inferred depositional environments provide a sedimentological context for the extraordinarily fossiliferous strata of the area.

Stratigraphic, sedimentologic, and ichnologic data were collected through detailed outcrop logging. Stratigraphic observations comprise assessment of rock-unit thicknesses, boundaries and distribution, and delineation of the key stratigraphic surfaces. The sedimentological data gathered include identification of lithology, texture, sedimentary and biogenic structures, and the documentation of the fossil content. Petrographic analysis of each documented lithofacies was conducted. The ichnological data collected include: identification of ichnogenera, the stratigraphic distribution of ichnofossils, characterization of ichnofossil suites and ichnofacies types, intensity of bioturbation (bioturbation index), ichnogenera diversity, and the size (maximum diameter) of trace fossils. Lithofacies were compiled into recurring facies associations (FA1 to FA5). The vertical distribution of lithofacies and the identification of stratigraphic surfaces permitted presentation of the data within a sequence stratigraphic framework.

GEOLOGIC SETTING AND STUDY AREA

The Fayum basin developed during the rifting event that led to the opening of the Tethys Sea during the Jurassic. The basin formed in association with extensional and strike-slip tectonics between Africa and Eurasia (Smith, 1971). The advent of the Late Cretaceous is marked by a period of compressional tectonics associated with strike-slip dextral shearing between Africa and Eurasia (Guiraud et al., 2005). The Fayum basin was uplifted during the Late Cretaceous Syrian Arc activity. Consequently, it was effectively subdivided into two major Paleocene-Eocene depocentres: the northern Tiba Basin and the southern Gindi or the lower Nile Basin (El Zarka, 1983). By the Middle Eocene, the southern depocentre Gindi (lower Nile) Basin attained a N-S orientation, and was the main depocentre between Assiut and Cairo. Since the Middle Eocene, the physiographic

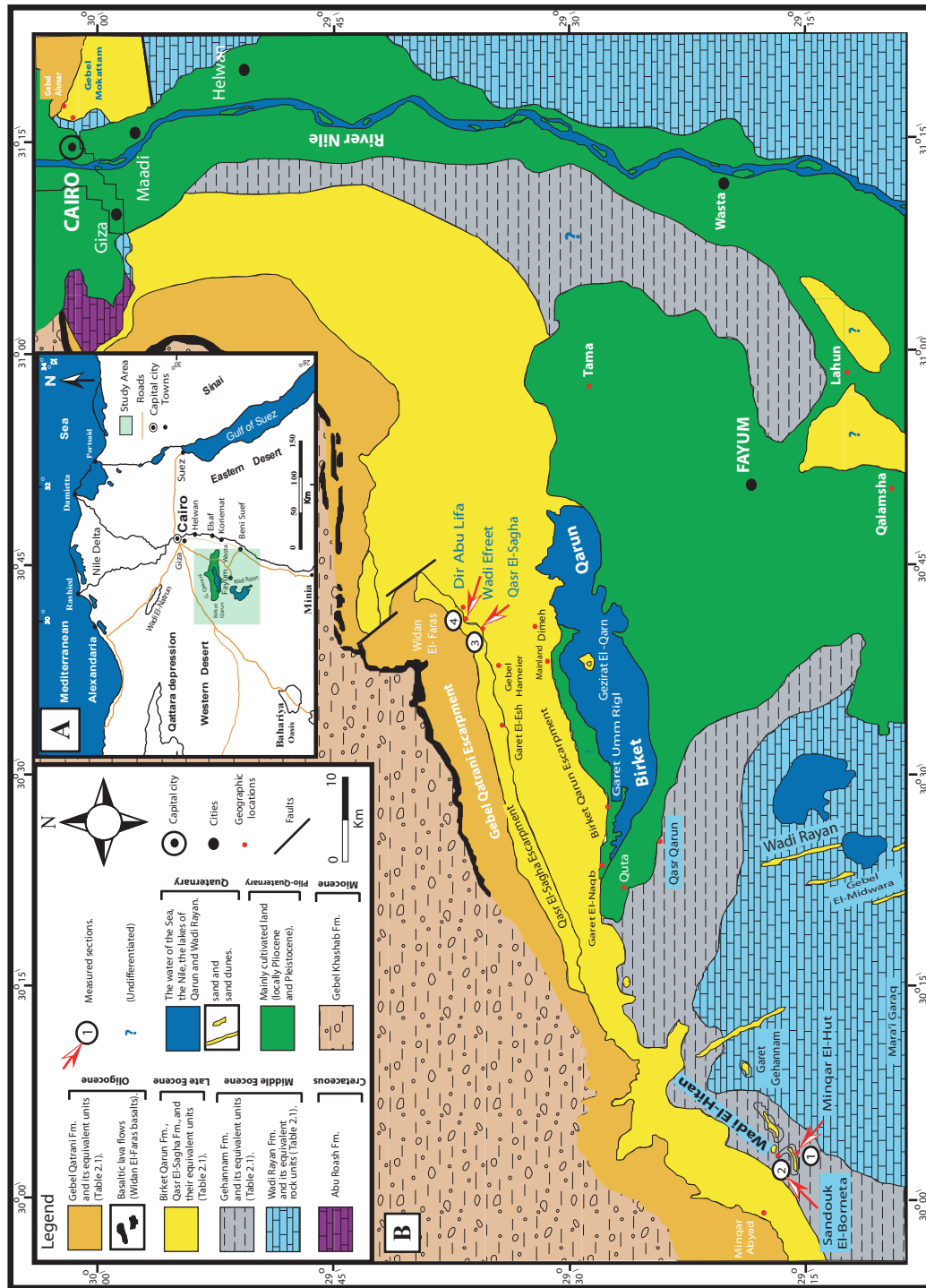


FIGURE 2.1. A- Location map of the Fayum depression, Egypt. B- Geological map of the Fayum and its adjacent area (Nile valley and northward to the greater Cairo). Compiled and modified after Beadnell (1905), Said (1962), GSE (1981, 1983), and Gingerich (1992).

margins of Egypt have been dominated by vertical movements associated with gradual subsidence of the Mediterranean Sea and the opening of the Red Sea (Sestini, 1984). The advent of the Late Eocene is marked by a continuous lowering of relative sea level, resulting in the progressive emergence and erosion of the structural highs that provided clastic sediments to Late Eocene basins of northern Egypt (Salem, 1976). The Oligocene was a time of uplift, regression, volcanicity and continental sedimentation (Cherif and El Afifi, 1983; Said, 1990) in the study area.

This work focuses on the Middle-Upper Eocene succession in the vicinity of the Fayum depression exposed in two areas: Wadi El-Hitan and Qasr El-Sagha (Fig. 2.1). Two sections (Fig. 2.1) were studied in the area of Wadi El-Hitan, SE Fayum. The first section is a composite section measured from Minqar El-Hut (N 29° 16' 02" - E 30° 03' 51") and the Old Camp site (N 29° 15' 55" - E 30° 01' 24"). The second section was measured entirely from exposures at Sandouk El-Borneta (N 29° 17' 00" - E 30° 03' 00"). Two sections were studied in the Qasr El-Sagha area, NW of Birket Qarun (Fig. 2.1): Qasr El-Sagha Temple section (N 29° 35' 42" - E 30° 40' 41") and the composite section of Dir Abu Lifa – Wadi Efreet (lies between: N 29° 36' 11" - E 30° 41' 46" and N 29° 37' 20" - E 30° 41' 45").

In the study area, five rock units are recognized (from base to top): the Middle Eocene Wadi Rayan and Gehannam formations; the Upper Eocene Birket Qarun and Qasr El-Sagha formations; and the Oligocene Gebel Qatrani Formation (Table 2.1). This work generally follows the lithostratigraphic classification of Beadnell (1905) and its emendation by Said (1962), as illustrated in Table (2.1). The Umm Rigl Member of Gingerich (1992) is used here to define the lowermost strata of the Qasr El-Sagha Formation in the area of Wadi El-Hitan. Upwards, the Bown and Kraus' (1988) lithostratigraphic subdivision of the Upper Eocene Qasr El-Sagha Formation in the area of Qasr El-Sagha into the Temple Member and upper Dir Abu Lifa Member is adopted.

TABLE 2.1. The lithostratigraphic classifications of the Middle Eocene – Oligocene succession of the Fayum area and its vicinities.

BEADNELL (1905)	Oligocene	E O C E N E									
		Middle					Late				
		The Wadi Rayan series					The Ravine beds	The Birket Qarun series	The Qasr El Sagha series	Fluvio-marine series	
ISKANDAR (1943)	Oligocene	Middle Eocene					Late Eocene				
		Wadi Rayan Group					Gehannam Formation				
		El Gharag Formation	Sath El-Hadid Formation	Midawara Formation	Muweilih Formation		Ravine beds member	Birket Qarun member	Qasr El Sagha member	Gebel Qatrani Formation	
SAID (1962)	Oligocene	Middle Eocene					Late Eocene				
		Wadi Rayan Formation					Gehannan Formation	Birket Qarun Formation	Qasr El Sagha Formation	Qatrani Formation	
BISHAY (1966) Nile Valley (between wasta and Samalut)		Middle Eocene					Late Eocene				
			Qarara Fm	El-Fashn Formation	Wadi Rayan Formation		Gehannan marl member	Gehannan shale member	Qasr El Sagha Formation	Gebel Qatrani Formation	
		Samalut Fm	Maghagha Fm								
SAID (1962)	Oligocene	Middle Eocene					Late Eocene				
		Wadi Rayan Formation					Gehannan Formation	Birket Qarun Formation	Qasr El Sagha Formation	Qatrani Formation	
ISMAIL and ABDEL-KAREEM (1971)	Oligocene	Middle Eocene					Late Eocene				
		Wadi Rayan Formation					Qasr El Sagha Formation				
		El-Mishgigah member	Gehannan Formation		Gehannan marl member	Gehannan shale member	Qasr El Sagha Formation	Gebel Qatrani Formation			
BASSIOUNI et al, (1984)	Oligocene	Middle Eocene					Late Eocene				
		Early	Middle		El Midawarah Formation	Gehannan Formation	Birket Qarun Formation	Qasr El Sagha Formation	El Qatrani Formation		
		Muweilih member	Wadi Rayan Formation		El Mishgigah member						
SAID (1990)	Oligocene	Middle Eocene					Late Eocene				
		Musalut Fm	Muweilih Fm	Midawara Formation	Sath El-Hadid Formation	Gharag Formation	Gehannan Formation	Qasr El Sagha Formation	Gebel Qatrani Formation		
SWEDAN (1992)	Oligocene	Middle Eocene					Late Eocene				
		Samalut Formation	Rayan Formation	Qazzun Formation	Mokattam Formation		Birket Qarun Formation	Qasr El Sagha Formation	Gebel Qatrani Formation		
PRESENT WORK	Oligocene	Middle Eocene					Late Eocene				
		Wadi Rayan Formation					Gehannan Formation	Birket Qarun Formation	Qasr El Sagha Formation	Gebel Qatrani Formation	

REPORTED TRACE FOSSILS

Some of the collected ichnological data are reported semi-quantitatively, in particular: (1) the bioturbation intensity, as expressed by the bioturbation index, which is a numerical scale (between 0 and 6) representing grades of bioturbation based on percentage ranges of disrupted primary fabric, which varies from nonbioturbated (BI 0) to completely bioturbated (BI 6) (*sensu*, Taylor and Goldring, 1993); and, (2) trace-fossil sizes, as represented by the maximum diameter through the use of five ranges, beginning with a diameter value < 2mm to those > 20mm.

Eighteen ichnospecies belonging to seventeen ichnogenera are reported and identified from the Middle-Upper Eocene strata in the study area. The stratigraphic distributions and illustrations of the reported ichnofossils (indicated in Fig. 2.2) are shown in Figs. 2.3-2.11. Also shown are (measured) maximum-burrow diameters and associated bioturbation intensities (BI) (Figs. 2.4, 2.7 and 2.10). Table 2.2 summarizes the mode of occurrence and physical characteristics of the ichnospecies identified in this study. Most of the ichnofossils are illustrated in Figs. 2.3, 2.5, 2.6, 2.8, 2.9 and 2.11. The trace fossils are generally characteristic elements of the *Cruziana*, *Skolithos* and *Psilonichnus* ichnofacies. Suites of the archetypal *Cruziana* Ichnofacies dominates lower parts of the section (e.g., Fig. 2.4; summarized in Table 2.3), with less diverse suites characteristic of stressed expressions of the *Skolithos* and *Psilonichnus* ichnofacies occurrences upwards (e.g., Fig. 2.7; Table 2.3).

Uncommon trace fossils (Figs. 2.3E and F) characteristic of continental settings are restricted to particular stratigraphic horizons in the study area. These include rare termite burrow nests observed in the upper part of the Dir Abu Lifa Member (Qasr El-Saga Formation) and other undiagnosed insect trace fossils (e.g., rarely preserved undiagnosed horizontal spreiten-bearing structures, Fig. 2.3F) that occur at the bounding stratigraphic horizon between Gehannam and Birket Qarun formations (Fig. 2.6D).

Traces ascribed to rhizoliths are also reported: these are differentiated from

TABLE 2.2. Description of the trace fossils reported from the Middle - Upper Eocene succession studied.

- 1- *Arenicolites* isp. (Fig. 2.3A) Simple, vertical to inclined U-shaped slender tubes have smoothed walls. Tubes are 2-3 mm in diameter, 8-12 mm apart (in horizontal plain view), with depths (vertical section) of 5-8 mm.
- 2- *Asterosoma* isp. (Fig. 2.5B) Star-shaped burrow system ranges from 50 to 90 mm across. These structures consist of radial arms (10-13 mm in diameter (max. width) and 20-30 mm in length). Arms are elongated, bulbous in the middle, tapering toward one end, though locally with some arms tapering on both ends. The internal structure has packed concentric laminations of sand (yellow) and clay (grayish).
- 3- *Chondrites* isp. (Fig. 2.3B) A complex dendritic burrow system (up to 40 mm across) consists of asymmetrically branching smooth-walled tunnels. These tunnels are neither anastomose nor converge, and are uniform in diameter (~2 mm). The lengths of some tunnels are traceable for > 30 mm, and ramify from a master shaft (commonly secondary to tertiary order of branching).
- 4- *Cylindrichnus* isp. (Fig. 2.3C) Horizontal, isolated, and non-branched structure is the only recorded form. Vertical and inclined structures are not exposed. The cross-section is large and has an elliptical form (max. diameter 60-70 mm, min. diameter 12-16 mm). The wall has multiple, concentrically yellowish and grayish alternating layers. Central core is grayish in color and elliptical (5-15mm in diameter) in shape.
- 5- *Diplocraterion* ? *parallelum* Torell, 1870 (Fig. 2.8G) Vertical to inclined, double entrance tubes have u-shaped spreiten with sediment fill darker than host sediment. Burrow width is up to 15 mm and total length of 30-70 mm. Tube diameter are 4 mm, and terminated upward with oval aperture (~3mm in diameter). The parallel tube and the above described characters are closest to those of *D. parallelum*.
- 6- *Monocraterion* isp. (Fig. 2.8G) Simple, slightly inclined vertical structure has a diagnostic funnel-shaped aperture. Burrow has a length up to 6 cm, average diameter of 15 mm, and a projected funnel aperture diameter of 30 mm.
- 7- *Ophiomorpha nodosa* Lundgren, 1891 (Figs. 2.6E, 2.11H) Simple to complex, horizontal, Y-shaped, and branched cylindrical burrow system. Tubes are 10-60 cm in length and 20-45 mm in diameter. The internal burrow lining is smooth and has an average thickness of 1 mm. The burrow walls are exteriorly mammalated by densely and more or less regular pellets. The pellets are ovoid to discoid in shape (1-3 mm in length and average height of 2 mm). The burrow fills are structureless and consist of sediments similar to the host sediment.
- 8- *Palaeophycus* isp. The plan view is not observed. Burrows are horizontal to inclined, branched and non-branched, lined cylindrical structures. Outline is oval to circular (diameter ranges between 5 and 20 mm). Passively filled with structureless sediments similar to host rock. It is distinguished from the *Planolites* by wall linings and their fills.
- 9- *Planolites montanus* Richter, 1937 (Figs. 2.3C, 2.8F, 2.9H) Burrows are horizontal to subhorizontal, unlined, unbranched, and smaller in size (average diameter of 2 mm). The shape is sinuous to tortuous and circular to elliptical in cross-section. Walls are mostly smooth. Burrow fills are structureless, and differ from the host sediments in color (grayish white) and grain size (finer sediments).
- 10- *Protovirgularia* isp. (Fig. 2.9H) Horizontal, slightly curved ridges that are almond-shaped to triangular in cross section. Ridges have lengths up to 80 mm and width of 5-8 mm. Internal structure has successive pads of sediment. Exterior ridges are hardly preserved.

TABLE 2.2. (in contin.)

11- *Psilonichnus upsilon*, Frey, Curran and Pemberton 1984 (Fig. 2.6C) Burrows are steeply inclined, rarely branched, unlined, and straight to slightly curved tubular structures. The morphology ranges from irregular shafts to J- and Y-shaped cylindrical forms, with a Y-shaped upper part if preserved. Burrow diameter varies between 3 and 6 cm, whereas the preserved depth or length is up to 18 cm. *Teichichnus*-appearance structure is referred to the passive burrow fills.

12- *Rhizocorallium irregulare* Mayer, 1954 (Fig. 2.5B) Burrows are tongue-shaped, and horizontally parallel to sub-parallel to bedding planes. Well-developed spreite exist between the limbs. The structures' lengths vary between 70 and 80 mm, whereas total widths ranges from 8 to 15 mm. Marginal tunnel is 2-3 mm wide, whereas spreite are 3-4 mm in width. Tube diameter/diameter of spreite ratio is typically > 1:5.

13- *Scolicia* isp. The plan view is not exposed. Well-developed association of vertical sections are documented. They are circular to oval with diameters range between 2.5 and 3.5 cm. The internal structures have circular, oval and sub-concentric laminae.

14- *Skolithos linearis* Haldeman, 1840 (Figs. 2.3A, 2.6E, 2.11G) Burrows are cylindrical, straight to curved, distinctly smoothed walled, rarely branched, and vertical to steeply inclined. Unornamented simple shafts are typically 2-4 mm in diameter with variable lengths.

15- *Teichichnus rectus* Seilacher, 1955 (Fig. 2.5G) Vertical and unbranched spreite consist of tightly packed, straight to broadly U-shaped laminae. Burrows have variable dimensions (max. lengths up to 150 mm max.; vertical extent 120 mm; and typical width of 20-30 mm). Longitudinal sections show nested burrows of simple, long, straight to sinuous, upward migrated, horizontal to sub-horizontal tunnels. These tunnels are mostly retrusive and merge upward at various angles with bedding planes.

16- *Thalassinoides suevicus* (Rieth, 1932) (Figs. 2.3D, 2.5B, 2.11C) The burrows are predominantly horizontal and regularly branched. They form bedding-parallel mazes, with an overall length >1m. Branches ramify at acute angles. The Y-shaped dichotomous bifurcations dominate T-shaped branches. The branches are cylindrical in shape and circular to oval in transverse section. The straight segments may extend to several decimeters in length. Diameters range from 2 to 3cm. Swollen and enlarged divergence areas (turning chambers) have expanded diameters up to 5cm. Burrow walls are mostly smooth and unlined. Burrow fills are structureless, but curvilinear-laminated meniscae are locally recorded.

17- *Thalassinoides paradoxicus* (Woodward, 1830) (Figs. 2.5E, 2.8B) Burrow system is complex, irregular branched box-work network. The network is oriented at various angles to the bedding planes, with an overall length up to 80 cm. Both Y-shaped bifurcations and T-shaped intersections are common. Subcylindrical to cylindrical branches, circular to elliptical occur in transverse section. Diameter varies between 10mm and 30 mm. Straight segments extend for 50 cm in length. The burrow walls are mostly smooth, but some rare knobs may be present.

18- *Teredolites longissimus* Kelly and Bromley, 1984 (Fig. 2.5C) Inclined molds occur as subcylindrical to club-shaped clusters of borings. Individual borings have diameters of 5-10 mm, and length of 30-70 mm. The length/diameter ratios are > 5. Apertures are circular to subcircular in cross-section. The boring walls are straight in their upper parts, and tend to be slightly sinuous and curved downward.

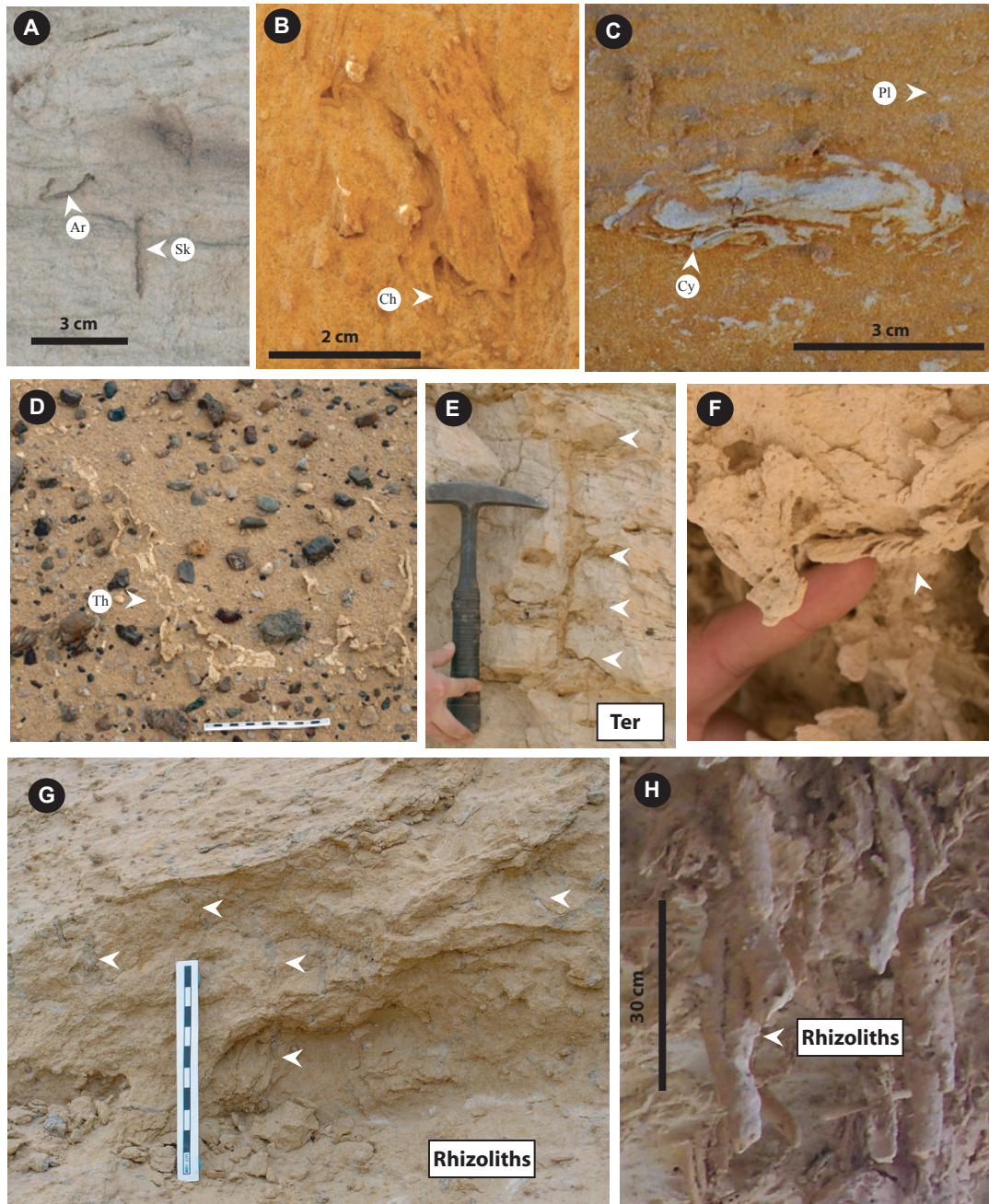


FIGURE 2.3. Trace fossils and rhizololiths found in the Middle-Upper Eocene succession, Fayum area. **A-** Ichnological suite of *Arenicolites* isp. (Ar) and *Skolithos linearis* (Sk) in the lower part of Dir Abu Lifa Member, Qasr El-Sagha area. **B-** Monospecific suite of *Chondrites* isp. (Ch) found in the bioturbated sandstone of the Gehannam Formation, Minqar El-Hut section. **C-** Horizontal *Cylindrichnus* isp. (Cy) and *Planolites montanus* (Pl) found as in (B), Sandouk El-Borneta section. **D-** Large horizontal maze of *Thalassinoides suevicus* (Th) from the same locality as in (B). **E-** Rare termite-burrow nest (Ter) preserved at the cross-bedded sandstone of Dir Abu Lifa Member, Wadi Efreet. White arrows point to the termite chambers. **F-** Undiagnosed horizontal spreiten-bearing structures (white arrow) found in the complex plaeoecologic horizon between Gehannam and Birket Qarun formations, Sandouk El-Borneta section. **G-** Dark-grey rhizololiths marking the top of the alluviated sandstone in the middle Birket Qarun Formation, Sandouk El-Borneta section. **H-** Brownish-coloured large rhizololiths (root cast) in the same locality as in (F).

Although trace fossils have a limited biostratigraphic importance owing to their long temporal ranges, their strongly facies-controlled nature (see Pemberton et al., 2001; Gingras et al., 2007) makes them a valuable and powerful tool in sedimentological and paleoenvironmental analyses. The softground and substrate-controlled ichnofacies (see MacEachern et al., 2007) are identified through careful ichnological analysis of the documented trace fossils and their suites in the studied succession. The firmground ichnofacies—*Glossifungites* Ichnofacies—are used here in the identification of discontinuity surfaces (Table 2.4 and Fig. 2.12). The recurring softground ichnofacies (e.g., archetypal *Cruziana* and *Skolithos* ichnofacies) and their departures from archetypal expressions impart important information regarding the paleoecological and paleoenvironmental conditions of the Middle-Upper Eocene succession (Table 2.3 and Fig. 2.12).

REPORTED FACIES ASSOCIATIONS

On the basis of the sedimentological and ichnological data, five facies associations (FA1-FA5) are identified from the Middle-Upper Eocene succession in the Fayum area (Table 2.3, Figs. 2.4, 2.7 and 2.12). Table 2.3 summarizes their sedimentological/ichnological characteristics, and presents a brief interpretation of the different facies associations' depositional environments. Ichnogenera are listed in order of decreasing abundance. The Middle Eocene Gehannam Formation is dominated by FA1 and FA2 (Figs. 2.4, 2.5 and 2.6). Facies Association 1 comprises the entire early Upper Eocene Birket Qarun Formation (Figs. 2.4 and 2.5). The late Upper Eocene Qasr El-Sagha Formation consists of FA3, FA4 and FA5 (Figs. 2.8, 2.9, 2.10 and 2.11).

The detailed sedimentary characteristics of the facies associations are listed in Table 2.3, with the most important observations summarized below. Primary sedimentary structures are rare in FA1 and FA2. Facies Association 3 is dominated by wavy-parallel lamination with rare wavy-ripple cross lamination. Facies Association 4 displays large-

TABLE 2.3. Summary of the characteristics of the identified facies associations and their depositional characters.

Facies Association	Character and Occurrence	Sedimentary Structures and Lithological Accessories	Ichnology / Fossil Content	Interpretation
FA1: Quiescent Bay / Gulf Deposits (Figs. 2.4 and 2.5)	<ul style="list-style-type: none"> • Medium- and fine- to very fine-grained bioturbated sandstones. • Comprises ~ 2/3 of Gehannam Fm and the entire Birket Qarun Fm. • Bed set thickness variable (~ 2-3 m in Gehannam; ~ 10 m in Birket Qarun Fm). 	<ul style="list-style-type: none"> • Very rare to rare (upwards) wave-ripple laminations in localized, thin horizons (Gehannam Fm). • Birket Qarun Fm characterized by large ovate to circular sandstone concretions. 	<ul style="list-style-type: none"> • Highly burrowed (BI 5), with high ichnogenera diversities. Trace fossils include: <i>Th</i>, <i>Pl</i>, <i>Op</i>, <i>Te</i>, <i>Sc</i>, <i>As</i>, <i>Rh</i>, and rare <i>Ch</i>, <i>Cy</i>, <i>Ar</i> and <i>Sk</i>. Archetypal <i>Cruziana</i> (Gehannam Fm) to proximal <i>Cruziana</i>-distal <i>Skolithos</i> Ichnofacies (Birket Qarun Fm). • Echinoids (<i>Schizaster</i> sp.), bivalves, gastropods, fish scales, shark teeth, whale skeletons, and allochthonous fossilized tree. 	<ul style="list-style-type: none"> • Distal marine (Gehannam Fm) to proximal marine (Birket Qarun Fm) broad bay or gulf environment, characterized by low energy, normal marine salinity and less restriction. FA1 deposits of Birket Qarun Fm suffers slightly higher energy levels than those of Gehannam Fm.
FA2: Low-Energy Bay-Margin to Supratidal Deposits (Figs. 2.4 and 2.6)	<ul style="list-style-type: none"> • Sandy shales and sandy siltstones/sandstones characterized by low angle cross-lamination through to massive-appearing bedding due to local rhizoturbation. • Interfingers with FA1 through a total thickness of 10 m. • Supratidal component caps the Gehannam Fm, with a thin (0.3 m -1m) subaerial unit. 	<ul style="list-style-type: none"> • Fissile, gypsiferous, and slightly ferruginous shale. • Abundant gypsum-filled joints, with very rare wave ripple and low-angle cross-lamination at the contact between the shale and siltstone facies. • Massive appearing upwards. 	<ul style="list-style-type: none"> • Sandy shale facies is weakly bioturbated (BI 0-2) and has low ichnogenera diversity. Upwards, rare <i>Te</i> and <i>Pl</i> are present. Bioturbation intensity (BI 0-3) and ichnogenera diversity of the sandy siltstone increase upward. The lower part contains rare to common <i>Te</i>. Upwards, trace fossils include: <i>Ps</i>, <i>Te</i>, <i>Th</i> and <i>Pl</i>. • Bioturbation increases upwards (BI 3). This is accompanied by the occurrence of rhizoliths, terrestrial arthropod burrows, <i>Op</i>, <i>Th</i>, <i>Sk</i>, <i>Pl</i>, <i>Ps</i>, and rare <i>Te</i>. • A firmground suite of the <i>Glossifungites</i> Ichnofacies occurs at the top of rhizolith-bearing sandstone locally. • Fossils abundant upwards, including whale-bone fragments, shark teeth, fish remains, and molluscan and crustacean fragments. 	<ul style="list-style-type: none"> • Physico-chemically stressed, quiescent sedimentation (low depositional energy), under fluctuating salinity stressed conditions along a bay-margin setting (i.e., shallow water). • Upwards, grades into intertidal and marginal-marine swamp deposits, probably along sheltered shorelines in tropical to subtropical coastal-bay margin environments. • The presence of a rooted (supratidal) complex horizon, capped by the ichnological suites of <i>Glossifungites</i> Ichnofacies suggests the presence of an amalgamated FS/SB surface.

TABLE 2.3. Continued.

Description	Character and Occurrence	Sedimentary Structures and Lithological Accessories	Ichnology / Fossil Content	Interpretation
FA3: Lagoonal / Low-Energy Brackish Bay Deposits (Figs. 2.4, 2.7 and 2.8)	<ul style="list-style-type: none"> Carbonaceous sandy shales interbedded with siltstones. Characterize the parasequences of Umm Rigl and Temple members. <p>Thickness varies between 0.3 and 5 m.</p>	<ul style="list-style-type: none"> Gypsiferous shales, coarsening upwards into sandy siltstones. Rare calccrete horizons are locally observed. Very rare wavy bedding and cross laminations. 	<ul style="list-style-type: none"> The weak bioturbation intensities (BI 0-3) and the low ichnogenera diversities increase upward. Trace fossil suites include <i>Sk</i>, <i>Te</i>, <i>Mo</i>, <i>Di</i>, <i>Pl</i>, and <i>Ps</i>, corresponding to an impoverished and distal expression of the distal <i>Skolithos</i> Ichnofacies. Muddier part has carbonaceous materials, while upper sandier part has rare thin-shelled bivalves. 	<ul style="list-style-type: none"> Marginal marine lagoonal-bay coastal waterways, partially restricted, relatively quiescent, with fluctuating and stressed salinities in an arid to semi-arid climate (tropical to subtropical).
FA4: Distributary Channel Deposits (Figs. 2.7 and 2.9)	<ul style="list-style-type: none"> Fine- to medium-grained, white sandstones, interbedded with mudstones. Forms a prominent cliff along the Qasr El-Sagha escarpment, typically overlying FA3 and underlying FA5. Total thickness varies between 30 and 35 m. 	<ul style="list-style-type: none"> Fining-upward channels, with unidirectional (N and NNW) lateral migration. Large-scale inclined stratification (IS) and inclined heterolithic stratification (IHS). Sedimentary rhythmites, tidal bundles, mudstone drapes, sigmoidal bedding, wavy and flaser bedding, and small-scale planar tabular- and trough cross-bedding common in association with the lower parts of channel deposits. 	<ul style="list-style-type: none"> Locally abundant <i>Sk</i> and <i>Pl</i>, with rare <i>Ar</i>, <i>Pr</i>, and rhizoliths. The autocyclic boundaries between the superposed channels are locally demarcated by firmground trace fossil suites attributed to the <i>Glossifungites</i> Ichnofacies (composed mainly of <i>Th</i>, rare <i>Sk</i>, and <i>Pa</i>). Rarely observed fossils, with locally small bivalves and gastropods, carbonaceous detritus, and rare terrestrial vertebrate bone fragments. 	<ul style="list-style-type: none"> Deltaic distributary-channel complexes. The depositional characters range from fluvial and estuarine point bars (e.g., IS and IHS, carbonaceous detritus and terrestrial vertebrate bone fragments) to tidal influences (e.g., tidal bundles, mudstone drapes, and sigmoidal bedding) and marine to brackish-marine expressions (e.g., <i>Glossifungites</i> Ichnofacies).

TABLE 2.3. Continued.

Description	Character and Occurrence	Sedimentary Structures and Lithological Accessories	Ichnology / Fossil Content	Interpretation
FA5: Estuarine Channel Deposits (Figs. 2.7, 2.10 and 2.11)	<ul style="list-style-type: none"> Weakly bioturbated sandstones / mudstones interbedded with minor coquinas. Three to four superimposed estuarine channels form the upper part of Dir Abu-Lifa Member, Qasr El-Sagha Fm. Overlie FA4 and abruptly pass into the overlying Oligocene Gebel-Qatrani Formation. Total thickness varies between 25 and 40 m. 	<ul style="list-style-type: none"> The lower estuary white clean sandstone deposits (positioned in the upper estuarine channel; channel III) are characterized by large-scale planar-tabular cross-bedding, and local small-scale sigmoidal bedding and trough cross-bedding. Paucity of physical sedimentary structures defines the distal middle estuary (green sandstone), proximal middle estuary/upper estuary (mudstone/siltstone/sandstone) deposits (found in channels I through III). Locally preserved IHS and well-developed gypsum veins are reported upward in channel III and within channel II, respectively. 	<ul style="list-style-type: none"> Lower-estuary deposits display weak, locally moderate, bioturbation intensities (BI 0-3) and low ichnofossil diversities. Trace fossils include: <i>Sk</i>, <i>Pl</i>, <i>Op</i>, <i>Ps</i>, <i>Ter</i>, and local rhizoliths, representing restricted <i>Skolithos-Psilonichnus</i> Ichnofacies. Distal middle estuary green sandstone is moderately to highly bioturbated (BI 3-4) with low diversity (a monospecific suite of <i>Th</i>, and rare <i>Ps</i> and <i>Te</i>). Proximal middle estuary/upper estuary deposits show weak bioturbation intensities (BI 0-1), and very low diversities of ichnogenera. Channel boundaries are demarcated by firmground ichnological suites attributed to the <i>Glossifungites</i> Ichnofacies, marking the TSE2 surfaces (Table 4). Green sandstone contains marine shells, fish and crustacean remains, and dispersed wood-fragments. Proximal middle-upper estuary deposits are poor in body fossils, with local rhizoliths in the muddy intervals. 	<ul style="list-style-type: none"> FA5 is interpreted as a complex of estuarine depositional environments comprising the lower estuary or estuarine mouth (e.g., cross-bedded sandstone), distal middle estuary or central bay (e.g., green sandstone), and proximal middle estuary (central bay) to upper estuarine (e.g., mudstone, sandstone/gypsum, and IHS).

scale inclined stratification (IS) and inclined heterolithic stratification (IHS). These are associated with sedimentary rhythmites, tidal bundles, mudstone drapes, and sigmoidal bedding, as well as wavy and flaser bedding. Basal units of FA4 may also contain small-scale planar-tabular and trough cross-bedding. Facies Association 5 contains large-scale planar-tabular cross-bedding, and small-scale sigmoidal and trough cross-bedding that both of which are interstratified with bioturbated sediments.

The most conspicuous aspects of the biological characteristics are summarized below, and detailed in Table 2.3. Facies Association 1 is thoroughly bioturbated (BI 5), and displays high ichnogenic diversities (11 ichnogenera; Table 2.3). The trace fossil suite represents the archetypal *Cruziana* Ichnofacies in the Gehannam Formation and a proximal expression of the *Cruziana* through distal expression of the *Skolithos* Ichnofacies in the Birket Qarun Formation. Also observed is an impressive array of skeletal material including echinoids, bivalves, gastropods, fish scales, sharks' teeth, whale skeletons, and an allochthonous fossilized tree trunk. Lower parts of FA2 are weakly bioturbated (BI 0-2) and have low ichnogenic diversities (2 common trace fossils observed). Upwards, FA2 displays increases in bioturbation intensity (BI 0 to 3) with increases in ichnogenic diversity (6 ichnogenera). The upwards increase in bioturbation is accompanied by the occurrence of rhizoliths and terrestrial arthropod burrows. Fossils of FA2 include abundant whale-bone fragments, sharks' teeth, and fish remains, in addition to mollusk and crustacean fragments. Facies Association 3 displays low bioturbation intensities (BI 0-3) and reduced ichnogenic diversities that increase upward (2 to 6 ichnogenera). The trace-fossil suite is ascribed to an impoverished expression of the distal *Skolithos* Ichnofacies. Muddy units of FA3 have abundant carbonaceous detritus, whereas the (upper) sandy parts contain rare, thin-shelled mollusks. Facies Association 4 contains very sporadically distributed trace fossils, with some levels barren, whereas others contain locally abundant trace fossils. The diversity of trace fossils is very low (3 ichnogenera observed). The boundaries between the

inclined bedsets are locally demarcated by firmground trace fossil suites attributed to the *Glossifungites* Ichnofacies. Facies Association 4 contains rare, small bivalves and gastropods, carbonaceous detritus, and rare terrestrial vertebrate bone fragments. Facies Association 5 displays low degrees of bioturbation (BI 0 to 3) and low ichnogenic diversities (up to 5 ichnogenera observed). Trace fossils are distributed sporadically and many levels are unburrowed. *Glossifungites* Ichnofacies-demarcated discontinuities are present at several levels. Although most levels have rare trace fossils, one horizon also contains marine bivalves, fish and crustacean remains, and dispersed wood fragments (Table 2.3, Figs. 2.11B-E).

Two types of transgressive surfaces of erosion (TSE) were observed in the field. Their characteristics are listed in Table 2.4. In short, the transgressive surface of erosion (Type 1 TSE) is characterized by the presence of an *Ostrea*-dominated shell lag and is completely bioturbated (BI 5 to 6) above the discontinuity. Transgressive surface of erosion (Type 2 TSE) dominantly possesses rip-up clasts, displays sporadically distributed bioturbation in facies lying above the discontinuity, and locally displays mudstone or interbedded sand- and mud-stone above the contact. Both Type 1 TSE and Type 2 TSE surfaces are demarcated by firmground suites attributed to the *Glossifungites* Ichnofacies. The Gehannam and Birket Qarun formations are separated by a coplanar Type 1 TSE/SB surface. Upwards in the Birket Qarun, several ravinement surfaces (Type 1 TSE) can be observed: these define several parasequences that characteristically thin upwards. Parasequences within the stratigraphically higher Qasr El Sagha Formation are bounded by Type 2 TSE.

TABLE 2.4. Summary of the characteristics of transgressively emplaced erosional discontinuities.

Discontinuity	Occurrence & Thickness	Sedimentology	Ichology / Fossil Content	Interpretation
Type 1 TSE (Figs. 2.4, 2.5E and 2.12)	<ul style="list-style-type: none"> Occurs beneath fine-grained coquina sandstones and discontinuous coquina beds. 	<ul style="list-style-type: none"> Commonly possesses a shell-lag deposit. No observed physical sedimentary structures (locally bioturbated to massive appearing). 	<ul style="list-style-type: none"> Weak to high bioturbation intensities (BI 0-5). Low to moderate diversities of ichnogenera. Trace fossils include: <i>Ps</i>, <i>Sk</i>, <i>Pl</i>, and rare <i>Te</i>, representing a distal expression of the <i>Skolithos</i> Ichnofacies. Underlain by firmground ichnological suites corresponding to the <i>Glossifungites</i> Ichnofacies. Bivalves (<i>Ostrea</i> sp.), gastropods (<i>Turritella</i> sp.), foraminifers (<i>Nummulites</i> sp.), echinoids and fragmented vertebrate bones. 	<ul style="list-style-type: none"> Wave ravinement accompanying transgression of an open-bay margin.
Type 2 TSE (Figs. 2.7, 2.8, 2.10, 2.11 and 2.12)	<ul style="list-style-type: none"> Occurs beneath coquina sandstones and coquina beds. Form the bases of the lagoonal parasequences and coincide with the bases of the estuarine channels. 	<ul style="list-style-type: none"> Erosive surface demarcated by rip-up clasts, coal and sulfur fragments. Local occurrences of wavy and flaser bedding. Sedimentary rhythmites locally observed Rarely cross-laminated. 	<ul style="list-style-type: none"> Weak to moderate bioturbation intensities (BI 0-3). A mixed trace fossil assemblage includes: <i>Ps</i>, <i>Sk</i>, <i>Pl</i>, with rare <i>Te</i> and <i>Th</i> attributable to a preservational expression of in situ fluctuating energy. Underlain by firmground ichnological suites corresponding to the <i>Glossifungites</i> Ichnofacies. Bivalves (<i>Carolia plucnoides</i>), the gastropods (<i>Turritella</i> sp.), large foraminifers, echinoids, abraded bones and teeth of vertebrates, and sporadic carbonized wood fragments. 	<ul style="list-style-type: none"> Wave and tidal ravinement accompanying transgression of shallow-water (lagoonal) deposits.

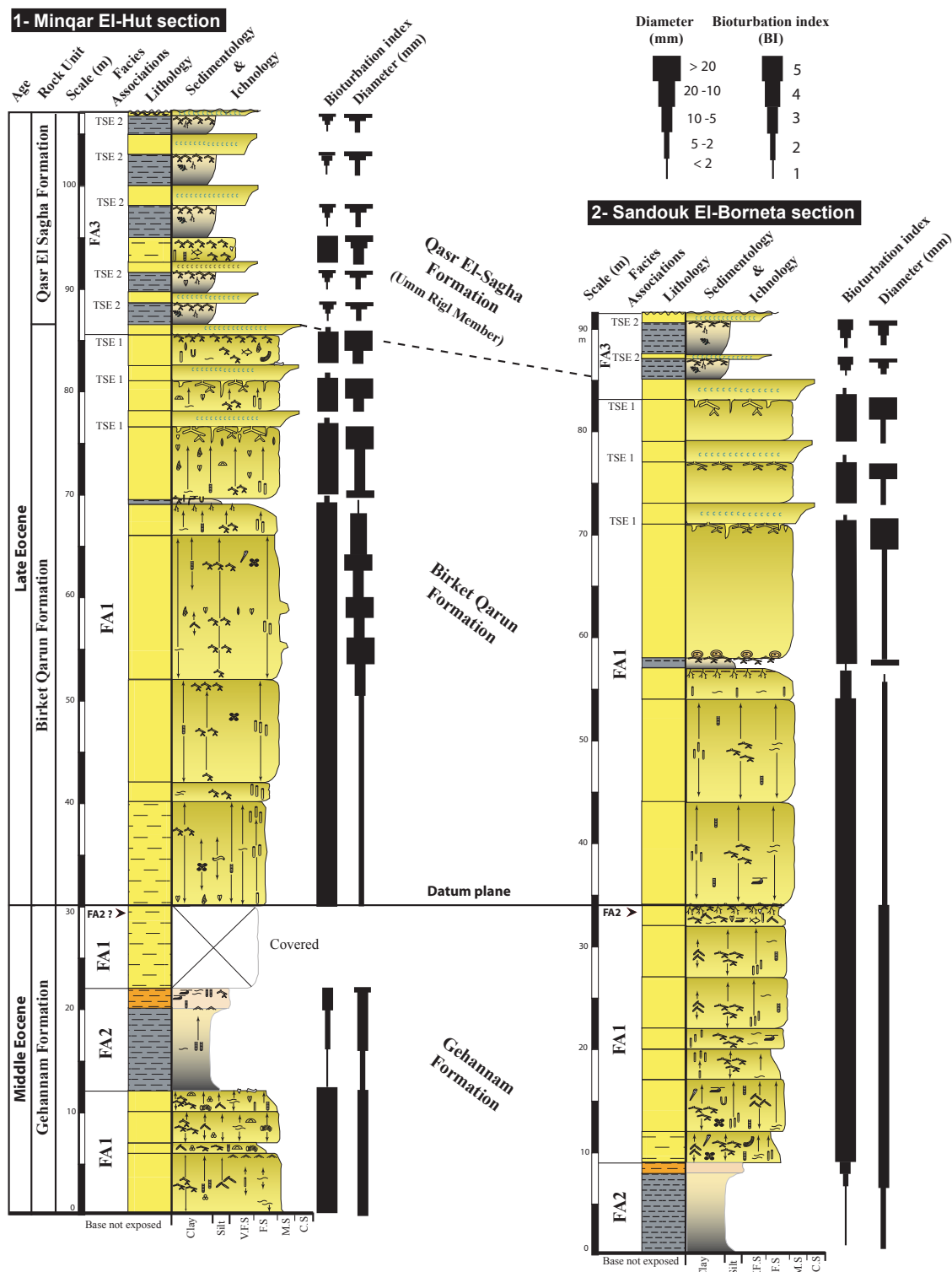
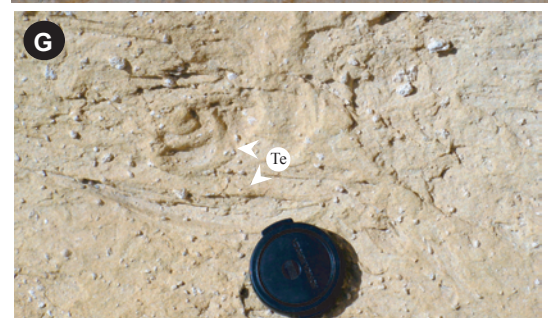
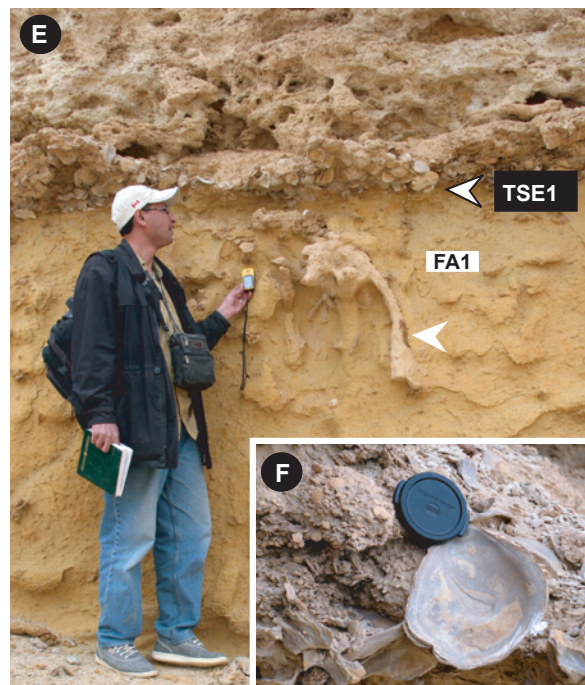
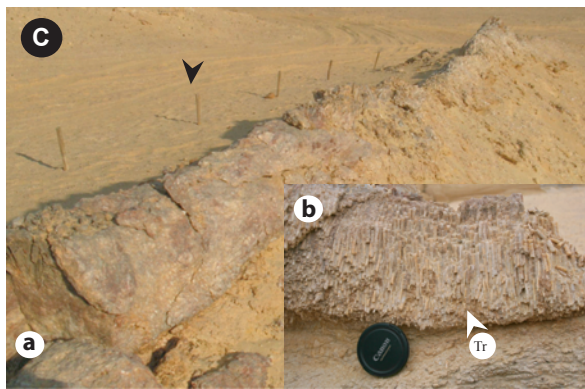
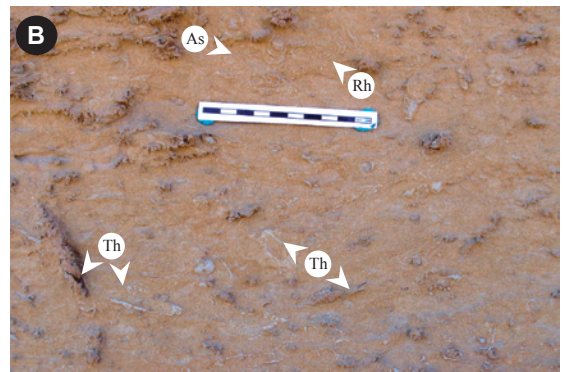
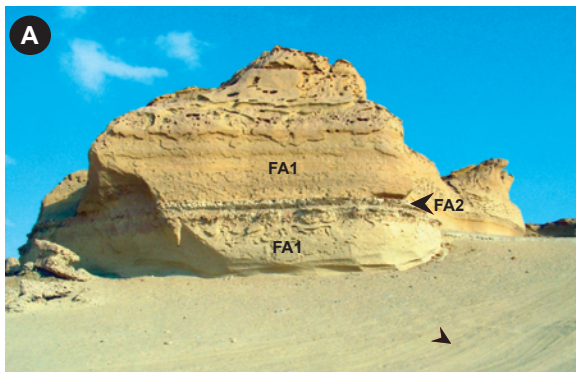


FIGURE 2.4. Correlation chart of the Middle-Upper Eocene succession in Minqar El-Hut and Sandouk El-Borneta sections in the area of Wadi El-Hitan (Whale Valley), SW Fayum.

FIGURE 2.5. Selected photographs of FA1 from Gehannam and Birket Qarun formations in the area of Wadi El-Hitan. **A-** General view of the outcrop between Sandouk El-Borneta and Minqar El-Hut, showing FA1 truncated by FA2. Black arrow points to a tire track for scale. **B-** Archetypal *Cruziana* Ichnofacies of the FA1, Sandouk El-Borneta section, dominated by *Thalassinoides suevicus* (Th), *Asterosoma* isp. (As) and *Rhizocorallium irregulare* (Rh). **C-** (a): Allochthonous tree trunk, recorded from the area between Sandouk El-Borneta and Minqar El-Hut (black arrow points to a tire track for scale). (b): Close-up view in (a) shows abundant borings of *Teredolites longissimus* (Tr), which are completely-filled with celestite and barite mineralization. **D-** Complex burrow-mottled ichnofabric of FA1 in Sandouk El-Borneta section. (Lens cap is 4 cm in diameter). **E-** General view of the upper parasequence of FA1 in Sandouk El-Borneta section; FA1 is demarcated by a large diameter *Thalassinoides paradoxicus* (Th) suite, typical of the *Glossifungites* Ichnofacies, and truncated upward by a well-developed coquina bed (white arrow) marking a Type 1 TSE surface. **F-** Close-up of the coquina bed in (E), illustrating oysters (mostly in-articulated) and abundant large foraminifers (e.g., *Nummulites* sp.). **G-** Monospecific suite of *Teichichnus rectus* (Te) recorded from FA1 in Sandouk El-Borneta. **H-** A complete, well-preserved whale skeleton (*Basilosaurus isis*) in FA1. A tire track to the right, ~20 m away from the site, for scale.



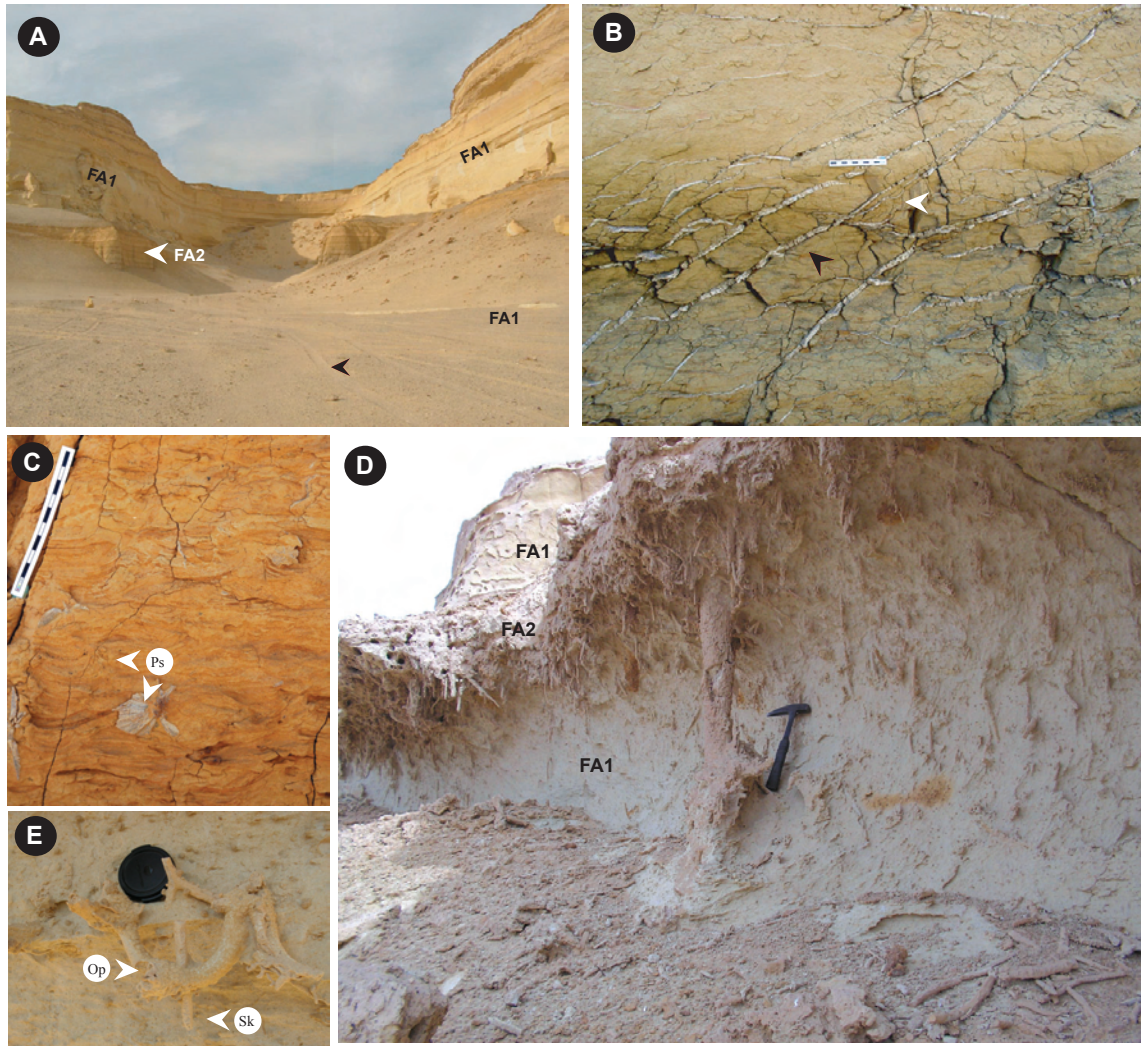


FIGURE 2.6. Selected lithofacies and ichnofacies of the bay-margin settings of FA2 from the Gehannam Formation in the area of Wadi El-Hitan. **A-** General view in Minqar El-Hut section, showing the FA1, which is interbedded with the slope-forming (forming cliffs locally) FA2. Black arrow points to a tire track for scale. **B-** Close-up view of FA2 in (A), showing the contact between the dark grey-green sandy shale below and the upper brownish-yellow siltstone above. The boundary is distinguished by ripple and low-angle cross-lamination (white arrow), as well as abundant diagonal and horizontal gypsum streaks (black arrow). Scale is 10 cm. **C-** Monospecific ichnofabric of abundant *Psilonichnus upsilon* (Ps) in the sandy siltstones of FA2. **D-** Complex ichnofabric of the swamp/supratidal rhizoliths-bearing sandstone facies of FA2, marking a FS/SB that separates FA2 (Gehannam Fm) below and the FA1 (Birket Qarun Fm) above. **E-** Close-up view of (D), showing *Skolithos linearis* (Sk) cross-cut *Ophiomorpha nodosa* (Op).

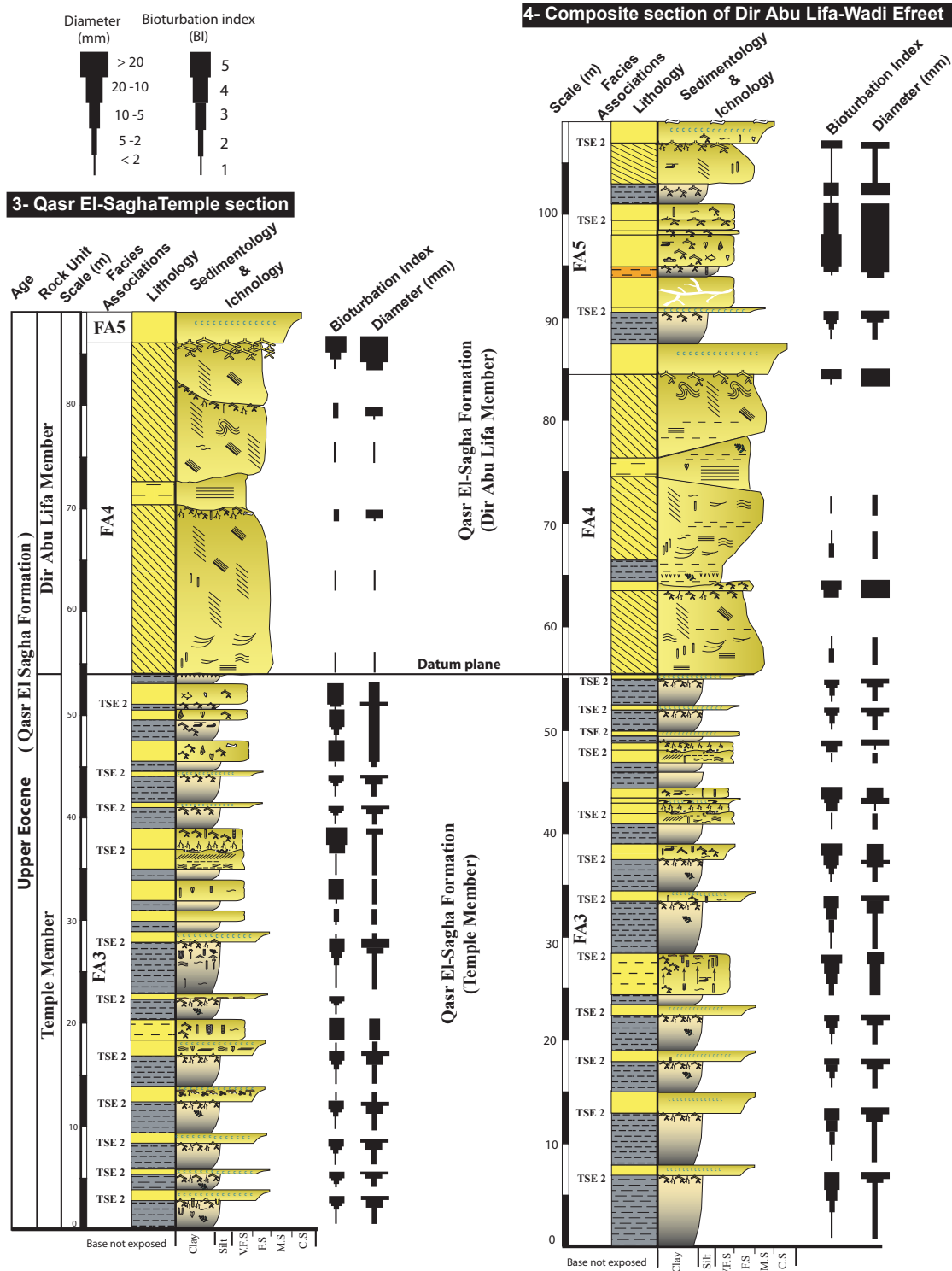


FIGURE 2.7. Correlation chart of the Upper Eocene Qasr El-Sagha Formation for the two composite sections; Qasr El-Sagha Temple and Dir Abu Lifa – Wadi Efreit in the area of Qasr El-Sagha, NE Fayum.

FIGURE 2.8. Selected lithofacies, ichnofacies and sedimentary structures of FA3 from the Temple Member, in the area of Qasr El-Sagha. **A-** Panoramic view shows the sequence boundary (SB) surface between the prograding parasequences of FA3 (black arrows) and FA4. In turn, FA4 is overlain by the transgressive surface (TS) and the FA5 (three small buildings to the lower right for scale). **B-** A contact between two parasequences in the Dir Abu Lifa - Wadi Efrete section. The sandy shale (Sh) of the lower parasequence is demarcated mainly by *Thalassinoides paradoxicus* (Th), attributed to the *Glossifungites* Ichnofacies. The overlying parasequence starts with a Type 2 TSE surface (black line) with lag deposits (L), and is overlain by interbedded sandstone (Ss) and coquina (C). **C-** Thickened sandstone with rhythmites (A) are truncated by an undulatory Type 2 TSE surface (white arrow), containing coal clasts and sulphur fragments, Temple section. This is overlain by root-bearing sandstone (B) and, in turn, by a burrowed sandstone (C). **D-** Close-up of the sandstone stratum (A) (described in C), showing wavy and flaser bedding. **E-** The contact between two parasequences in the Temple section, showing shale (A) grading upward to siltstone (B), with convolute bedding (white arrow), which is demarcated by firmground suites of the *Glossifungites* Ichnofacies and white ovate calcrete (Calc), marking a Type 2 TSE surface (white line), associated with sandstone/coquina (C). **F-** Close-up view of the sandy shale facies of FA3, showing fissility, gypsum streaks (white arrow), *Planolites montanus* (Pl), in addition to the rhizoliths and disseminated carbonaceous detritus (black arrow). **G-** Complex ichnofabric of FA3 in the Temple section, dominated by *Diplocraterion* isp. (Di), *Monocraterion* isp. (Mo), *Planolites* isp. (Pl), and *Skolithos* isp. (Sk), with convolute bedding upward (black arrow).

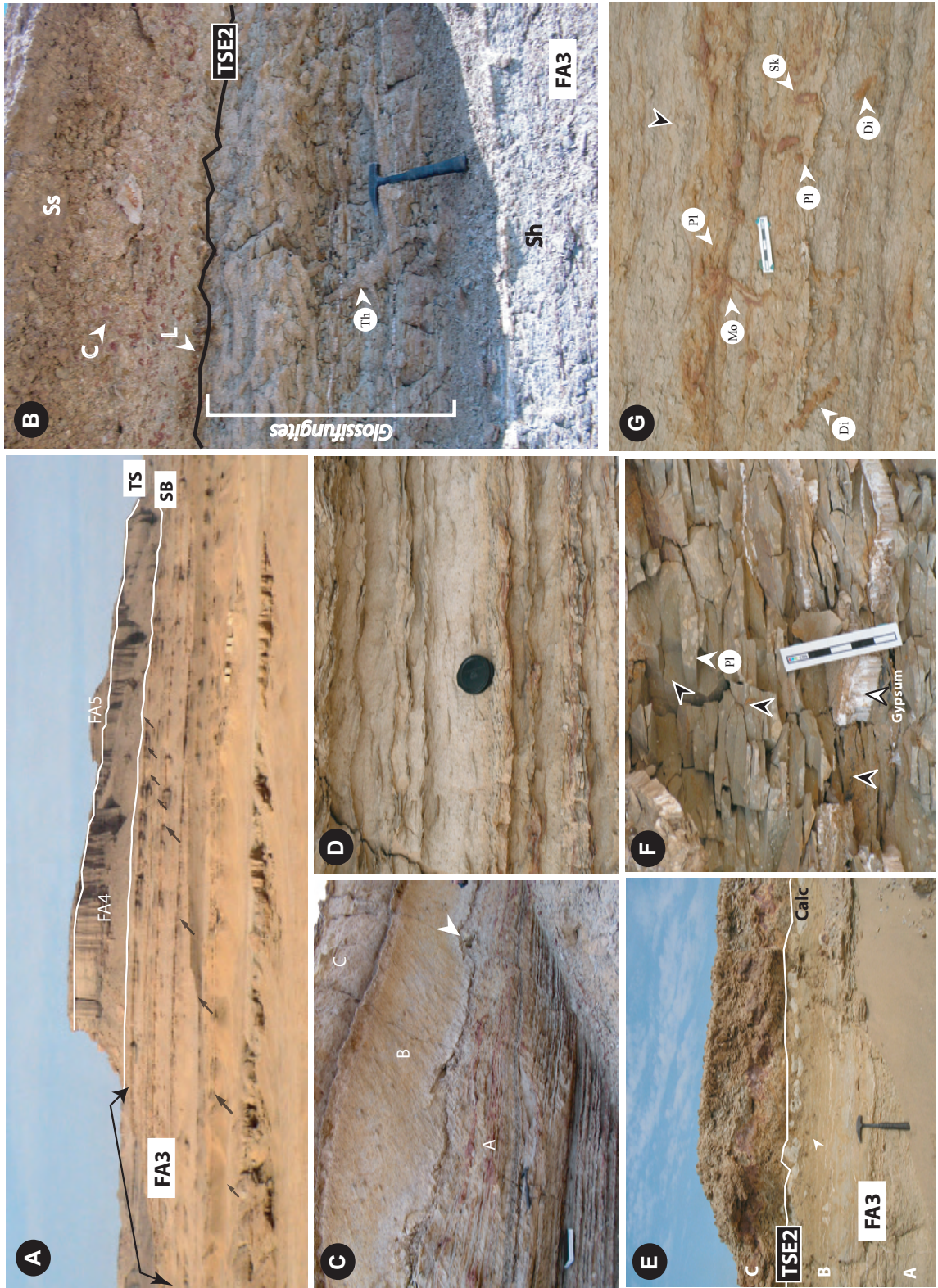
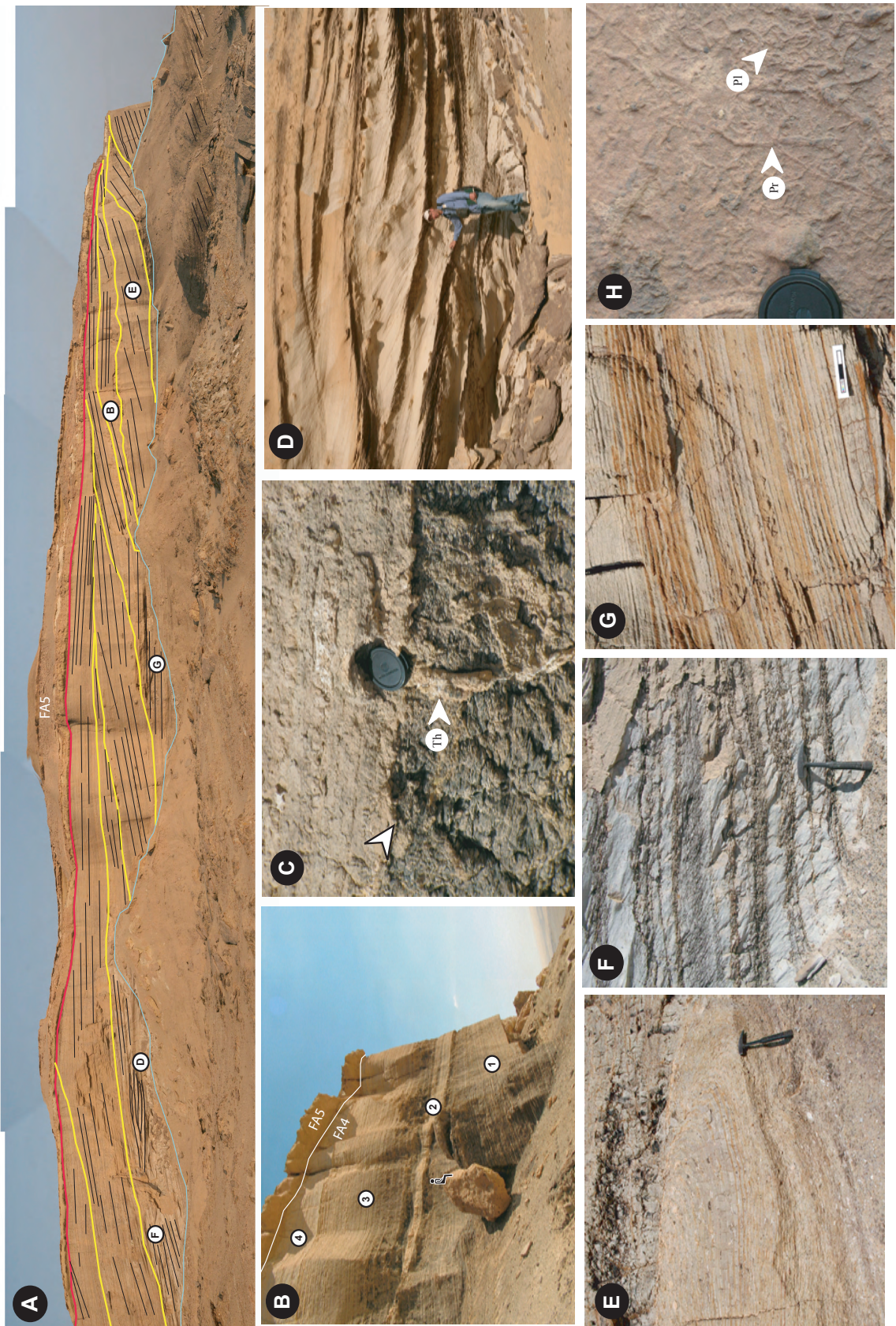


FIGURE 2.9. Lithofacies, ichnofacies and sedimentary structures of the deltaic distributary channels of FA4, Dir Abu Lifa Member in the area of Qasr El-Sagha. **A-** Panoramic view of the distributary channels of the FA4, vertical cliff behind Qasr El-Sagha temple (with a height of ~32 m from the foreground). **B-** Close-up view of (A), showing four superimposed and fining-upward distributary channels that have migrated laterally in the N and NNW direction. This channel succession is capped by a Type 2 TSE (white line), which separates FA4 below from FA5 above. The cartoon figure sits on the fallen boulder for scale. **C-** Close-up view of (A), showing the scour surface (black-framed white arrow) between two superimposed channels, associated with rhizoliths and *Thalassinoides* (Th). **D-** Close-up view of (A), showing the large-sized sigmoidal cross-bedding. **E-** Close-up view of (A), showing a relatively large-scale slump and convolute deformational structures. **F-** Close-up view of (A), showing tidal rhythmites and mudstone-drape structures. **G-** Close-up view of (A), showing the well-developed tidal bundles. **H-** Ichnofabric of FA4, dominated by *Planolites montanus* (Pl) and *Protovirgularia* isp. (Pr).



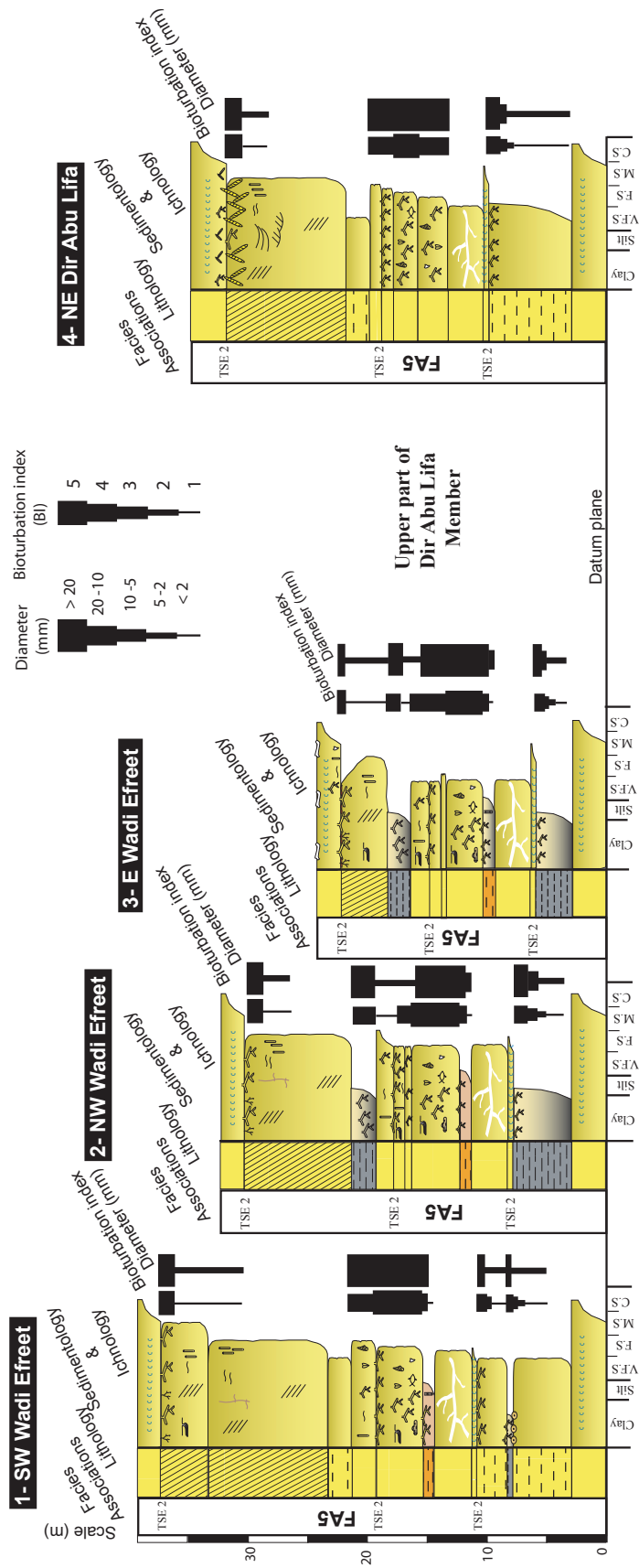
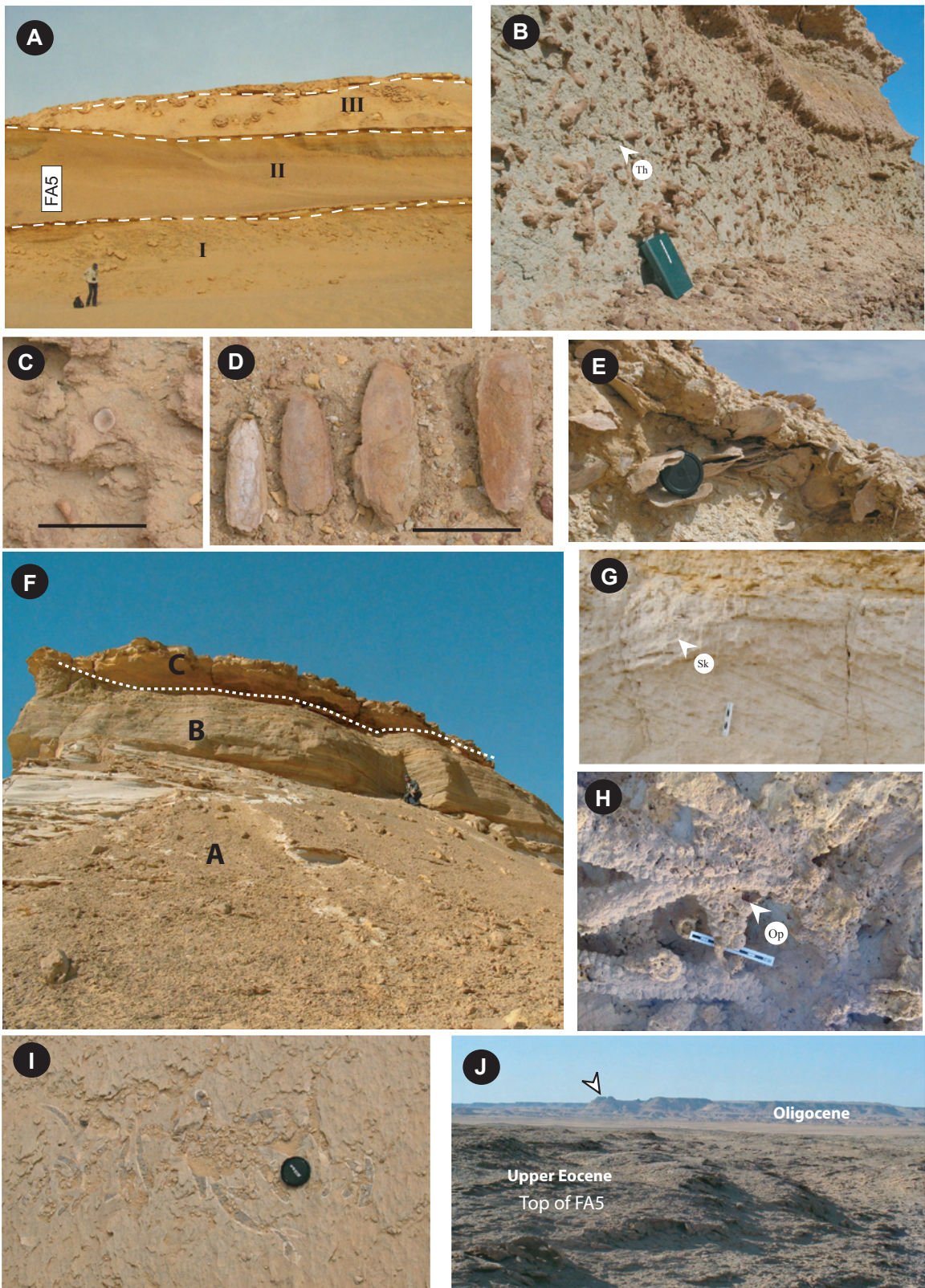


FIGURE 2.10. Correlation chart of the upper part of Dir Abu Lifa Member (Qasr El-Sagha Formation) exposed in the area between West Wadi Efreet and East Dir Abu Lifa (not to scale horizontally).

FIGURE 2.11. Selected lithofacies, biofacies, ichnofacies and sedimentary structures of the estuarine channels (FA 5) forming the upper part of Dir Abu Lifa Member in the area of Qasr El-Sagha. **A-** The three main successive estuarine channels (I-III) of FA5, Wadi Efreet. **B-** The green sandstone cliff crops out NE of the Dir Abu Lifa section, and shows abundant resistively weathering (ferruginous) *Thalassinoide suevicus* (Th). **C-** Ray tooth from the same locality as in (B). **D-** Ferruginous moulds of articulated clams from the same locality as in (B). Bar scale is 4 cm in C and D. **E-** Close-up of the transgressive sandstone / coquina, showing *Carolia plucnoides* and small *Turritella* sp. (lens cap is 4cm in diameter). **F-** Cross-bedded sandstone (A) underlies the local IHS (B) that is truncated upward by a Type 2 TSE surface (white dashed-line), associated with the transgressive deposits (C), SW of Wadi Efreet. **G-** Close-up view of (F), showing N- and NNE-trending cross-bedding that is locally burrowed by abundant *Skolithos linearis* (Sk). **H-** Monospecific suite of well-preserved *Ophiomorpha nodosa* (Op), demarcating the top of a cross-bedded sandstone, NE Dir Abu Lifa section. **I-** The mammalian vertebrate Sirenians (dugongs) skeleton on the transgressive deposits (NE Wadi Efreet section). **J-** The basal transgressive facies, NE of Dir Abu Lifa, forms the top surface of the plateau, which extends to the foot of the high hills of the Oligocene Gebel Qatrani escarpment (arrow).



INTERPRETATION

The five facies associations (FA1-FA5) show a gradual shallowing upwards (Fig. 2.12), which is discussed below in detail. In general, the vertical succession represents sedimentation in a low-energy, distal, broad open-marine bay or gulf environment (Gehannam Formation: FA1) that shoaled to bay-margin setting (FA2). The overlying Birket Qarun Formation is dominated by FA1 and indicates a continuous aggradation of quiescent (marine) bay fill. The base of the Qasr El-Sagha Formation is dominantly muddy, and represents shallow lagoonal deposits. Large deltaic distributary channels (FA4) cut into these lagoonal strata (Fig. 2.8), which are, in turn, cut by transgressive (or abandonment phase) estuarine channel (FA5) successions (Figs. 2.7, 2.8, 2.10 and 2.12).

GEHANNAM FORMATION

The Middle Eocene Gehannam Formation comprises the bioturbated sandstones of FA1, and bedded mudstones and rhizolith-bearing sandstones of FA2. Interpretations of Gehannam Formation deposition are controversial. Neritic to epibathyal (e.g., Elewa et al., 1998), open-marine offshore (e.g., Gingerich, 1992), and shallow-marine littoral to outer neritic (e.g., Blondeau et al., 1984; Bassiouni et al., 1984) environments have been suggested. However, the presence of ichnological suites attributable to the archetypal *Cruziana* Ichnofacies (Fig. 2.5B), thoroughly bioturbated very fine-grained sandstones, and very rare preservation of primary physical sedimentary structures show that the lower Gehannam Formation was characterized by low sedimentation rates, in a minimally physico-chemically stressed, quiescent environment. Based on these parameters, it is most likely that the lower 2/3 of the Gehannam Formation (FA1) was deposited in a distal, open-marine bay or gulf that was characterized by low depositional energy. The absence of notable vertical facies variation (typically associated with offshore/shoreface transition), and the intercalated transition of FA1 into the bay-margin deposits of FA2 (described below) suggest that, although dominated by low-energy conditions, FA1

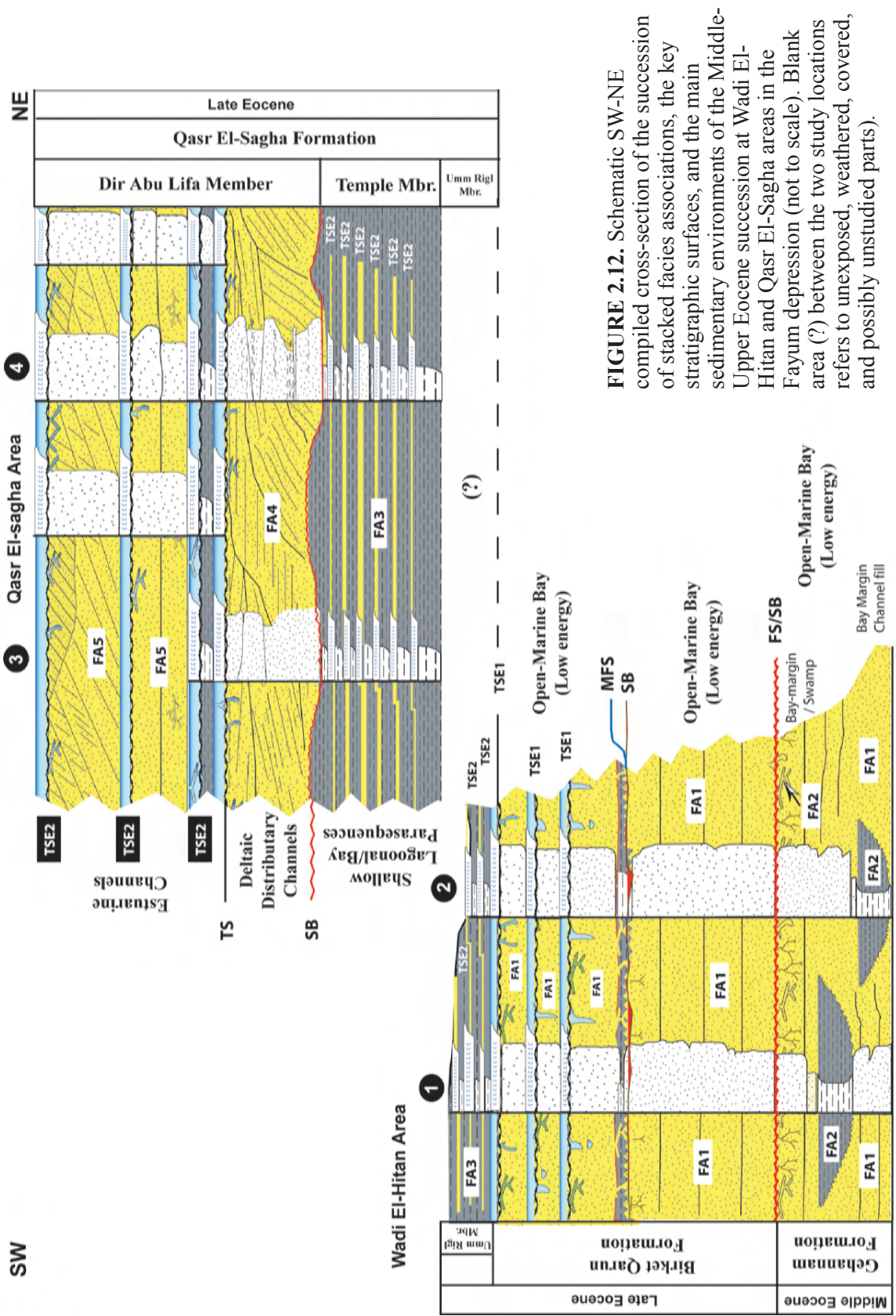


FIGURE 2.12. Schematic SW-NE compiled cross-section of the succession of stacked facies associations, the key stratigraphic surfaces, and the main sedimentary environments of the Middle-Upper Eocene succession at Wadi El-Hitan and Qasr El-Sagha areas in the Fayum depression (not to scale). Blank area (?) between the two study locations refers to unexposed, weathered, covered, and possibly unstudied parts).

accumulated in relatively shallow waters. The presence of abundant whale bones (locally semi-articulated), planktonic foraminifera and coccoliths, with the teredinid-bored allochthonous tree trunk (Table 2.3) further attest to an open marine bay setting for FA1.

Upwards, the Gehannam Formation is locally represented by FA2. The sandy shale lithology of FA2, with weak bioturbation and low ichnological diversities, reflects moderate sedimentation rates in a physico-chemically stressed sedimentary environment (Gingras et al., 2007; MacEachern et al., 2007). The general absence of wave-generated sedimentary structures suggests deposition in a quiescent bay-margin setting. However, the presence of gypsum streaks (Fig. 2.6B) and some carbonaceous detritus is attributed to sedimentation and evaporation in a near-shore setting. The trace-fossil suite of FA2 contains a mixture of inferred suspension-feeding and deposit-feeding structures that do not represent an archetypal ichnofacies, and may be attributable to bioturbation in a tidal-flat setting (Gingras et al., 1999). Taken together, FA2 is interpreted to indicate sedimentation along a bay margin, perhaps as shallow, low-energy channel-fill deposits, or accumulation within intertidal to supratidal environments (e.g., Gingras et al., 2002a; Dashtgard and Gingras, 2005; Nesbitt and Campbell, 2006). An abrupt shallowing-upward of relative sea level is reflected by the presence of marginal-marine swamp/supratidal deposits (FA2), which cap the Gehannam Formation. The presence of a root-bearing (supratidal) complex paleoecologic horizon, crosscut by Type 1 TSE, suggests that the contact between the Gehannam Formation and the Birket Qarun Formation represents an amalgamated FS/SB (Figs. 2.5A, 2.6D and 2.12). The FS/SB coplanar surface defines a facies dislocation from the bay-margin (swampy/supratidal) deposits of the Middle-Eocene Gehannam Formation (FA2), below, to low-energy open-bay sandstones (FA1) of the Upper Eocene Birket Qarun Formation, above. This FS/SB marks a major discontinuity between Middle (Bartonian) and Late (Priabonian) Eocene, and can be correlated with the regional Bart2/Pr1 sequence boundary of Hardenbol et al. (1998) (Fig. 2.13).

BIRKET QARUN FORMATION

The planktonic foraminifers in the Birket Qarun Formation (e.g., Abdou and Abdel-Kireem, 1975; Strougo and Haggag, 1984; Haggag and Bolli, 1995, 1996), as well as the nannoplanktonic *Chiasmolithus oamaruensis* Zone “NP18” (Zalat, 1995) indicate a Late Eocene age. The Birket Qarun Formation has been interpreted to represent winnowed platform-edge sands (e.g., Elewa et al., 1998), with *Nummulites* banks developed as bars in restricted shallow lagoons (e.g., Swedan et al., 1982). A setting of an offshore barrier-bar complex, paralleling the shoreline of the ancient Tethys, was suggested by Gingerich (1992).

However, the diverse suites of the *Cruziana* Ichnofacies and the presence of a diverse marine fauna (Table 2.3) suggest that the Birket Qarun Formation accumulated in less restricted conditions than previously suggested. As with the lower part of the Gehannam Formation, the Birket Qarun Formation represents proximal broad bay or sheltered gulf environments characterized by low hydraulic energy. The lower two-thirds of the Birket Qarun Formation are characterized by thoroughly bioturbated (Figs. 2.5D and G) fine-grained sandstones (FA1), containing trace fossil suites attributed to proximal expressions of the *Cruziana* Ichnofacies. Some ichnofossil suites are more characteristic of distal expressions of the *Skolithos* Ichnofacies. Low sedimentation rates and a generally low-energy wave climate permitted the broad bay to become thoroughly bioturbated and led to the destruction of all physical sedimentary structures. The middle part of the Birket Qarun Formation contains a dark grey shale bed (Fig. 2.4). This bed varies in thickness from a few decimeters to 3m. It is described as “black shale” and is interpreted to contain a MFS, separating a transgressive/regressive succession at Wadi Hitan (Dolson et al., 2002). The sporadic presence of a TSE1 shows that this horizon marks a local coplanar FS/SB (Fig. 2.12). The FS/SB indicates a facies dislocation from the lower, thickly bedded sandstone (FA1) to either a regional transgressive shale marker bed, which is locally absent due to erosion, or the upper parasequences of the Upper

Eocene Birket Qarun Formation. This surface exhibits evidence of subaerial exposure, such as the occurrence of varicolored alluviated sandstone below the undulatory erosive surface, the local abundance of rhizoliths (Fig. 2.3G), and localized erosion of the dark-grey shale marker bed. This surface can be correlated with the regional Pr2 sequence boundary of Hardenbol et al. (1998) (Fig. 2.13).

The upper third of the Birket Qarun Formation accumulated during a period of rapid relative sea-level change largely attributable to local tectonics (discussed below). Three parasequences are preserved (Figs. 2.4 and 2.12). Each parasequence was initiated with a ravinement (Type 1 TSE) surface. These are best interpreted as transgressive sediments deposited in the higher energy (i.e., shallow) bay-margin setting (Table 2.4, Figs. 2.5E-F). Parasequences are otherwise composed of FA1. The uppermost ravinement surface represents a marker flooding surface (Type 1 TSE; Fig. 2.12) that marks the transition from open-marine bay parasequences of the Birket Qarun Formation to marginal-marine lagoonal parasequences of the Umm Rigl Member of the Qasr El-Sagha Formation.

QASR EL-SAGHA FORMATION

Previous work asserts that the Qasr El-Sagha Formation was deposited in coastal and marginal-marine environments associated with rapid relative sea level fluctuations, active tectonics, and a tropical to subtropical climate (e.g., Beadnell, 1905; Said, 1962; Blondeau et al., 1984). Paleopole and paleolatitude studies indicate that during the Eocene and Oligocene, Africa was south of its present-day position, and was within a tropical to subtropical climate zone (Abd El Dayem and Nabawy, 1999; Lotfy and Van der Voo, 2007). The nannoplanktonic *Isthmolithus recurvus* zone (NP19) is recognized in the Qasr El Sagha Formation, indicating a Late Eocene age (Zalat, 1995, p.239) (Fig. 2.13).

Umm Rigl and Temple Members

The Umm Rigl and Temple members are represented by shallow lagoon/bay parasequences (FA3; Table 2.3). Facies Association 3 can be correlated with Vondra's (1974, p.85-86) Facies 1 (*arenaceous bioclastic carbonate facies*; displaying shoreward migration of subaqueous dunes as offshore bars and barrier beaches) and Facies 2 (*gypsiferous carbonaceous laminated claystone and siltstone facies*; attributed to restricted shallow lagoons along the lee sides of barrier islands). Observed coquina beds, emplaced at Type 2 TSE, are synonymous with the terms "harte bank" of Blanckenhorn (1903), "arenaceous bioclastic facies" of Vondra (1974), and "hard beds" by Gingerich (1992).

The Umm Rigl and Temple members, consisting of FA3, are characterized by several 1-8 m thick parasequences (Figs. 2.7 and 2.8A). The parasequences are bound by Type 2 TSE, which are interpreted to correspond to transgressive tide and wave ravinement, followed by low-energy, shallow-water deposition (Table 2.4, Figs. 2.8B and E). Deposits emplaced on Type 2 TSE thicken upward, with local preservation of well-developed sedimentary structures (e.g., wavy bedding, flaser bedding, rhythmites, and cross-bedding; Figs. 2.8C-D). These are interpreted to record more markedly tide-influenced sedimentation. The uppermost Type 2 TSE is mantled with rip-up clasts, and local coal and sulfur fragments, indicating that the erosional surface was close spatially to the Upper Eocene shoreline and overall progradation extent of the parasequences (Figs. 2.8 and 2.12). These strata are characterized by a reduced intensity of bioturbation, and low-diversity (stressed) ichnological suites containing mixed elements of the *Skolithos* (see Fig. 2.8G) and *Cruziana* Ichnofacies (see FA3; Table 2.3) (e.g., Gingras et al., 2007; MacEachern et al., 2007). Also present are disseminated carbonaceous detritus and plant remains, and abundant fibrous and massive gypsum streaks (Fig. 2.8F). The depositional environment of the Umm Rigl and Temple members is interpreted to reflect marginal-marine lagoonal settings, with locally distributed supratidal marshland. This environment

was quiescent, with fluctuating salinity in an arid to semi-arid climate and tropical to subtropical paleoenvironment. The presence of the firmground suites corresponding to the *Glossifungites* Ichnofacies and local calcretes (Figs. 2.8B and E) on the tops of the Temple Member parasequences is related to iterative, small-scale adjustments of relative sea level.

Dir Abu Lifa Member

The lower part of the Dir Abu Lifa Member is represented by deltaic distributary channels (FA4). Based on the presence of “foresets” with dips less than 5° to the northwest and depositional lengths from 100 to 200 m, Vondra (1974, p.89) interpreted these sediments to have been deposited on the sloping surface of a delta front. The contrasting dip-direction disparity between the giant foresets and the large-scale intrasets led to the Bown and Kraus (1988, p.46-47) assertion that the giant cross-bedded unit is non-deltaic and represents lateral accretion within stream channels. A thin, hummocky cross-stratified sandstone and mudstone composite bedset locally occurs at the base of the laterally accreting channel fills. This has been taken to represent a marine shoreface or wave-influenced delta front that was locally cannibalized by overlying channels (Dolson et al., 2002, p.49).

Our observations show that the Dir Abu Lifa Member is dominated by locally bioturbated, inclined heterolithic stratification (IHS). The IHS consists of sandstone, siltstone and mudstone beds that are intercalated at the cm to dm scale. Locally, the beds are bioturbated predominantly with *Skolithos* and *Planolites*. Although the bioturbation is extremely sporadically distributed, it can generally be observed locally in any of the IHS sets. The style of bioturbation is consistent with that observed in tidally influenced channels at other locales, including the Cretaceous McMurray Formation (Pemberton et al., 1982), Pleistocene tidal bar deposits at Willapa Bay, Washington (Gingras et al., 1999) and modern deposits in the Bay of Fundy (Pearson and Gingras, 2006). Below the

IHS sets are sigmoidal cross-beds that represent channel thalweg deposits under tidal conditions. Moreover, the ichnological suite is typical of facies accumulating in brackish-water channels (see MacEachern and Gingras, 2007 for a thorough discussion). The sedimentary and ichnological criteria are most consistent with sedimentation in deltaic distributary-channel complexes (Table 2.3; Fig. 2.12). The (local) absence of delta-front deposits in the area is not deemed problematic, as deltaic distributary complexes commonly lack fringing delta-front sandstones in cratonic basins settings (e.g., Bhattacharya and Walker, 1992; Olariu and Bhattacharya, 2006). The above interpretation is further based on the following criteria: (1) preferred unidirectional dip of sigmoidal foresets; (2) unidirectional (N and NNW) lateral migration (Figs. 2.9A and B); (3) the presence of fining-upwards units (Fig. 2.7); (4) the presence of abundant carbonaceous detritus; (5) large-scale syn-sedimentary convolute bedding (Fig. 2.9E); and (6) the presence of bone fragments of terrestrial vertebrates. Additionally, tidal influence (Figs. 2.9F and G) is expressed by tidal bundles, mudstone drapes, flaser and wavy bedding, small-scale trough- and planar tabular cross-bedding, and sigmoidal bedding (e.g., Dalrymple, 1992; Gingras et al., 2002b; Rebata-h et al., 2006); and abundant ichnological evidence for brackish-water sedimentation (Table 2.3, Fig. 2.9H). From the above, we infer that a large river debouched into the Fayum basin from the SW (e.g., Salem, 1976; Said, 1990). The delta front and deltaic sediments were likely deposited northward / basinward of the study area (e.g., Salem, 1976).

The upper part of the Dir Abu Lifa Member is represented by FA5. Facies Association 5 is equivalent to the quartz sandstone facies of Vondra (1974), and the seven units (green and gold muddy sandstone; sandstone and gypsum; green sandstone; gypsiferous golden sandstone; lower cross-bedded sandstone and mudstone; bare limestone, and upper cross-bedded sandstone and mudstone) of Bown and Kraus (1988). This unit has been interpreted as distributary channel deposits (Vondra, 1974), and as fluvial-dominated deposits (Bown and Kraus, 1988). In the studied sections, Facies

Association 5 comprises at least three stacked estuarine channel complexes (Channels I, II, III; Figs. 2.10 and 2.11). The base of each estuarine channel succession is marked by a Type 2 TSE (Figs. 2.11A and E). The lower estuary (estuarine mouth) is represented by the clean, white, friable sandstone located in channel III (Figs. 2.11A and F). These lithologies, combined with large-scale cross bedding (Fig. 2.11G) and local small-scale trough- and sigmoidal cross-bedding, indicate deposition in a shallow, marginal-marine, tidally influenced environment. The reduced bioturbation intensity, the very low diversity of ichnogenera, and the absence of body fossils are also consistent with high sedimentation rates and turbid water in a marginal-marine setting. These deposits are tentatively interpreted to record sediment accumulation within tidal inlet channels or flood-tidal deltas of the estuary mouth.

The distal middle estuary (central basin) is represented by the green sandstones positioned in Channel II (Figs. 2.11A and B). The fine- to very fine-grained sandstone lithology and the paucity of wave-generated sedimentary structures indicate deposition in a relatively quiescent depositional environment. The presence of the marine shells (Fig. 2.11D), sharks' and fish teeth (Fig. 2.11C), crustacean-shell fragments, and dispersed wood fragments indicate a marine to brackish-water environment. However, the high bioturbation intensities, reduced ichnogenic diversities, and the presence of a monospecific suite of large-diameter *Thalassinoides* (Fig. 2.11B) probably indicate a brackish-water setting (e.g., Pemberton et al., 1982, 2001; Pemberton and Wightman, 1992; Ranger and Pemberton, 1992; Gingras et al., 1999, 2007; MacEachern and Gingras, 2007). The green sandstone is interpreted to have been deposited in an estuarine central-basin environment under conditions of relative quiescence, and suffering overall brackish-water conditions.

The proximal middle estuary (central basin) to upper estuarine (bay-head delta?) is represented by the mudstone/siltstones, sandstone/gypsum, and the IHS units present in channels I, II, and III, respectively (Fig. 2.10). Sandy gypsiferous mudstone/siltstone

lithologies, the absence of fossils, and the general absence of wave-generated sedimentary structures, coupled with the weak bioturbation and low diversity of ichnofauna suggest deposition in a quiescent, (fluctuating) salinity-stressed environment (e.g., Gingras et al., 2007; MacEachern et al., 2007). The sandstone/gypsum lithologies and the general absence of both current- and wave-generated sedimentary structures indicate deposition in a low-energy setting. Additionally, the absence of body fossils and very rare occurrences of ichnofossils, in association with the well-developed thick gypsum veins, suggest a restricted central/lagoonal bay estuary to upper estuarine environment. Sandstone / mudstone IHS locally crop out (Fig. 2.11F). The IHS, combined with the presence of some marginal marine expressions of trace fossils and the local presence of rhizoliths in muddy intervals, are best interpreted as meandering, tidally influenced estuarine-channel point-bar deposits (e.g., Thomas et al., 1987; Ranger and Pemberton, 1992; Gingras et al., 1999, 2002b).

In brief, the upper Dir Abu Lifa Member represents a complicated assemblage of estuary deposits (e.g., Howard et al., 1975; Dorjes and Howard, 1975). These reflect an increase in relative sea level, or could be interpreted to result from autogenic occupation of the distributary channel complex following lobe abandonment. Several parts of an estuary system are exposed. *The lower estuary (estuarine mouth)* is represented by cross-bedded sandstones, interpreted to have accumulated in tidal inlet channels or flood-tidal deltas within the estuary mouth. *The distal middle estuary (central basin)* is represented by the green sandstones, interpreted to have been deposited under relatively quiescent brackish-water conditions. *The proximal middle estuary (central basin) to upper estuary* is represented by the mudstone/siltstones (restricted central basin environment), sandstone/gypsum (restricted basin – upper estuary), and the IHS units (meandering, tidally influenced, estuarine-channel point bar).

SEA-LEVEL HISTORY

Key stratigraphic surfaces (Figs. 2.12 and 2.13) indicate a history of episodic and complex shoreline retreat and advance during late Middle - Late Eocene. Facies Association 1 of Gehannam Formation (base not exposed) was deposited in a late-stage highstand of relative sea level during the Late Bartonian. The Late Bartonian relative low sea level and/or tectonic uplift were followed by the Early Priabonian relative sea level rise. This Middle Eocene (Bartonian) - Late Eocene (Priabonian) boundary is expressed herein by the coplanar FS/SB surface between the Gehannam Formation (FA2) and the Birket Qarun Formation (FA1). Lowstand systems tract (LST) and transgressive systems tract (TST) deposits were either not deposited or deposited and subsequently eroded. The lower part of the Birket Qarun Formation (FA1) was deposited during a relative sea-level highstand. Upwards, the Birket Qarun Formation is highly rooted and alluviated, and amalgamated with Type 1 TSE, forming a FS/SB. A thin transgressive shale bed (locally eroded) overlies a FS/SB surface. Overall, the parasequences of the upper Birket Qarun Formation, Umm Rigl and Temple members were deposited during a highstand stage of relative sea level that was associated with minor sea-level fluctuations (expressed by the abundant parasequences and TSE surfaces). The Late Priabonian marks a relatively low sea level position, which is characterized by laterally migrating distributary channels (FA4) that crosscut the lagoonal parasequences (FA3) at a sequence boundary (Fig. 2.12). Estuarine channel deposits (FA5) were deposited during an ensuing transgressive pulse that corresponds to inferably higher-order sea-level cycles.

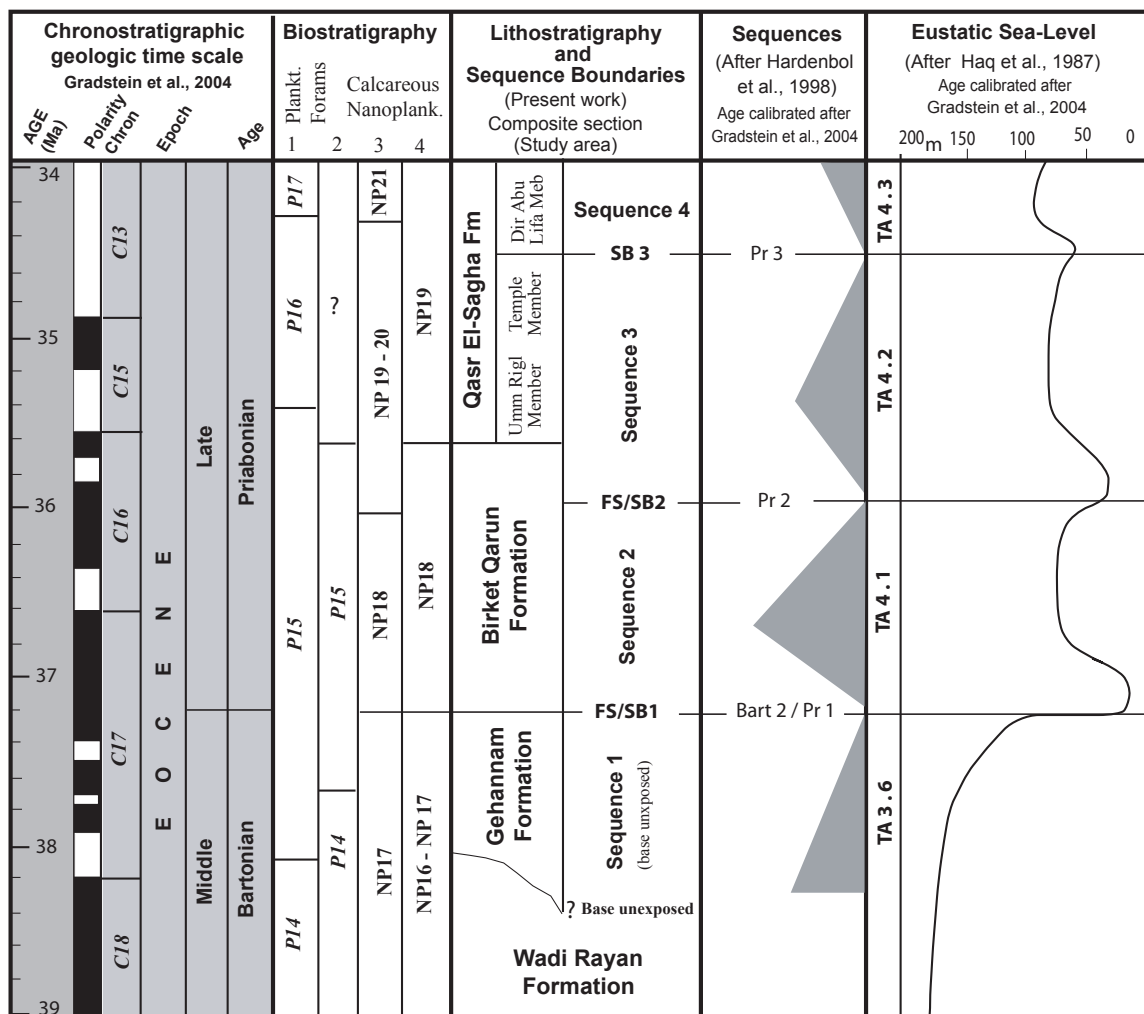


FIGURE 2.13. Correlation chart of the lithostratigraphy, the identified sequences and sequence boundaries of the compiled Middle-Upper Eocene succession in the study area, with the regional sequences of Hardenbol et al. (1998) and the global eustatic sea-level curve of Haq et al. (1987). The age is calibrated after the global Eocene chronostratigraphic time scale of Gradstein et al. (2004), the planktonic biozones of (1) Berggren et al. (1995) and (2) Haggag and Bolli (1996), and the nanoplanktonic biozones of (3) Martini (1971) and (4) Zalat (1995).

DISCUSSION

Some aspects of the reported facies associations are unusual and merit discussion. Facies Association 1 is impressive in that throughout its thickness, no physical sedimentary structure were observed. Intense bioturbation and the presence of ichnogenera consistent with the *Cruziana* Ichnofacies attest to deposition of FA1 below fair-weather wave base (e.g., Walker and Plint, 1992; Pemberton et al., 2001). Another

interesting characteristic of FA1 (Table 2.3) is the absence of gradational progradation to shoreface/foreshore deposits or a deltaic succession; rather, FA1 abruptly passes into the bay margin/supratidal deposits of FA2. These observations lead us to infer that FA1 was deposited under conditions of low tide- and wave-generated energies in a shallow marine bay or gulf. The resulting gulf to bay-margin succession differs greatly from the coarsening-upwards profiles commonly generated in other shallowing-upwards units (e.g., shoreface, delta). Additionally, the profile differs from typical bay-margin successions in that the ichnological features are most consistent with fully marine conditions and bear no evidence of physico-chemical stresses normally associated with embayed near-shore settings. The depositional setting associated with FA1 likely played a role in how and where the abundant whale fossils were preserved (discussed below).

The rhizolith-bearing part of FA2 displays a horizon of large root casts, trace fossils, and invertebrate/vertebrate fossils. The presence of a complex association of marginal-marine and continental trace-fossil assemblages attests to a near-shore position on a very shallow-gradient coastline. In a similar fashion, approximately twenty well-preserved lagoonal parasequences are reported from FA3. The lagoonal units are bounded by wave / tidal ravinement surfaces that are easily identified by the presence of *Glossifungites*-Ichnofacies demarcated surfaces. The parasequence boundaries are therefore very well displayed and serve as unusually good examples of the *Glossifungites* Ichnofacies.

Facies Association 4 is also notable due to the presence of unusually large-scaled inclined heterolithic stratification (IHS). The vertical succession of the reported IHS varies between 30 and 35 m thick, and are laterally extensive (i.e., exceed the outcrop scale, which is up to 1 km exposure). The IHS comprise cm- to dm- scale interbeds of sandstone, siltstone and mudstone. Therein, bioturbation is rare to absent and sporadically distributed. The middle and upper portions commonly display well-developed tidal rhythmites, with the basal bedsets containing large sigmoidal cross-beds that represent

channel thalweg deposits. Taken together, the sedimentological evidence strongly supports tidally influenced sedimentation within the realm of brackish water. Studies of Pleistocene and modern IHS deposits have generally focused on much smaller tidal bars (up to 10 m thick) (e.g., Gingras et al., 1999; Pearson and Gingras, 2006). However, Choi et al. (2004) document a tidally influenced point bar on the distributary of the macrotidal Han River Delta, Korea to be 25 m thick. In the rock record, very thick examples of similar IHS (up to 28 m thick) have been reported only from subsurface datasets: e.g., the Cretaceous McMurray (estuarine) and Dunvegan (tidal incised-valley fills) formations in the Western Canada Sedimentary Basin (e.g., Pemberton et al., 1982; Ranger and Pemberton, 1992; Plint and Wadsworth, 2003). Thus, these outcrops provide an important large-scale example of heterolithic, fluvially influenced channel deposits.

Facies Association 5 contains variant sandstone/mudstone sedimentary facies that represent quiescent to energetic, fluvial to brackish to marine depositional waters. Facies Association 5 represents the most complex units observed in the local stratigraphy. Further work should emphasize assessing the lateral variability, and perhaps subdivision of FA5. In the context of this study, the presence of FA5 is useful to demonstrate the upwards encroachment of continental sedimentary environments.

PALEOENVIRONMENT AND DISTRIBUTION OF THE EOCENE WHALES IN THE FAYUM DEPRESSION

The depositional model (Figs. 2.12 and 2.13) of the Middle – Upper Eocene succession provides successive paleoenvironments that strongly controlled the distribution of the Eocene-whale fossils in the Fayum, all of which occur in the highstand systems tracts (HST) sequences 1, 2 and 3. Thus, the whale skeletons occur sporadically at the top of the Gehannam Formation (FA1) and are concentrated in the sandstones (FA1) of the Birket Qarun Formation. The biological and sedimentological characteristics of FA1 attest to many physical, chemical and biotic paleoenvironmental parameters.

The pertinent physical factors comprise low depositional energy, low to moderate sedimentation rate, sandy soft-ground substrate and generally euphotic zone. Normal marine salinity and high levels of oxygenation are the two main revealed chemical-controlling factors. The previous paleoecologic physical and chemical factors resulted in abundant food resources and biomass. These paleoecological factors, coupled with an open marine bay setting in the HST represent a typical environment for the Eocene whales in the area of Wadi El-Hitan. Upwards, *Basilosaurus isis* and *Dorudon atrox* are not recorded in Qasr El-Sagha Formation (FA3-5). Rather, only a smaller whale (3 m long), *Saghacetus osiris*, is observed in lagoon-associated strata (FA3).

Overall, the depositional characters of the FA2, FA4 and FA5 reflect shallow-water environments that were locally characterized by fluctuating salinities. These units seemed to offer neither space nor food for the whales to exploit.

OCCURRENCES OF EOCENE WHALES

A more global comparison of the sedimentary paleoenvironments characterized by Eocene whales helps to understand the origin and evolution of the Eocene (archaeocete) whales. The earliest whales are found in Pakistan. These are represented by the wolf-sized *Pakicetus* sp., which were found with a land-mammal fauna in fluvial sediments of the Lower Eocene Kuldana Formation (Gingerich et al., 1983). The Middle Eocene *Ambulocetus* sp. (walking whale) skeletons were found in the same locality as *Pakicetus* sp. in Pakistan, but 120 m higher in the section (Thewissen et al., 1994). In these strata, the presence of mixed molluscs and leaf impressions attests to the presence of a proximal, shallow-marine environment. The Middle Eocene *Rhodocetus* sp. (partly terrestrial tail-swimming whale) bones are found in green shale deposited in deep fully marine waters; Domanda Formation, in Pakistan (Gingerich et al., 1994).

The lowermost occurrence of the Fayum's *Basilosaurus isis* and *Dorudon atrox* is in the late Middle Eocene in the Gehannam Formation. Whale-fossil occurrences are most

abundant in the early Late Eocene in the Birket Qarun Formation. The residence of late Middle–Late Eocene Fayum whales in fully open marine bay or gulf habitats confirms the transition of Early Eocene and early Middle Eocene whales (described above) from land and marginal-marine settings into fully marine environments.

CONCLUSIONS

Five recurring facies associations (FA1-FA5) are identified from the Middle-Upper Eocene succession from the Wadi El-Hitan and Qasr El-Sagha areas in the Fayum depression. The ichnological characteristics found in the depositional units of FA1 are attributed to archetypal- and proximal expressions of the *Cruziana* Ichnofacies. These ichnofacies, combined with the thorough bioturbation, high ichnogenera diversities, and paucity of preserved wave-generated sedimentary structures indicate that deposition occurred in low-energy, distal to proximal, broad, open bays or gulfs. The gypsiferous mudstone/siltstone of FA2 combined with reduced bioturbation and low ichnological diversities are indicative of physico-chemically stressful conditions (e.g., low energy and fluctuating salinity stresses due to proximity to the coastal margin in a tropical to subtropical climate) in a low-energy bay-margin setting. Upwards, the rhizolith-bearing sandstone of FA2 contains continental trace fossils, marine to brackish marine trace fossils, and a marine invertebrate and vertebrate fossil association, indicating a marginal marine to coastal swamp/supratidal setting. The weakly bioturbated carbonaceous mudstones of FA3 (impoverished trace fossil suites attributed to distal expressions of *Skolithos* Ichnofacies), with low trace-fossil diversities indicate a partially restricted shallow lagoonal or bay setting, in an arid to semi-arid climate. Facies Association 4 is interpreted to record deltaic distributary-channel complexes. This interpretation is based on the incorporation of sedimentological and ichnological characters consistent with marginal-marine point bars (e.g., IS and IHS), which were tidally influenced (e.g., tidal bundles and sigmoidal bedding) and deposited under conditions of brackish water

(e.g., impoverished marine to brackish-marine trace fossil suites). Facies Association 5 represents a complex stratigraphic assemblage of mudstone- and sandstone-bearing estuarine channels. Physical sedimentary structures (e.g., large tabular planar cross-bedding) combined with the presence of impoverished expressions of the *Skolithos* – *Psilonichnus* Ichnofacies characterize the lower estuary deposits. A paucity of physical sedimentary structures is observed in the middle estuary green sandstone, which displays high degrees of bioturbation and low ichnofossil diversities), and the upper estuary mudstones/sandstones display reduced degrees of bioturbation and low-diversity ichnological suites.

The depositional model (Fig. 2.12) shows that the facies associations and their corresponding depositional environments record a gradual shallowing-upward succession. This shallowing-upward is coincident with a regional vertical tectonic movement of the northern margin of Egypt during the Eocene that was perturbed by contemporaneous local tectonics. The Middle Eocene (Bartonian) Gehannam Formation (FA1) was deposited in a low-energy distal broad bay or gulf, locally interrupted by low-energy bay-margin processes (FA2), which abruptly shallowed upward to marginal-marine swamps (FA2). The Birket Qarun Formation (FA1) indicates a proximal, low-energy bay or gulf setting, and incorporates a thin, transgressive, dark-grey shale unit. The upper Birket Qarun Formation displays repeated wave ravinement and coastal transgressive sediments in a bay-margin setting. The lower Temple Member of the Late Eocene (Priabonian) Qasr El-Sagha Formation is represented by shallow lagoonal or bay parasequences (FA3) in arid to semi-arid (tropical to subtropical) climates. Facies Association 3 is truncated upward by a SB that heralds the deposition of the deltaic distributary channels (FA4) of the upper Dir Abu Lifa Member. The upper part of the Dir Abu Lifa Member is represented by stacked estuarine channels (FA5), recording a return to relative sea-level rise and transgressive conditions in the study area.

Finally, many of the intervals display unusual ichnological-sedimentological

associations such as highly bioturbated sandstones of FA1 and the large-scale IHS of FA4 that may serve to interpret the stratigraphic record elsewhere. Our studies show that the whales of the Fayum are restricted to the HST, and lived under conditions of low depositional energy and moderate-sedimentation rates, in fully marine waters of environments characterized by a high biomass. The residence of the Fayum Middle-Upper Eocene whales in a fully marine environments within the highstand systems tracts confirms the transition of the early Eocene whales from land and land/shallow sea margins to fully marine environments.

REFERENCES

- Abd El Dayem, A.L. and Nabawy, B.S., 1999, Tertiary sedimentary rocks, Fayum, Egypt: Magnetic fabric and paleomagnetic study: *Sedimentology of Egypt*, v. 7, p. 185-196.
- Abdou, H.F. and Abdel-Kireem, M.R., 1975, Planktonic foraminiferal zonation of the middle and upper Eocene rocks of Fayum province, Egypt: *Revista Española de Micropalantología*, v. 7, p. 15-64.
- Ahmed, S.M., 2001, Contribution to sedimentary nature of Eocene sequence, Fayum, Egypt: *Sedimentology of Egypt*, v. 9, p. 27-41.
- Bassiouni, M., Boukhary, M., Shama, K. and Blondeau, A., 1984, Middle Eocene Ostracodes from Fayoum, Egypt: *Géologie Méditerranéenne*, v. 11, p. 181-192.
- Beadnell, H.J.L., 1905, The topography and geology of the Fayum Province of Egypt: Egyptian Survey Department, Cairo, 101 pp.
- Berggren, W.A., Kent, D.V., Swisher, C.C. and Aubry, M.-P., 1995, A revised Cenozoic geochronology and chronostratigraphy, *in* Berggren, W.A., Kent, D.V., Aubry, M.-P. and Hardenbol, J., eds., *Geochronology, time scales and global stratigraphic correlation*: Society of Economic Paleontologists and Mineralogists Special Publication, v. 54, p. 129–212.

- Bhattacharya, J. and Walker, R.G., 1992, Deltas, *in* Walker R.G. and James, N.P., eds., Facies Models: Response to Sea Level Change: Geological Association of Canada, St John's, NF, p. 157-178.
- Bishay, Y., 1966, Studies on the larger foraminifera of the Eocene of the Nile Valley between Assiut, Cairo and SW Sinai: Unpublished Ph.D. Thesis, Alexandria University, 244 pp.
- Blanckenhorn, M., 1903, Neue geologisch-stratigraphische Beobachtungen in Aegypten: Sitzungsberichte der Mathematisch-physikalischen Classe der Königlischen Bayerischen Akademie der Wissenschaften, v. 32, p. 353-433.
- Blondeau, A., Boukhary, M. and Shamah, K., 1984, Les microfacies de l'Eocene et de l'Oligocene de la Province du Fayoum, Egypte: Revue de Paléobiologie, v. 3, p. 243-267.
- Bown, T.M. and Kraus, M.J., 1988, Geology and paleoenvironment of the Oligocene Jebel Qatrani Formation and adjacent rocks, Fayum depression, Egypt: United States Geological Survey Professional Paper, v. 1452, p. 1-60.
- Cherif, O.H. and El Afifi, F.I., 1983, Remarks on the stratigraphy and tectonism of the main Oligocene exposures in Egypt: Annals of the Geological Survey of Egypt, v. 13, p. 247-255.
- Choi, K.S., Dalrymple, R.W., Chun, S.S. and Kim, S-P., 2004, Sedimentology of modern inclined heterolithic stratification (IHS) in the Macrotidal Han River Delta, Korea. Journal of Sedimentary Research, v. 74, p. 667-689.
- Dalrymple, R.W., 1992, Tidal Depositional Systems, *in* Walker, R.G. and James, N.P., eds., Facies Models: Response to Sea Level Change: Geological Association of Canada, St John's, NF, p. 195-218.
- Dashtgard, S.E. and Gingras, M.K., 2005, The temporal significance of bioturbation in backshore deposits: Waterside Beach, New Brunswick, Canada: Palaios, v. 20, p. 589-595.

- Dolson, J., El Barkooky, A., Gingerich, P.D., Prochazka, N. and Shann, M., 2002, The Eocene and Oligocene Paleo-Ecology and Paleo-Geography of Whale Valley and the Fayum Basins: Implications for Hydrocarbon Exploration in the Nile Delta and Eco-Tourism in the Greater Fayum Basin: AAPG, Search Discovery Article # 10030: <http://www.searchanddiscovery.com/documents/cairo/index.htm>.
- Dorjes, J. and Howard, J. D., 1975, Estuaries of the Georgia Coast, U.S.A.: sedimentology and biology. IV. Fluvial-marine indicators in an estuarine environment, Ogeechee River-Ossabaw Sound: *Senckenbergiana Maritima*, v. 7, p. 137-179.
- Elewa, A.M.T, Omar, A.A. and Dakrory, A.M., 1998, Biostratigraphical and paleoenvironmental studies on some Eocene ostracodes and foraminifers from the Fayoum depression, Western Desert, Egypt: *Egyptian Journal of Geology*, v. 42, p. 439-469.
- El Zarka, M.H., 1983, Mode of hydrocarbon generation and prospects of the northern part of the Western Desert, Egypt: *Journal of African Earth Sciences*, v. 1, p. 295-304.
- Geological Survey of Egypt 'GSE', 1981, Geological Map of Egypt, scale 1: 2,000,000: Egyptian Geological Survey and Mining Authority, Ministry of Industry and Mineral Resources, Cairo, 1 sheet.
- Geological Survey of Egypt 'GSE', 1983, Geological Map of Greater Cairo Area, scale 1: 100,000: Egyptian Geological Survey and Mining Authority, Ministry of Industry and Mineral Resources, Cairo, 1 sheet.
- Gingerich, P.D., 1992, Marine mammals (Cetacea and Sirenia) from the Eocene of Gebel Mokattam and Fayum, Egypt; stratigraphy, age and paleoenvironments: *University of Michigan Papers in Paleontology*, v. 30, p. 1-84.
- Gingerich, P. D., S. M. Raza, M. Arif, M. Anwar, and X. Zhou, 1994, New whale from the Eocene of Pakistan and the origin of cetacean swimming: *Nature*, v. 368, p. 844-847.

- Gingerich, P. D., Wells, N. A., Russell, D. E. and Shah, S. M. I., 1983, Origin of whales in epicontinental remnant seas: new evidence from the early Eocene of Pakistan: *Science*, v. 220, p. 403-406.
- Gingras, M.K., Bann, K.L., MacEachern, J.A., Waldron, J. and Pemberton, S.G., 2007, A conceptual framework for the application of trace fossils, *in* MacEachern, J.A., Bann, K.L., Gingras, M.K. and Pemberton, S.G., eds., *Applied Ichnology: Society of Economic Paleontologists and Mineralogists Short Course Notes*, v. 52, p. 1-25.
- Gingras, M.K., Pemberton, S.G., Saunders, T. and Clifton, H.E., 1999, The ichnology of modern and Pleistocene brackish-water deposits at Willapa Bay, Washington; variability in estuarine settings: *Palaios*, v. 14, p. 352–374.
- Gingras, M.K., Räsänen, M.E., Pemberton, S.G. and Romero, L.P., 2002a, Ichnology and sedimentology reveal depositional characteristics of bay-margin parasequences in Miocene Amazonian foreland basin: *Journal of Sedimentary Research*, v. 72, p. 871–883.
- Gingras, M.K., Räsänen, M. and Ranzi, A., 2002b, The significance of bioturbated inclined heterolithic stratification in the southern part of the Miocene Solimoes Formation, Rio Acre, Amazonia Brazil: *Palaios*, v. 17, p. 591–601.
- Gradstein, F.M., Ogg, J.G. and Smith, A.G., 2004, *A Geologic Time Scale 2004*: Cambridge University Press, London, 589 pp.
- Guiraud, R., Bosworth, W., Thierry, J. and Delplanque, A., 2005, Phanerozoic geological evolution of Northern and Central Africa: An overview: *Journal of African Earth Sciences*, v. 43, p. 83-143.
- Haggag, M.A. and Bolli, H.M., 1995, Globigerinatheka index aegyptiaca, a new late Eocene planktonic foraminiferal subspecies from Fayoum, Egypt: *Revista Española de Micropaleontología*, v. 27, p. 143-147.

- Haggag, M.A. and Bolli, H.M., 1996, The origin of *Globigerina* *theke* *semiinvoluta* (Keijzer), Upper Eocene, Fayoum area, Egypt: *Neues Jahrbuch für Geologie und Paläontologie Monatshefte*, v. 6, p. 365-374.
- Haq, B.U., Hardenbol, J. and Vail, P.R., 1987, Chronology of fluctuating sea level since the Triassic: *Science*, v. 235, p. 1156-1167.
- Hardenbol, J., Thierry, J., Farley, M.B., Jacquin, T., de Graciansky, P.C. and Vail, P.R., 1998, Mesozoic and Cenozoic sequence chronostratigraphic framework of European basins, *in* de Graciansky, P.C., Hardenbol, J., Jacquin, T. and Vail, P.R., eds., *Mesozoic and Cenozoic Sequence Stratigraphy of European Basins*: Society of Economic Paleontologists and Mineralogists Special Publication, v. 60, p. 3-13.
- Howard, J.D., Elders, C.A. and Heinbokel, J.F., 1975, Animal-sediment relationships in estuarine point bar deposits, Ogeechee River-Ossabaw Sound, Estuaries of the Georgia Coast, U.S.A.: *Sedimentology and Biology*, V: *Senckenbergiana Maritima*, v. 7, p. 181-203.
- Iskandar, F., 1943, Geological survey of the Gharaq El Sultani Sheet No. 68/54: The Standard Oil Company of Egypt. S. A., Report No. 57, 36 pp.
- Ismail, M.M. and Abdel-Kireem, M.R., 1971, Contributions to the stratigraphy of the Fayoum Province: *Bulletin Faculty of Science Alexandria University*, v. 11, p. 57-63.
- Klappa, C.F., 1980, Rhizoliths in terrestrial carbonates: classification, recognition, genesis and significance: *Sedimentology*, v. 27, p. 613-629.
- Lotfy, H. and Van der Voo, R., 2007, Tropical northeast Africa in the middle-late Eocene: Paleomagnetism of the marine-mammals sites and basalts in the Fayum province, Egypt: *Journal of African Earth Sciences*, v. 47, p. 135-152.

- MacEachern, J.A., Bann, K.L., Gingras, M.K. and Pemberton, S.G. (2007) The Ichnofacies Paradigm: High-resolution Paleoenvironmental Interpretation of the Rock Record, *in* MacEachern, J.A., Bann, K.L., Gingras, M.K. and Pemberton, S.G., eds., *Applied Ichnology: Society of Economic Paleontologists and Mineralogists Short Course Notes*, v. 52, p. 26-63.
- MacEachern, J.A. and Gingras, M.K. (2007) Recognition of brackish-water trace fossil suites in the Cretaceous Western Interior Seaway of Alberta, *in* Bromley, R.G., Buatois, L.A., Mángano, M.G., Genise, J.F. and Melchor, R.N., eds., *Sediment–Organism Interactions: a Multifaceted Ichnology: Society of Economic Paleontologists and Mineralogists Special Publication*, v. 88, p. 147–192.
- Martini, E., 1971, Standard Tertiary and Quaternary calcareous nannoplankton zonation, *in* Farinacci, A., ed., *Proceedings of the II Plankton Conference: Roma*, p. 739–785.
- Nesbitt, E.A. and Campbell, K.A., 2006, The paleoenvironmental significance of *Psilonichnus*: *Palaios*, v. 21, p. 187-196.
- Olariu, C. and Bhattacharya, J.P., 2006, Terminal distributary channels and delta front architecture of river-dominated delta systems: *Journal of Sedimentary Research*, v. 76, p. 212-233.
- Pearson, N.J. and Gingras, M.K., 2006, An ichnological and sedimentological facies model for muddy point-bar deposits. *Journal of Sedimentary Research*, v. 76, p. 771-782.
- Pemberton, S.G., Flach, P.D. and Mossop, G.D., 1982, Trace fossils from the Athabasca oil sands, Alberta, Canada: *Science*, v. 217, p. 825-827.
- Pemberton, S.G., Spila, M., Pulham, A. J., Saunders, T., MacEachern, J.A., Robbins, D. and Sinclair, I.K., 2001, *Ichnology and Sedimentology of Shallow to Marginal Marine Systems: Ben Nevis and Avalon Reservoirs, Jeanne D’ Arc Basin: Geological Association of Canada, St. John’s NF*, 343 pp.

- Pemberton, S.G. and Wightman, D.M., 1992, Ichnological characteristics of brackishwater deposits, *in* Pemberton, S.G., ed., Applications of Ichnology to Petroleum Exploration, A Core Workshop: Society of Economic Paleontologists and Mineralogists Core Workshop Note, v. 17, p. 141–167.
- Plint, A.G. and Wadsworth, J.A., 2003, Sedimentology and palaeogeomorphology of four large valley systems incising delta plains, western Canada Foreland Basin: implications for mid-Cretaceous sea-level changes: *Sedimentology*, v. 50, p. 1147-1186.
- Ranger, M.J. and Pemberton, S.G., 1992, The Sedimentology and ichnology of estuarine point bars in the McMurray Formation of the Athabasca Oil Sands Deposit, northeastern Alberta, Canada, *in* Pemberton, S.G., ed., Applications of Ichnology to Petroleum Exploration, A Core Workshop: Society of Economic Paleontologists and Mineralogists Core Workshop Note, v. 17, p. 401-421.
- Rebata-h, L.A., Gingras, M.K., Räsänen, M.E. and Barberi, M. (2006) Tidal-channel deposits on a delta plain from the Upper Miocene Nauta Formation, Marañón Foreland Sub-basin, Peru: *Sedimentology*, v. 53, p. 971-1013.
- Said, R., 1962, The geology of Egypt: Elsevier, Amsterdam and New York, 377 pp.
- Said, R., 1990, The geology of Egypt: A. A. Balkema, Rotterdam, 734 pp.
- Salem, R., 1976, Evolution of Eocene-Miocene sedimentation patterns in parts of northern Egypt: *American Association of Petroleum Geologists Bulletin*, v. 60, p. 34-64.
- Sestini, G., 1984, Tectonic and sedimentary history of NE African margin (Egypt/Libya), *in* Dixon, J.E. and Robertson, A.H.F., eds., The geological evolution of the eastern Mediterranean: Geological Society of London Special Publication, v. 17, p. 161-175.
- Smith, A.G., 1971, Alpine deformation and the oceanic areas of Tethys, Mediterranean and Atlantic: *Geological Society of American Bulltten*, v. 82, p. 2039-2070.

- Strougo, A. and Haggag, M.A.Y., 1984, Contribution to the age determination of the Gehannam Formation in the Fayum Province, Egypt: *Neues Jahrbuch für Geologie und Paläontologie Monatshefte*, v. 1, p. 46-52.
- Swedan, A.H., 1992, Stratigraphy of the Eocene sediments in the Fayum area: *Annals of the Geological Survey of Egypt*, v. 18, p. 157-166.
- Swedan, A., Ibrahim, A., El Nattar, I. and Abbas, M., 1982, Geology of the area north of Bahariya Oasis and south of Qattara depression, Western Desert, Egypt: *Annals of the Geological Survey of Egypt*, v. 12, p. 283-303.
- Thewissen, J. G. M., Hussain, S. T. and Arif, M., 1994, Fossil evidence for the origin of aquatic locomotion in Archaeocete whales: *Science*, v. 263, p. 210-212.
- Thomas, R.G., Smith, D.G., Wood, J.M., Visser, J., Calverley-Range, E.A. and Koster, E.H., 1987, Inclined heterolithic stratification – terminology, description, interpretation and significance: *Sedimentary Geology*, v. 53, p. 123-179.
- Taylor, A.M. and Goldring, R., 1993, Description and analysis of bioturbation and ichnofabric: *Journal of the Geological Society, London*, v. 150, p. 141–148
- Vondra, C.F., 1974, Upper Eocene transitional and near-shore marine Qasr el Sagha Formation, Fayum Depression, Egypt: *Annals of the Geological Survey of Egypt*, v. 4, p. 79-94.
- Walker, R.G. and James, N.P., 1992, Facies models: Response to Sea Level Change: Geological Association of Canada, St John's, NF, 454 pp.
- Walker, R.G. and Plint, A.G., 1992, Wave- and storm-dominated shallow marine systems, *in* Walker, R.G. and James, N.P., eds., *Facies Models: Response to Sea Level Change*: Geological Association of Canada, St John's, NF, p. 219-238.
- Zalat, A.A., 1995, Calcareous nanoplankton and diatoms from the Eocene / Pliocene sediments, Fayoum depression, Egypt: *Journal of African Earth Sciences*, v. 20, p. 227-244.

CHAPTER 3: MIDDLE - UPPER EOCENE FACIES ARCHITECTURE AND TRACE FOSSILS INTERPRETING THE PALEOENVIRONMENT AND SEDIMENTOLOGIC SETTING OF THE WHALE-BEARING GEHANNAM AND BIRKET QARUN FORMATIONS, WADI EL-HITAN, FAYUM - EGYPT *

INTRODUCTION

Wadi El-Hitan (Whale Valley) is located at the SW corner of the Fayum depression (Fig. 3.1). This area was known in late 18th and early 19th centuries for the occurrence of abundant vertebrate (especially whale) fossils within Middle-Upper Eocene strata (e.g., Schweinfurth, 1877; Dames, 1894; Beadnell, 1905). In 2005, Wadi El-Hitan was added to UNESCO's World Heritage list. Only a few geological studies had been conducted in Wadi El-Hitan (e.g., Beadnell, 1905; Gingerich, 1992; Dolson et al., 2002, Peters et al., 2009), as most of the published efforts focused on the vertebrate fossils. The present chapter presents the first consideration of the abundant trace fossils that occur within Eocene strata at Wadi El-Hitan, and discusses their paleoenvironmental and sedimentologic applications in this World heritage area.

Trace fossils are excellent paleoenvironmental indicators, as they help elucidate paleoenvironmental parameters such as depositional energy, salinity and oxygen content (e.g., Ekdale et al., 1984; Savrda and Bottjer, 1989; Gingras et al., 1999, 2000, 2002; McIlroy, 2004; MacEachern et al., 2005, 2007; Nesbitt and Campbell, 2006; Hembree and Hasiotis, 2007; Bromley et al., 2007). Integrated ichnological and sedimentological data have been used repeatedly to interpret the character of sedimentary environments (see Seilacher, 1982; Pemberton and MacEachern, 1997; Taylor et al., 2003; Bann et al., 2004; Buatois et al., 2005; Gingras et al., 2007; MacEachern et al., 2007).

* A version of this chapter has been submitted for publication in PALAIOS journal as "Middle-Upper Eocene facies architecture and trace fossils interpreting the paleoenvironment and sedimentologic setting of the whale-bearing Gehannam and Birket Qarun formations, Wadi El-Hitan, Fayum - Egypt", by: Zaki A. Abdel-Fattah, Murray K. Gingras, Michael W. Caldwell and S. George Pemberton.

Although the whale-bearing strata at Wadi El-Hitan are investigated partly in Chapter 2, Chapter 3 introduces additional and detailed sedimentological and ichnological data, which are integrated to interpret and discuss the paleoenvironment, source of sediments and Eocene-whale preservation in this World heritage area. The main objectives of this chapter are twofold: (1) the integration of the detailed ichnological data (i.e., biogenic sedimentary structures and ichnofacies analyses), with sedimentological data (i.e., detailed facies analysis) to interpret the paleoenvironment and develop a depositional model for the whale-bearing deposits of the Fayum; and (2) to consider potential relationships between sedimentary processes, paleogeography and the occurrence of the well-preserved whale skeletons.

STUDY AREA LOCATIONS

The Middle - Upper Eocene successions (Fig. 3.1) were measured at three localities in the vicinity of Wadi El-Hitan area: (1) Minqar El-Hut (between N 29° 15' 48" - E 30° 02' 47" and N 29° 16' 02" - E 30° 03' 51"); (2) Old Camp site (N 29° 15' 55" - E 30° 01' 24"); and (3) Sandouk El-Borneta section (N 29° 17' 00" - E 30° 03' 00").

METHODS

Documentation of the stratigraphic, sedimentologic and ichnological data have been carried out through detailed field work in the study area. The descriptive ichnological data gathered include the identification and description of observed ichnogenera and ichnospecies, trace fossil assemblages, and ichnofacies types. Semi-quantitative ichnological data comprise the degree of bioturbation (recorded as bioturbation index or BI; *sensu*, Reineck, 1963; Taylor and Goldring, 1993), and the maximum diameter of the ichnofossils. Sedimentological data include lithic designations and rock textures, nature of bedding and bed contacts, physical sedimentary structures, and fossil content. To supplement the outcrop data, fifteen standard petrographic thin-

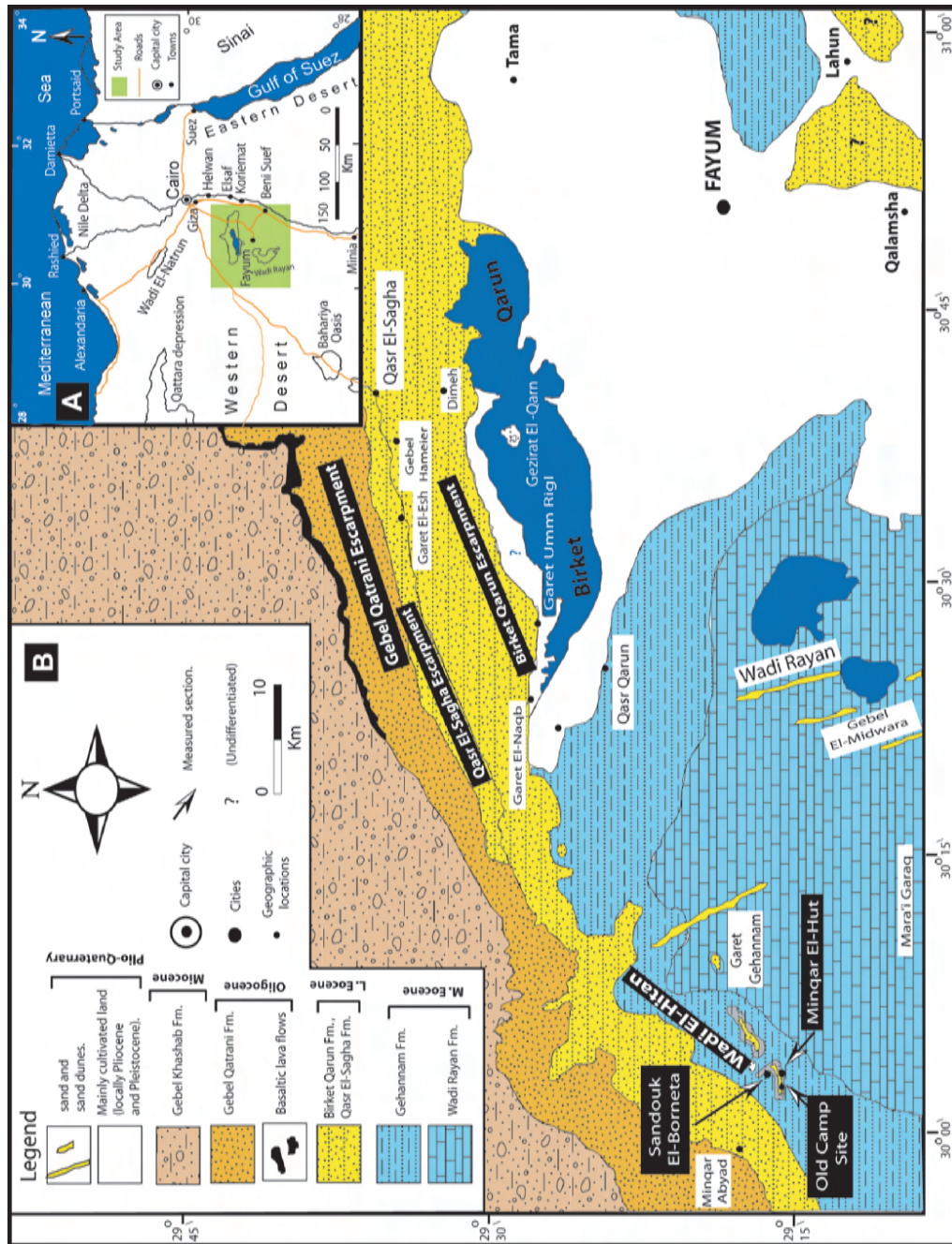


FIGURE 3.1. A- Location map of the Fayum depression, Egypt. **B-** Geological map of the Fayum depression and the studied sections in the area of Wadi El-Hitan. Redrawn and modified after Beadnell (1905), Said (1962) and Gingerich (1992).

sections were studied using a petrographic microscope. Some representative samples were analyzed using a JEOL 6301F Field Emission SEM.

GEOLOGIC AND STRATIGRAPHIC SETTING

The pre-Eocene sedimentary succession of the Fayum sag basin is characterized by complex subsurface structures (synclinal/anticlinal and fault systems) that are overlain unconformably by nearly horizontal Eocene/Oligocene sedimentary strata (Fig. 3.1). The Fayum basin developed during Jurassic rifting, which was characterized by extensional and strike-slip movement between Africa and Eurasia (Smith, 1971). Uplift and tectonic inversion occurred during the Late Cretaceous Syrian Arc event. Since the Middle Eocene, the tectonic margins of Egypt have been dominated by vertical movements, associated with gradual subsidence of the Mediterranean Sea and the opening of the Red Sea (Sestini, 1984). The Late Eocene was marked by a general lowering of relative sea level, resulting in the progressive emergence and erosion of structural highs that provided clastic sediments to Late Eocene basins of northern Egypt (e.g., Salem, 1976).

In the area of Wadi El-Hitan, the outcrop stratigraphy is represented by the slope-forming Middle Eocene Gehannam Formation (base unexposed), which is overlain by the characteristically thick, cliff-forming Upper Eocene Birket Qarun Formation. In turn, the Birket Qarun Formation is overlain upward by the late-Upper Eocene Qasr El-Sagha Formation. The ravine beds (fish-scale beds) and the Birket Qarun series (*Operculina* – *Nummulites* beds) of Beadnell (1905) were formally renamed as Gehannam and Birket Qarun formations, respectively, by Said (1962). Biostratigraphic data (e.g., Beadnell, 1905; Strougo and Haggag, 1984; Zalat, 1995; Elewa et al., 1998; Morsi et al., 2003) indicates that the Gehannam Formation is Middle Eocene (Bartonian) in age. The Late Eocene (Priabonian, ~37 Ma) age of the Birket Qarun Formation is also based on previous biostratigraphic studies (e.g., Zalat, 1995; Haggag and Bolli, 1996; Morsi et al., 2003; Seiffert et al., 2008).

FACIES ARCHITECTURE

Middle-Upper Eocene deposits of the Gehannam and Birket Qarun formations are divided into two facies associations: (FA1) open-marine bay deposits; and (FA2) bay margin/coastal deposits (see Chapter 2). Symbols used in figures and illustrations are shown in Fig. 3.2. These facies associations can be further subdivided into five sedimentary facies (Figs. 3.3-3.6). Table 3.1 summarizes the stratigraphical, sedimentological, paleontological and ichnological characteristics of the sedimentary facies, and provides a brief paleoenvironmental/sedimentological interpretation of those facies.

FACIES ASSOCIATION 1: OPEN-MARINE BAY DEPOSITS

The vertebrate-bearing sandstones of Facies Association 1 (FA1) include fossils of the whale *Basilosaurus isis* and *Dorudon atrox*, as well as marine-vertebrate bones of sea cows (*Protosiren* sp.), crocodiles (*Crocodilus* sp.), sharks and fish scales. Facies Association 1 (FA1) comprises two genetically related sedimentary facies (F1 and F2) that are interpreted to have accumulated within a quiescent marine embayment (Table 3.1). Facies 1 and 2 (Fig. 3.3) constitute the main facies in the Gehannam and Birket Qarun formations, respectively. Although F1 and F2 share similar characteristics, they vary in some of their sedimentological, paleontological and ichnological properties.

Facies 1 (F1): Fine- to Very Fine-Grained Bioturbated Sandstones

Facies 1 is dominantly represented by grayish white, fine- to very fine-grained, texturally and mineralogically mature, calcareous quartz arenite (Figs. 3.4E, F). Facies 1 comprises two thirds of the exposed sections of the Gehannam Formation (Figs. 3.3, 3.4A, 3.6A), and exhibit stratal thicknesses of 20 to 25 m. Bed thicknesses vary between 1 and 5 m, with an average thickness of 2 m. The basal bedding contacts are generally sharp, but gradational basal bedding contacts are also observed. Primary physical

TABLE 3.1. Summary of the characteristics of the facies associations (FA1 and FA2) and their identified sedimentary facies (F1-F5).

Facies Assoc.	Occurrence & Thickness	Sediment. Characters	Ichnology & Fossil Content	Interpretation
FA1: Open Marine Bay Deposits				
F1 (Fine- to very fine-grained sandstones)	<ul style="list-style-type: none"> Up to 2/3 of Gehannam Fm, base not exposed, interbedded with FA2. Bed thickness ~ 1-5 m. 	<ul style="list-style-type: none"> Very rare wave ripple laminations in locally thin horizons. Dominated by calcareous quartz arenite microfacies 	<ul style="list-style-type: none"> Highly burrowed (BI 5), with high ichnogenera diversity. Trace fossils include: <i>Th</i>, <i>Pl</i>, <i>Op</i>, <i>Te</i>, <i>Sc</i>, <i>As</i>, <i>Rh</i>, and rare <i>Ch</i>, <i>Cy</i>, <i>Ar</i> and <i>Sk</i>. Archetypal <i>Cruziana</i> Ichnofacies. Echinoids (<i>Schizaster</i> sp.), bivalves, fish scales, sharks' teeth, and poorly preserved whale skeletons. 	<ul style="list-style-type: none"> Distal-marine bay or gulf environment, characterized by low energy, normal salinity and less restriction.
F2 (Medium- to fine-grained sandstones)	<ul style="list-style-type: none"> Constitutes roughly the entire of Birket Qarun Fm, overlying FA2. Bed thickness ~3-10 m. 	<ul style="list-style-type: none"> Paucity of physical sedimentary structures. Truncated upwards by TSE surfaces, displaying 3 to 4 parasequences. Dominated by dolomitic-calcareous quartz arenite microfacies. 	<ul style="list-style-type: none"> Highly burrowed (BI 5) with high ichnogenera diversity. Trace fossils include: <i>Th</i>, <i>Pl</i>, <i>Op</i>, <i>Te</i>, <i>As</i>, <i>Pa</i>, <i>Rh</i>, <i>Sk</i>, <i>Cy</i>, <i>Ar</i> and <i>Ps</i>. Proximal expression of <i>Cruziana</i> Ichnofacies. Bivalves, gastropods, echinoids, shark teeth, common marine vertebrate bones of whales and crocodiles. 	<ul style="list-style-type: none"> Proximal marine bay or gulf environment, characterized by low energy, normal marine salinity, and less restriction. F2 displays evidences of slightly higher energy levels than F1.
FA2: Bay-Marine / Coastal Deposits				
F3 (sandy shale)	<ul style="list-style-type: none"> Interfingers with F1. Total thickness 8 m. 	<ul style="list-style-type: none"> Fissile, gypsiferous, and slightly ferruginous shale. 	<ul style="list-style-type: none"> Sandy shale is weakly bioturbated (BI 0-2) and has low ichnogenera diversity. Upwards, rare <i>Te</i> and <i>Pl</i> are present. No observed fossils. 	<ul style="list-style-type: none"> Physico-chemically stressed, quiescent sedimentation (low depositional energy) along a bay-margin setting.
F4 (Sandy siltstone)	<ul style="list-style-type: none"> Overlies F3, underlies F1. Total thickness 2 m. 	<ul style="list-style-type: none"> Abundant gypsum-filled joints, with very rare wave ripple and low-angle cross-lamination at the contact between the shale and siltstone facies. 	<ul style="list-style-type: none"> Bioturbation intensity (BI 0-3) and ichnogenera diversity increase upward. The lower part contains rare to common <i>Te</i>. Upwards, trace fossils include: <i>Ps</i>, <i>Te</i>, <i>Th</i> and <i>Pl</i>. No observed fossils. 	<ul style="list-style-type: none"> Bay margin (low to moderate depositional energy), perhaps as a shallow, low-energy channel-fill, or possibly within intertidal to supratidal environments.
F5 (Fine-grained sandstone)	<ul style="list-style-type: none"> Outcrops on top of F1 and underlies F2, and marking the boundary between the Gehannam and Birket Qarun formations. Thickness 0.3 m - 1m. 	<ul style="list-style-type: none"> No observed physical sedimentary structures. 	<ul style="list-style-type: none"> Moderate bioturbation intensity (BI 3) and diversity of ichnogenera. Trace fossils include: Rhizoliths, <i>Op</i>, <i>Th</i>, <i>Sk</i>, <i>Pl</i>, <i>Ps</i>, and rare <i>Te</i>. The firmground suites of the <i>Glossifungites</i> Ichnofacies cap the rhizolith-bearing sandstones of F5. Whale-bone fragments, shark teeth, fish remains, molluscan and crustacean shell fragments. 	<ul style="list-style-type: none"> Marginal-marine swamps to supratidal setting along sheltered shorelines in tropical to subtropical coastal bay-margin environment.

sedimentary structures are very rarely preserved, generally comprising wave-ripple laminations in thinly bedded horizons. Fossils in F1 contain irregular echinoids (e.g., *Schizaster* sp.; Fig. 3.4C), common bivalves and gastropods, crab-carapace fragments, common fish scales, abundant sharks' teeth (Fig. 3.4D), and poorly preserved bones of the whale *Basilosaurus isis*. Petrographic thin sections and SEM investigations reveal relatively abundant planktonic foraminifera (Fig. 3.4E) and nannoplankton (coccoliths) (Fig. 3.4G).

Facies 1 is generally highly burrowed (BI 5) and contains a diverse ichnological assemblage (Fig. 3.4B). Trace-fossil diameters mostly lie between 5 and 10 mm, with some large (> 2 cm in diameter) *Thalassinoides* and *Ophiomorpha* present. This trace-fossil assemblage contains a diverse mixture of deposit feeding structures, as well as vertical dwellings of detritus feeders and/or filter feeders, which represents the archetypal *Cruziana* Ichnofacies. Observed ichnogenera (Table 3.3, Figs. 3.7, 3.8) include, in decreasing order of abundance, *Thalassinoides*, *Planolites*, *Ophiomorpha*, *Teichichnus*, *Scolicia*, *Asterosoma*, *Rhizocorallium*, and rare *Chondrites*, with *Cylindrichnus*, *Arenicolites*, and *Skolithos* increasing in abundance upwards. The upper part of F1



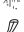





















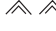







Ichnofossils		
	<i>Arenicolites</i> (Ar)	
	<i>Asterosoma</i> (As)	
	<i>Chondrites</i> (Ch)	
	<i>Cylindrichnus</i> (Cy)	
	<i>Ophiomorpha</i> (Op)	
	<i>Planolites</i> (Pl)	
	<i>Psilonichnus</i> (Ps)	
	<i>Rhizocorallium</i> (Rh)	
	<i>Scolicia</i> (Sc)	
	<i>Skolithos</i> (Sk)	
	<i>Teichichnus</i> (Te)	
	<i>Thalassinoides</i> (Th)	
	<i>Teredolites</i> (Tr)	
	Rhizoliths (Root traces/casts)	
Fossils		
	Bivalves	
	Gastropods	
	Echinoids	
	Foraminifers, in general	
	Large foraminifers	
	Fish remains	
	Vertebrates & bones	
	Teeth	
	Plant remains, leaf imprints	
	Wood	
Others		
	Ripple laminations (wave)	
	Concretionary sandstone	
	Alluviation	
	Gypsum streak	
	Coquina	
	Unconformity	
	Th	} <i>Glossifungites</i> Ichnofacies
	Giant burrows	

FIGURE 3.2. Legend and key to symbols used in figures and illustrations.

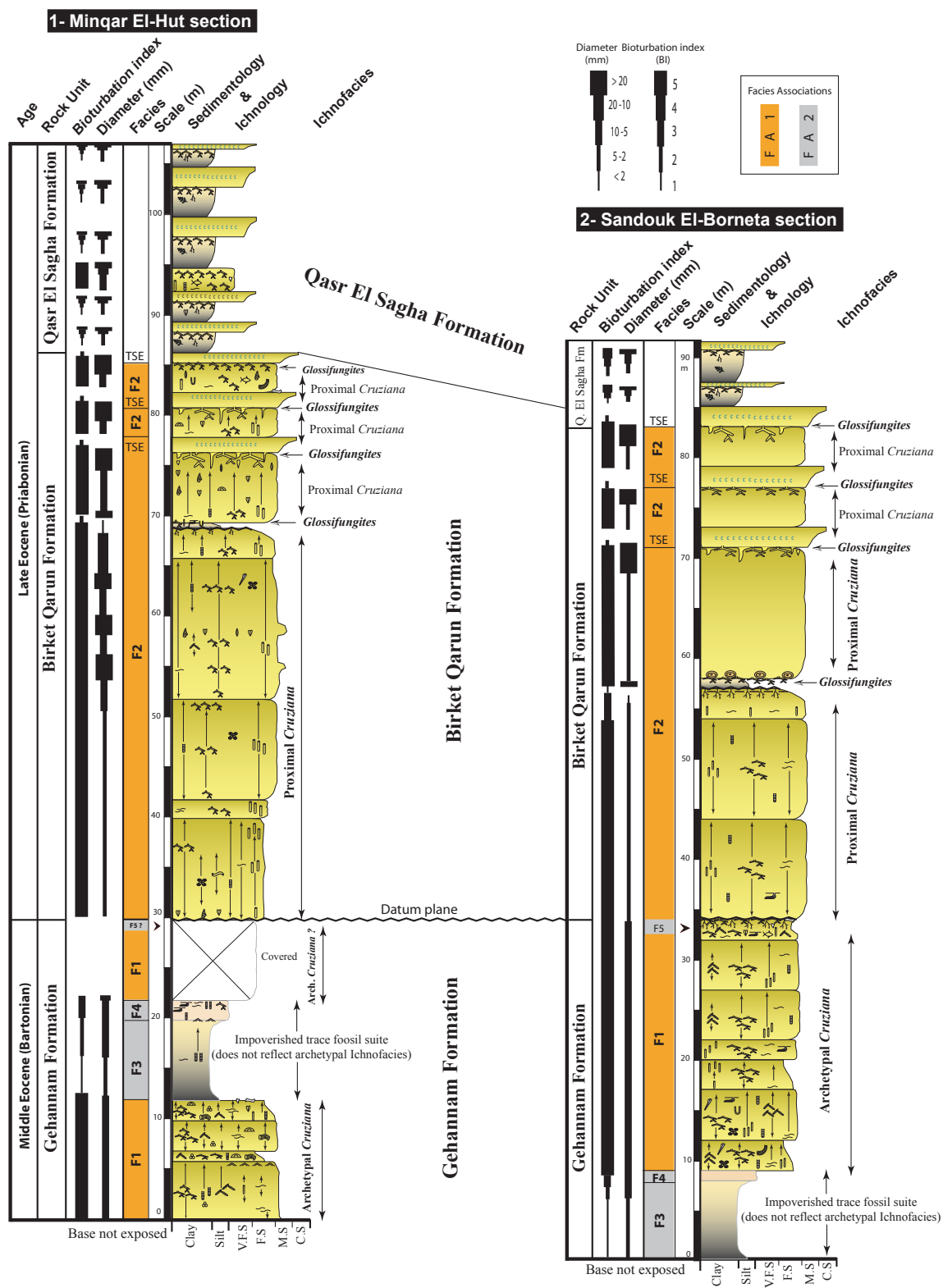


FIGURE 3.3. Correlation chart of the Middle-Upper Eocene succession in the composite section of Minqar El-Hut and Sandouk El-Borneta section in the area of Wadi El-Hitan.

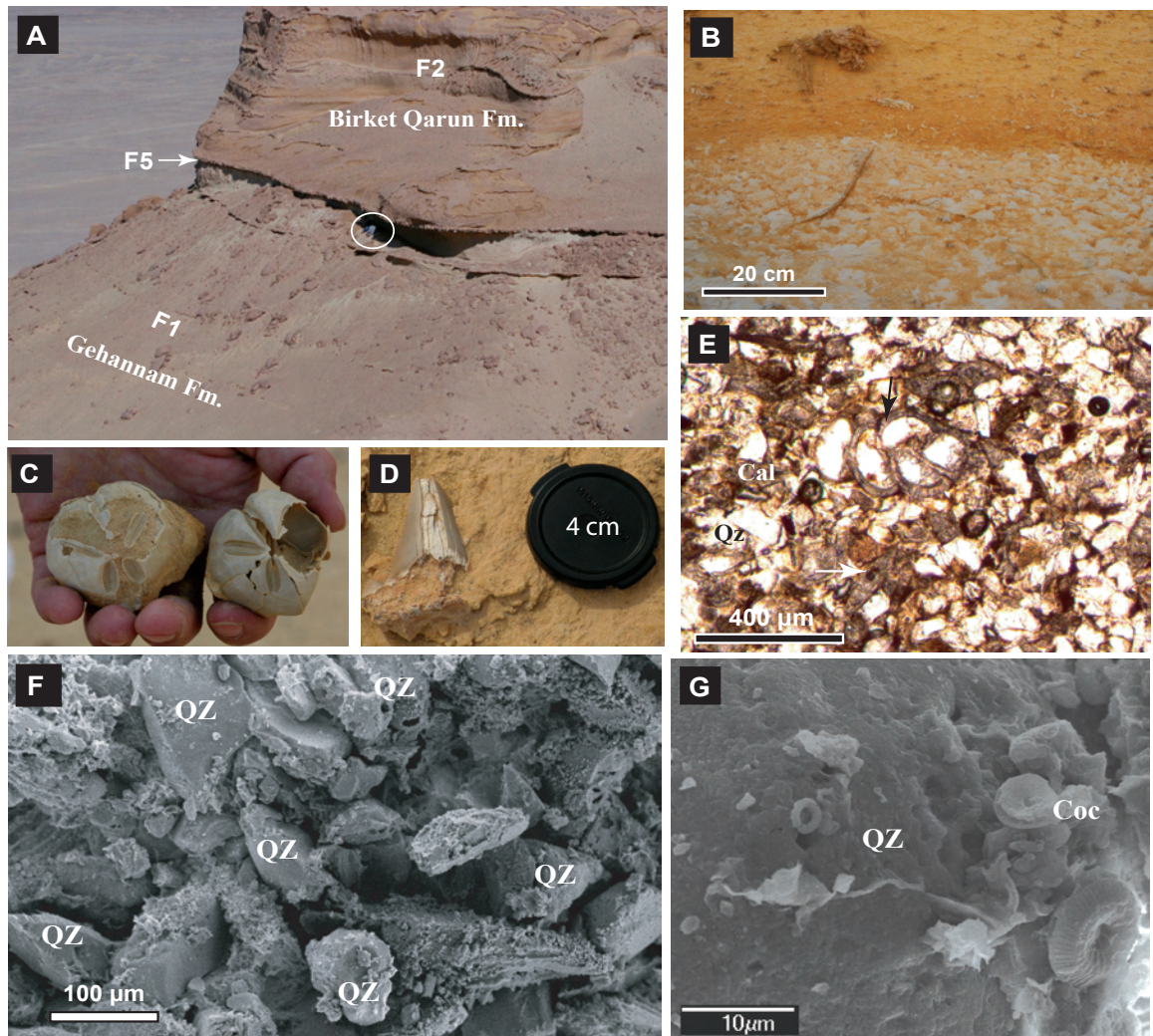


FIGURE 3.4. Selected photographs, showing the characteristics of Facies 1 (FA1). **A-** Rhizolith/ trace-fossil bearing sandstone (F5) marking the boundary between Gehannam Formation (F1) below and Birket Qarun Formation (F2) above, Sandouk El-Borneta section. (Man in the white circle for scale). **B-** Intensive bioturbation (BI 5) and burrow mottles found in the sandstone of F1 at the base of Sandouk El-Borneta section. **C-** Irregular echinoid *Shizaster* sp. found in F1, Minqar El-Hut section. **D-** Large-sized shark's tooth found in F1, Minqar El-Hut section. **E-** Transmitted light photomicrograph, showing the textural and mineralogical maturity of the calcareous quartz-arenite microfacies of F1. Planktonic foraminifera (black arrow), benthonic foraminifera (white arrow), and brownish calcareous bioclastics are associated with the dominantly monocrystalline quartz grains (Qz). Quartz overgrowth (resulted in the angular appearance of quartz grains) and the carbonate cement (Cal, brownish color) constitute the main cement types. **F-** SEM micrograph showing the pore filling, pervasive authigenic marine calcite, cementing the quartz grains (Qz) in Facies 1. **G-** SEM micrograph showing an assemblage of nannoplankton (coccoliths) stacked on the surface of quartz grain (rough surface is due to micro-quartz overgrowth).

includes one large (approximately 10 meter long) allochthonous tree trunk that is thoroughly bored with *Teredolites longissimus* (Fig. 3.8G).

Facies 2 (F2): Medium- to Fine-Grained Bioturbated Sandstones

Facies 2 is composed of grayish white to yellow, very fine- to medium-grained dolomitic-calcareous quartz arenite (Figs. 3.5C-D). Sandstones of F2 show mature textural and mineralogical characteristics that are broadly similar to F1. Facies 2 constitutes almost the entire Birket Qarun Formation (Fig. 3.3). Stratal thicknesses range between 44 and 52 m. Beds thicknesses vary between 3 and 10 m, with an average thickness of 7 m. The beds are cliff forming, with sharp basal bedding contacts, and upward sporadic bioturbated-based bedding contacts. The base of F2 locally overlies F5 (described below). Upwards, F2 is truncated by successive wave ravinement surfaces that demarcate several parasequence boundaries (Fig. 3.3). The ravinement surfaces are overlain by lag deposits and sporadically distributed coquina beds. Due to high degrees of bioturbation, primary physical sedimentary structures are rarely preserved. Fossils recorded in F2 include bivalves (thin-shelled pectinids, oysters, *Lucina pharaonis*, and sea pens), common gastropods (*Turritella pharaonica*), echinoid fragments, barnacles, crab carapace fragments, fish scales, sharks' teeth, well-preserved whale skeletons (e.g., *Basilosaurus isis*; Fig. 3.5B, and *Dorudon atrox*), crocodiles and other (commonly disarticulated) marine-vertebrate bones. Planktonic foraminifera and coccoliths are common in F2 (Figs. 3.5C-D).

Facies 2 is highly burrowed (BI 5) and contains a high diversity of ichnogenera (Fig. 3.5A). Burrow diameters mostly lie between 5-10 mm, but some large (> 2 cm diameter) burrows are present. This trace-fossil suite is attributed to the proximal expression of the *Cruziana* Ichnofacies. Trace fossils (Table 3.3, Figs. 3.7, 3.8) include, in decreasing order of abundance, *Thalassinoides*, *Planolites*, *Ophiomorpha*, *Teichichnus*, *Asterosoma*, *Palaeophycus*, *Rhizocorallium*, *Skolithos*, *Cylindrichnus*, *Arenicolites*,

and *Psilonichnus*. This trace-fossil suite contains a mixture of deposit-feeding and dwelling structures, with rare to moderately abundant inferred suspension-feeding structures. Ravinement surfaces are demarcated by trace fossil suites dominated by robust firmground *Thalassinoides*. The large *Thalassinoides* are unlined, passively infilled, descend from a sharp contact, and are characteristic of the *Glossifungites* Ichnofacies (Figs. 3.3, 3.8F).

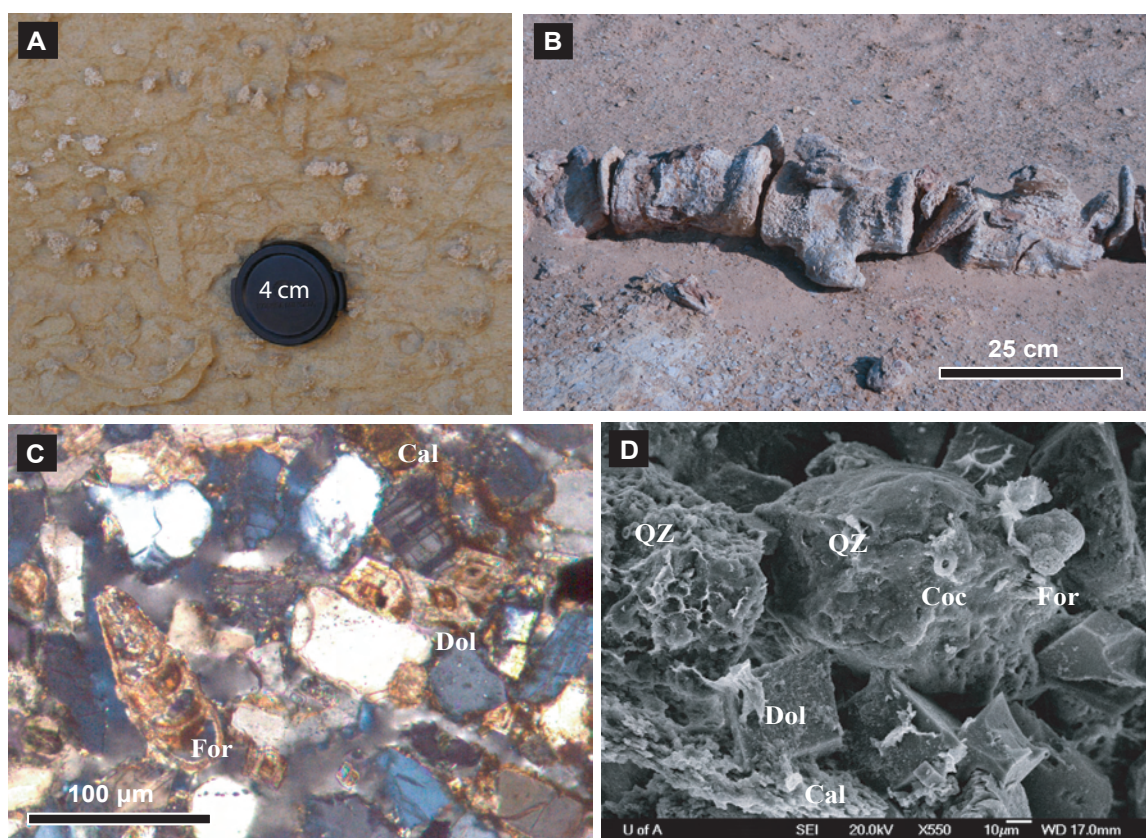


FIGURE 3.5. Selected photographs, showing the characteristics of Facies 2 (FA1). **A-** Burrow-mottled ichnofabric of the sandstone, Sandouk El-Borneta section. **B-** Large-sized segment of fossil-whale (*Basilosaurus isis*) skeleton in Facies 2. **C-** Optical photomicrograph (crossed nicols) showing the dolomitic quartz arenite microfacies of Facies 2. The dominantly monocrystalline quartz grains, rare feldspar (microcline grain, upper right corner), and the dolomitized foraminiferal test (For) are cemented by pervasive marine-dolomite cement (dol), quartz-overgrowth cement, and calcite (Cal) cement. **D-** SEM micrograph of (C), showing planktonic foraminifera test (For) and a coccolith (Coc) on the surface of a quartz grain (Qz), cemented by the characteristic pore-filling dolomite rhombs (Dol) and the calcite (Cal) cements.

FACIES ASSOCIATION 2: BAY MARGIN/COASTAL DEPOSITS

Facies Association 2 represents less than one third of the exposed outcrop of the Gehannam Formation and is absent in the Birket Qarun Formation. Occurrences of FA2 vary in thickness between 10 and 15 m. Facies Association 2 is dominated by three sedimentary facies: F3 (laminated sandy shale), F4 (locally bioturbated sandy siltstone), and F5 (fine-grained sandstone) (Figs. 3.3, 3.4A, 3.6A, E).

Facies 3 (F3): Laminated Sandy Shale

Facies 3 is represented by gray, fissile shale. The shale is sandy to silty, gypsiferous, and ferruginous (Figs. 3.6A-C). Facies 3 contains black manganese (Mn) micro-veins and black flecks, and disseminated dark carbonaceous detritus. Facies 3 has a total thickness of 8 m. This facies interfingers with F1 and underlies F4 (described below; Figs. 3.6A-B). Facies 3 is planar bedded to massive appearing. Body fossils are generally absent. Facies 3 is weakly bioturbated (BI 0-2), and has a very low diversity of ichnogenera. Upwards, rare *Teichichnus* and very rare *Planolites* (Fig. 3.7H) are present. Burrow diameters vary between 5 and 10 mm.

Facies 4 (F4): Sandy Siltstone

Facies 4 consists of brownish yellow, gypsiferous, locally ferruginous sandy siltstone (Figs. 3.6B, D). Occurrences of F4 vary in thickness between 1 and 2 m. This facies typically overlies F3 and underlies F1 (Figs. 3.6A-B). Abundant gypsum-filled joints, obliquely and horizontally oriented, demarcate the boundary between F3 and F4. Wave-ripple and low-angle cross-lamination are rarely preserved. No fossils were observed. Facies 4 shows an upward increase in both bioturbation intensity (BI 0-3) and ichnogenera diversity. The lower part of F4 contains rare to common *Teichichnus*. Upwards, trace fossils include abundant *Psilonichnus*, *Teichichnus*, *Thalassinoides* and *Planolites*. Although the trace fossil suites do not represent a clear archetypal ichnofacies,

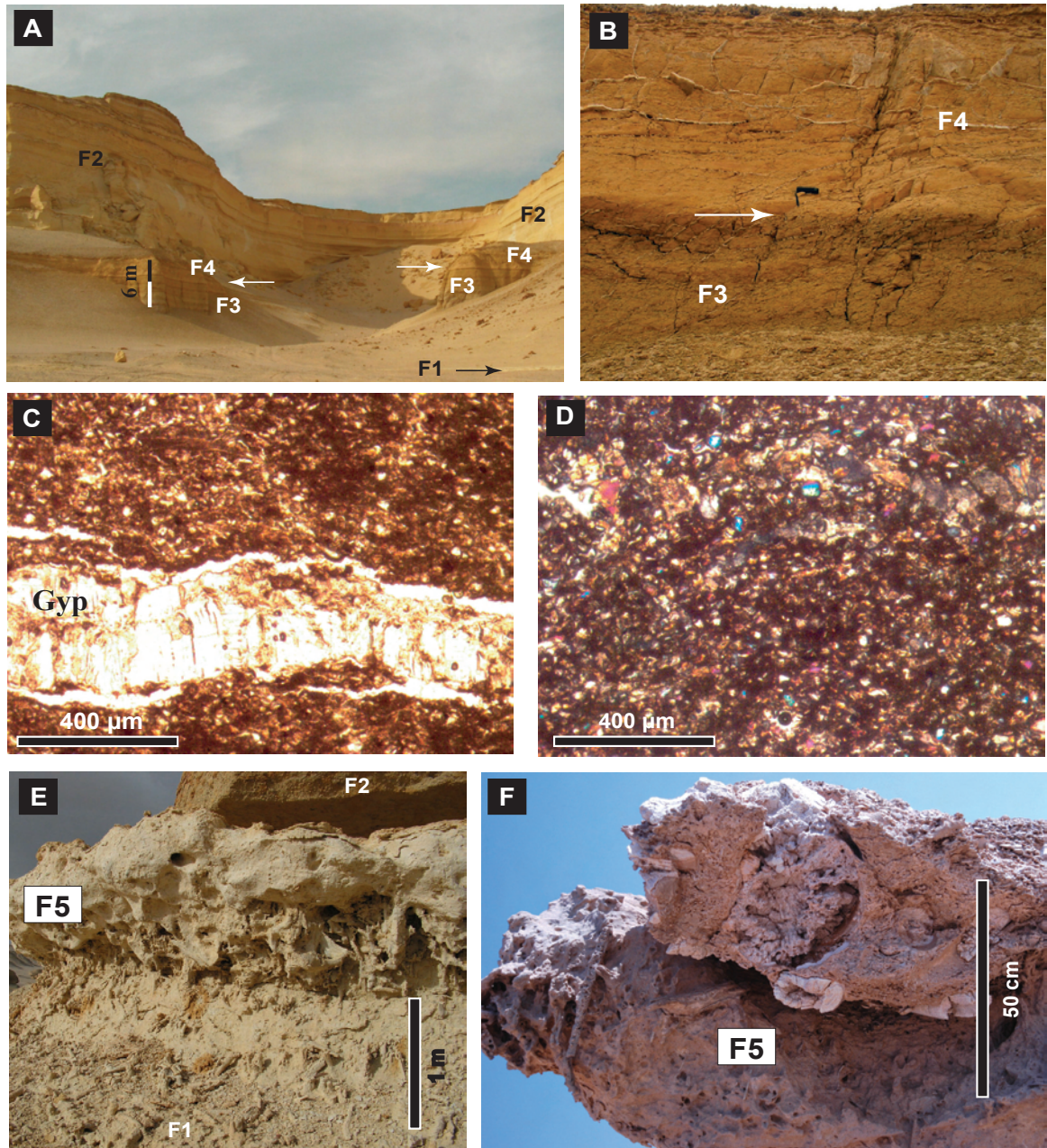


FIGURE 3.6. Selected photographs, showing the characteristics of Facies 3 through 5 (FA2). **A-** Facies Association 2 (sandy siltstone F4 overlies gypsiferous shale F3) is sandwiched between F1 and F2 of the FA1 in Minqar El-Hut. **B-** Close up of (A), showing the contact (white arrow) between the sandy shale (F3) below and the sandy siltstone (F4) above (black GPS is 15 cm long). **C-** Transmitted light photomicrograph of the silty and sandy shale (F3), showing the characteristic micro-vein gypsum (Gyp). **D-** Optical photomicrograph (crossed nicol) of the sandy siltstone (F4), showing gypsum (upper bright-color crystals). **E-** Fine-grained sandstone (F5), associated with a complex paleoecologic horizon between F1 and F2 in the area between Minqar El-Hut and Sandouk el-Borneta sections. **F-** Fragmented fossil-whale bones, associated with rhizoliths and invertebrate trace fossils in the sandstone of Facies 5 (FA2), Sandouk El-Borneta section.

the ichnological suite displays the characteristics of the *Psilonichnus* Ichnofacies, locally (e.g., Fig. 3.7I).

Facies 5 (F5): Fine-Grained Sandstone

Facies 5 comprises grayish white, very fine-grained sandstone. The thickness of F5 varies between 30 cm and 2 m. In the study area, Facies 5 outcrops sporadically as a diagnostic boundary separating F1 and F2, and marking the boundary between Gehannam and Birket Qarun formations (Figs. 3.4A, 3.6E). Physical sedimentary structures are very rare to absent. Fossils are common (e.g., marine vertebrate bone fragments, fish-remains, molluscan- and arthropod shell fragments) (Figs. 3.6F, 3.9D). Facies 5 displays rhizoliths, and moderate to locally high bioturbation intensities (BI 3-4). Ichnogenera diversities are moderate. Trace fossils include *Ophiomorpha*, *Thalassinoides*, *Skolithos*, *Planolites*, *Psilonichnus*, and rare *Teichichnus*. Also common within F5 are rhizoliths (i.e., sediment- and/or cemented sediment-filled root moulds; *sensu* Klappa, 1980) (Figs. 3.9A-D) and various potential trace fossils of terrestrial arthropods, such as horizontal spreiten-bearing structures (*Naktodemasis*) and ichnofossils assigned to *Scoyenia*.

BIOGENIC SEDIMENTARY STRUCTURES

INVERTEBRATE TRACE FOSSILS

Seventeen ichnospecies belonging to thirteen ichnogenera are identified from the Eocene whale-bearing strata in the area of Wadi El-Hitan. Table 3.2 summarizes the recorded ichnogenera, their type ichnospecies, summary diagnoses, generalized ethologies / trophic behaviors and commonly associated trace-making organisms. Descriptions of the identified ichnospecies—and the characters used to identify the ichnofossils in the study area—are summarized in Table 3.3. The vertical and stratigraphic distributions of the reported ichnofossils are shown in Fig. 3.3. Most of the

TABLE 3.2. Type ichnospecies, short diagnoses, ethologies, trophic behaviors, and possible trace-maker organisms of the Middle - Upper Eocene ichnogenera in the area of Wadi El-Hitan.

Ichnogenera	Type ichnospecies	Short diagnosis	Ethology	Trophic	Tracemaker
<i>Arenicolites</i>	<i>A. carbonaria</i> Binney, 1852	Vertical U-tubes without spreite, variable size, and smooth to sculptured walls can occur (Chamberlain, 1971).	Domicinia	Suspension-, Deposit- or Filter-Feeder	Polychaetes or Amphipods
<i>Asterosoma</i>	<i>A. radiciforme</i> von Otto, 1854	Radial 3 to 9 horizontal bulbous burrows starting from an axial tube, simple or budding dichotomously or in a fan-shaped pattern (Häntzschel, 1975).	Fodinichnia	Deposit-Feeder	Crustaceans and vermiform organisms
<i>Chondrites</i>	<i>C. targionii</i> Sternberg, 1833	Dendritic, smooth-walled, regular, asymmetric ramifying burrow system, neither interpenetration nor interconnection, constant diameter (Frey and Howard, 1985).	Chemichnia, Fodinichnia	Chemosymbiont/Deposit-Feeder	Polychaetes and Sipunculids
<i>Cylindrichnus</i>	<i>C. concentricus</i> Howard, 1966	Long subcylindrical burrows, vertical to horizontal, straight to gently curved, rarely branched, having multiple, concentrically layered walls (Frey and Howard, 1985).	Domicinia	Suspension- or Filter-Feeder	Terebellids
<i>Ophiomorpha</i>	<i>O. nodosa</i> Lundgren, 1891	Simple to complex burrow systems, lining smooth interiorly and densely to sparsely mamillated or nodose with pellets exteriorly (Frey et al., 1978).	Domicinia, Fodinichnia	Deposit-, Suspension-Feeder	Decapod Crustaceans
<i>Planolites</i>	<i>P. vulgaris</i> Nicholson & Hinde, 1874	Unlined, rarely branched, straight to tortuous, smooth to irregularly walled or annulated burrows, infillings distinct and structureless (Pemberton and Frey, 1982).	Fodinichnia, Pascichnia	Deposit-Feeder	Polychaetes
<i>Psilonichnus</i>	<i>P. tubiformis</i> , Fürsich, 1981	Vertical U-tube spreite, unlined burrows, of variable diameter, ranging from irregular shafts to J-, Y-, or U-shaped structures (Frey et al., 1984).	Domicinia	Suspension-, Deposit-Feeder	Decapod Crustaceans
<i>Rhizocorallium</i>	<i>R. jenense</i> Zenker, 1836	U-shaped spreiten-burrows, parallel or oblique to bedding plane, with distinct and more or less parallel limbs (Fürsich, 1974).	Fodinichnia	Deposit-Feeder	? Crustaceans
<i>Scolicia</i>	<i>S. prisca</i> de Quatrefages, 1849	Meandering trails, broadly U-shaped in section, with floor and lateral walls, floor shows a single or biserially alternating series of laminae (Smith and Crimes, 1983).	Fodinichnia	Deposit-Feeder	Echinoids and Gastropods
<i>Skolithos</i>	<i>S. linearis</i> Haldeman, 1840	Cylindrical to subcylindrical burrows, straight to gently curved, distinctly walled, vertical to steeply inclined burrows, up to meter long (Alpert, 1974).	Domicinia	Suspension-Feeder or Carnivore	Polychaete and ?Arthropods
<i>Teichichnus</i>	<i>T. rectus</i> Seilacher, 1955	Spreiten structures, rarely branched, composed of longitudinally nested burrows, showing retrusive or protrusive displacement (Frey and Howard, 1985).	Fodinichnia, Domicinia	Deposit-Feeder	Vermiform organisms
<i>Thalassinoides</i>	<i>T. callianassae</i> Ehrenberg, 1944	Three-dimensional burrow system composed of smooth, cylindrical tubes branching at Y- to T-shaped, enlarged at points of bifurcation (Häntzschel, 1975).	Domicinia, Fodinichnia	Deposit-, Suspension-Feeder	Decapod Crustaceans
<i>Teredolites</i>	<i>T. clavatus</i> Leymerie, 1842	Clavate borings in woody substrates, acutely turbinate, tapered and elongate to short, more or less circular in cross-section (Kelly and Bromley, 1984).	Domicinia / Fodinichnia	(Wood) Suspension-Feeder	Bivalves

reported ichnofossils are moderately to well preserved in full relief, but some biogenic structures show hyporelief preservation (Figs. 3.7, 3.8).

TABLE 3.3. Description of the ichnospecies identified in the whale-bearing Gehannam and Birket Qarun formations, Wadi El-Hitan area. Some of these ichnospecies are described and presented in Chapter 2.

1- *Arenicolites* isp. (Fig. 3.7A) Simple, vertical to inclined U-shaped slender tubes have smoothed walls. Tubes are 2-3 mm in diameter, 8-12 mm apart (in horizontal plain view), and with depths (vertical section) of 5-8 mm.

2- *Asterosoma* isp. (Fig. 3.7B) Star-shaped burrow system ranges from 50 to 90 mm across. These structures consist of radial arms (10-13 mm in diameter (max. width) and 20-30 mm in length). Arms are elongated, bulbous in the middle, tapering in one end, but some arms tapering on both ends. The internal structure has packed concentric laminations of sand (yellow) and clay (grayish).

3- *Chondrites* isp. (Fig. 3.7C) A complex dendritic burrow system (up to 40 mm across) consists of asymmetrically branching smooth-walled tunnels. These tunnels are neither anastomose nor converge, and are uniform in diameter (~2 mm). The lengths of some tunnels are traceable for > 30 mm, and ramifying from a master shaft (commonly secondary to tertiary order of branching).

4- *Cylindrichnus* isp. (Fig. 3.7D) Horizontal, isolated, and non-branched structure is the only recorded form. Vertical and inclined structures are not exposed. The cross-section is large and has an elliptical form (max. diameter 60-70 mm, min. diameter 12-16 mm). The wall has multiple, concentrically yellowish and grayish alternating layers. Central core is grayish in color and elliptical (5-15 mm in diameter) in shape.

5- *Ophiomorpha nodosa* Lundgren, 1891 (Figs. 3.7E, G) Simple to complex, horizontal to Vertical, Y-shaped, and branched cylindrical burrow system is the common morphology in FA1. The straight parts of the tubes are 10-60 cm in length and 20-45 mm in diameter. The internal burrow lining is smooth and has an average thickness of 1 mm. The burrow walls are exteriorly mammalated by densely and more or less regular pellets. The pellets are ovoid to discoid in shape (1-3 mm in length and average height of 2 mm). The burrow fills are structureless and consist of sediments similar to the host sediment.

6- *Ophiomorpha irregulaire* Frey, Howard & Pryor 1987 (Fig. 3.7F) horizontal Y-shaped structures are rare to common morphology, but locally observed upward in F1. The burrow system has irregular, sparsely mastoid wall exterior and better developed roof lining than floor lining.

7- *Planolites montanus* Richter, 1937 (Fig. 3.7D) Burrows are horizontal to subhorizontal, unlined, unbranched, and smaller in size (average diameter of 2 mm). The shape is sinuous to tortuous and circular to elliptical in cross-section. Walls are mostly smooth. Burrow fillings are structureless, and differs from the host sediments in color (grayish white) and grain size (finer sediments).

8- *Planolites beverleyensis* (Billings, 1937) (Fig. 3.7H) These burrows are straight, slightly curved, and larger in size (5-10 mm in diameter and > 30 mm in length). Some structures are stoutly flattened and have an elliptical cross-section. The walls are irregular and non-smoothed. Burrow infills differ from host sediments (grayish white gypsiferous claystone to reddish brown ferruginous very fine-grained sandstone).

9- *Psilonichnus upsilon*, Frey, Curran and Pemberton 1984 (Fig. 3.7I) Burrows are steeply inclined, rarely branched, unlined, and straight to slightly curved tubular structures. The morphology ranges from irregular shafts to J- and Y-shaped cylindrical forms, with a Y-shaped upper part if preserved. Burrow diameter varies between 3 and 6 cm, while the preserved depth or length is up to 18 cm.

10- *Rhizocorallium irregulare* Mayer, 1954 (Fig. 3.7B) Burrows are tongue-shaped, horizontally parallel to sub-parallel to bedding planes. Well-developed spreite exist between the limbs. The structure's length varies between 70 and 80 mm, whereas the total width ranges from 8 to 15 mm. Marginal tunnel is 2-3 mm wide, whereas spreite are 3-4 mm in width. Tube diameter/diameter of spreite ratio is generally > 1:5.

TABLE 3.3. (continued)

11- *Scolicia* isp. The plan view is not exposed. Well-developed groups of vertical sections are documented. They are circular to oval with diameters ranging between 2.5 and 3.5 cm. The internal structures have circular, oval and sub-concentric laminae.

12- *Skolithos linearis* Haldeman, 1840 (Figs. 3.7E, J) Burrows are cylindrical, straight to curved, distinctly smoothed walls, rarely branched, vertical to steeply inclined. Unornamented simple shafts are typically 2-4 mm in diameter with variable lengths.

13- *Skolithos ingens* (Hall, 1843) (Fig. 3.8K) These burrow structures are rare and have a characteristic bulged wall.

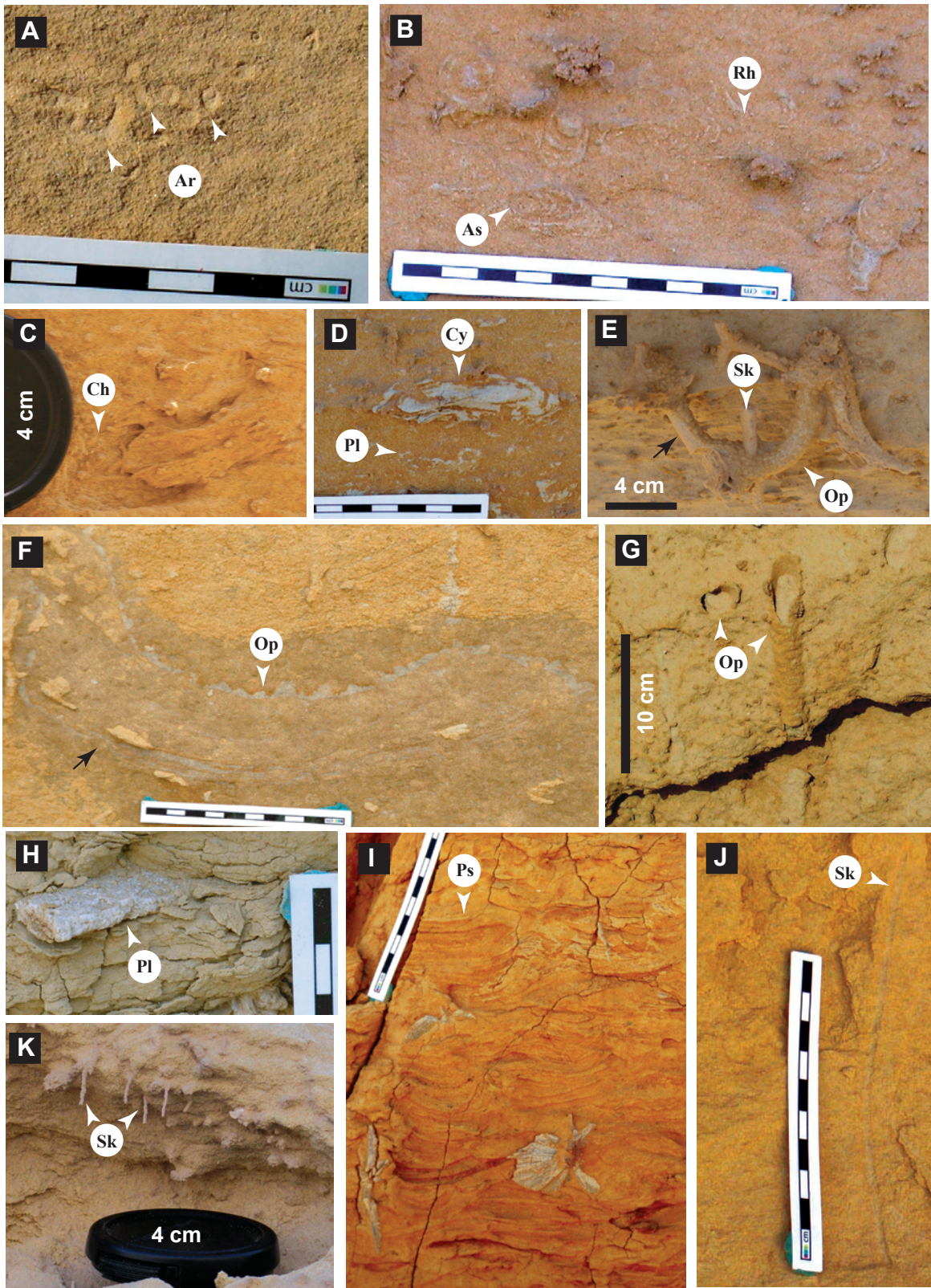
14- *Teichichnus rectus* Seilacher, 1955 (Figs. 3.8A-B) Vertical and unbranched spreiten structures consist of tightly packed, straight to broadly U-shaped laminae. Burrows have variable dimension sizes (max. length up to 150 mm; max. height up to 120 mm; widths between 20-30 mm). Longitudinal sections show nested burrows of simple, long, straight to sinuous, upward migrated, horizontal to sub-horizontal tunnels. These tunnels are mostly retrusive and merge upward with various angles with respect to bedding planes.

15- *Thalassinoides suevicus* (Rieth, 1932) (Figs. 3.8C-E) The burrows are predominantly horizontal, regularly branched. They form bedding-parallel mazes, with an overall length >1m. Branches ramify at acute angles. The Y-shaped dichotomous bifurcations dominate T-shaped branches. The branches are cylindrical in shape and circular to oval in transverse section. The straight segments may extend to several decimeters long. Diameter ranges from 2 to 3 cm. Swollen and enlarged divergence areas, turning chambers, have expanded diameters up to 5 cm. Burrow walls are mostly smooth and unlined. Burrow fills are structureless, but curvilinear- laminated meniscae are locally recorded.

16- *Thalassinoides paradoxicus* (Woodward, 1830) (Fig. 3.8F) Burrow system is complex, irregular branched box-work network. The network is oriented at various angles to the bedding planes, with an overall length up to 80 cm. Both Y-shaped bifurcations and T-shaped intersections are common. Subcylindrical to cylindrical branches, circular to elliptical in transverse sections. Diameter varies between 10 mm and 30 mm. Straight segments extend for 50 cm long. The burrow walls are mostly smooth, but some rare knobs may be reported.

17- *Teredolites longissimus* Kelly and Bromley, 1984 (Fig. 3.8G) Inclined molds occur as subcylindrical to club-shaped clusters of borings in xylic substrate. The individual boring has a diameter of 5-10 mm and length of 30-70 mm. The length/diameter ratio is > 5. Apertures are circular to subcircular in cross-section. The boring walls are straight in their upper parts and tend to be slightly sinuous and curved downward. The external borings' walls are mostly smooth, but some molds show sub-parallel series of ridges and grooves.

FIGURE 3.7. Invertebrate trace fossils: **A-** Monospecific suite of *Arenicolites* isp. (Ar) (F2: Sandouk El-Borneta section). **B-** Complex ichnofabric, showing *Asterosoma* isp. (As) and *Rhizocorallium irregulare* (Rh) (F1: Sandouk El-Borneta section). **C-** Rare *Chondrites* isp. (F1: between Sandouk El-Borneta and Minqar El-Hut sections). **D-** Complex ichnofabric of *Cylindrichnus* isp. (Cy) and *Planolites montanus* (Pl) (F1: Sandouk El-Borneta section). **E-** *Skolithos linearis* (Sk) (7 cm long) cross cut the *Ophiomorpha nodosa* (Op) (F5: Sandouk El-Borneta section). **F-** Horizontal large-sized *O. irregulare* (black arrow) (F1: Minqar El-Hut section). **G-** Vertical form of *Ophiomorpha nodosa* (Op) (F5: between Sandouk El-Borneta and Minqar El-Hut sections), note the thin lining in burrow to the middle left. **H-** Flattened large-sized *Planolites beverleyensis* (Pl) (F3: Minqar El-Hut section). **I-** Monospecific suite of *Psilonichnus upsilon* (Ps) (F4: Minqar El-Hut section). **J-** Long and smoothed-walled *Skolithos linearis* (Sk) (F2: Old Camp Site). **K-** Short rough-walled *Skolithos ingens* (Sk) (F2: Sandouk El-Borneta section).



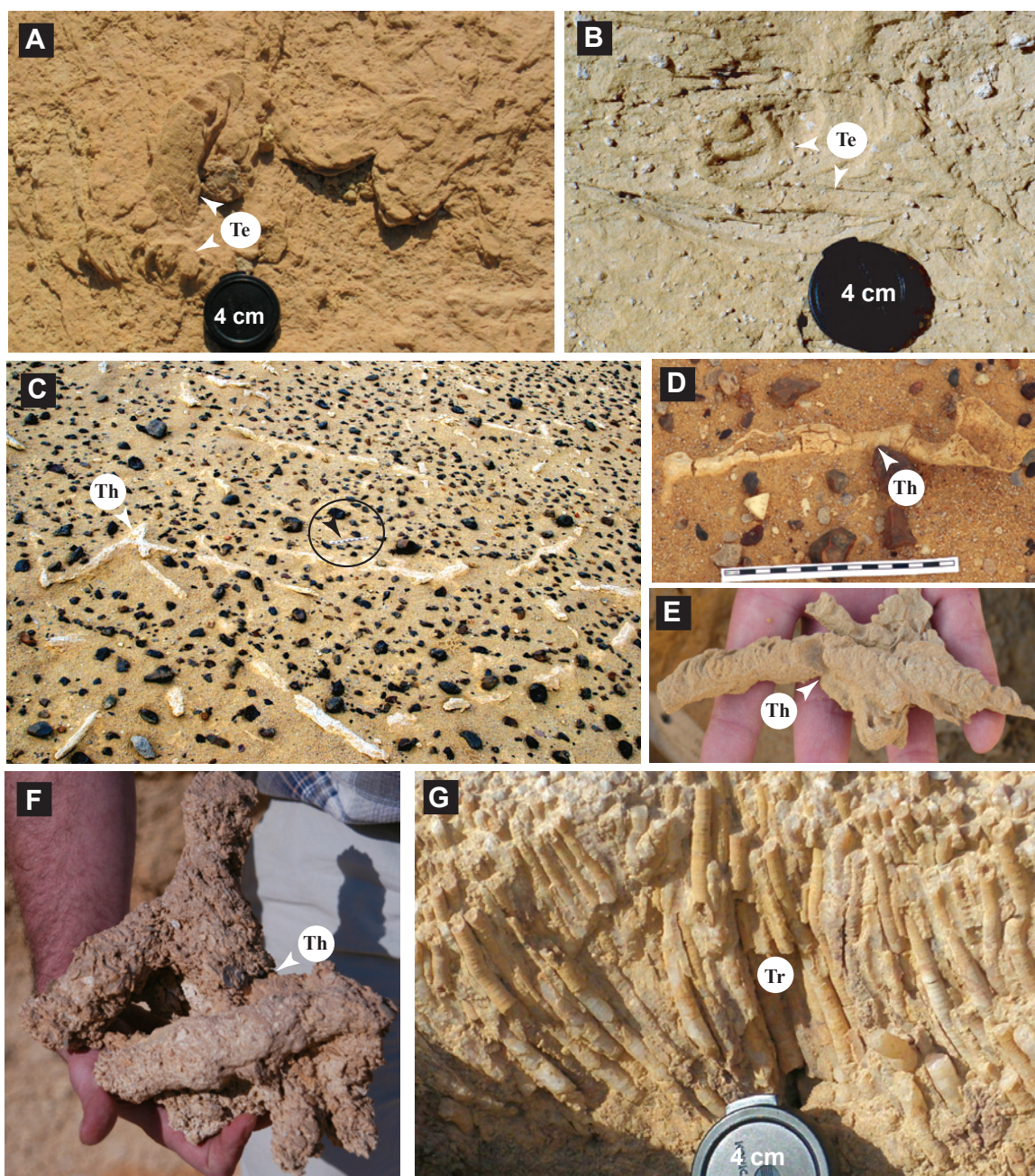


FIGURE 3.8. Invertebrate trace fossils: **A-** Plan view of monospecific suite of *Teichichnus rectus* (Te) (F2: Sandouk El-Borneta section). **B-** Longitudinal and vertical cross sections of *Teichichnus rectus* (Te) (F2: Sandouk El-Borneta section). **C-** Horizontal maze of *Thalassinoides suevicus* (Th) (F1: Minqar El-Hut section) (bar scale, black arrow, is 20 cm long). **D-** Close-up view of (C), showing *Thalassinoides suevicus* (Th) tube with a large swollen and enlarged divergence area (turning chamber) to the right. **E-** Rare *Thalassinoides suevicus* (Th) with curvilinear-laminated meniscae (F4: Minqar El-Hut section). **F-** Irregularly branched, passively filled box-work network of *T. paradoxicus* (Th) (F2: Old Camp site). **G-** Allochthonous *Teredolites longissimus* (Tr) (F1: between Sandouk El-Borneta and Minqar El-Hut sections).

PLANT-ROOT FOSSILS (RHIZOLITHS)

Two types of rhizoliths, restricted to two stratigraphic horizons, have been identified in the Middle-Upper Eocene succession (Figs. 3.3, 3.9). The first type (Type 1 rhizoliths) is associated with a paleoecologically complex horizon that marks the boundary between the Gehannam and Birket Qarun formations. The second type (Type 2 rhizoliths) is constrained to a thin stratigraphic horizon in the middle part of the Birket Qarun Formation (Fig. 3.3).

Type 1 Rhizoliths

Rhizolith clusters outcrop sporadically in a distinctive association with *Thalassinoides*, *Ophiomorpha*, *Psilonichnus*, and *Naktodemasis* (Figs. 3.6E-F, 3.7E, G, 3.9A-D)—between F1 and F2 of the FA1 (Figs. 3.3, 3.4A, 3.6E). Rhizoliths are associated with marine- to marginal-marine fossils (Figs. 3.6F, 3.9D). Type 1 rhizoliths are medium to large in size. They are preserved in upright to inclined and horizontal growth positions (Figs. 3.9A-D). These root casts are preserved as branched, irregular tubes that are filled with calcareous sandstone. Root casts show various branching patterns, which are dichotomized into smaller downward-tapering branches (Figs. 3.9A-D). Rhizoliths are weather resistantly, and have a brownish-yellow color.

The varied dimensions and morphologies of the Type 1 rhizoliths (Figs. 3.9A-D) are similar to those associated with bush and tree plants of arid to semi-arid climates (e.g., Sarjeant, 1975; Retallack, 2001; Gregory et al., 2004). These are not the product of a single plant type. They were formed by a variety of unidentified Middle Eocene plants, occupying bay-margin swamps to supratidal settings.

Type 2 Rhizoliths

Type 2 rhizoliths locally and sporadically demarcate the alluviated sandstone horizon of F2 (FA1) in the middle Birket Qarun Formation (Fig. 3.9E). These structures

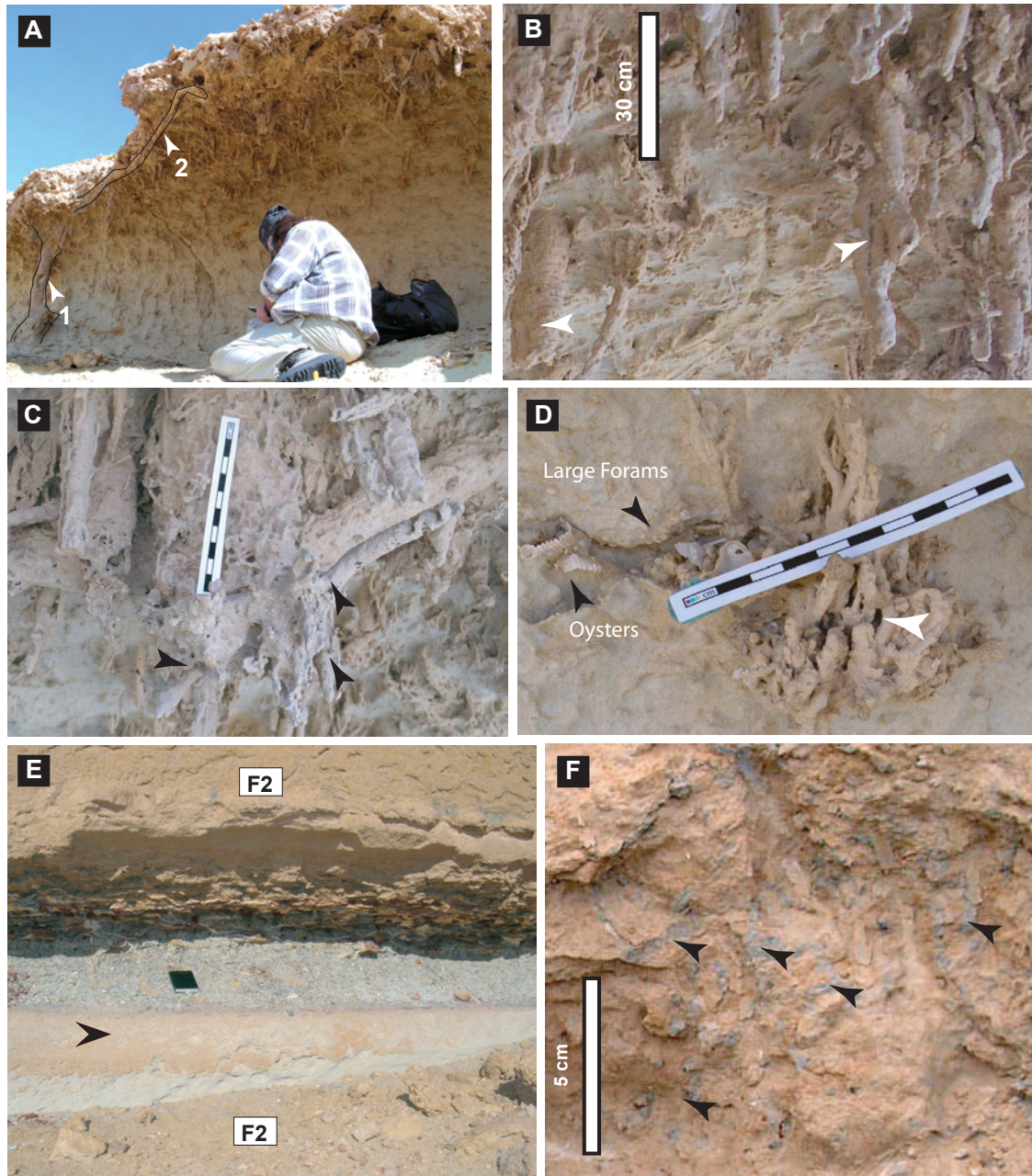


FIGURE 3.9. Type 1 and Type 2 rhizoliths: **A-** Three-dimensional roof gallery of the complex paleoecologic horizon in Facies 5, bounding the Gehannam and Birket Qarun formations, Sandouk El-Borneta section. Type 1 rhizoliths; a horizontal root (2) radiates laterally for more than a meter, with a diameter up to 5 cm, with a possible vertical bush (1) up to 1 m high and >20 cm in diameter. **B-** Close-up view of (A), showing the Type 1 rhizoliths (white arrows), with their diagnostic downward dichotomization and tapering. **C-** Close-up view of (A), showing another branching type (black arrows) of the Type 1 rhizoliths. **D-** Close-up view of (A), showing another isolated branching of the Type 1 rhizoliths (white arrow), associated with oysters and the large foraminifera (*Nummulites* sp.). **E-** Type 2 rhizoliths, demarcating the upper alluviated sandstone of Facies 2 (black arrow), Sandouk El-Borneta Section (notebook is 25 cm long). **F-** Dark grey, small-sized Type 2 rhizoliths (black arrows) are preserved in upright, inclined, and horizontal growth position, Sandouk El-Borneta section.

are preserved as root casts, and rare root moulds and root tubules in upright and horizontal growth positions (Fig. 3.9F). The density of rhizoturbation is locally moderate to high. The rhizoliths are characterized by their smaller dimensions and dark gray color (Fig. 3.9F). Diameter ranges between 3 and 6 mm. The exposed excavated height is up to 10 cm.

The small dimensions and the moderate to high degree of rhizoturbation associated with the Type 2 rhizoliths (Figs. 3.9E-F) are good indicators of rhizoliths associated with grass plants (e.g., Klappa, 1980; Retallack, 2001; Hasiotis, 2004).

PALEOENVIRONMENTAL AND SEDIMENTOLOGIC SETTING

The defined facies associations and their genetically related sedimentary facies are integrated with the reported ichnofossils and their corresponding ichnofacies to propose the paleoenvironmental and sedimentologic model illustrated in Fig. 3.10. Facies Association 1 is interpreted to have accumulated in a low-energy fully-marine bay. Facies Association 2 represents shallowing episodes and / or progradation of the sheltered bay-margin paleoenvironment.

INTERPRETATION OF FACIES ASSOCIATION 1

High degrees of bioturbation and very rare preservation of sedimentary structures are consistent with slow and continuous sedimentation. Rarely preserved oscillation ripple lamination suggests that physical reworking that accompanied sedimentation was dominated by waves.

The reported ichnological suites reveal several paleoecological factors that accompanied the deposition of FA1. Abundant occurrences of *Thalassinoides* (Figs. 3.8C-D) and *Planolites montanus* (Fig. 3.7D) indicate (basinwards) low-energy oxygenated conditions. Copious large, horizontal domichnia, represented by *Ophiomorpha nodosa* and *O. irregulairae* (Figs. 3.7E-G), are indicators of useful nutrients within low-energy

environments (e.g., Frey et al., 1978; Howard and Frey, 1984; Pollard et al., 1993). Likewise, *Scolicia*, *Chondrites* (Fig. 3.7C), *Asterosoma* and *Rhizocorallium irregulare* (Fig. 3.7B) are reasonable indicators of low-energy marine environments. More specifically, *Rhizocorallium* and *Asterosoma* reflect the activity of organisms that favor sublittoral depths generally near or below wave-base (e.g., Farrow, 1966; Fürsich, 1998). Rare, large and horizontal forms of *Cylindrichnus* (Fig. 3.7D) (e.g., Fürsich, 1974; Frey et al., 1990) and the paucity of domicinia of suspension feeders, such as represented by *Skolithos* (Fig. 3.7J) and *Arenicolites* (Fig. 3.7A), further support deposition in a low-energy depositional environment.

Finally, the intercalated transition of FA1 into the locally rooted FA2 (bay-margin deposits, interpreted below) and absence of gradational progradation to shoreface or a delta succession suggest that although dominated by low-energy conditions, FA1 accumulated in relatively shallow waters. Thereby, the deposits of FA1 are ascribed to sedimentation in a low-energy embayment with limited fluvial influx and open connection to consistently marine conditions (Figs. 3.10, 3.11).

INTERPRETATION OF FACIES ASSOCIATION 2

The abrupt vertical facies change from FA1 to FA2, combined with the sporadic and spatially varied stratigraphic distributions of FA2 (Figs. 3.3, 3.4A, 3.6A, E) are attributed to dynamic facies-belt shifting in a nearshore locale. The gypsiferous sandy shale lithology of F3 (Figs. 3.6B-C), the presence of gypsum streaks and carbonaceous detritus, and the general absence of current-generated sedimentary structures coupled with reduced bioturbation intensities (BI 0-2) and low ichnological diversities indicate deposition in an energy-sheltered locale that was influenced by fluctuating evaporation and therefore was physico-chemically stressed (e.g., Gingras et al., 2007; MacEachern and Gingras, 2007).

Facies 4 shows an upward increase in both bioturbation intensities (BI 0-3) and

ichnogenera diversities. The monospecific suite of *Psilonichnus upilon* (Fig. 3.7I) reflects typical facies deposited in the upper beach to lower dune environment (e.g., Curran, 1984; Frey et al., 1984), intertidal to subtidal conditions in a brackish, sheltered bay setting (e.g., Gingras et al., 2000), or in supratidal/backshore locales (Frey et al., 1984). Upwards abundance of *Teichichnus* and *Thalassinoides* (Fig. 3.8E) in F4 likely represents shallow subtidal and intertidal sedimentation with rare supratidal zones locally preserved.

Rhizolith / trace-fossil bearing sandstones (i.e., F5) of FA2 represent bay-margin swamps that encroached or interfingered with intertidal-flat and low-relief tidal channel, and supratidal deposits. Similar swamps have been reported mainly from tropical to subtropical coastal waterways of weakly tidal-influenced bay-margin paleoenvironments (e.g., Taylor et al., 2001; Gingras et al., 2002; Gregory et al., 2004). This interpretation is based on: (1) the presence of diverse rhizolith morphologies, displaying various types and orders (second and third orders) of dichotomization (Figs. 3.9A-D); (2) the presence of trace fossils attributable to the activities of insects (e.g., undiagnosed horizontal spreiten-bearing structure and possible *Naktodemasis*); and (3) commonly observed marginal-marine through to brackish-water trace-fossil assemblages (e.g., *Ophiomorpha*, *Thalassinoides*, *Skolithos*, *Planolites*, *Psilonichnus*, and rare *Teichichnus*). Reddish and brownish oxidation colors of the root-cast sediments and the preservation of root moulds and casts imply that swampy and/or intertidal/supratidal substrates were at least partly consolidated during subaerial exposure (see Klappa, 1980).

The vertical succession through FA2 indicates persistent progradation of the bay margin from shallow, restricted sedimentation to subaerially exposed, low-relief backshore settings (Figs. 3.10A, C). In summary, deposits of FA2 are best attributed to low-energy, shallow-water regimes, with a locally channelized bay margin. These grade upwards into intertidal/supratidal sediments and backshore swamp deposits (Fig. 3.10).

DISCUSSION

SOURCE OF SEDIMENTS IN FACIES ASSOCIATION 1

The accumulation of a thick (60-80 m composite thickness) succession of sandstones of FA1, the high intensities of uniformity bioturbation (BI 5), and the general absence of preserved primary physical sedimentary structures, combined with the local intercalation of bay-margin deposits (FA2) and notable absence of vertical facies change into shoreface or deltaic successions lead us to beg the question: what is the source and transport mechanism of the abundant clastic sediments? Three possible sediment transport mechanisms are suggested: nearshore Tethyan currents, hypopycnal plumes, and wind-blown sand (eolian).

Overall low relative sea levels and/or tectonic uplift during the late Middle Eocene (Late Bartonian) and Late Eocene (Priabonian) led to the emergence of the Cretaceous/Eocene highs as a land mass (Fig. 3.11). These Cretaceous-Eocene highs are considered as the main source of sediments in the northern cratonic basins of Egypt during Middle-Upper Eocene (see Salem, 1976). Streams feeding large delta systems (e.g., the Eocene El Bahr Depression system) and smaller delta systems transported these clastic sediments from the Cretaceous-Eocene structural high, and deposited them into the Eocene Tethys Sea (Fig. 3.11). The textural and mineralogical maturity of the sandstone and the presence of a single allochthonous *Teredolites*-bored tree trunk may be explained as the result of long-shore transport over considerable distances (Fig. 3.11). However, the paucity of physical sedimentary structures and the presence of intense bioturbation suggest that long-shore Tethyan paleocurrents were not sufficiently strong to stand alone as a dominant sediment transport mechanism in the Wadi El-Hitan area.

It seems more likely that river-born fine- and very fine-grained sand was introduced as hypopycnal plumes. In this hypothesis, fluvial systems (Fig. 3.11B) supply a substantial suspended sediment load into the Tethys Sea. The fine- and very fine-grained

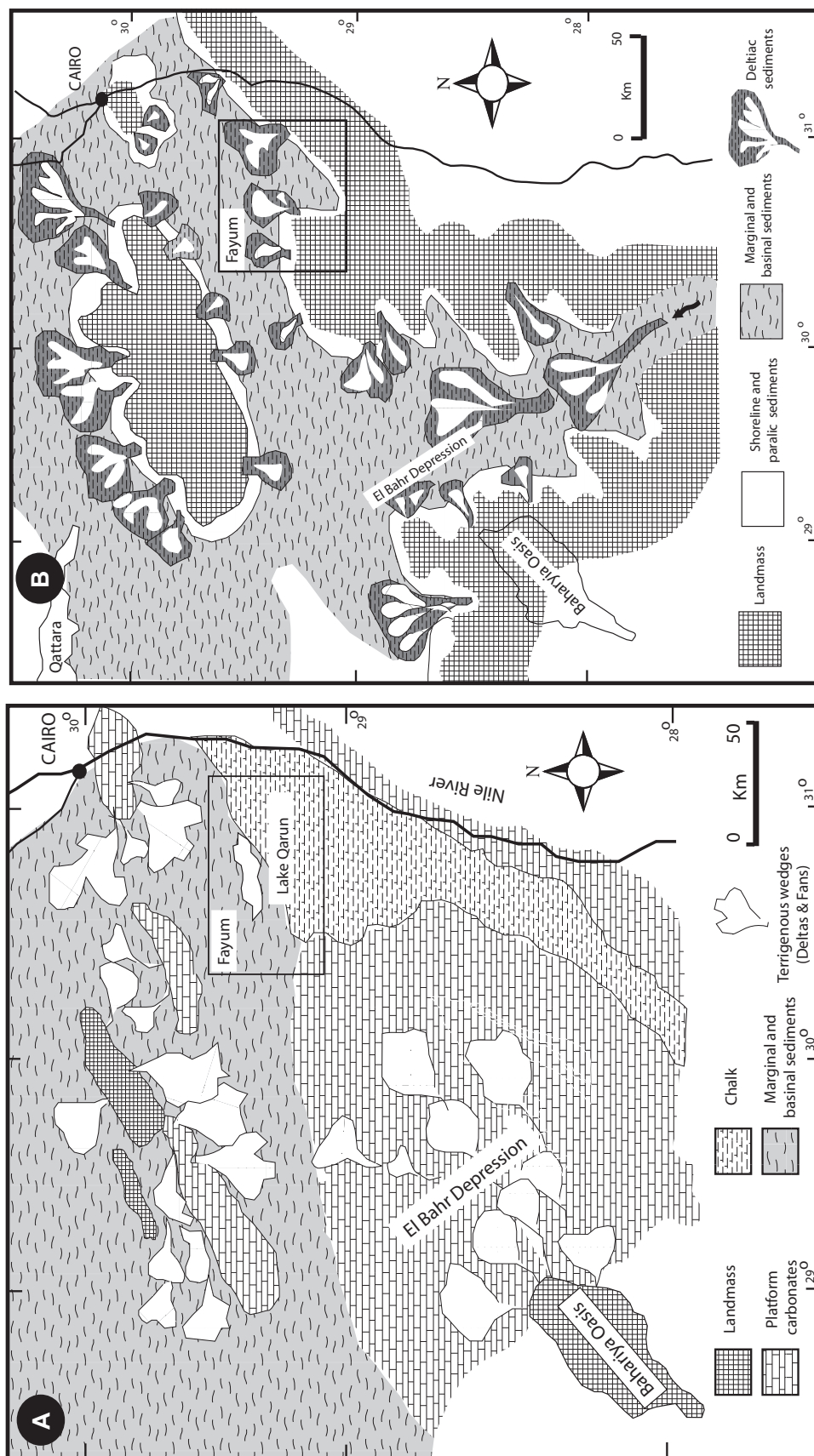


FIGURE 3.11. Generalized sedimentary depositional models of northern Egypt, comprising Fayum area, during Middle Eocene (A) and Late Eocene (B) (Modified after Salem, 1976). The structural highs (bounding Faym Basin) provided clastic sediments to the Fayum (Gindi) Basin. A large delta system (see El Bahr Depression) and smaller delta systems conducted the clastic sediments to the Tethyan paleocurrents, which distributed these sediments to the Fayum (Gindi Basin) in a less-restricted strait or gulf.

sands are derived from suspension from a hypopycnal plume—the sediments of which were subsequently remobilized (see Wright and Nittrouer, 1991) from near the river mouths and transported by the low-energy marine processes of waves and longshore currents along depositional strike into the Fayum embayment. In this scenario, most of the muddy fraction would have to be buoyed and deposited elsewhere in the basin. The merits of this two-stage transport hypothesis are consistent with the evidently low-energy depositional character of FA1. The resulting strata differ from those formed in shelf-sand plume models (e.g., Scheihing and Gaynor, 1991), and modern examples of dispersal of river sediments in coastal seas (e.g., Wright and Nittrouer, 1991), in that in our studied intervals no physical sedimentary structures are preserved. Neoichnological experiments (see Gingras et al., 2008) showed that a moderate population of bioturbating fauna of the *Cruziana* Ichnofacies can churn bottom sediments to a depth of 10 cm in 42 days. However, under high population densities, the deposit-feeding animals could bioturbate the same sediments in less than a day (e.g., Gingras et al., 2008). This high burrowing rate highlights the role of bioturbation in obliterating the physical sedimentary structures under low-energy depositional processes.

An eolian source could also explain the observed textural and mineralogical maturity. Eolian transport also has the merits of being able to supply continuous sediment at modest rates, thereby facilitating the highly bioturbated character of FA1 under conditions of constant slow aggradation. However, the residence of the Fayum province in a tropical climatic zone (Lotfy and Van der Voo, 2007), the long time span of the accumulations of FA1, and the transition of FA1 into the locally rooted and swampy facies of FA2 suggest that an eolian transport mechanism is less likely to be the dominant sediment transport mechanism. Nevertheless, eolian sand could still have been an occasional and local source of sediment, where wind acted as an important transport mechanism in the study area.

**PALEOENVIRONMENT AND PALEO GEOGRAPHIC DISTRIBUTION OF
THE FAYUM EOCENE WHALES**

The robust skeletons of *Basilosaurus isis* (~18 m long) and *Dorudon* sp. (5 m long) are abundantly interred within the sandstones of FA1. The whale bones are poorly preserved and occur sporadically near the top of F1 in the Gehannam Formation. Well-preserved skeletons of these whales are most abundant in Facies 2 of FA1 within the Birket Qarun Formation. These large- and medium-sized whales became extinct during the late Priabonian.

The proposed depositional models (Figs. 3.10, 3.11) indicate that the Eocene whales of the Wadi El-Hitan were completely aquatic, and resided in a large, quiescent fully-marine bay. The paleoecological physical parameters characteristic of FA1 include: shallow water depths within the euphotic zone, low depositional energy, low- to moderate-sedimentation rates, and the presence of sandy soft-ground substrates. Chemical parameters are interpreted to have included normal marine salinities and well oxygenated conditions. The optimal physico-chemical parameters resulted in an abundance of food resources and a correspondingly rich marine biodiversity. Therefore, the low-energy marine bay paleoenvironment of FA1 represents a typical environment for the flourishing of the Eocene whales and other marine vertebrates in the area of Wadi El-Hitan.

The Early-Middle Eocene whales (e.g., *Pakicetus* sp., *Ambulocetus* sp. and *Rhodocetus* sp.) were not fully aquatic (see Gingerich et al., 1983; 1994; Thewissen et al., 1994), and thus had a limited paleogeographic distribution (endemic to SE Asia). Unlike the previous early whales, the fully marine nature of *Basilosaurus* spp. (the largest creatures on Earth during the Middle-Late Eocene) and *Dorudon* sp. led to a broad paleogeographic distribution during the late Middle-Late Eocene. Global correlations of *Basilosaurus*-bearing strata show common sedimentological characteristics attributable to quiescent depositional energies and low to moderate sedimentation rates in offshore to open-marine gulf and bay paleoenvironments. The Middle Eocene (late Bartonian) *B.*

dazinda was recorded by Gingerich et al. (1997) from offshore shales in the middle part of Drazinda Formation, Pakistan. In North America, *Basilosaurus cetoids* and *Dorudon* sp. have been found in the Upper Eocene Pachuta Marl and Shubuta Marl members of the Yzoo Formation of Alabama, the strata of which were interpreted to reflect the slow accumulation of sediments in a shallow gulf coast / sea (e.g., Kellogg, 1936). Finally, bones of *B. isis* were also discovered from the glauconitic phosphorite-calcarenite bed in the Upper Eocene (Priabonian) Wadi Esh-Shallala Formation of Jordan (Zalmout et al., 2000).

PRESERVATION OF THE FOSSIL-WHALE BONES

The fossil-whale bones are well preserved as disarticulated to locally semi-articulated skeletons. Fully articulated skeletons are rare and sporadically distributed. Encrustation of the vertebrate skeletons is largely absent. Fossil-bone degradation and pyrite mineralization have not been observed. These characteristics are not consistent with whale skeletons interred on modern ocean floors, nor can such features be related to a beaching or stranding mechanism.

Modern (deep-marine) whale falls (e.g., Allison et al., 1991; Smith and Baco, 2003) yield fully articulated whale skeletons, dense (encrusting) colonization, intensive borings, marked bone degradation, and pyrite mineralization. Conversely, the stranding and beaching mechanism is rejected as a cause for the occurrences in the study area for a number of reasons. Firstly, there is no sedimentological evidence in FA1 for strong waves or currents capable of driving whales into the shallows of the coastline. Secondly, the fossil whales are not constrained to a single stratigraphic horizon, but they are spatially and vertically distributed throughout FA1. Thirdly, there is an absence of the parallel arrangement of the fossilized skeletons. The orientations of the heads relative to the trailing of *Basilosaurus isis* skeletons lie in two opposite directions in the area of Wadi El-Hitan (*sensu* Dolson et al., 2002). Fourthly, the reported fossil whale bones are not

assigned to a single-species community, a common condition associated with stranding. Finally, the stratigraphic occurrence of the whale skeletons is well below and above the shallow bay-margin deposits of FA2: whale-fossil occurrence is thereby stratigraphically lower and upper than stranding mechanisms would predict.

We suggest that the low-energy environment permitted gentle disarticulation of the deceased whales during resting to the bay floor. The sedimentation rates must have been at least moderate (especially upwards in Birket Qarun Formation) in order to bury the whales before they became encrusted and bored. Notably, this hypothesis is at odds with the fact that bioturbation eradicated sedimentary lamination, suggesting that sedimentation rates, although moderate, were relatively consistent and permitted thorough bioturbation. Peters et al. (2009) proposed a physical mechanism linking the distribution of the articulated to semi-articulated vertebrate remains to offshore marine flooding surfaces of a transgressive systems tract (TST), and attributed the disarticulated and isolated skeletons to lag deposits on the sequence boundaries. Our data indicate that the complete and semi-articulated whale skeletons (Fig. 3.4B) reside within the strata of the highstand systems tracts HST (see Chapter 2) in the low-energy deposits of Facies Association 1. However, these whale skeletons were buried or gently transported along the sea floor before burial. The fragmented whale bones are commonly associated with the high-energy TSE, which may have served to erode the vertebrate-bearing sediments and transport the whale bones, other vertebrate remains, and invertebrate shells for relatively long distances before accumulation as ravinement deposits (Fig. 3.5F).

SUMMARY

1. Middle-Upper Eocene deposits of the whale-bearing Gehannam and Birket Qarun formations can be divided into two main facies associations (FA1 and FA2). Facies Association 1 encompasses two genetically related sandstone facies (F1 and F2). Facies Association 2 is represented by shale (F3), siltstone (F4), and sandstone (F5) facies.

2. Seventeen ichnospecies belonging to thirteen ichnogenera of invertebrate trace fossils and two rhizoliths types are identified from these whale-bearing rock units. These include *Arenicolites* isp., *Asterosoma* isp., *Chondrites* isp., *Cylindrichnus* isp., *Ophiomorpha nodosa*, *O. irregulaire*, *Planolites montanus*, *P. beverleyensis*, *Psilonichnus upsilon*, *Rhizocorallium irregulare*, *Scolicia* isp., *Skolithos linearis*, *S. ingens*, *Teichichnus rectus*, *Thalassinoides suevicus*, *T. paradoxicus*, and allochthonous *Teredolites longissimus*.
3. The high bioturbation intensity, paucity of the physical sedimentary structures, and presence of ichnological suites attributable to archetypal and proximal expressions of the *Cruziana* Ichnofacies are taken together as indicative of FA1 deposition in a low-energy, open-marine bay setting.
4. Facies Association 2 represents a landward, shallow bay-margin setting. Ichnological and sedimentological characters of FA2 attest to deposition in a low-energy (locally channelized) bay margin that prograded into intertidal/supratidal and swampy settings.
5. The high intensity of bioturbation and an absence of preserved evidence of hydraulic reworking (i.e., wave- / current-generated sedimentary structures) in FA1 suggest that clastic point-sources are a combination of hypopycnal—nominally suggesting flashy point-source discharge—and weak Tethyan longshore currents. Eolian sand may be an occasional and important source of sediment.
6. The physical- (e.g., shallow water depths, low energy, and low to moderate sedimentation rates) and chemical-parameters (e.g., marine salinity and well oxygenated conditions) of the Eocene marine bay in Wadi El-Hitan resulted in an abundance of food resources, richness in marine biodiversity, and consequently a flourishing of the Eocene Whales in the marine-bay paleoenvironment.
7. The low-energy conditions (weak wave and currents) resulted in gentle disarticulation of the deceased whales during resting on the bay floor. The sedimentation rates must have been sufficiently rapid in order to inter the whales, but slow enough that bioturbation was able to eradicate any primary physical structures.

REFERENCES

- Allison, P. A., Smith, C. R., Kukert, H., Deming, J.W. and Bennett, B.A., 1991, Deep-water taphonomy of vertebrate carcasses: a whale skeleton in the bathyal Santa Catalina Basin: *Paleobiology*, v. 17, p. 78–89.
- Alpert, S.P., 1974, Systematic review of the genus *Skolithos*: *Journal of Paleontology*, v. 48, p. 661-669.
- Bann, K.L., Fielding, C.R., MacEachern, J.A. and Tye, S.C., 2004, Differentiation of estuarine and offshore marine deposits using integrated Ichnology and sedimentology: Permian Pebbly Beach Formation, Sydney basin, Australia, *in* McIlroy, D., ed., *The application of Ichnology to Palaeoenvironmental and Stratigraphic analysis: Geoleological Society of London Special Publication*, v. 228, p. 179-212.
- Beadnell, H.J.L., 1905, *The topography and geology of the Fayum Province of Egypt*: Egyptian Survey Department, Cairo, 101 pp.
- Bromley, R.G, Buatois, L.A., Mángano, G.M., Genise, J.F. and Melchor, R.N., 2007, *Sediment-Organisms Interactions: A Multifaceted Ichnology*: Society of Economic Paleontologists and Mineralogists Special Publication No. 88, 387 pp.
- Buatois, L.A., Gingras, M.K., MacEachern, J., Mángano, M.G., Zonneveld, J-P., Pemberton, S.G., Netto, R.G. and Martin, A., 2005, Colonization of brackish-water systems through time: Evidence from the trace-fossil record: *Palaaios*, v. 20, p. 321-347.
- Chamberlain, C.K., 1971, Morphology and ethology of trace fossils from the Ouachita Mountains, southeast Oklahoma: *Journal of Paleontology*, v. 45, p. 212-246.
- Curran, H.A., 1984, Ichnology of Pleistocene carbonates on San Salvador, Bahamas: *Journal of Paleontology*, v. 58, p. 312-321.

- Dames, W.B., 1894, Über Zeuglodonten aus Aegypten und die Beziehungen der archaeoceten zu den übrigen Cetaceen: Géologische und Paläontologische Abhandlungen, Jena, v. 5, p. 189-222.
- Dolson, J., El Barkooky, A., Gingerich, P.D., Prochazka, N. and Shann, M., 2002, The Eocene and Oligocene Paleo-Ecology and Paleo-Geography of Whale Valley and the Fayum Basins: Implications for Hydrocarbon Exploration in the Nile Delta and Eco-Tourism in the Greater Fayum Basin: American Association of Petroleum Geologists, Search Discovery Article # 10030: <http://www.searchanddiscovery.com/documents/cairo/index.htm>.
- Ekdale, A.A., Bromley, R.G. and Pemberton, S.G., 1984, Ichnology: The use of trace fossils in sedimentology and stratigraphy: Society of Economic Paleontologists and Mineralogists Short Course, v. 15, 317 pp.
- Elewa, A.M.T, Omar, A.A. and Dakrory, A.M., 1998, Biostratigraphical and paleoenvironmental studies on some Eocene ostracodes and foraminifers from the Fayoum depression, Western Desert, Egypt: Egyptian Journal of Geology, v. 42, p. 439-469.
- Farrow, G.E, 1966, Bathymetric zonation of Jurassic trace fossils from the coast of Yorkshire, England: Palaeogeography, Palaeoclimatology, Palaeoecology, v. 2, p. 103–151.
- Frey, R.W., Curran, H.A. and Pemberton, S.G., 1984, Trace making activities of crabs and their environmental significance: the ichnogenus *Psilonichnus*: Journal of Paleontology, v. 58, p. 333-350.
- Frey, R.W. and Howard, J.D., 1985, Trace Fossils from the Panther Member, Star Point Formation (Upper Cretaceous), Coal Creek Canyon, Utah: Journal of Paleontology, v. 59, p. 370-404.

- Frey, R.W., Howard, J.D and Pryor, W.A., 1978, *Ophiomorpha*: its morphologic, taxonomic, and environmental significance: *Palaeogeography, Palaeoclimatology, Palaeoecology*, v. 23, p. 199-229.
- Frey, R.W, Pemberton, S.G. and Saunders, T.D.A., 1990, Ichnofacies and bathymetry: A passive relationship: *Journal of Paleontology*, v. 64, p. 155-158.
- Fürsich, F.T., 1974, Ichnogenus *Rhizocorallium*: *Paläontologische Zeitschrift*, v. 48, p. 16–28.
- Fürsich, F.T., 1998, Environmental distribution of trace fossils in the Jurassic of Kachchh (Western India): *Facies*, v. 39, p. 243–272.
- Gingerich, P.D., 1992, Marine mammals (Cetacea and Sirenia) from the Eocene of Gebel Mokattam and Fayum, Egypt; stratigraphy, age and paleoenvironments: *University of Michigan Papers in Paleontology*, v. 30, p. 1-84.
- Gingerich, P. D., Arif, M., Bhatti, M. A., Anwar, M. and Sanders, W. J., 1997, *Basilosaurus drazindai* and *Basiloterus hussaini*, new Archaeoceti (Mammalia, Cetacea) from the middle Eocene Drazinda Formation, with a revised interpretation of ages of whale-bearing strata in the Kirthar Group of the Sulaiman Range, Punjab (Pakistan): *University of Michigan, Contributions from the Museum of Paleontology*, v. 30, p. 55–81.
- Gingerich, P. D., S. M. Raza, M. Arif, M. Anwar and Zhou, X., 1994, New whale from the Eocene of Pakistan and the origin of cetacean swimming: *Nature*, v. 368, p. 844-847.
- Gingerich, P. D., Wells, N. A., Russell, D. E. and Shah, S. M. I., 1983, Origin of whales in epicontinental remnant seas: new evidence from the early Eocene of Pakistan: *Science*, v. 220, p. 403-406.

- Gingras, M.K., Bann, K.L., MacEachern, J.A., Waldron, J. and Pemberton, S.G., 2007, A conceptual framework for the application of trace fossils, *in* MacEachern, J.A., Bann, K.L., Gingras, M.K. and Pemberton, S. G., eds., *Applied Ichnology: Society of Economic Paleontologists and Mineralogists Short Course Note*, v. 52, p. 1-25.
- Gingras, M.K., Hubbard, S.M., Pemberton, S.G. and Saunders, T.A., 2000, The significance of Pleistocene *Psilonichnus* at Willapa Bay, Washington: *Palaaios*, v. 15, p. 142–151.
- Gingras, M.K., Pemberton, S.G., Dashtgard, S. and Dafoe, L., 2008, How fast do marine invertebrates burrow?: *Palaeogeography, Palaeoclimatology, Palaeoecology*, v. 270, p. 280–286.
- Gingras, M.K., Pemberton, S.G., Saunders, T. and Clifton, H.E., 1999, The ichnology of modern and Pleistocene brackish-water deposits at Willapa Bay, Washington; variability in estuarine settings: *Palaaios*, v. 14, p. 352–374.
- Gingras, M.K., Räsänen, M.E., Pemberton, S.G. and Romero, L.P., 2002, Ichnology and sedimentology reveal depositional characteristics of bay-margin parasequences in Miocene Amazonian foreland basin: *Journal of Sedimentary Research*, v. 72, p. 871–883.
- Gregory, M.R., Martin, A.J. and Campbell, K.A., 2004, Compound trace fossils formed by plant and animal interactions: Quaternary of northern New Zealand and Sapelo Island, Georgia (USA): *Fossils and Strata*, v. 51, p. 88–105.
- Haggag, M.A. and Bolli, H.M., 1996, The origin of *Globigerinatheka semiinvoluta* (Keijzer), Upper Eocene, Fayoum area, Egypt: *Neues Jahrbuch für Geologie und Paläontologie, Monatshefte*, v. 6, p. 365-374.
- Häntzschel, W., 1975, *Trace Fossils and Problematica* (2nd ed.): *Treatise on Invertebrate Paleontology, Part W, Supplement*: Geological Society of America and University of Kansas, Boulder and Lawrence, 269 pp.

- Hasiotis, S.T., 2004, Reconnaissance of Upper Jurassic Morrison Formation ichnofossils, Rocky Mountain region, USA: environmental, stratigraphic, and climatic significance of terrestrial and freshwater ichnocoenoses: *Sedimentary Geology*, v. 167, p. 277–368.
- Hembree, D.I. and Hasiotis, S.T., 2007, Paleosols and ichnofossils of the White River Formation of Colorado: Insight into soil ecosystems of the North American mid-continent during the Eocene-Oligocene transition: *Palaios*, v. 22, p. 123-142.
- Howard, J.D. and Frey, R.W., 1984, Characteristic trace fossils in nearshore to offshore sequences, Upper Cretaceous of east-central Utah: *Canadian Journal of Earth Sciences*, v. 21, p. 200-219.
- Kellogg, R., 1936, A review of the Archaeoceti: *Carnegie Institution of Washington Publications*, v. 482, p. 1–366.
- Kelly, S.R.A. and Bromley, R.G., 1984, Ichnological nomenclature of clavate borings: *Palaeontology*, v.27, p. 793-807.
- Klappa, C.F., 1980, Rhizoliths in terrestrial carbonates: classification, recognition, genesis and significance: *Sedimentology*, v. 27, p. 613-629.
- Lotfy, H., and Van der Voo, R., 2007, Tropical northeast Africa in the middle–late Eocene: Paleomagnetism of the marine-mammals sites and basalts in the Fayum province, Egypt: *Journal of African Earth Sciences*, v. 47, p. 135–152.
- MacEachern, J.A., Bann, K.L., Bhattacharya, J.P. and Howell, C.D., 2005, Ichnology of deltas: organism responses to the dynamic interplay of rivers, waves, storms and tides, in Bhattacharya, B.P. and Giosan, L., eds., *River Deltas: Concepts, Models and Examples*: Society of Economic Paleontologists and Mineralogists Special Publication, v. 83, p. 49-85.

- MacEachern, J.A., Bann, K.L., Gingras, M.K. and Pemberton, S.G., 2007, The Ichnofacies Paradigm: High-resolution Paleoenvironmental Interpretation of the Rock Record, in MacEachern, J.A., Bann, K.L., Gingras, M.K. and Pemberton, S. G., eds., Applied Ichnology: Society of Economic Paleontologists and Mineralogists Short Course Note, v. 52, p. 26-63.
- McIlroy, D., 2004, The Application of Ichnology to palaeoenvironmental and Stratigraphic Analysis: Geological Society of London Special Publication, v. 288, 490 pp.
- Morsi, A.M., Boukhary, M. and Strougo, A., 2003, Middle-upper Eocene ostracods and Nummulites from Gebel Na'alun, southeastern Fayum, Egypt: *Revue de Micropaléologie*, v. 46, p. 143-160.
- Nesbitt, E.A. and Campbell, K.A., 2006, The paleoenvironmental significance of *Psilonichnus*: *Palaios*, v. 21, p. 187-196.
- Pemberton, S.G. and Frey, R.W., 1982, Trace fossil nomenclature and the Planolites-Palaeophycus Dilemma: *Journal of Paleontology*, v. 56, p. 843-881.
- Pemberton, S.G. and MacEachern, J.A., 1997, The ichnological signature of storm deposits: the use of trace fossils in event stratigraphy, in Brett, C.E, ed., *Palaeontological Event Horizons Ecological and Evolutionary Implications*: Columbia University Press, p. 73-109.
- Peters, S.E., Antar, M.S.M., Zalmout, I.S. and Gingerich, P.D., 2009, Sequence stratigraphic control on preservation of late Eocene whales and other vertebrates at Wadi Al-Hitan, Egypt: *Palaios*, v. 24, p. 290–302.
- Pollard, J.E., Goldring, R. and Buck, S.G., 1993, Ichnofabrics containing Ophiomorpha: significance in shallow-water facies interpretation: *Journal of the Geological Society of London*, v. 150, p. 149–164.
- Reineck, H.E., 1963, Sedimentgefüge im Bereich der südlichen Nordsee: *Abhandlungen der Senckenbergischen Naturforschenden Gesellschaft*, v. 505, p. 1–107.

- Retallack, G.J., 2001, *Soils of the Past*, 2nd edition: Blackwell Science, Oxford, 404 pp.
- Said, R., 1962, *The geology of Egypt*: Elsevier, Amsterdam and New York, 377 pp.
- Salem, R., 1976, Evolution of Eocene-Miocene sedimentation patterns in parts of northern Egypt: *American Association of Petroleum Geologists Bulletin*, v. 60, p. 34-64.
- Sarjeant, W.A.S., 1975, Plant trace fossils, *in* Frey, R.W., ed., *The Study of Trace Fossils*: Springer-Verlag, New York, p. 163–179.
- Savrda, C.E. and Bottjer, D.J., 1989, Trace fossil models for reconstructing oxygenation histories of ancient marine bottom waters: application to Upper Cretaceous Niobrara Formation, Colorado: *Palaeogeography, Palaeoclimatology, Palaeoecology*, v. 74, p. 49-74.
- SCHEIHING, H.M. and GAYNOR, G.C., 1991, The shelf sand-plume model: a critique: *Sedimentology*, v. 38, p. 433-444.
- Schweinfurth, G., 1877, Reise die Wüste von Heluan bis Qeneh, 24 März bis 18 Mai 1877: *Petermanns Geographische Mitteilungen (Gotha)*, v. 23, p. 387-389.
- Seiffert, E.R., Bown, T.M., Clyde, W.C. and Simons, E.L., 2008, Geology, paleoenvironment, and age of Birket Qarun locality 2 (BQ-2), Fayum Depression, Egypt, *in* Fleagle, J.G. and Gilbert, C.C., eds., *Elwyn L. Simons: A Search for Origins*: Springer-Verlag, New York, p. 71-86.
- Seilacher, A., 1982, Distinctive features of sandy tempestites, *in* Einsele G. and Seilacher, A., eds., *Cyclic and event stratification*: Springer-Verlag, Berlin, 333-349p.
- Sestini, G., 1984, Tectonic and sedimentary history of NE African margin (Egypt/Libya), *in* Dixon, J.E. and Robertson, A.H.F., eds., *The geological evolution of the eastern Mediterranean*: Geological Society of London Special Publication, v. 17, p. 161-175.
- Smith, A.G., 1971, Alpine deformation and the oceanic areas of Tethys, Mediterranean and Atlantic: *Geological Society of America Bulletin*, v. 82, p. 2039-2070.

- Smith, C.R. and Baco, A.R., 2003, Ecology of whale falls at the deep-sea floor: *Oceanography and Marine Biology: an Annual Review*, v. 41, p. 311-354.
- Smith, A.B. and Crimes, T.P., 1983, Trace fossils formed by heart urchins - a study of *Scolicia* and related traces: *Lethaia*, v. 16, p. 79-92.
- Strougo, A. and Haggag, M.A.Y., 1984, Contribution to the age determination of the Gehannam Formation in the Fayum Province, Egypt: *Neues Jahrbuch für Geologie und Paläontologie, Monatshefte*, v. 1, p. 46-52.
- Taylor, A.M. and Goldring, R., 1993, Description and analysis of bioturbation and ichnofabric: *Journal of the Geological Society, London*, v. 150, p. 141-148.
- Taylor, A.M., Goldring, R. and Gowland, S., 2003, Analysis and application of ichnofabrics: *Earth-Science Reviews*, v. 60, p. 227-259.
- Taylor, D., Yen, O.H., Sanderson, P.G. and Dodson, J., 2001, Late Quaternary peat formation and vegetation dynamics in lowland tropical swamp; Nee Soon, Singapore: *Palaeogeography, Palaeoclimatology, Palaeoecology*, v. 171, p. 269-287.
- Thewissen, J. G. M., Hussain, S. T. and Arif, M., 1994, Fossil evidence for the origin of aquatic locomotion in Archaeocete whales: *Science*, v. 263, p. 210-212.
- Wright, L.D. and Nittrouer, C.A., 1991, Dispersal of river sediments in coastal seas: six contrasting cases: *Sedimentology*, v. 18, p. 494-508.
- Zalat, A.A., 1995, Calcareous nanoplankton and diatoms from the Eocene / Pliocene sediments, Fayoum depression, Egypt: *Journal of African Earth Sciences*, v. 20, p. 227-244.
- Zalmout, I.S., Mustafa, H.A. and Gingerich, P.D., 2000, Priabonian *Basilosaurus isis* (Cetacea) from Wadi Esh-Shallala Formation: First marine mammal from the Eocene of Jordan: *Journal of Vertebrate Paleontology*, v. 20, p. 201-204.

CHAPTER 4: SIGNIFICANCE OF HYPOBURROW NODULE FORMATION ASSOCIATED WITH LARGE BIOGENIC SEDIMENTARY STRUCTURES IN THE UPPER EOCENE BIRKET QARUN FORMATION, WADI EL-HITAN, FAYUM-EGYPT *

INTRODUCTION

This chapter aims to reveal the origin of unusually large sedimentary features found in the upper Birket Qarun Formation in the Fayum area, Egypt. The structures are discordant with bedding, display dm-scale diameters and commonly exceed a meter in length. The morphology of the structures is crudely conical to columnar with rare branching elements. All of the structures are observed at parasequence boundaries. As such, their interpretation potentially can be related to the sequence stratigraphic framework of the succession.

Large sedimentary features (dm- to m-scale) that are also discordant with bedding are attributable to at least five main processes. Water / gas escape (i.e., seepage, fluidization and liquefaction) constitutes one of the most important non-biogenic mechanisms (e.g., Lowe, 1975; Bailey and Newman, 1978; Flint, 1983; Massari et al., 2001). Concretionary calcite cementation represents another common mechanism capable of generating discordant structures in sedimentary media (e.g., Abdel-Wahab and McBride, 2001; McBride et al., 2003; Mozley and Davis, 2005; Wanas, 2008). The collapse and infilling of karstic dissolution cavities (e.g., Hunter et al., 1992) is a very common mechanism of generating discordant sedimentary bodies, but is mainly limited to carbonate successions. More rarely, whirlpool structures had been identified as steeply scouring into sedimentary bedding (Dionne and Laverdiere, 1972). Finally, biogenic

* A version of this chapter has been submitted for publication in SEDIMENTARY GEOLOGY journal as “Significance of hypoburrow nodule formation associated with large biogenic sedimentary structures in the Upper Eocene Birket Qarun Formation, Wadi El-Hitan, Fayum-Egypt”, by: Zaki A. Abdel-Fattah, Murray K. Gingras and S. George Pemberton.

sedimentary structures are variable in scale and commonly are discordant to bedding. Many examples of unusually large biogenic sedimentary structures have been reported (e.g., Bromley et al., 1975; Pemberton et al., 1988; Sendden, 1991; Nara, 1995; Savrda, 2002; Buck and Goldring, 2003; Abad et al., 2006). Some of these structures are related to the dwelling and escape structures of sea anemones (e.g., Shinn, 1968; Frey and Howard, 1981). Others are attributed to molluscan burrowing activities (e.g., Goldring, 1964; Bromley et al., 1975). Several larger burrows are interpreted as the result of excavations of marine vertebrates such as whales, walruses and rays (e.g., Howard et al., 1977; Nelson et al., 1987; Gingras et al., 2007a).

This chapter uses ichnological and sedimentological observations to interpret previously unreported large sedimentary structures in the study area. Additionally, petrographic and stable isotopic analyses ($\delta^{13}\text{C}$ and $\delta^{18}\text{O}$) are used to develop a paragenetic model that is integrated into a sequence stratigraphic framework.

GEOLOGIC SETTING AND STUDY AREA

The Fayum intracratonic basin was generated during Jurassic rifting, characterized by extensional and strike-slip tectonics between Africa and Eurasia (Smith, 1971). The Fayum Basin was uplifted during the Late Cretaceous Syrian Arc Orogeny. Since the Middle Eocene, the northern margin of Egypt had been dominated by further uplift (Sestini, 1984). Then, the Late Eocene was marked by a general lowering of relative sea level, accompanied by progressive emergence and erosion of the structural highs that provided clastic sediments to Late Eocene basins of northern Egypt (e.g., Salem, 1976). The Fayum Basin is characterized by complex pre-Eocene subsurface structure and relatively simple (horizontal to gently inclined) Eocene-Oligocene geology. The outcrop stratigraphy is represented by five units (from base to top): Middle Eocene Wadi Rayan and Gehannam formations, the Upper Eocene Birket Qarun and Qasr El-Sagha formations, and the Oligocene Gebel Qatrani Formation (Fig. 4.1).

Two Middle-Upper Eocene sections were measured and studied at three locations in the vicinity of Wadi El-Hitan area (Fig. 4.1). The composite section from Minqar El-Hut (between N 29° 15' 48" - E 30° 02' 47" and N 29° 16' 02" - E 30° 03' 51") and the Old Camp site (N 29° 15' 55" - E 30° 01' 24") is correlated with the Sandouk El-Borneta section (N 29° 17' 00" - E 30° 03' 00") (Figs. 4.1, 4.2). The present work focuses on the Upper Eocene (Priabonian) succession of the upper part of Birket Qarun Formation (Fig. 4.2).

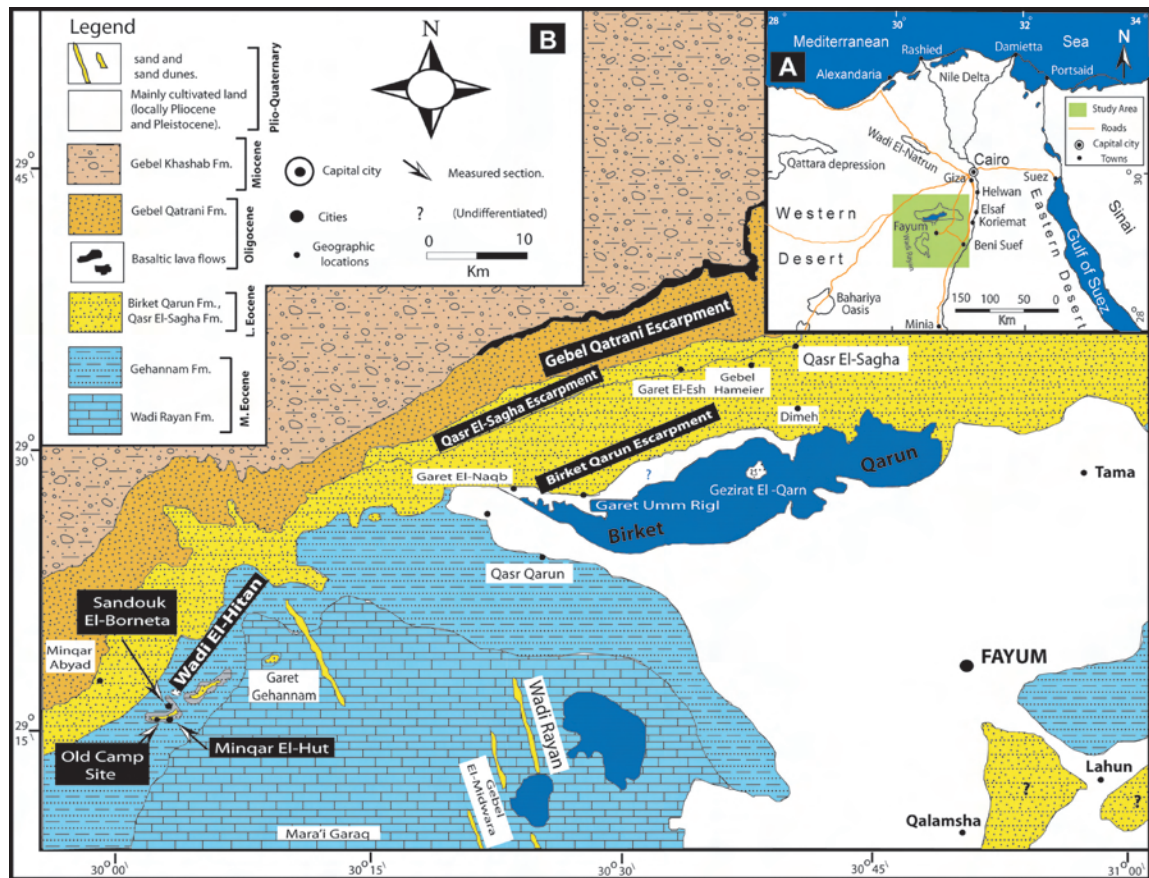


FIGURE. 4.1. A- Location map of the study area. B- Geological map of the Fayum depression and the studied sections in the area of Wadi El-Hitan, redrawn and modified after Beadnell (1905), Said (1962), and Gingerich (1992).

The average thickness of the Birket Qarun Formation varies between 50 and 55 m at the Minqar El-Hut composite section and the Sandouk El-Borneta section, respectively. The lithology is mainly grayish white to yellow, highly bioturbated and fossiliferous, fine- to very fine-grained sandstones. The sandstones typically incorporate a grayish black shale bed in the middle part of the Birket Qarun Formation. Upwards, the sandstone strata of the Birket Qarun Formation are truncated by several sandstone/coquina beds (Fig. 4.2). The age of the Birket Qarun Formation is assigned to the Late Eocene (Priabonian, ~37 Ma) (e.g., Zalat, 1995; Haggag and Bolli, 1996; Morsi et al., 2003; Seiffert et al., 2008).

METHODOLOGY

The stratigraphic relations, as well as the sedimentary and ichnological characters of the large sedimentary structures and their associated strata were documented in the field. The ichnological data includes both qualitative and semi-quantitative data. The descriptive ichnological data comprise identification of ichnogenera, and details of the ichnofossil suites. Semi-quantitative data include morphometric measurements of the large sedimentary structures (e.g., maximum height, maximum diameter, and the diameter/height ratio), intensity of bioturbation in the surrounding media (bioturbation index or BI), ichnogenic diversities, and size distributions (maximum diameter) of the associated trace fossils.

Two large polished cross-sectional and longitudinal slabs were cut through a sampled representative structure. Additionally, a large petrographic thin-section (10 x 8 cm) was carefully cut across a representative sedimentary structure for petrographic analysis. Twelve standard petrographic thin-sections of the structure-associated depositional units were stained with Alizarin Red S (ARS) and studied with a petrographic microscope. Some representative samples were examined with a JEOL 6301F (Field Emission) Scanning Electron Microscope (SEM).

Carbon and oxygen stable-isotope analyses of the bulk calcite and bulk dolomite

were carried out on twenty two samples. Four samples were collected from the hosting sandstone unit, whereas eighteen samples represent the large sedimentary structure. Two longitudinal and two transverse slices (1 cm thick) were cut through large sedimentary structures. These slices are easily differentiated into three zones: matrix sandstone (m zone), nodular hypoburrow (see Gingras et al., 2007b) cemented sandstone (hc zone), and preferentially cemented burrow (b zone). Examples from each zone were ground manually into powder. The resulting samples contained both calcite and dolomite. Therefore, chemical separation (using phosphoric acid 100%) treatments of Degens and Epstein (1964) and Al-Aasm et al. (1990) were used. Carbon dioxide was extracted and analyzed in a Finnigan-MAT252 mass spectrometer. Both carbon and oxygen stable-isotopic data are expressed by δ notation relative to the Vienna PDB and SMOW standards.

LARGE SEDIMENTARY STRUCTURES

Curiously large-sized structures occur sporadically along the boundary between units I and II (Table 4.1) in the upper Birket Qarun Formation (Figs. 4.2, 4.3). The depositional environment is interpreted to represent a fully marine embayment punctuated by wave ravinement surfaces. The depositional nature of the entire Birket Qarun Formation is discussed in detail in chapters 2 and 3.

MORPHOLOGY AND SIZE

The large, massive-appearing structures display variable sizes and morphologies between localities (Fig. 4.3). In Sandouk El-Borneta and along Wadi El-Hitan, the structures have large-diameter (up to dm-scale) branched pillars and/or large boxwork morphology (Figs. 4.3A-D). At the Old Camp site, the structures are more strongly perpendicular to the bedding planes (angles varying between 85° and 95°) (Figs. 4.3E-H). Some structures are well displayed and weather prominently, whereas others are eroded,

TABLE 4.1. Summary of the characteristics and depositional affinities of the structure-associated depositional units.

Main Characteristics	Depositional Unit I (<i>Hosting sandstone deposits</i>) (Figs. 2 and 3)	Depositional Unit II (<i>Sandstone/lag/coquina deposits</i>) (Figs. 2 and 3)
Occurrences	Cliff-forming strata, comprising the upper part of Birket Qarun Fm, truncated by ravinement surfaces and the depositional unit II.	Truncating the structure-hosted sandstones (depositional unit I), upper Birket Qarun Fm, associated with ravinement surfaces, passively fill the large structures.
Thickness	Bed thicknesses ranging between 3 and 7 m.	Average bed thickness of ~ 2 m.
Lithofacies	Fine- to very fine-grained sandstone.	Heterolithic unit, interbedded/intercalated fine- to coarse-grained sandstone and lag/coquina lithofacies.
Microfacies	Dolomitic quartz arenite microfacies.	Calcareous quartz arenite and rudite microfacies.
Sedimentary Structures	No preserved physical sedimentary structures.	No preserved physical sedimentary structures.
Fossil Content	Bivalves (thin-shelled pectinids, oysters, sea pens and <i>Lucina pharaonis</i>), common gastropods (<i>Turritella pharaonica</i>), irregular echinoids, crab-carapace fragments, and marine vertebrate-bone fragments. Petrographic thin sections and the SEM investigations show an abundant association of planktonic foraminifera and nannoplankton (coccoliths).	Bivalves (e.g., <i>Ostrea</i> sp., <i>Crassostrea</i> sp., <i>Carolia plucnoides</i> , and <i>Lopha verleti</i>); gastropods (e.g., <i>Turritella pharoanum</i> and <i>Terebra</i> sp.); foraminifera (e.g., <i>Nummulites</i> sp. and <i>Operculina</i> sp.), echinoid- and crustacean-carapace fragments, and vertebrate-bone fragments.
Ichnology	Highly burrowed (BI 5), with high ichnogenera diversities, burrow diameters range from 5 to 10 mm, but large (> 2 cm diameter) <i>Th</i> and <i>Op</i> are present. Trace-fossil suites include in decreasing order of abundance: <i>Th</i> , <i>Pl</i> , <i>Op</i> , <i>Te</i> , <i>As</i> , <i>Rh</i> , <i>Sk</i> , <i>Cy</i> , <i>Ar</i> , and <i>Ps</i> . Proximal <i>Cruziana</i> -distal <i>Skolithos</i> ichnofacies.	Weak to moderate bioturbation intensities (BI 1-3), and low to locally moderate ichnogenera diversities. Trace-fossil suites include <i>Sk</i> , <i>Pl</i> , <i>Ps</i> , and rare <i>Te</i> , attributed to the softground <i>Skolithos</i> Ichnofacies. Diameters vary between 5 and 10 mm. Depositional unit II is underlain by firmground trace-fossil suites—dominated by <i>Th</i> , <i>Ar</i> and <i>Sk</i> —attributed to the <i>Glossifungites</i> Ichnofacies.
Interpretation	Low- to moderate-energy, open-marine bay or gulf, with normal salinity and minimal restriction, in a tropical to subtropical climatic zone.	Moderate- to high-energy transgressive conditions, mostly associated with wave ravinement surfaces in a bay margin to coastal setting.

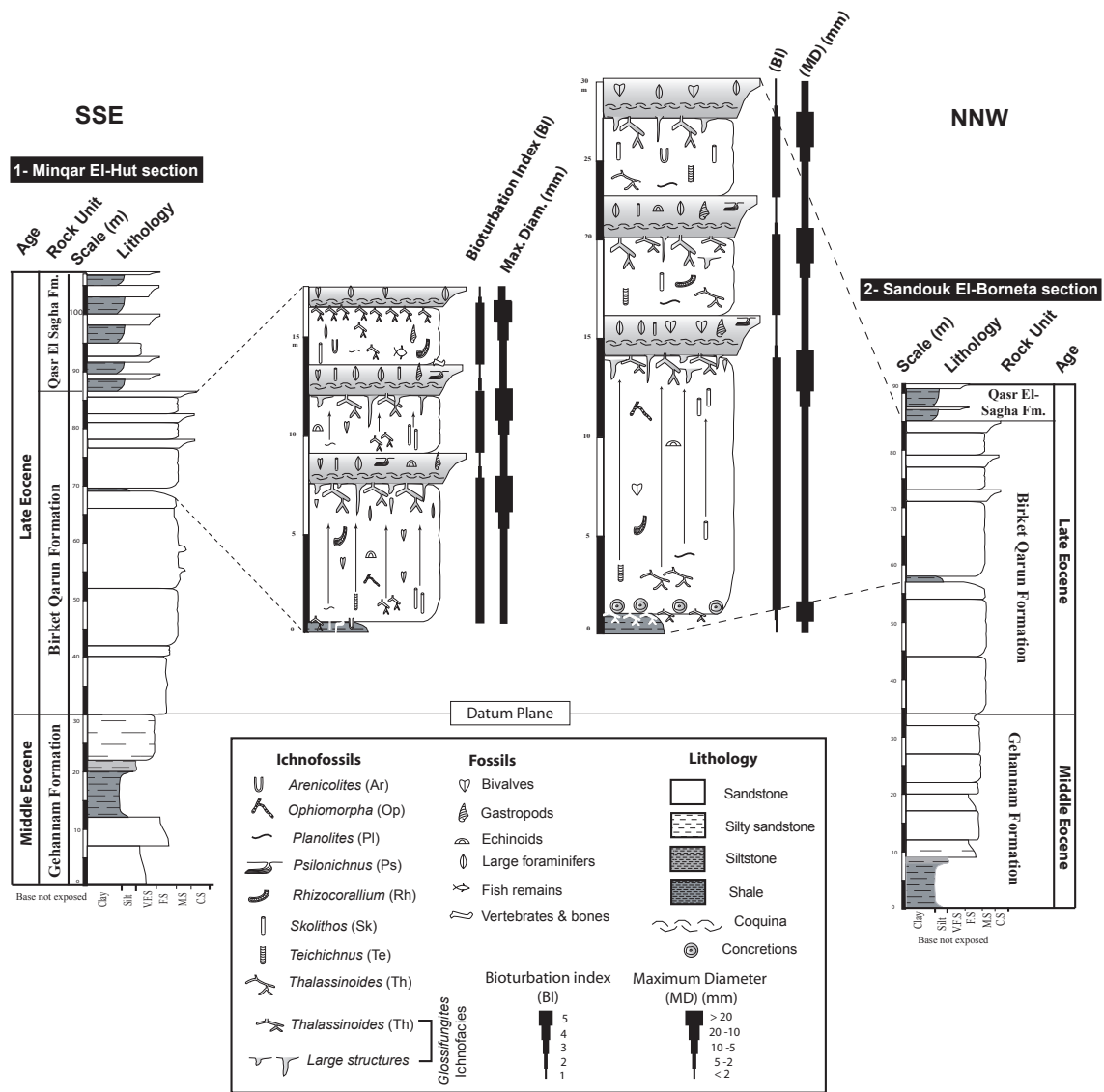
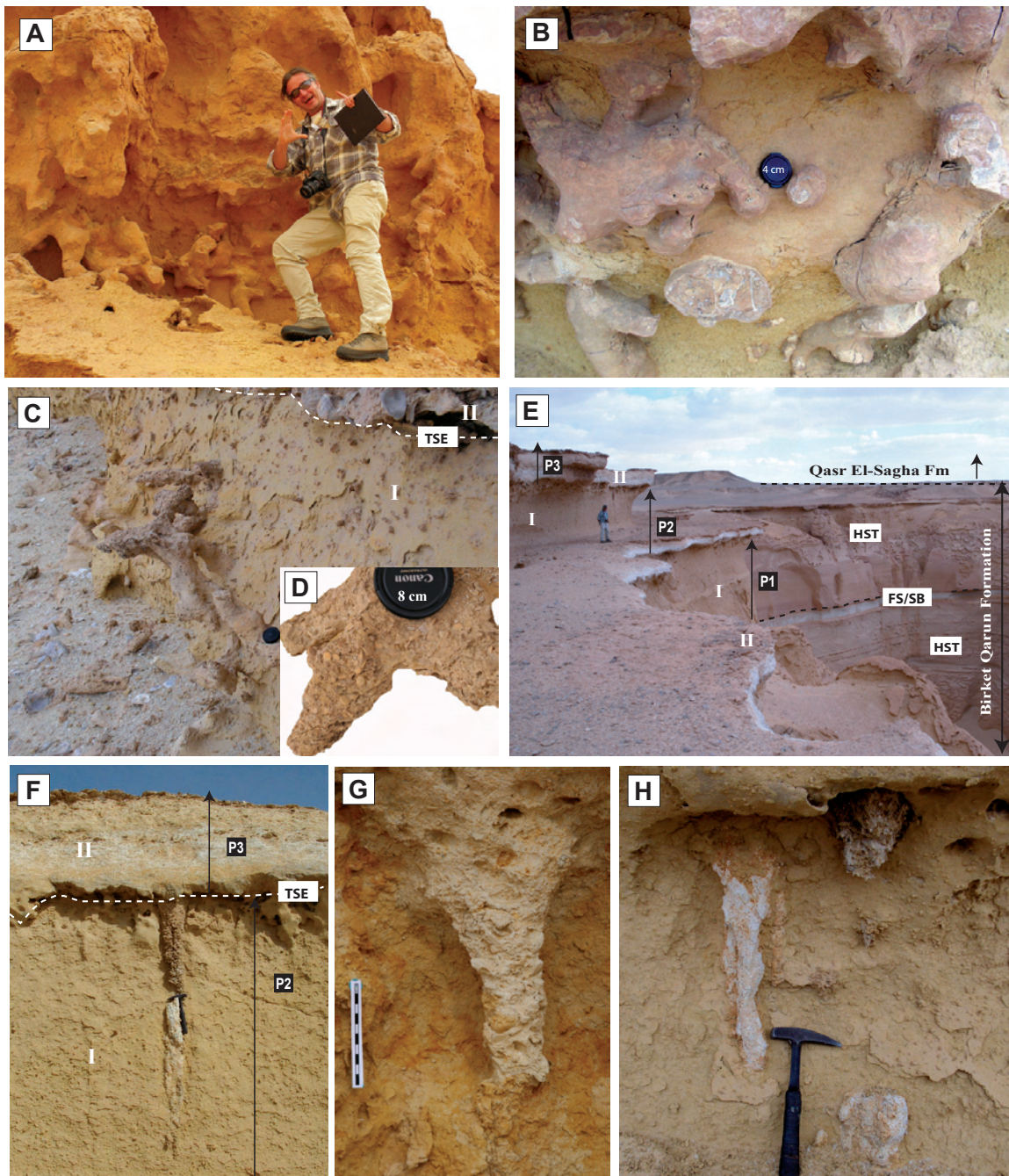


FIGURE. 4.2. Correlation of the Upper Eocene Birket Qarun Formation at the composite Minqar El-Hut and Old Camp site section with Sandouk El-Borneta section, in the area of Wadi El-Hitan, SW Fayum.

FIGURE. 4.3. Large-sized sedimentary structures and their associated depositional units. **A-** Large-sized branched pillars, defining the upper Birket Qarun Formation in the area of Wadi El-Hitan. **B-** Close up of A, showing the concretionary large sedimentary structures. **C-** Box-work (T- and Y-shaped morphology) structures hosted in the sandstones of the depositional unit I, truncated upward by the TSE and the coquina deposits of depositional unit II, Sandouk El-Borneta section. **D-** Close up of a structure on C, showing the passive-fill character (note the abundant lenticular large foraminifera). **E-** Outcrop view of three stacked parasequences (P1-P3) of a HST that overlies the coplanar FS/SB surface, Birket Qarun Formation, Old Camp site. **F-** Close-up view of E, showing a large conical vertical sedimentary structure at the contact between the parasequences P2 and P3. **G-** Close up view of E, showing an amphora-like sedimentary structure at the contact between the parasequences P1 and P2. Note the white color, resistant weathering, and passively filled character (shell hash and coarse-grained sandstone) of these structures. **H-** Close-up view of E, showing vertically extended sedimentary structure (left), discrete vertical structures (middle), and totally eroded structures forming widespread cavities (upper right).

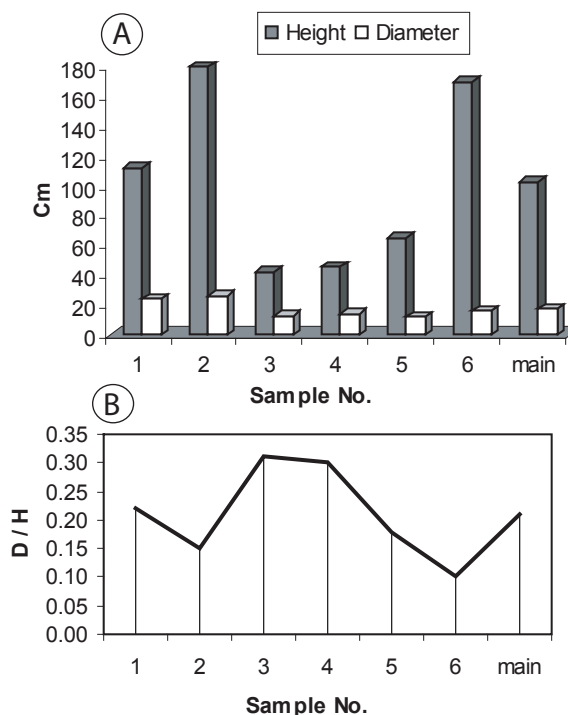


forming moldic cavities (Fig. 4.3H). The features most commonly display conical to elongate sub-cylindrical and amphora-like morphologies (Figs. 4.3E-H). Cross-sections are circular to oval. Six morphometric measurements of the vertical conical structures, comprising the maximum height, the maximum diameter and the diameter/height ratio, are shown in Table (4.2). The statistical relationships between these three parameters are presented in (Fig. 4.4). The maximum height varies between 42 and 180 cm, with an average value of 102 cm. The maximum diameter ranges from 12 to 26 cm, with an average maximum diameter of 17 cm. The diameter/height ratio varies between 0.1 and 0.31, with an average ratio of 0.21.

TABLE 4.2. Morphometric measurements of six large amphora-like sedimentary structures in the Old Camp site, Wadi El-Hitan area.

Sample no.	Max. Height (cm)	Max. Diameter (cm)	Diameter / Height
1	112	24	0.22
2	180	26	0.15
3	42	13	0.31
4	46	14	0.30
5	65	12	0.18
6	170	16	0.10
Main	102.5	17.5	0.21

FIGURE. 4.4. A- Columnar chart, showing the relationship between the maximum height (H) and the maximum diameter (D) for the six morphometric measurements illustrated in Table 4.2. **B-** Drop-line chart representing the distribution of the diameter/height (D / H) ratios of the six morphometric measurements illustrated in Table 4.2.



ICHTHOLOGICAL TEXTURE AND CHARACTERS

Cross-sections through the structures reveal circular cross-sections of one or more 3 to 4 cm diameter *Thalassinoides* (Fig. 4.5). The *Thalassinoides* locally interpenetrate and branch. The trace fossils are passively filled, sharp walled and unlined, suggesting that these burrows belong to the firmground-associated *Glossifungites* Ichnofacies. The reported large-sedimentary structures are associated with trace-fossil suites, attributed to the *Glossifungites* Ichnofacies. These firmground ichnological suites contain abundant dwellings of inferred deposit-feeding organisms (mainly *Thalassinoides*). Rare to common domiciles of inferred suspension-feeding and/or filter-feeding organisms (e.g., *Arenicolites* and *Skolithos*) are locally present. These firmground trace-fossil suites are passively filled with massive to concentrically aligned shell hash, large foraminifera's tests, lags and sandstone deposits of the heterolithic depositional unit II.

Longitudinal- and cross-sectional slabs (Fig. 4.5) reveal a complex ichnological fabric of cross-cutting and amalgamated burrows. Smaller trace fossils (circular to oval in cross section and ~ 0.5 cm in diameter) are also present. These burrows are not passively filled, and may be interpreted as *Planolites*.

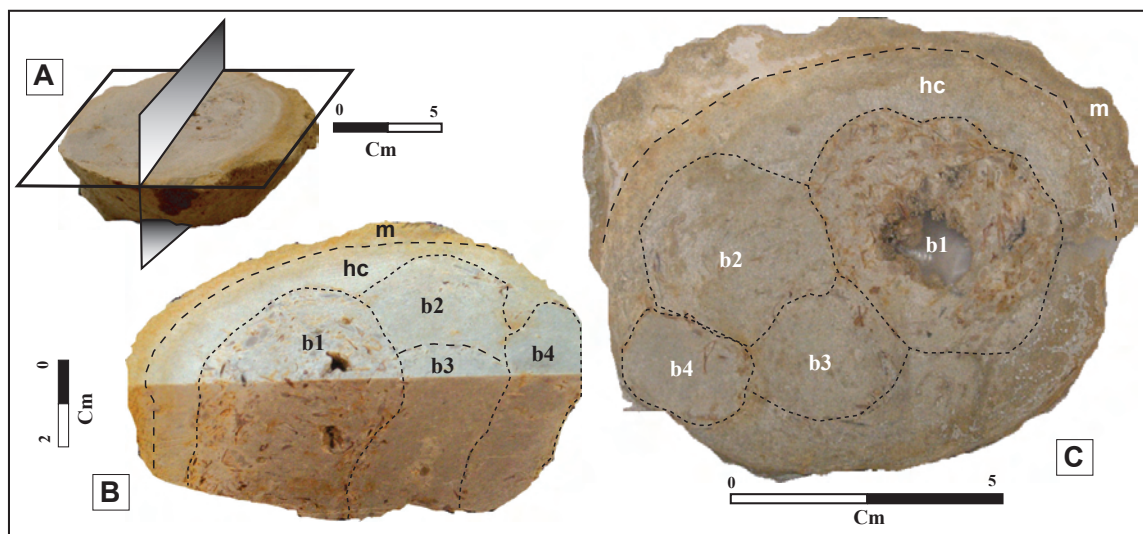


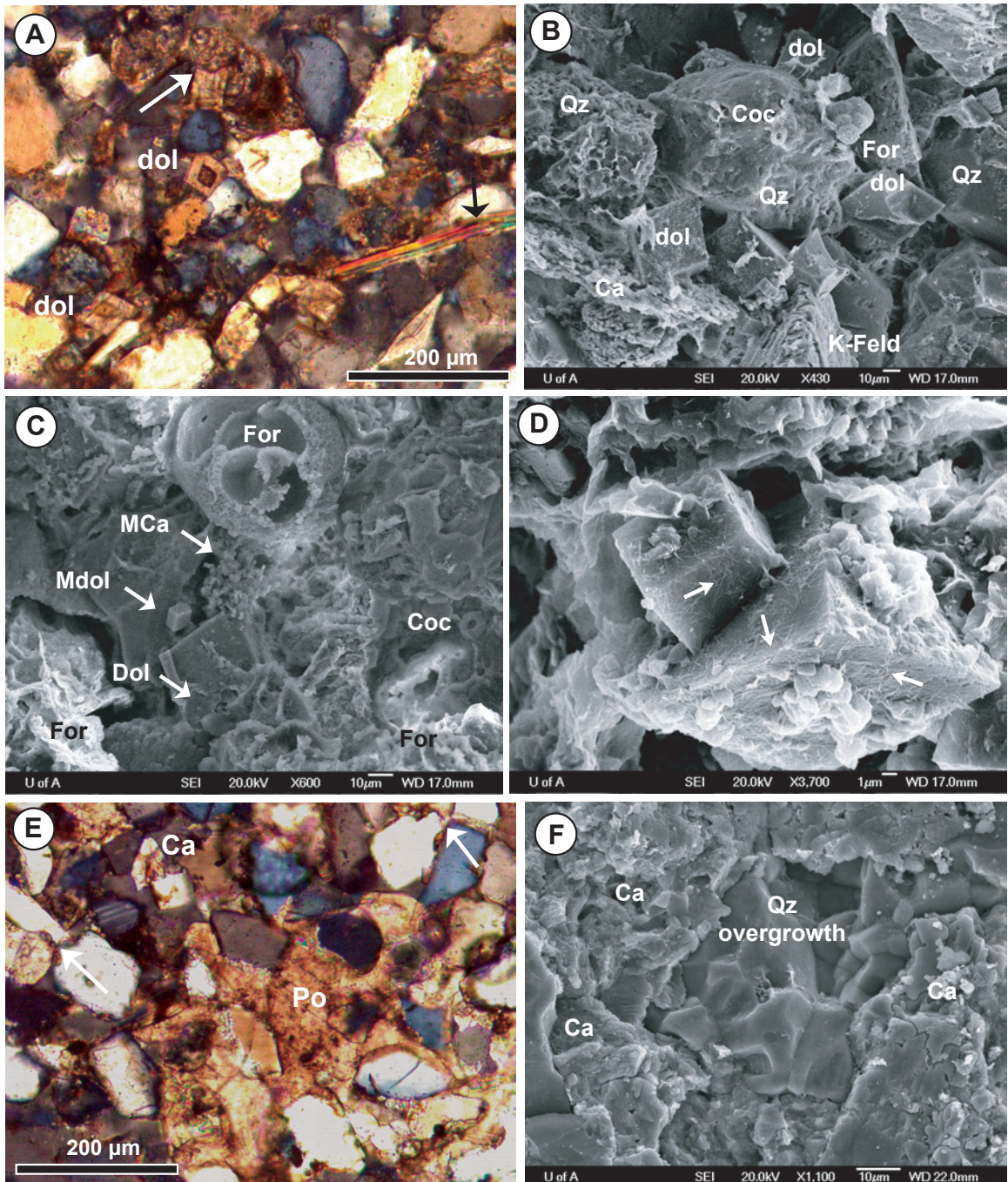
FIGURE. 4.5. Large longitudinal (B) and cross-sectional (C) polished slabs were cut through a large sedimentary structure (A). Four passively-filled *Thalassinoides* burrows (b1-b4) are cemented together by hypoburrow concretionary sandstone (hc). Note the color and texture contrast between the yellow matrix sandstone (m), and the yellowish white hypoburrow cemented sandstone (hc zone) and burrow zone (b1-b4).

PETROGRAPHY AND DIAGENESIS

DEPOSITIONAL UNIT I (HOST SANDSTONE)

The matrix sandstone is dominated by a dolomitic quartz arenite microfacies (Fig. 4.6). This microfacies has a moderately mature to mature texture that is fine to very fine grained, subrounded, and moderately to well sorted. Detrital quartz grains constitute > 95% of the mineralogical framework elements ($Q_{>95\%}$ $F_{<3\%}$ $L_{<0.5\%}$). The quartz grains are mainly monocrystalline, with very rare polycrystalline grains (Figs. 4.6A, E). Detrital

FIGURE. 4.6. Optical (crossed nicols) photomicrographs and SEM images of the quartz arenite microfacies (depositional unit I). **A-** Dolomitized foraminifera test (white arrow) and pore-filling microcrystalline dolomite, engulfed by the pore-filling zoned dolomite rhombs (dol), with a rare mica flake (black arrow). **B-** SEM image, showing the pervasive dolomite (dol) and calcite (Ca) cement. Note the stacked planktonic foraminifera (For) and the coccoliths (Coc) on the surface of the quartz grain (Qz). **C-** SEM photograph, illustrating partially dissolved planktonic foraminifera (For) and coccoliths (Coc). The precipitated microcrystalline calcite (MCA) is engulfed by pore-filling microcrystalline dolomite (Mdol) that is covered by the zoned dolomite rhombs (Dol). **D-** SEM image of the growing microcrystalline calcite and microcrystalline/coarse-crystalline dolomite rhombs on a bio-carbonate shell fragment. Note the growth of fibrous microbial dolomite (white arrow) on dolomite-rhomb surfaces. **E-** Pore-filling microcrystalline calcite (white arrows), engulfed by the pore-filling mosaic and coarse crystalline calcite (Ca) and large-pore filling poikilotopic calcite crystal (Po), engulfing several quartz grains. **F-** SEM image, showing the contact between the quartz overgrowth (smooth-surface prisms) and the microcrystalline/mosaic calcite (Ca) cement.



feldspars occur in small amounts, and are dominated by plagioclase (Fig. 4.6E) and K-feldspar grains (Fig. 4.6B). Lithic fragments are very rarely observed. Mica (Fig. 4.6A) and glauconite are very rare. Bio-carbonate grains—averaging 15-20% of the total volume of the rock—include bioclastic-shell fragments, foraminifera (abundant planktonic and benthonic types), and nannoplankton (coccoliths). These bioclasts are highly corroded and partially dolomitized (Figs. 4.6A, C).

Authigenic carbonates and quartz overgrowths represent the main cement types in the matrix sandstone (Fig. 4.6). The quartz cement occurs as a euhedral, smoothed, prismatic and syntaxial crystal overgrowth on the monocrystalline detrital quartz grains (Fig. 4.6F). The authigenic carbonate cement contains calcite and dolomite. The calcite cement comprises microcrystalline calcite, mosaic equigranular calcite, and coarse-crystalline calcite. Microcrystalline calcite ($< 10\ \mu\text{m}$) commonly fringes the bioclasts and rarely detrital grains, and locally occurs as pore-filling cement (Figs. 4.6A, C, D). The precursor microcrystalline calcite cement is engulfed by an equigranular mosaic calcite ($< 100\ \mu\text{m}$; averaging between 40 and 80 μm) that is the most common pore-filling cement. Coarse crystalline calcite ($> 100\ \mu\text{m}$) and sporadically distributed poikilotopic calcite crystals encrust, and thus postdate, the mosaic calcite cement (Fig. 4.6E). Authigenic dolomite cement includes microcrystalline dolomite aggregates ($< 10\ \mu\text{m}$) that are succeeded by pore-filling Fe^{+2} -rich zoned dolomite rhombs ($\sim 50\ \mu\text{m}$) (Figs. 4.6A-D). Rare post-dated fibrous microbial dolomites (e.g., Rao et al., 2003) have grown on the smooth surfaces of some dolomite rhombs (Fig. 4.6D).

DEPOSITIONAL UNIT II (OVERLYING SANDSTONE / COQUINA)

Unit II is represented mainly by intercalated sandstones and coquinas. These lithofacies are dominated by the calcareous quartz arenite and rudite microfacies.

The quartz arenite microfacies is immature to submature, and it is fine to coarse grained; grains are angular to sub-rounded and poorly to moderately sorted (Figs. 4.7A,

B). This microfacies is mineralogically mature: monocrystalline quartz grains constitute >95% of the mineralogical framework elements ($Q_{>95\%}$ $F_{<2\%}$ $L_{<0.5\%}$). Detrital feldspars (plagioclase and K-feldspars) and lithic fragments are rare. Bio-carbonate grains—average 30% of the total volume of the rock and include larger benthic foraminifera, oysters, bivalves, gastropods, bryozoans and ostracodes (Fig. 4.7A). Authigenic minerals are represented mainly by the carbonate cements and rare syntaxial quartz overgrowth (Figs. 4.7A-B). Pervasive calcite cementation is represented mainly by microcrystalline calcite (< 10 μm), which was succeeded the equigranular calcite mosaic (~ 20-60 μm) and later by coarse-crystalline calcite (>100 μm). The calcite cement replaces and displaces framework and bioclastic grains, and fills the inter-granular pores in the framework (Figs. 4.7A-B). Microcrystalline dolomite and zoned dolomite rhombs are sporadically distributed.

The rudite microfacies is composed of gravel-sized shells and bioclasts (> 50% of the total volume of the rock) (Figs. 4.7C-D, 4.8A, D, E) in a sandstone (calcareous quartz arenite) matrix with pervasive authigenic calcite cement. The shells and bioclasts include abundant oysters, bivalves and gastropods shell fragments, large foraminifera (e.g., *Nummulites* sp., *Operculina* sp.) and small foraminifera (e.g., miliolids), bryozoans, ostracodes and echinoids (Figs. 4.7C, 4.8A, D). This microfacies is characterized by moldic porosity (Figs. 4.7C-D, 4.8D-E). The pervasive calcite cement includes microcrystalline-, prismatic-, mosaic- and coarse-crystalline calcite habits (Figs. 4.7C-D). Microcrystalline calcite (<10 μm) commonly envelopes the bioclastic grains, but also occurs as pore-filling cement. Prismatic calcite engulfs microcrystalline calcite around the bioclastic grains and along the margins of bio-moulds (Figs. 4.7D, 4.8E). This was followed by mosaic equigranular (< 100 μm) coarse-crystalline calcite (> 100 μm), which represents the main pore-filling phase. Dolomite and quartz overgrowth cements are sporadically and locally present.

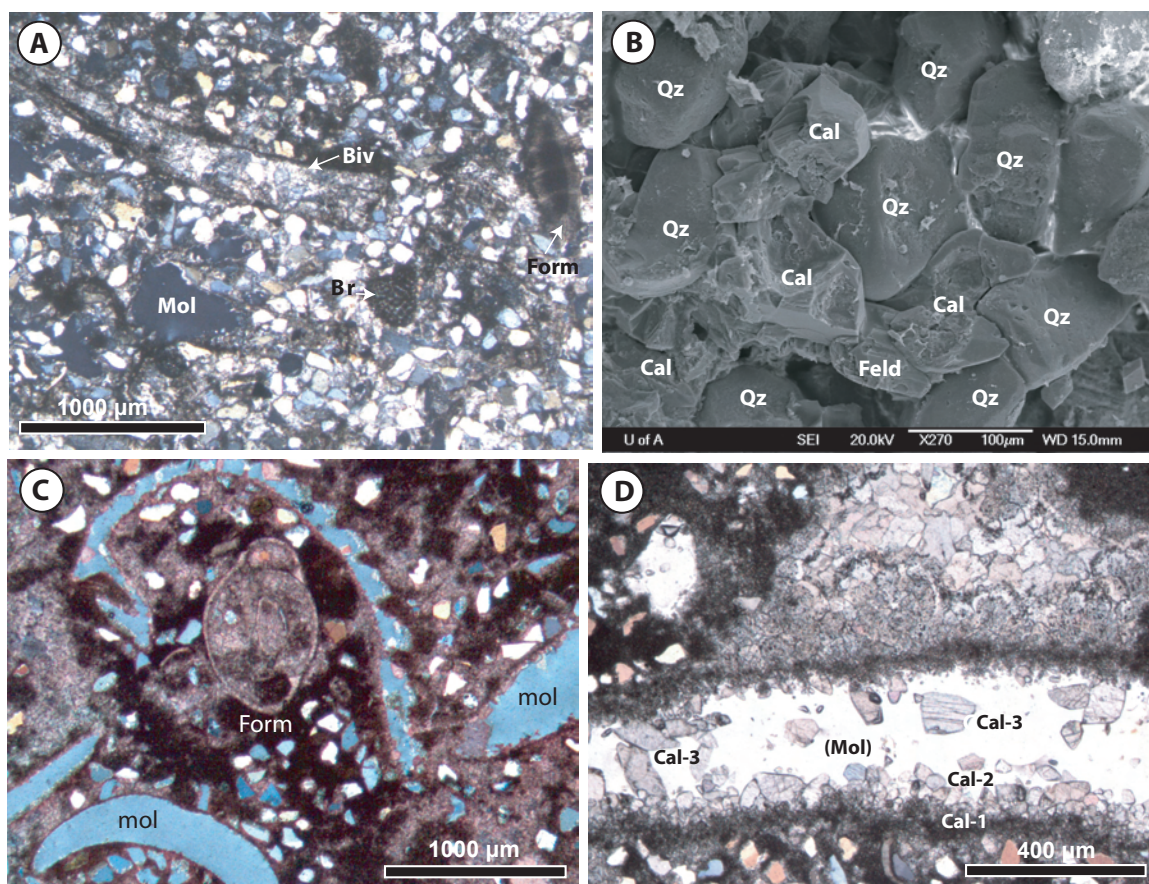
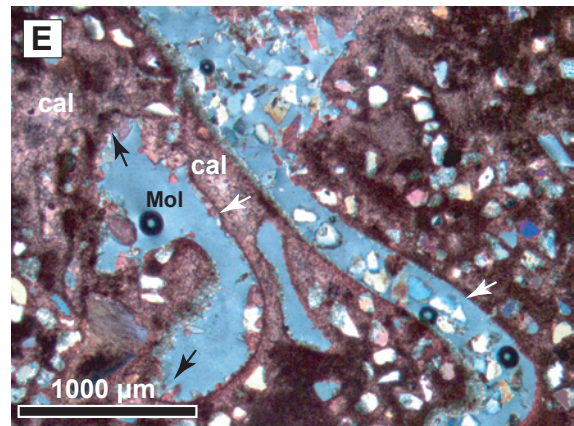
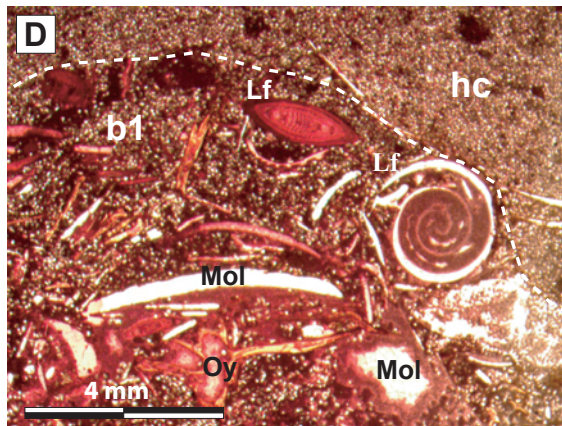
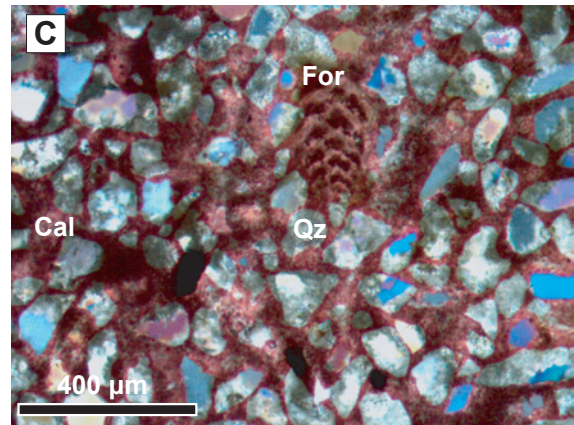
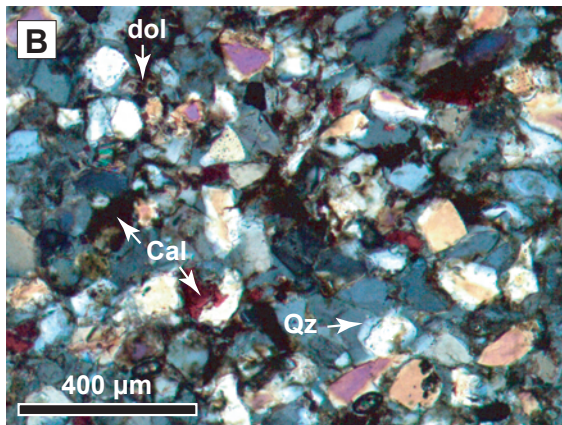
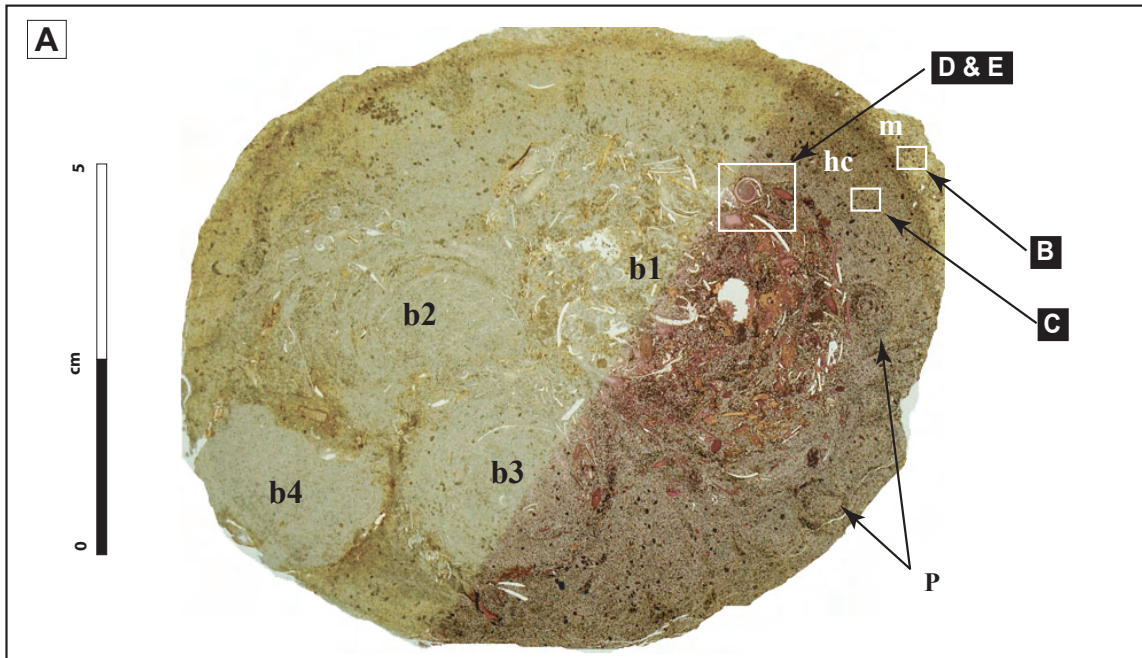


FIGURE. 4.7. Optical (crossed nicols) photomicrographs and SEM images of the depositional unit II. **A-** Moderately mature texture with abundant bio-carbonate fragments—bivalves (Biv), larger foraminifera (Form), bryozoans (Br)—bio-moldic porosity (Mol) and pervasive calcite cementation in the calcareous quartz arenite microfacies. **B-** SEM photograph, showing the pervasive pore-filling microcrystalline and mosaic calcite (Cal) and rare dolomite, cementing the dominant quartz (Qz) and rare feldspar (Feld) grains in the framework of the quartz arenite microfacies. **C-** Gravel-sized bivalves/bioclasts, small miliolid foraminifera (Form) and molds (mol) set in calcareous quartz arenite matrix and pervasive calcite cementation (stained reddish with ARS) in the rudite microfacies. **D-** The sequential order of the different types of calcite-cement—microcrystalline calcite (Cal-1), prismatic calcite (Cal-2) and mosaic / coarse crystalline calcite (Cal-3)—precipitation in a bio-mold (mol) of the rudite microfacies.

LARGE SEDIMENTARY STRUCTURES

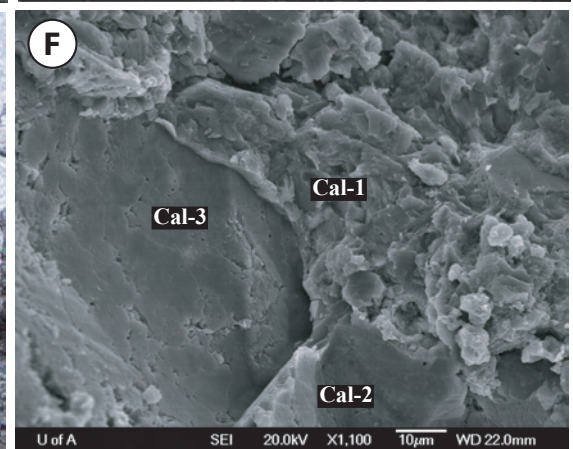
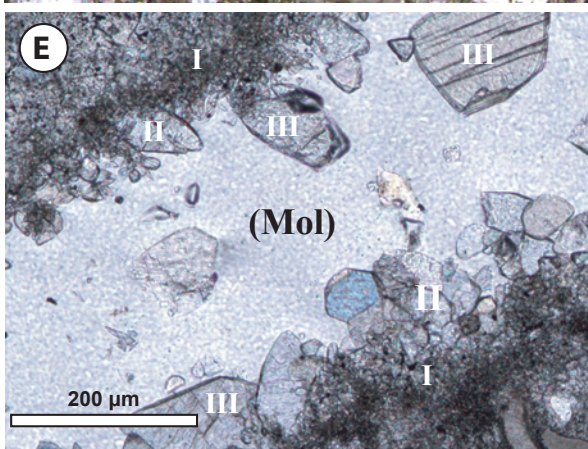
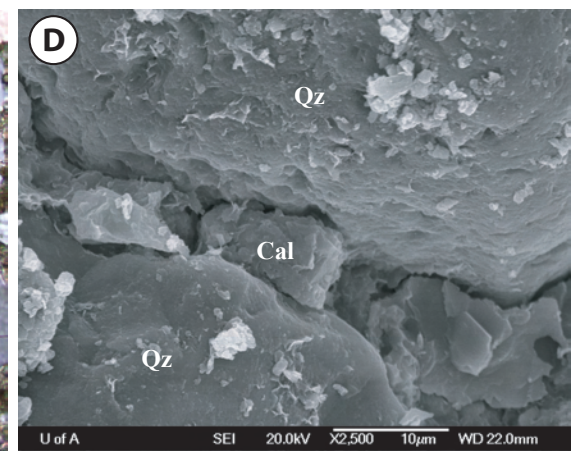
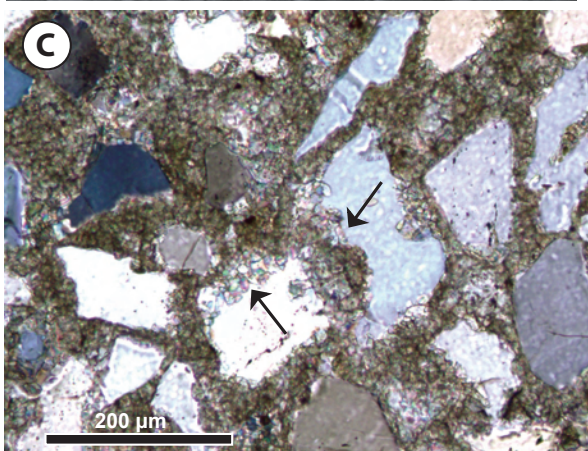
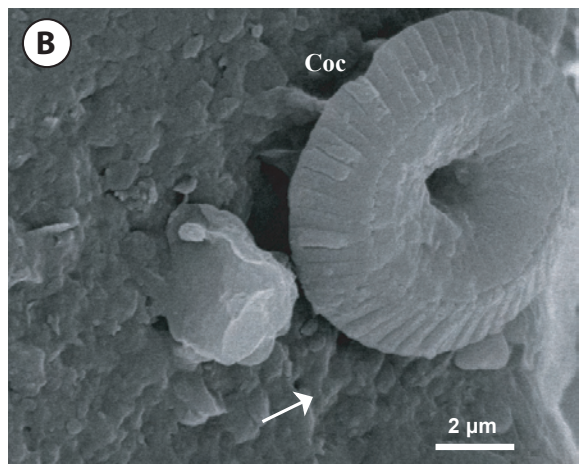
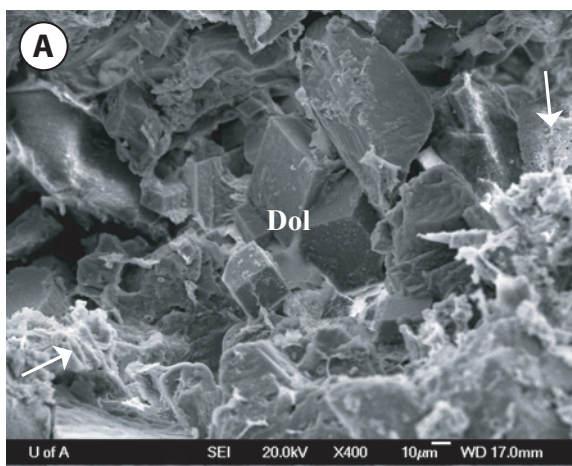
Petrographic thin sections and SEM investigations of the large structures show diagnostic textural, petrographic and diagenetic changes. The structure's wall (Fig. 4.8A) appears as dark line that marks a change from the yellowish, slightly stained, matrix sandstone (Figs. 4.8A-B, 4.9A-B) to the light purple hypoburrow-cemented sandstone (Figs. 4.8A, C, 4.9C-D). The concretionary hypoburrow-cemented sandstone envelops the large *Thalassinoides* (b1-b4) that together form the core of the large sedimentary structures (Fig. 4.8A). These unlined internal burrows are passively filled with the quartz arenite and/or rudite microfacies (Figs. 4.8A, D, E). The burrow fills have most of the petrographic characters of the depositional unit II, but differ in that they are pervasively cemented (Figs. 4.8D-E, 4.9E-F). Likewise, the preferentially cemented-burrow sandstone (quartz arenite microfacies) is lithologically similar to the main matrix sandstone, but for the pervasive authigenic concretionary-calcite cement (reddish staining) (Fig. 4.8C). The calcite cement replaces and displaces the bioclastic and framework grains (Figs. 4.9C-D). These are represented by the earlier grain-coating

FIGURE. 4. 8. Plain-light and crossed-nicols photomicrographs of the large sedimentary structures. **A-** Plain-light photograph of a large petrographic thin section (partly stained with ARS) showing a diagnostic diagenetic change from lightly-stained matrix sandstone (m) to the purple-stained hypoburrow cemented sandstone (hc) that binds four passively filled *Thalassinoides* (b1-b4). Note the well-developed spreite of burrow b2, and the two small burrows *Planolites* (p) (lower right). **B-** Optical photomicrograph (crossed nicols) of the matrix sandstone (m zone) in A, showing the authigenic calcite (cal) cement (stained dark red), zoned dolomite rhombs (dol), and the syntaxial quartz overgrowth (Qz). **C-** Optical photomicrograph (crossed nicols) of the hc zone in A, showing monocrystalline quartz grain (Qz) framework and common foraminifera (for) tests, sitting in the pervasive eodiagenetic calcite (reddish-stained) cement (cal). **D-** Plain-light photomicrograph of the contact between the burrow b1 and the hc zone in A. The burrow b1 is sharp walled (dotted line) and passively filled with the rudite—gravel-sized large foraminifera (Lf), oyster shell fragments (Oy), moldic porosity (Mol)—and calcareous quartz arenite microfacies, with pervasive calcite cementation (reddish stained). **E-** Close-up optical photomicrograph (crossed nicols) of D, showing different cement types. Microcrystalline calcite (white arrow), prismatic calcite (black arrow)—infilling the large-sized bio-molds (Mol)—and the pervasive purple-stained pore-filling mosaic and coarse-crystalline calcite (Cal).



and pore-filling microcrystalline calcite that is enveloped by the pore-filling equigranular mosaic calcite, and later by coarse-crystalline calcite (Figs. 4.9E-F). The dolomite cement and quartz overgrowth are sporadically observed in the preferentially cemented burrow zone.

FIGURE. 4.9. Optical photomicrographs (crossed nicols) and SEM images of the different structure zones. **A-** The microcrystalline and euhedral dolomite rhombs (Dol) replacing the foraminifera-test fragments (white arrows) in the matrix sandstone zone. **B-** Nannoplankton coccoliths (Coc) stacked on a rough surface—due to micro-quartz overgrowth, white arrow—of a quartz grain in the matrix sandstone zone. **C-** Pervasive micro-crystalline and mosaic calcite, displacing and replacing the monocrystalline quartz grains (black arrows) and filling the loosely packed framework grains in the hypoburrow cemented zone. **D-** Microcrystalline and mosaic calcite (Cal), cementing two quartz (Qz) grains in the hypoburrow cemented zone. **E-** The microcrystalline calcite (I) is engulfed by the prismatic calcite (II) that is post-dated by mosaic and coarse-crystalline calcite (III) in the internal burrow zone. **F-** Common three types of the pore-filling calcite cement in the burrow zone: microcrystalline calcite (Cal-1); mosaic calcite (cal-2); and the coarse-crystalline calcite (Cal-3).



STABLE ISOTOPE GEOCHEMISTRY

ISOTOPIC SIGNATURE

The carbon and oxygen stable isotopic data—analyzed bulk calcite and bulk dolomite samples of the host sediments and the different diagenetic zones (Figs. 4.5, 4.8A)—are shown in Table (4.3). Discernible is an overall and general depletion trend in isotopic values ($\delta^{13}\text{C}_{\text{PDB}}$ and $\delta^{18}\text{O}_{\text{PDB}}$) of both bulk calcite and bulk dolomite cements from the host sandstone through the outer structure zones (m and hc zone) into the most depleted internal structure burrow zones (b1-b4) (Fig. 4.10).

The host sandstone shows bulk calcite isotopic compositions of ($\delta^{13}\text{C}_{\text{PDB}}$ -0.94 to -1.45% , and $\delta^{18}\text{O}_{\text{PDB}}$ -4.78 to -4.95%), and bulk dolomite isotopic values of ($\delta^{13}\text{C}_{\text{PDB}}$ -2.05 to -2.61% and $\delta^{18}\text{O}_{\text{PDB}}$ -2.14 to -2.93%) (Fig. 4.10, field A). Matrix sandstone (m zone) exhibits a gradual depletion in the bulk calcite ($\delta^{13}\text{C}_{\text{PDB}}$ -1.62 to -2.69% and $\delta^{18}\text{O}_{\text{PDB}}$ -5.37 to -7.20%) and bulk dolomite ($\delta^{13}\text{C}_{\text{PDB}}$ -2.36 to -3.62% and $\delta^{18}\text{O}_{\text{PDB}}$ -5.87 to -9.87%) (Fig. 4.10, field B). Nodular hypoburrow cemented sandstone (hc zone) reveals a continual depletion in the isotopic values of the bulk calcite and the bulk dolomite (Fig. 4.10, field C). This zone can be subdivided into the outer (yellow white color) and internal (white) sub-zones (Table 4.3). Bulk calcite isotopic compositions have a range of $\delta^{13}\text{C}_{\text{PDB}}$ from -3.13 to -4.75% , and of $\delta^{18}\text{O}_{\text{PDB}}$ from -4.63 to -6.75% . Bulk dolomite displays isotopic compositions range of $\delta^{13}\text{C}_{\text{PDB}}$ from -4.44 to -7.23% , and of $\delta^{18}\text{O}_{\text{PDB}}$ from -4.80 to -7.91% . Preferentially cemented burrow zone (b zone) is highly depleted in both carbon and oxygen isotopic compositions (Fig. 4.10, field D). Bulk calcite isotopic compositions exhibit a range of $\delta^{13}\text{C}_{\text{PDB}}$ from -3.99 to -4.98% and of $\delta^{18}\text{O}_{\text{PDB}}$ from -4.80 to -7.22% . Bulk dolomite has an isotopic-composition range of $\delta^{13}\text{C}_{\text{PDB}}$ from -4.21 to -8.23% , and of $\delta^{18}\text{O}_{\text{PDB}}$ from -1.41 to -11.2% .

TABLE 4.3. Carbon and oxygen stable isotope data of the bulk calcite cement (microcrystalline, prismatic, mosaic and coarse crystalline calcite \pm bioclasts) and the bulk dolomite cement (microcrystalline and zoned rhombs \pm dolomitized bioclasts).

Sample Name	Description	Bulk Calcite			Bulk Dolomite		
		$\delta^{13}\text{C}$	$\delta^{18}\text{O}$	$\delta^{18}\text{O}$	$\delta^{13}\text{C}$	$\delta^{18}\text{O}$	$\delta^{18}\text{O}$
		‰ PDB	‰ PDB	‰ SMOW	‰ PDB	‰ PDB	‰ SMOW
Host sandstone (depositional unit I)							
Mh10-1	Yellow Sst. (far from structures)	-0.94	-4.78	25.99	-2.61	-2.93	27.89
Mh10-2	Yellow Sst. (far from structures)	-1.45	-4.95	25.80	-2.05	-2.14	28.71
Mh14-1	Yellow Sst. (close to structures)	-2.30	-6.75	23.95	-2.44	-6.65	24.05
Mh14-2	Yellow Sst. (close to structures)	-1.62	-5.37	25.37	-3.62	-9.77	20.83
Matrix sandstone (m zone)							
C1-1	Yellow Sst. (outer zone)	-2.46	-6.78	23.92	-3.51	-5.26	25.48
C2-1	Yellow Sst. (outer zone)	-2.48	-6.84	23.86	-2.36	-5.87	24.86
C3-1	Yellow Sst. (outer zone)	-2.69	-7.20	23.49	-3.24	-9.87	20.73
Hypoburrow cemented sandstone (hc zone)							
C1-2	Outer yellow/white hc sub-zone	-3.13	-5.41	25.33	-4.95	-7.87	22.79
C2-2	Outer yellow/white hc sub-zone	-3.96	-4.63	26.13	-4.64	-5.64	25.09
C3-2	Outer yellow/white hc sub-zone	-4.28	-5.37	25.37	-4.44	-7.03	23.67
C4-1	Outer yellow/white hc sub-zone	-4.73	-5.28	25.65	-4.75	-6.78	23.92
C1-3	Internal white hc sub-zone	-4.11	-5.10	25.65	-5.07	-6.44	24.27
C2-3	Internal white hc sub-zone	-4.73	-5.17	25.57	-7.23	-7.91	22.75
C3-4	Internal white hc sub-zone	-4.75	-6.75	23.95	-4.60	-4.80	25.97
Cemented burrow zone (b zone)							
C1-4	Internal burrow zone (b1)	-4.09	-5.63	25.11	-4.51	-5.93	24.80
C1-5	Internal burrow zone (b1)	-4.15	-5.91	24.81	-4.23	-6.06	24.66
C2-4	Internal burrow zone (b1)	-4.67	-7.12	23.57	-4.80	-8.08	22.58
C3-3	Internal burrow zone (b1)	-4.62	-6.85	23.85	-5.25	-1.41	29.45
C4-2	Internal burrow zone (b1)	-4.98	-7.22	23.46	-4.95	-7.87	22.79
C3-5	Internal burrow zone (b2)	-4.60	-4.80	25.97	-4.21	-8.95	21.68
C4-3	Internal burrow zone (b2)	-4.51	-6.54	24.16	-4.43	-6.93	23.77
C4-4	Internal burrow zone (b3)	-3.99	-5.77	24.96	-8.23	-11.20	19.36

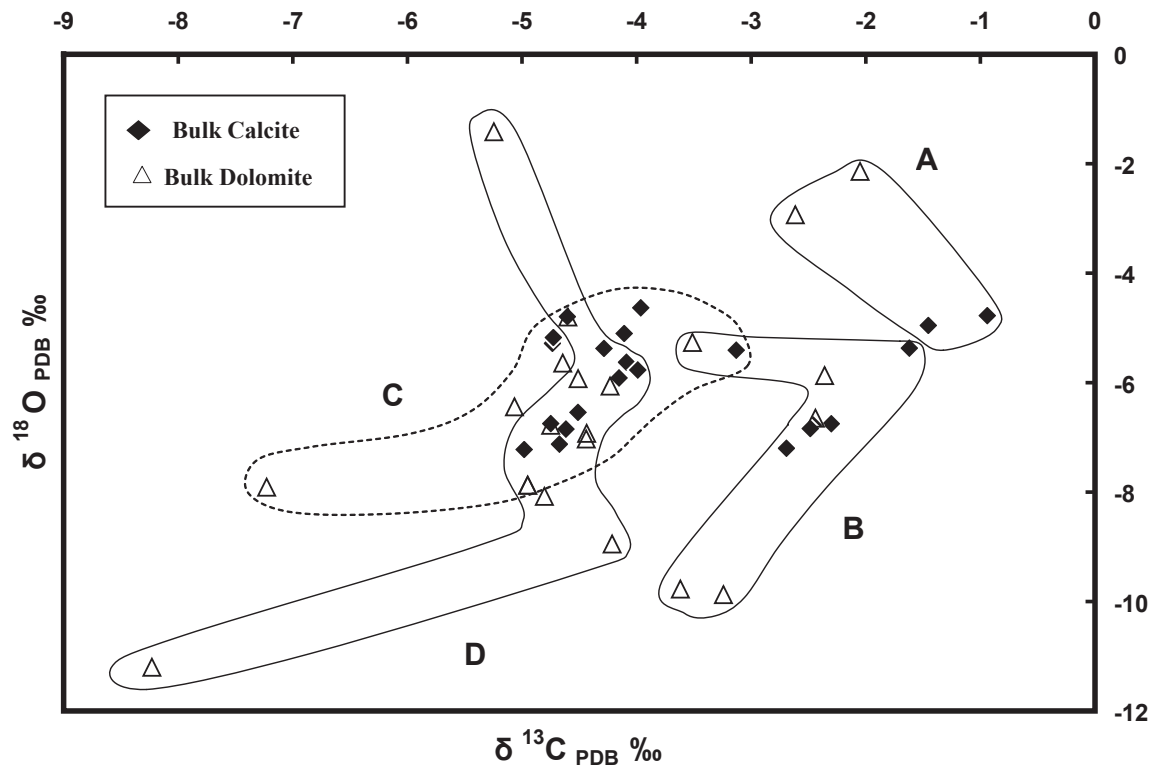


FIGURE. 4.10. A cross plot of $\delta^{13}\text{C}_{\text{PDB}} \text{ ‰}$ versus $\delta^{18}\text{O}_{\text{PDB}} \text{ ‰}$ of the bulk calcite and bulk dolomite. Field A corresponds to the host sandstone. Field B is the matrix sandstone (m zone). Field C marks the hypoburrow concretionary sandstone (hc zone). Field D is the internal burrow zone (b zone).

INTERPRETATION OF BULK CALCITE AND DOLOMITE ISOTOPIC SIGNATURE

Bulk Calcite Isotopic Signature

The $\delta^{13}\text{C}_{\text{PDB}}$ values of the bulk calcite show a systematic depletion compared to the host sediments (-0.94 to -2.30‰) from the matrix sandstone (m zone) (-2.46 to -2.69‰) through the hypoburrow concretion (hc zone) (-3.13 to -4.75‰), into the cemented burrow (b zone) (-3.99 to -4.98‰) (Fig. 4.10). The biasing of the $\delta^{13}\text{C}_{\text{PDB}}$ values towards negative values indicates that the pore-water carbon was derived from seawater and dissolution of metastable carbonate coupled with bacterial decomposition of

organic matter (Fig. 4.11) in the sulfate reduction zone. The anoxic and anaerobic sulfate reduction zone generated high alkalinity, thereby increasing the total dissolved carbon and prompting the precipitation of calcite from pore water biased towards light $\delta^{13}\text{C}_{\text{PDB}}$ values during shallow diagenesis (between sediment/water interface and shallow depths of ~3m).

The depleted range of the oxygen in bulk calcite $\delta^{18}\text{O}_{\text{PDB}}$ from -4.63 to -7.22‰, and the $\delta^{18}\text{O}_{\text{SMOW}}$ between 23.46 and 26.13‰ (similar to the fresh-water range; see Taylor, 1967) indicates mixing of marine pore water and meteoric ground water during the precipitation of the authigenic calcite. Using the $\delta^{18}\text{O}_{\text{PDB}}$ range of the bulk calcite (-4.63 to -7.22‰), the calcite-water fractionation equation $10^3 \ln \alpha_{\text{calcite-water}} = 2.78 \times 10^6 T^{-2} - 2.89$ (Freidman and O'Neil, 1977) and assuming the $\delta^{18}\text{O}_{\text{SMOW}}$ values of pore water between -2 and -4‰ (as assumed for the Recent and Eocene meteoric water in this area by Yurtsever and Gat, 1981 and Abdel-Wahab and McBride, 2001) the precipitation of the calcite is interpreted to have occurred between ~15° and 35° C (Fig. 4.12A).

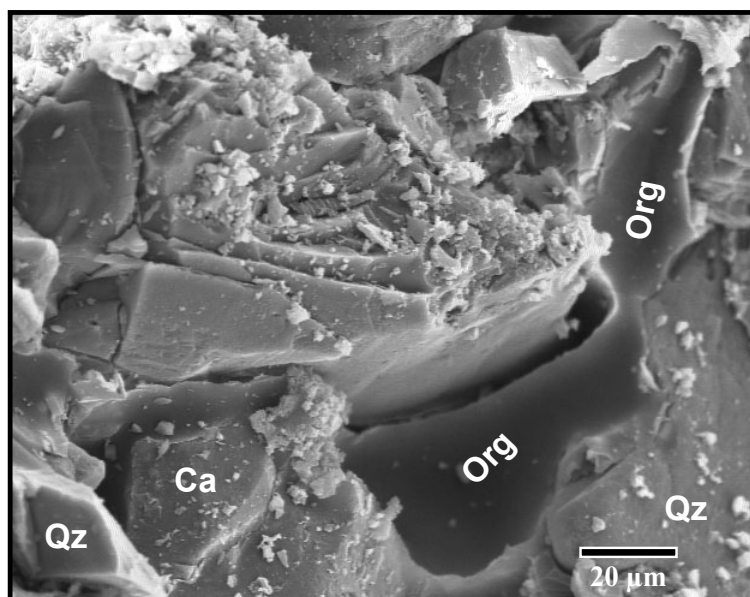


FIGURE. 4.11. SEM photograph showing well-preserved dark organic material (Org) in the structure-adjacent host sandstone zone (Qz is quartz and Ca is calcite).

Bulk Dolomite Isotopic Signature

Bulk dolomite isotopic values provide additional clues to the origin of the dolomite precipitation. The increasingly depleted $\delta^{13}\text{C}_{\text{PDB}}$ values from the matrix sandstone to the center of the burrow structures show a range of -2.05 to -8.23‰ (Fig. 4.10). The light bulk-dolomite $\delta^{13}\text{C}_{\text{PDB}}$ values point to a significant contribution of biogenic CO_2 to the total dissolved inorganic carbon (e.g., Freidman and Murata, 1979). The preservation of organic carbon in the hosting sandstone (Fig. 4.11), the formation of Fe^{+2} -rich dolomite rhombs, and the depletion in the bulk dolomite $\delta^{13}\text{C}_{\text{PDB}}$ are taken together as indicators of the dolomite growth in an anoxic and anaerobic sulfate reduction zone through to early-stage methanogenesis. The surfaces of some dolomite rhombs are covered by fibrous microbial dolomite (Fig. 4.6D) that post dates the microcrystalline- and zoned- dolomite rhombs in the early methanogenesis zone.

The biasing of the bulk dolomite $\delta^{18}\text{O}_{\text{PDB}}$ measurements toward light (warm) values of -1.41 to -11.20‰ indicates the presence of meteoric water in the pore water during the precipitation of the dolomite. Dolomite more depleted than $\delta^{18}\text{O}_{\text{PDB}}$ of -2‰ likely records formation in, or modification by, depleted (meteoric) water and/or under elevated temperatures (even allowing for depleted seawater as light as $\delta^{18}\text{O}_{\text{PDB}}$ -4‰) (e.g., Land, 1983). Using the wide $\delta^{18}\text{O}_{\text{PDB}}$ range of bulk dolomite (-1.41 to -11.20‰), the dolomite-water fractionation equation $10^3 \ln \alpha_{\text{dolomite-water}} = 3.2 \times 10^6 \text{ T}^{-2} - 3.3$ (Land, 1983), assuming the pore-water $\delta^{18}\text{O}_{\text{SMOW}}$ of -2 to -4‰ (e.g., Yurtsever and Gat, 1981; Abdel-Wahab and McBride, 2001), the dolomite was precipitated in temperatures between $\sim 20^\circ$ and 65° C (Fig. 4.12B). The higher range of the calculated bulk-dolomite formation temperature may be due to more depleted pore-water $\delta^{18}\text{O}_{\text{SMOW}}$ values ($< -4\text{‰}$) during the precipitation of dolomite and/or probable contamination of high-temperature dolomite.

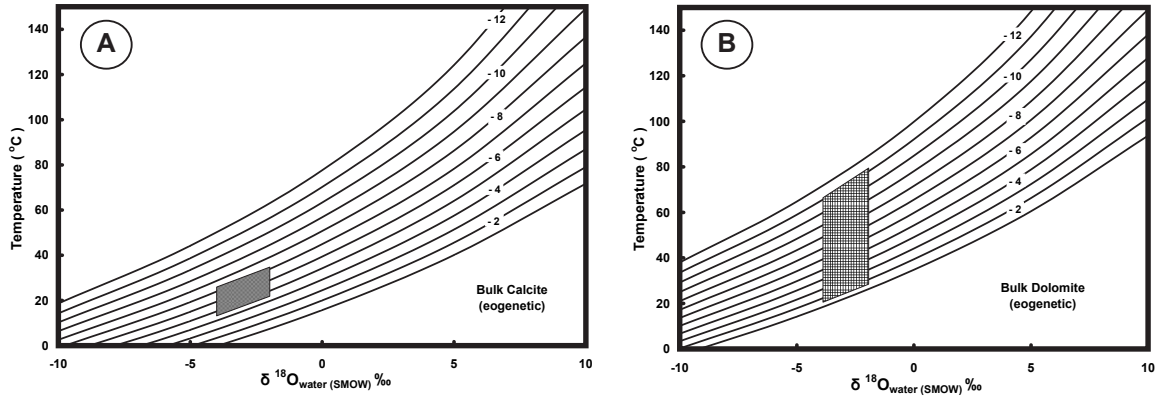


FIGURE. 4.12. **A-** Range of temperature and the calculated $\delta^{18}\text{O}_{\text{SMOW}}$ value of pore fluids constructed for the analyzed $\delta^{18}\text{O}_{\text{PDB}}$ range of the bulk calcite (-4.63 to -7.22‰) using the calcite-water fractionation equation of Friedman and O'Neil (1977). The bulk calcite field marks the calculated temperature, assuming that the $\delta^{18}\text{O}_{\text{SMOW}}$ value of pore fluids lies between -2 and -4‰. **B-** Range of temperature and the calculated $\delta^{18}\text{O}_{\text{SMOW}}$ value of pore fluids constructed for the analyzed $\delta^{18}\text{O}_{\text{PDB}}$ range of the bulk dolomite (-1.41 to -11.20‰), using the dolomite-water fractionation equation of Land (1983). The bulk-dolomite field marks the calculated temperature, assuming that the $\delta^{18}\text{O}_{\text{SMOW}}$ value of the pore fluids was between -2 and -4‰.

ORIGIN OF THE LARGE SEDIMENTARY STRUCTURES

Pertinent ichnological and sedimentologic data are integrated with sequence stratigraphy in order to propose a bio-sedimentological model. This model interprets the origin and the development of the anomalous large sedimentary structures. The terms sea-level fall, sea-level rise, and sea-level still stand are used herein to describe the relative sea-level phases of the parasequences (see Chapter 2). The suggested bio-sedimentological model (Fig. 4.13) comprises five stages (A to E).

STAGE A

The hosting sandstone was deposited during sea-level still stand (Fig. 4.13). The presence of bio-carbonate grains (e.g., foraminifera, coccoliths and bioclasts), the prolonged residence time (low sedimentation rate) of the sediments close to sediment-water interface (e.g., Taylor et al., 1995; Ketzer et al., 2002; El-Ghali et al., 2006), and

the concomitant thorough bioturbation (reflected by suites of the *Cruziana* Ichnofacies; Fig. 4.2) (e.g., Aller, 1994; Konhauser and Gingras, 2007) together resulted in early diagenetic changes. Stable isotope $\delta^{13}\text{C}_{\text{PDB}}$ and $\delta^{18}\text{O}_{\text{PDB}}$ values (Fig. 4.10) of the bulk calcite and the bulk dolomite of the host sandstone show an affinity to marine pore-water and low meteoric ground water influence.

Eodiagenesis (Fig. 4.13) commenced through dissolution and diffusion of Ca^{+2} and CO_3^{-2} from bio-carbonate grains. Petrographic evidence (Fig. 4.6) indicates that the carbonate cement growth initiated as fringing and/or pore-filling microcrystalline calcite cement. The microcrystalline calcite dolomitized into microcrystalline dolomite that was covered by zoned dolomite. In turn, the dolomites were engulfed by the mosaic and coarse-crystalline calcite (Figs. 4.6, 4.13). The microcrystalline calcite fringes around bioclasts, and the presence of pore-filling microcrystalline and coarse-crystalline calcite in the framework are good indications of precipitation prior to significant compaction, typically of a near surface origin (e.g., Morad and Al-Aasm, 1997, El-Ghali et al., 2006).

STAGE B

Stage B represents the discontinuity and/or non-deposition episodes. Subaerial erosion and/or exposure (due to tectonic uplift and/or relative sea-level fall) and/or submarine exhumation (due to transgressive ravinement) resulted in the dewatering, burial and compaction of the hosting-unit sediments. During this stage, the substrate became firm but unlithified (Fig. 4.13). The pore-water likely was influenced by meteoric water and/or an elevated meteoric groundwater table during this stage.

STAGE C

With onset of early relative sea-level rise, the benthonic organisms (e.g., crustaceans and worms) colonized the firmground substrate. The resulting firmground ichnological suites (dominated by *Thalassinoides*) correspond to the *Glossifungites*

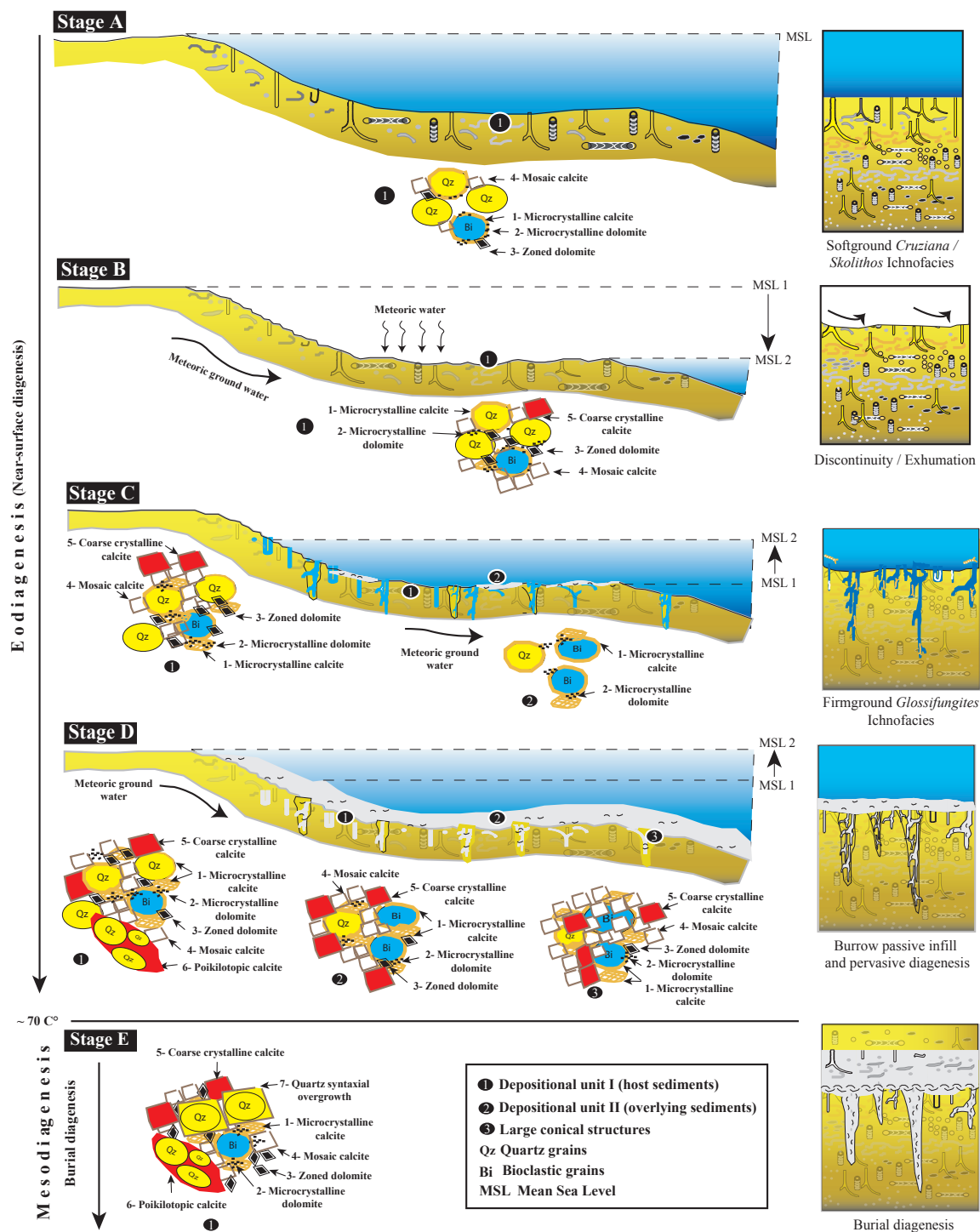


FIGURE. 4.13. Schematic diagrams of the five stages of the bio-sedimentological model, summarizing the development of the parasequence-constrained, large-sized sedimentary structures in the upper part of the Birket Qarun Formation.

Ichnofacies (Fig. 4.13). During this stage, the hosting sandstone showed progressive eodiagenetic changes and increased lithification (Fig. 4.13).

STAGE D

Stage D defines the late relative sea-level rise and early relative sea-level still stand phase of a parasequence-order cycle. The open vacated burrows (especially *Thalassinoides*) of the *Glossifungites* Ichnofacies were passively filled with post-omission sediments. During this stage, the overlying transgressive sandstone/lags/coquina deposits, the passively filled burrows, and the host sandstone suffered intensive diagenetic events and pervasive growth of the carbonate cement (Fig. 4.13). The light isotopic $\delta^{13}\text{C}_{\text{PDB}}$ and $\delta^{18}\text{O}_{\text{PDB}}$ of the bulk calcite and dolomite values (Table 4.3, Fig. 4.10) point to a significant contribution of biogenic CO_2 to the total dissolved inorganic carbon in the sulfate reduction zone and meteoric ground-water influence under a range of shallow diagenetic temperatures (Fig. 4.12).

The sandstone/lag/coquina deposits capping the parasequence boundary, as well as the burrow fills, suffered substantial eodiagenetic calcite cementation (Figs. 4.7-9, 4.13). These changes can be attributed to: 1- abundant bioclastics/lag deposits (source of carbonate cement) (e.g., Bjørkum and Walderhaug, 1990, Ketzer et al., 2002); 2- passive-filled nature and textural heterogeneity (e.g., Pemberton and Gingras, 2005) may enhance the permeability and localize the migration of carbonate-bearing fluxing fluids; and 3- conditions associated with a tropical climate (e.g., Lotfy and Van der Voo, 2007) promoted chemical flux and encouraged cementation. Nevertheless, the anoxic and anaerobic conditions in the sulfate reduction zone led to high alkalinity and precipitation of the pervasive carbonate cements (Figs. 4.8-9, 4.13). Local isopachous or irregular prismatic calcite cement enveloped the pre-dated microcrystalline calcite, and are post-dated by the mosaic calcite and coarse crystalline calcite (Figs. 4.8, 4.9, 4.13). Microcrystalline dolomites and zoned dolomite rhombs are uncommon and occur locally

(Figs. 4.7-9, 4.13). These may be due to reduced and localized occurrences of bioclasts that are rich in aragonite and low-magnesium calcite.

The hosting sandstone shows progressive and pervasive coarse-crystalline calcite and sporadically distributed poikilotopic calcite crystals (Figs. 4.6E, 4.13) that are interpreted to represent late-stage eodiagenesis.

STAGE E

Subsequent burial depths and compaction resulted in mesodiagenesis (burial diagenesis). The syntaxial quartz overgrowth cement near sites of inter-granular dissolution of the hosting sandstone (Figs. 4.6F, 4.8B, 4.13) is attributed to subsequent burial at considerable depth (> 1 km) as a mesogenetic authigenetic mineral (e.g., McBride, 1989). In many sedimentary basins, quartz cement overgrowth becomes common where the temperatures exceed 90°-100° C (Walderhaug, 1996). The mesodiagenetic changes did not affect the sandstone/lag deposits or the anomalous large structures (Figs. 4.7-9). This can be attributed to: 1- concretionary carbonate cement freezes the early texture, resisting later chemical and mechanical alterations (e.g., Mozley, 2003); 2- the calcite cement inhibited the development of the quartz overgrowth cement (e.g., Tucker, 2001); and 3- the abundance of bioclasts and lack of inter-granular contact of quartz grains.

DISCUSSION AND IMPLICATIONS

BIOTURBATION AND DIAGENESIS

The general depletion of the bulk calcite and bulk dolomite $\delta^{13}\text{C}_{\text{PDB}}$ values (Table 4.3) from the matrix sandstone (m zone) through hypoburrow cemented sandstone (hc zone) into the internal burrow zone (b zone) (Fig. 4.10) were strongly influenced by bioturbation. The biological activities changed and modified both the physical and chemical parameters of the sedimentary microenvironments. Burrowing activities (e.g.,

feeding, irrigation, and excretion) directly introduce plenty of organic matter in the form of mucus (generally polysaccharides), fecal pellets or primary organic materials (e.g., Aller, 1994; Bird et al., 2000), and the burrows thereby act directly or indirectly as source of organic carbon.

The organic matter constitutes a good substrate for microbial communities in an aerobic and anoxic sulfate reduction zone. The decomposition of organic carbon during sulfate reduction resulted in high alkalinity, increased total dissolved carbon, and precipitation of carbonate minerals from pore water that are biased towards light $\delta^{13}\text{C}_{\text{PDB}}$ values. Therefore, the localization of organic carbon toward the internal burrow zone accounts for the tendency toward general depletion of the $\delta^{13}\text{C}_{\text{PDB}}$ values from the matrix sandstones into the preferentially cemented burrow zone (Table 4.3, Fig. 4.10). This further led to the pervasive nucleation of the concretionary authigenic carbonate minerals in and around the burrows.

The general depletion of the bulk calcite and bulk dolomite $\delta^{18}\text{O}_{\text{PDB}}$ values is interpreted herein as a result of meteoric water invasion in the marine pore water during the precipitation of the authigenic carbonate minerals. The large-sedimentary structures are spatially constrained to the parasequence boundaries (Figs. 4.2, 4.3). These parasequence boundaries mark shallowing-upward surfaces of short-lived subaerial erosion and/or (transgressive) submarine exhumation. This setting favors invasion of meteoric water and/or meteoric groundwater mixing with marine pore waters.

Moreover, the burrow-system nature of the firmground ichnogenera of the *Glossifungites* Ichnofacies—e.g., excavation of firmground shortly after subaerial and/or marine exhumation, infaunal colonization followed by passive fills of burrows with sandstone/lags transgressive deposits—led to vertical and lateral textural heterogeneity and enhancement of the vertical permeability (e.g., Pemberton and Gingras, 2005). The enhanced permeability resulted in localization of the flowing meteoric/marine pore waters preferentially in and around burrows. This can account for the pervasive carbonate

cement with depleted $\delta^{18}\text{O}_{\text{PDB}}$ values in and round the burrows.

SEDIMENTOLOGIC AND SEQUENCE STRATIGRAPHIC IMPLICATIONS

Sedimentary Environment

The high bioturbation intensity (BI 5), high ichnogenera diversities and the presence of ichnological suites attributable to proximal expressions of the *Cruziana* Ichnofacies and distal expressions of the *Skolithos* Ichnofacies (Table 4.1, Fig. 4.2) are good indicators of normal-marine salinities (minimally stressed conditions) and low- to moderate depositional energies during the accumulation of the host sandstones (depositional unit I). The paucity of primary physical sedimentary structures, prevalence of fine- to very fine-grained sandstones, introduction of marine authigenic carbonate cement, and the absence of evidence for physico-chemical stress (e.g., syneresis cracks or evaporite beds) strongly support a paleoenvironment that was quiescent and marine. Abundant mixed benthic fauna (Table 4.1) planktonic foraminifera, and coccoliths add additional evidence of a shallow but fully marine, low- to moderate-energy paleoenvironment. Recent paleomagnetic data places the Fayum province at a lower paleolatitude than present under a tropical climate during the Middle and Late Eocene (Lotfy and Van der Voo, 2007). Thus, depositional unit I (host sandstone) is best interpreted to have been deposited under a low to moderate energy, open-marine bay or gulf paleoenvironment in tropical climatic zone (Fig. 4.14).

Heterolithic depositional unit II shows weak to moderate bioturbation intensities (BI 0-3), general reduced ichnogenera diversities, and locally common softground trace-fossil suites attributable to the *Skolithos* Ichnofacies (Table 4.1, Fig. 4.2). These ichnological characters point to a moderate- to high-energy shallow-marine environment. The base of the depositional unit II is characterized by the presence of lag deposits, the large bio-sedimentary structures, and firmground ichnological suites, attributable to the *Glossifungites* Ichnofacies. The base of this unit is interpreted as ravinement (TSE)

surfaces that record transgressive and high-energy conditions (Fig. 4.14). The mixed vertebrate and benthic invertebrate fauna (Table 4.1) are indicative of normal-marine salinities and agitated shallow-marine conditions. The sandstone/lags/coquina deposits (depositional unit II) accumulated during transgression under moderate- to high-energy conditions, mostly in bay margin and/or coastal waterway settings (Fig. 4.14).

Sequence Stratigraphy

The large sedimentary structures and firmground ichnological suites are restricted to parasequence boundaries, which are demarcated by wave ravinement (TSE) surfaces (Figs. 4.2, 4.3, 4.13, 4.14). These TSE define the boundaries of three to four prograding and thinning-upward parasequences in the upper Birket Qarun Sandstone (Figs. 4.3E, 4.14). The parasequences constitute the base of a highstand systems tract (HST) of a third-order sequence (Figs. 4.2, 4.3E, 4.14) (see Chapter 2). Each parasequence was initiated with the deposition of fine-grained sandstone (depositional unit I) in a low-energy open-marine bay. The sandstone shoaled upward (Figs. 4.13, 4.14) until truncated by a wave ravinement (TSE) surface that corresponds to a parasequence-bounding marine flooding surface. Ravinement surfaces are overlapped by the sandstone/shell hash/lag deposits (depositional unit I) in bay margin/coastal setting under moderate- to high-energy conditions.

The relative sea-level cyclicity (Fig. 4.14) during the deposition of the structure-associated parasequences appeared to be rapid, and were associated with noticed tectonic activity. Subsidence/uplift tectonics (EGPC, 1992) were controlled by the SE-throwing of the NW-SE striking faults bounding the Fayum (Gindi) sag-basin. Local basin tectonics associated with the glacio-eustatic sea-level fall and rise adjusted relative sea levels and accommodation space during the deposition of these structure-associated parasequences.

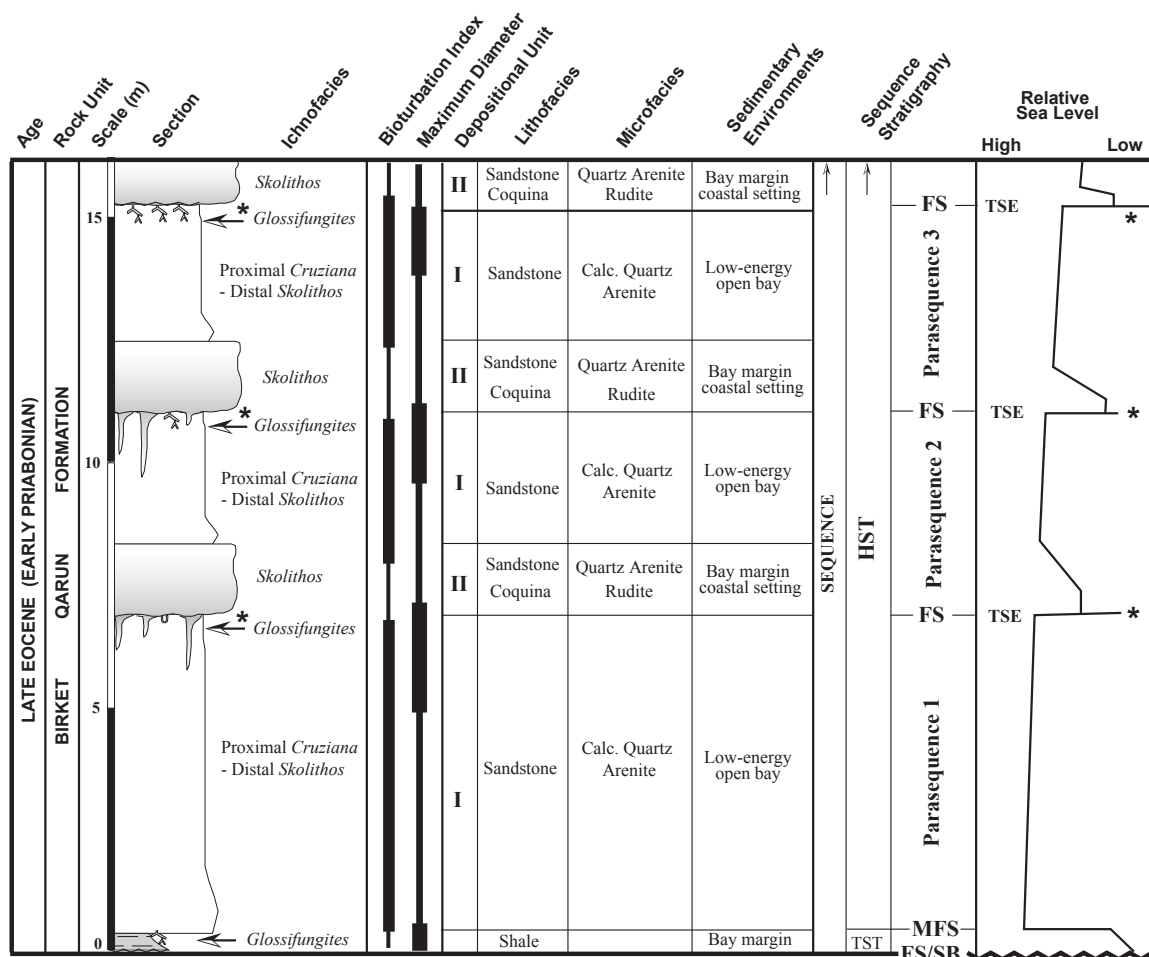


FIGURE. 4.14. Detailed chart of the integrated stratigraphic, sedimentological and ichnological data, summarizing the sedimentary environments and sequence stratigraphic architecture of the structure-associated depositional units in the Birket Qarun Formation.

CONCLUSIONS

- 1- Unusual large-sized branched pillars and/or large boxworks and conical sedimentary structures define the upper Birket Qarun Formation, in the area of Wadi El-Hitan.
- 2- Polished longitudinal- and cross-sectional slabs of these large structures reveal a complex ichnofabric. Firmground *Thalassinoides*, belonging to the *Glossifungites* Ichnofacies, are bounded by hypoburrow concretionary zone within the matrix sandstone.
- 3- Petrographic thin sections and the SEM investigations indicate a progressive diagenetic change from the matrix sandstone into the internal structure zones. Nodular hypoburrow

cemented sandstone (quartz arenite microfacies) and burrow-zone fills (rudite / quartz arenite microfacies) show grain-coating and pore-filling microcrystalline calcite, pore-filling equigranular mosaic calcite, and coarse-crystalline/poikilotopic calcite textural habits. The dolomite cement and quartz overgrowth are common in the matrix sandstone, and locally observed within the different structure zones.

4- Stable isotopic data of the bulk calcite ($\delta^{13}\text{C}_{\text{PDB}}$ from -0.94 to -4.98‰ and $\delta^{18}\text{O}_{\text{PDB}}$ from -4.63 to -7.22‰) and bulk dolomite ($\delta^{13}\text{C}_{\text{PDB}}$ from -2.05 to -8.23‰ and $\delta^{18}\text{O}_{\text{PDB}}$ from -1.41 to -11.20‰) are biased towards light (warm) values. These data indicate that the marine pore-water carbon was highly influenced by bacterial decomposition of organic matter and suffered a mixing of meteoric ground water during the precipitation of the authigenic carbonate cement under shallow diagenetic conditions.

5- Based on the integrated ichnological data, petrography, paragenetic events, and stable isotope data, a bio-sedimentological model has been suggested. The bioturbation mediated and enhanced the shallow diagenetic events. Calcite-dominated carbonate precipitation in and around the burrows led to development of these large concretionary sedimentary structures.

6- The large sedimentary structures are confined to parasequence boundaries. Each parasequence was initiated with the deposition of highly bioturbated, fine-grained host sandstones (depositional unit I) in low-energy open-marine bay. These record upward shoaling, and were truncated by the wave-ravinement surfaces (TSE) corresponding to parasequence-bounding marine flooding surfaces. These surfaces are overlain by and associated with weakly bioturbated, medium- to high-energy bay margin to coastal sandstone/shell hash/lag deposits of the depositional unit II.

REFERENCES

- Abad, M., Ruiz, F., Pendón, J.G., Tosquella, J. and González-Regalado, L., 2006, Escape and equilibrium trace fossils in association with *Conichnus conicus* as indicators of variable sedimentation rates in Tortonian littoral environments of SW Spain: *Geobios*, v. 39, p. 1–11.
- Abdel-Wahab, A. and McBride, E.F., 2001, Origin of giant calcite-cemented concretions, Temple Member, Qasr El Sagha Formation (Eocene), Fayum depression, Egypt: *Journal of Sedimentary Research*, v. 71, p. 70–81.
- Al-Aasm, I.S., Taylor, B.E. and Southmm, B., 1990, Stable isotope analysis of multiple carbonate samples using selective acid extraction: *Chemical Geology*, v. 80, p. 119–125.
- Aller, R.C., 1994, Bioturbation and remineralization of sedimentary organic matter: Effects of redox oscillation: *Chemical Geology*, v. 114, p. 331–345.
- Bailey, R.H. and Newman, W.A., 1978, Origin and significance of cylindrical sedimentary structures from Boston Bay Group, Massachusetts: *American Journal of Science*, v. 278, p. 703-714.
- Beadnell, H.J.L., 1905, The topography and geology of the Fayum province of Egypt: Egyptian Survey Department, Cairo, 101 pp.
- Bird, F.L., Boon, P.I. and Nichols, P.D., 2000, Physiochemical and microbial properties of burrows of the deposit-feeding thalassinidean ghost shrimp *Biffarius arenosus* (Decapoda: Callianassidae): *Estuarine, Coastal and Shelf Science*, v. 51, p. 279–291.
- Bjørkum, P.A. and Walderhaug, O., 1990, Geometrical arrangement of calcite cementation within shallow marine sandstones: *Earth-Science Reviews*, v. 29, p. 145-161.

- Bromley, R.G., Curran, H.A., Frey, R.W., Gutschick, R.C. and Suttner, L.J., 1975, Problems in interpreting unusually large burrows, *in* Frey, R.W., ed., *The Study of Trace Fossils*: Springer-Verlag, New York, p. 351–376.
- Buck, S.G. and Goldring, R., 2003, Conical sedimentary structures, trace fossils or not? Observations, experiments, and review: *Journal of sedimentary Research*, v. 73, p. 338–353.
- Degens, E.T. and Epstein, S., 1964, Oxygen and carbon ratios in coexisting calcites and dolomites from recent and ancient sediments: *Geochimica et Cosmochimica Acta*, v. 28, p. 23–44.
- Dionne, J-C. and Laverdiere, C., 1972, Structure cylindrique verticale dans un dépôt meuble Quaternaire, au nord de Montréal, Québec: *Canadian Journal of Earth Sciences*, v. 9, p. 528–543.
- EGPC, 1992, Western Desert, oil and gas fields (A comprehensive overview): The Egyptian General Petroleum Corporation, Cairo, 431 pp.
- El-ghali, M.A.K., Mansurbeg, H., Morad, S., Al-Aasm, I. and Ajdanlisky, G., 2006, Distribution of diagenetic alterations in fluvial and paralic deposits within sequence stratigraphic framework: Evidence from the Petrohane terrigenous Group and the Svidol Formation, Lower Triassic, NW Bulgaria: *Sedimentary Geology*, v. 190, p. 299–321.
- Frey, R.W. and Howard, J.D., 1981, Conichnus and Schaubcylindrichnus: redefined trace fossils from the upper Cretaceous of the Western Interior: *Journal of Paleontology*, v. 55, p. 800-804.
- Friedman, I. and Murata, K.J., 1979, Origin of dolomite in Miocene Monterey shale and related formations in the Temblor Range, California: *Geochimica et Cosmochimica Acta*, v. 42, p. 1357-1365.

- Friedman, I. and O'Neil, J.R., 1977, Compilation of stable isotopic fractionation factors of geochemical interest: U.S. Geological Survey, Professional Paper 440-KK, 6th edition, 12 p.
- Gingerich, P.D., 1992, Marine mammals (Cetacea and Sirenia) from the Eocene of Gebel Mokattam and Fayum, Egypt; stratigraphy, age and paleoenvironments: University of Michigan Papers in Paleontology, v. 30, p. 1-84.
- Gingras, M.K., Armitage, I.A., Pemberton, S.G. and Clifton, H. E., 2007a, Pleistocene walrus herds in the Olympic Peninsula area: trace-fossil evidence of predation by hydraulic jetting: *Palaaios*, v. 22, p. 539-545.
- Gingras, M.K., Bann, K.L., MacEachern, J.A., Waldron, J. and Pemberton, S.G., 2007b, A conceptual framework for the application of trace fossils, *in* MacEachern, J.A., Bann, K.L., Gingras, M.K. and Pemberton, S. G., eds., *Applied Ichnology: Society of Economic Paleontologists and Mineralogists Short Course Note*, v. 52, p. 1-25.
- Goldring, R., 1964, Trace fossils and the sedimentary surface in shallow water marine sediments, *in* van Straaten, L. M. J. U., ed., *Deltaic and shallow water deposits: Developments in Sedimentology*, v. 1, p. 136–143.
- Haggag, M.A. and Bolli, H.M., 1996, The origin of *Globigerina* *semiinvoluta* (Keijzer), Upper Eocene, Fayoum area, Egypt: *Neues Jahrbuch für Geologie und Paläeontologie, Monatshefte*, v. 6, p. 365-374.
- Howard, J.D., Mayout, V. and Heardr, W., 1977, Biogenic structures formed by rays: *Journal of Sedimentary Petrology*, v. 47, p. 339-346.
- Hunter, R.J., Gelfenbaum, G. and Rubin, D.M., 1992, Clastic pipes of probable solution-collapse origin in Jurassic rocks of the southern San Juan basin, New Mexico: U.S. Geological Survey Bulletin, v. 1808-L, p. L12-L19.

- Ketzer, J.M., Morad, S., Evans, R. and Al-Aasm, I.S., 2002, Distribution of diagenetic alterations in fluvial, deltaic, and shallow marine sandstones within a sequence stratigraphic framework: evidence from the Mullaghmore Formation (Carboniferous), NW Ireland: *Journal of Sedimentary Research*, v. 72, p. 760–774.
- Konhauser, K.O. and Gingras, M.K., 2007, Linking geomicrobiology with ichnology in marine sediments: *Palaaios*, v. 22, p. 339–342.
- Land, L.S., 1983, The application of stable isotopes to studies of the origin of dolomite and to problems of diagenesis of clastic sediments, *in* Arthur, M.A., ed., *Stable Isotopes In Sedimentary Geology*: Society of Economic Paleontologists and Mineralogists Short Course Note, v. 10, p. 4.1–4.22.
- Lotfy, H. and Van der Voo, R., 2007, Tropical northeast Africa in the middle–late Eocene: Paleomagnetism of the marine-mammals sites and basalts in the Fayum province, Egypt: *Journal of African Earth Sciences*, v. 47, p. 135–152.
- Lowe, D.R., 1975, Water escape structures in coarse-grained sediments: *Sedimentology*, v. 22, p. 157–204.
- Massari, F., Ghibaudo, G., D’Alessandro, A. and Davaud, E., 2001, Water-upwelling pipes and soft-sediment-deformation structures in lower Pleistocene calcarenites (Salento, southern Italy): *Geological Society of America Bulletin*, v. 113, p. 545–560.
- McBride, E.F., 1989, Quartz cement in sandstones: A review. *Earth-Science Reviews*, v. 26, p. 69–112.
- McBride, E.F., Picard, M.D. and Milliken, K.L., 2003, Calcite- cemented concretions in Cretaceous sandstone, Wyoming and Utah, U.S.A: *Journal of Sedimentary Research*, v. 73, p. 462–483.

- Morad, S. and Al-Aasm, I.S., 1997, Conditions for rhodochrosite-nodule formation in Neogene–Pleistocene deep-sea sediments: evidence from O, C and Sr isotopes: *Sedimentary Geology*, v. 114, p. 295–304.
- Morsi, A.M., Boukhary, M. and Strougo, A., 2003, Middle–Upper Eocene ostracods and nummulites from Gebel Na'alun, southeastern Fayum, Egypt: *Revue de micropaleontology*, v. 46, p. 143–160.
- Mozley, P., 2003, Diagenetic Structures, *in* Middleton, G.V., Church, M.J., Coniglio, M., Hardie, L.A. and Longstaffe, F.J., eds., *Encyclopedia of Sediments and Sedimentary Rocks: Encyclopedia of Earth Sciences series*: Dordrecht, Kluwer Academic Publishers, p. 219-223.
- Mozley, P.S. and Davis, J.M., 2005: Internal structure and mode of growth of elongate calcite concretions: Evidence for small-scale, microbially induced, chemical heterogeneity in groundwater: *Geological Society of America Bulletin*, v. 117, p. 1400–1412.
- Nara, M., 1995, *Rosselia socialis*: A dwelling structure of a probably terebellid polychaete: *Lethaia*, v. 28, p. 171–178.
- Nelson, C.H., Johnson, K.R. and Barber, Jr.J.H., 1987, Gray whale and walrus feeding excavation on the Bering Shelf, Alaska: *Journal of Sedimentary Petrology*, v. 57, p. 419-430.
- Pemberton, S.G., Frey, R.W. and Bromley, R.G., 1988, The ichnotaxonomy of *Conostichus* and other plug-shaped ichnofossils: *Canadian Journal of Earth Sciences*, v. 25, p. 866-892.
- Pemberton, S.G. and Gingras, M.K., 2005, Classification and characterizations of biogenically enhanced permeability. *American Association of Petroleum Geologists Bulletin*, v. 89, p. 1493–1517.

- Plint, A.G., 1983, Liquefaction, fluidization and erosional structures associated with bituminous sands of the Bracklesham Formation (Middle Eocene) of Dorset, England: *Sedimentology*, v. 30, p. 525-535.
- Rao, V.P., Kessarkar, P.M., Krumbein, W.E., Krajewski, K.P. and Schneider, R.J., 2003, Microbial dolomite crusts from the carbonate platform off western India: *Sedimentology*, v. 50, p. 819–830.
- Said, R., 1962, *The geology of Egypt*: Elsevier, Amsterdam and New York, 377 pp.
- Salem, R., 1976, Evolution of Eocene-Miocene sedimentation patterns in parts of northern Egypt: *American Association of Petroleum Geologists Bulletin*, v. 60, p. 34-64.
- Savrda, C.E., 2002, Equilibrium responses reflected in a large *Conichnus* (Upper Cretaceous Eutaw Formation, Alabama, USA): *Ichnos*, v. 9, p. 33–40.
- Seiffert, E.R., Bown, T.M., Clyde, W.C. and Simons, E.L., 2008, Geology, paleoenvironment, and age of Birket Qarun locality 2 (BQ-2), Fayum Depression, Egypt, *in* Fleagle, J.G. and Gilbert, C.C., eds., *Elwyn L. Simons: A Search for Origins*: Springer-Verlag, New York, p. 71-86.
- Sendden, J.W., 1991, Origin and sequence stratigraphic significance of large dwelling traces in the Escondido Formation (Cretaceous, Texas, USA): *Palaios*, v.6, p. 541-552.
- Sestini, G., 1984, Tectonic and sedimentary history of NE African margin (Egypt/Libya), *in* Dixon, J.E., and Robertson, A.H.F., eds., *The geological evolution of the eastern Mediterranean*: Geological Society of London Special Publication, v. 17, p. 161-175.
- Shinn, E.S., 1968, Burrowing in recent lime sediments of Florida and the Bahamas: *Journal of Paleontology*, v. 42, p. 879-894.

- Smith, A.G., 1971, Alpine deformation and the oceanic areas of Tethys, Mediterranean and Atlantic: Geological Society of America Bulletin., v. 82, p. 2039-2070.
- Taylor, H.P. JR., 1967, Oxygen isotope studies of hydrothermal mineral deposits, *in* Barnes, H.L., ed., Geochemistry of Hydrothermal Ore Deposits: Holt, Rinehart & Winston, New York, p. 109–142.
- Taylor, K.G., Gawthorpe, R.L. and Van Wagoner, J.C., 1995, Stratigraphic control on laterally persistent cementation, Book Cliffs, Utah: Journal of the Geological Society, London, v. 152, p. 225-228.
- Tucker, M.E., 2001, Sedimentary Petrology; An introduction to the Origin of Sedimentary Rocks: Blackwell Scientific, Oxford, U.K., 262pp.
- Walderhaug, O., 1996, Kinetic modeling of quartz cementation and porosity loss in deeply buried sandstone reservoirs: American Association of Petroleum Geologists Bulletin, v. 80, p. 731–745.
- Wanas, H.A., 2008, Calcite-cemented concretions in shallow marine and fluvial sandstones of the Birket Qarun Formation (Late Eocene), El-Faiyum depression, Egypt: Field, petrographic and geochemical studies: Implications for formation conditions: Sedimentary Geology, v. 212, p. 40-48.
- Yurtsever, Y. and Gat, J.R., 1981, Atmospheric waters, *in* Gat, J.R., and Gonfianti R., eds., Stable Isotope Hydrology: Deuterium and Oxygen-18 in the Water Cycle: International Atomic Energy Agency, Vienna, Technical Report, Serial no. 210, p. 103–142.
- Zalat, A. A., 1995, Calcareous nanoplankton and diatoms from the Eocene / Pliocene sediments, Fayoum depression, Egypt: Journal of African Earth Sciences, v. 20, p. 227-244.

CHAPTER 5: THE *GLOSSIFUNGITES* ICHNOFACIES AND SEQUENCE STRATIGRAPHIC ANALYSIS: A CASE STUDY FROM THE MIDDLE-UPPER EOCENE SUCCESSION, FAYUM DEPRESSION, EGYPT

INTRODUCTION

The substrate-controlled ichnofacies: firm-ground *Glossifungites* (erected by Seilacher, 1964, 1967a,b), hardground *Trypanites* (added by Frey and Seilacher, 1980), and woodground *Teredolites* (introduced by Bromley et al., 1984) are extensively used in genetic stratigraphic analysis (e.g., Savrda, 1991b; MacEachern et al., 1992b). In particular, the *Glossifungites* Ichnofacies is useful in the identification of omission surfaces, and makes a substantial contribution in sequence stratigraphic analysis (e.g., Vossler and Pemberton, 1988; MacEachern et al., 1992b; Pemberton et al., 1992a,b, 2001, 2004; Frey and Goldring, 1992; Savrda, 1995; Holz, 2003; De Gibert and Robles, 2005; Fielding et al., 2006; Morris et al., 2006; MacEachern et al., 2007).

Moreover, the *Glossifungites* Ichnofacies subsists in wide-ranging environments. Examples of the *Glossifungites* Ichnofacies have been observed in association with wave ravinement and channel erosion in modern intertidal environments (Frey and Seilacher, 1980; Pemberton and Frey, 1985; Gingras et al., 2000, 2001), bay margins (Gingras et al., 2002a,b), brackish and estuarine environments (Buatois et al., 2002), estuarine incised valleys (Savrda, 1991a; MacEachern and Pemberton, 1994; MacEachern and Hobbs, 2004), forced regressive and lowstand shorefaces (MacEachern et al., 1992b; Pemberton and MacEachern, 1995), transgressively incised shorefaces (Raychaudhuri et al., 1992; MacEachern et al., 1999), transgressive offshore settings (MacEachern et al., 1992a), distal offshore settings (MacEachern and Burton, 2000) and deep-marine slope to bathyal environments (Hayward, 1976; Savrda et al., 2001a,b).

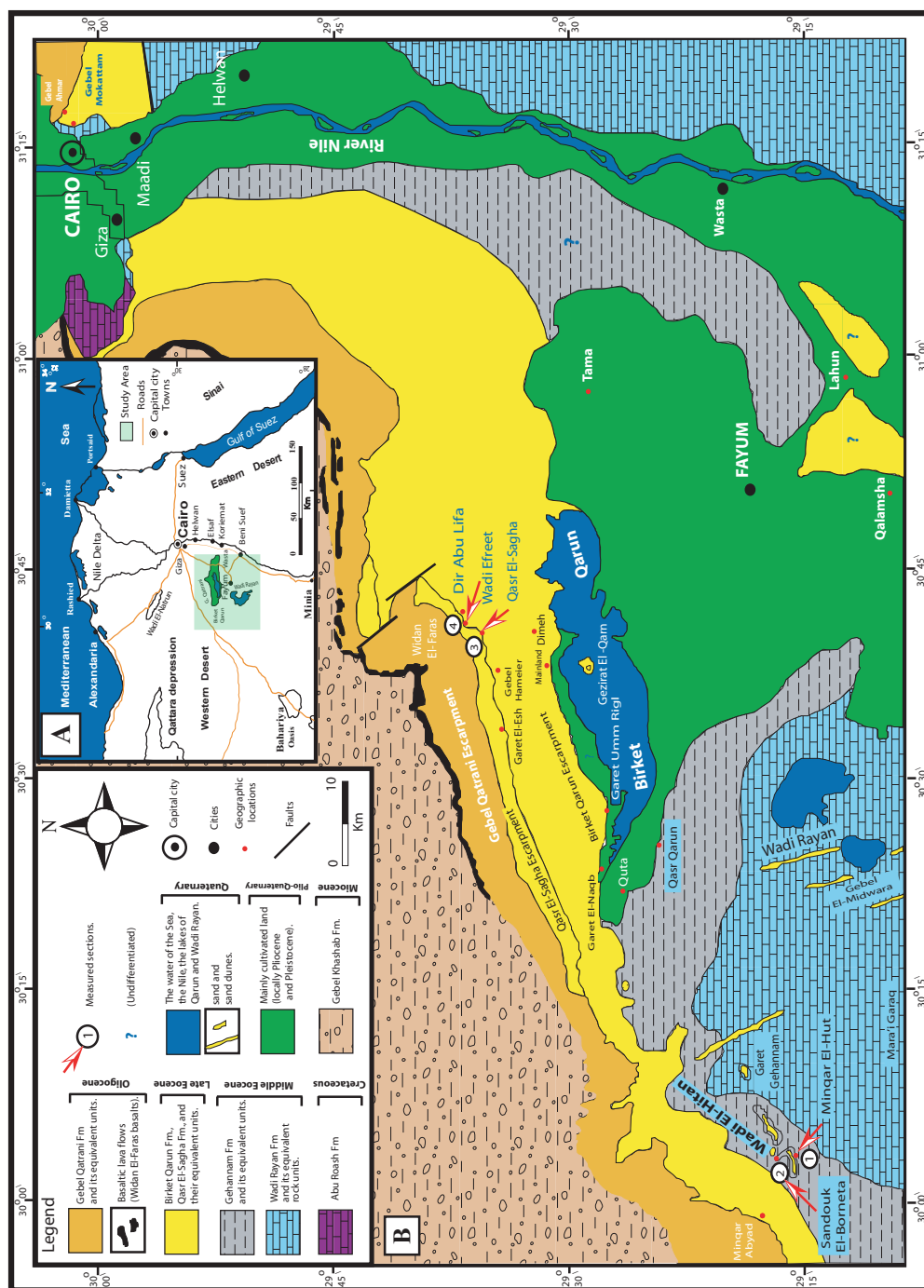
Almost any effort to classify *Glossifungites* Ichnofacies–demarcated surfaces apart from their geological settings is likely to be over-simplified. The present work

proposes a genetic approach, based on the integrated sedimentological, stratigraphical and ichnological data, to classify the examined *Glossifungites* Ichnofacies–demarcated surfaces within a sequence stratigraphic framework. This classification proves to be substantially useful in sequence stratigraphic analysis of the Middle-Upper Eocene succession in the Fayum Depression.

Four sections of the Middle-Upper Eocene outcrop succession were examined in two areas: Wadi El-Hitan (Whale Valley) and Qasr El-Sagha (El-Sagha Temple), in the vicinity of the Fayum Depression (Fig. 5.1). The four measured sections are numbered as follow (Fig. 5.1): 1) the composite section between Minqar El-Hut and Old Camp site; 2- the Sandouk El-Borneta section; 3) Qasr El-Sagha Temple section; and 4) the composite section between Dir Abu Lifa and Wadi Efreet. The sedimentological data (facies association analysis) and ichnological data (trace fossils, bioturbation intensity or BI, burrow density, ichnological diversity, and ichnofacies analysis) are combined with sequence stratigraphic data in a detailed study of more than twenty-five *Glossifungites* Ichnofacies– demarcated surfaces. The burrowing densities are detected herein as the bioturbation index (BI) immediately below the discontinuities. The symbols used in figures and illustrations are shown in Fig. 5.2. A comprehensive review of the concepts of sequence stratigraphy lies beyond the scope of this chapter. The pertinent sequence-stratigraphic terms and definitions that are used throughout the present study are drawn from various sources (e.g., Mitchum et al., 1977; Vail et al., 1977; Brown and Fisher, 1977; Van Wagoner, 1988, 1990; Posamentier et al., 1988; Posamentier and Allen, 1999), and are summarized in Chapter 1.

GEOLOGIC SETTING

The Fayum depression (Fig. 5.1) has a sub-triangular shape and occupies an area of 17,000 km². The Fayum or Gindi basin is one of the northern (intracontinental)



lowering of the sea level that resulted in progressive emergence and erosion of the structural highs that provided clastic sediments to the Late Eocene basins of northern Egypt (Salem, 1976). The Oligocene was a time of uplift, regression, volcanism and continental sedimentation (Cherif and El Afifi, 1983; Said, 1990).

The Fayum (Gindi) Basin is located in the unstable shelf belt (e.g., Said, 1990). This basin is characterized by a complex subsurface structural framework (synclinal/anticlinal structures and NW-SE striking fault system) that is masked by the relatively simple surface geology in the Fayum depression. The outcropping sedimentary successions blanket the underlying strata, and dip northward with a gentle dip angle averaging between 2° and 3°. There are small, localized faults that occur in different parts of the Fayum depression (Fig. 5.1).

The present work follows (with some modifications) the lithostratigraphic classification of Beadnell (1905) and the emendation of Said (1962). The lithostratigraphic subdivision of the Upper Eocene Qasr El-Sagha Formation into the lower Umm Rigl Member (Gingerich, 1992), and the middle Temple and the upper Dir Abu Lifa members (Bown and Kraus, 1988) is adopted. In the studied sections (Fig. 5.1), the outcrop stratigraphy is represented mainly by the following four rock units (from the base to top): the Middle Eocene Gehannam Formation, the Upper Eocene Birket Qarun and Qasr El-Sagha formations, and the Oligocene Gebel Qatrani Formation. The age assigned to these rock units is based on previous biostratigraphic studies (e.g., Strougo and Haggag, 1984; Zalat, 1995; Haggag and Bolli, 1996).

DEFINED FACIES ASSOCIATIONS

Five main facies associations (FA1 through FA5) are identified from the Middle-Upper Eocene succession in the Fayum depression (Table 5.1). The reported facies associations were described in detail in Chapter 2. The sedimentological, ichnological, and paleontological criteria of facies associations and a brief interpretation

Table 5.1. Summary of the stratigraphic, sedimentologic and depositional characters of the identified facies associations (FA1 – FA5).

Facies Ass.	Thickness (m)	Rock units	Lithology	Phys. Sed. Structures	Ichnofacies & Ichnogenera	Sed. environment
FA1: Low-energy marine-bay deposits.	Total compiled thickness: (60-80). Bed thickness: 2-10 m.	Gehannam and Birket Qarun formations	Medium- and fine- to very fine-grained sandstones.	Very rare wave ripple laminations in thin horizons (Gehannam Fm) and large ovoid concretionary sandstones (Birket Qarun Fm).	High bioturbation (BI 4-5), with high ichnogenera diversity. Ichnogenera include <i>Th</i> , <i>Pl</i> , <i>Op</i> , <i>Te</i> , <i>Sc</i> , <i>As</i> , <i>Rh</i> , <i>Ch</i> , <i>Cy</i> , <i>Ar</i> , <i>Sk</i> , and <i>Ps</i>). Archetypal (lower) to proximal (upward) expressions of the <i>Cruziana</i> Ichnofacies.	Low-energy and less- restricted open-marine bay.
FA2: Bay-margin deposits.	Total compiled thickness: ~12 m. Bed thickness: 0.5 – 8 m.	Gehannam Formation	Sandy shale grades upwards to siltstone and sporadically upward to fine- grained sandstone.	Very rare wave ripple, low-angle cross-lamination and gypsum joints are observed at the shale/ siltstone contact. Massive- appearing structures occur upwards (sandstone facies).	Bioturbation increases upwards (BI 0-3). Lower shale/siltstone facies has common <i>Ps</i> <i>Pl</i> and <i>Th</i> . Upwards, complex associations of <i>Op</i> , <i>Th</i> , <i>Sk</i> , <i>Pl</i> , <i>Ps</i> , rhizoliths, and vertebrate/invertebrate fossils are present in sandstone facies.	Low-energy bay margin (locally channelized) to swampy / supratidal environment (tropical to subtropical).
FA3: Lagoonal- brackish deposits.	Total thickness: 30-50 m. Bed thickness: 0.3 - 5 m.	Umm Rigl and Temple Mbrs. (Qasr El-Sagha Formation)	Carbonaceous sandy shale, grades upward to sandy siltstone and very fine-grained sandstone.	Tidal rhythmites, rare wavy bedding, and cross-lamination are locally observed upwards in sandier and silty parts.	Increasing-upward bioturbation intensities (BI 0-3) and ichnogenera diversities. Trace fossils suites (<i>Sk</i> , <i>Te</i> , <i>Mo</i> , <i>Di</i> , <i>Pl</i> , and <i>Ps</i>) are attributed to an impoverished distal expression of the <i>Skolithos</i> Ichnofacies.	Quiescent marginal- marine lagoonal / bay, partially restricted in arid to semi-arid climate (tropical to subtropical).
FA4: Distributary channel deposits.	Total thickness: 30- 35 m. Bed Thickness 1- 10 m.	Base of Dir Abu-Lifa Member (Qasr El-Sagha Formation)	Fine- to medium- grained sandstone and mudstone.	Inclined stratification (IS) and inclined heterolithic stratification (IHS), sigmoidal-bedding, planar- cross-bedding, tidal rhythmites, mud drapes, wavy/flaser bedding, and convoluting bedding.	Local occurrences of trace fossil suites of <i>Sk</i> , <i>Pl</i> , rare <i>Ar</i> , <i>Pr</i> , and rhizoliths, not attributed to archetypal Ichnofacies. Autocyclic <i>Glossifungites</i> Ichnofacies (Mainly <i>Th</i> , rare <i>Pa</i> and <i>Sk</i>) locally marks the channel boundaries.	Deltaic distributary- channel complexes.
FA5: Estuarine deposits.	Total thickness: 25- 40 m. Bed thickness: 0.5 – 5 m.	Dir Abu-Lifa Member (Qasr El-Sagha Formation)	Very fine- to coarse- grained sandstones, mudstones, lags and coquina deposits.	Upper estuarine channel is characterized by planar-tabular cross-bedding, sigmoidal bedding, and local IHS.	Weak to moderate bioturbation intensities (BI 0-3), with low ichnofossil diversities. <i>Skolithos</i> Ichnofacies (<i>Sk</i> , <i>Ar</i> and <i>Ps</i>) and local abundance of monospecific suites of <i>Th</i> , with rare <i>Ps</i> and <i>Te</i> .	Estuarine (lower-, middle-, and upper estuary) environment.

of their different depositional paleoenvironments are summarized in Table (5.1).

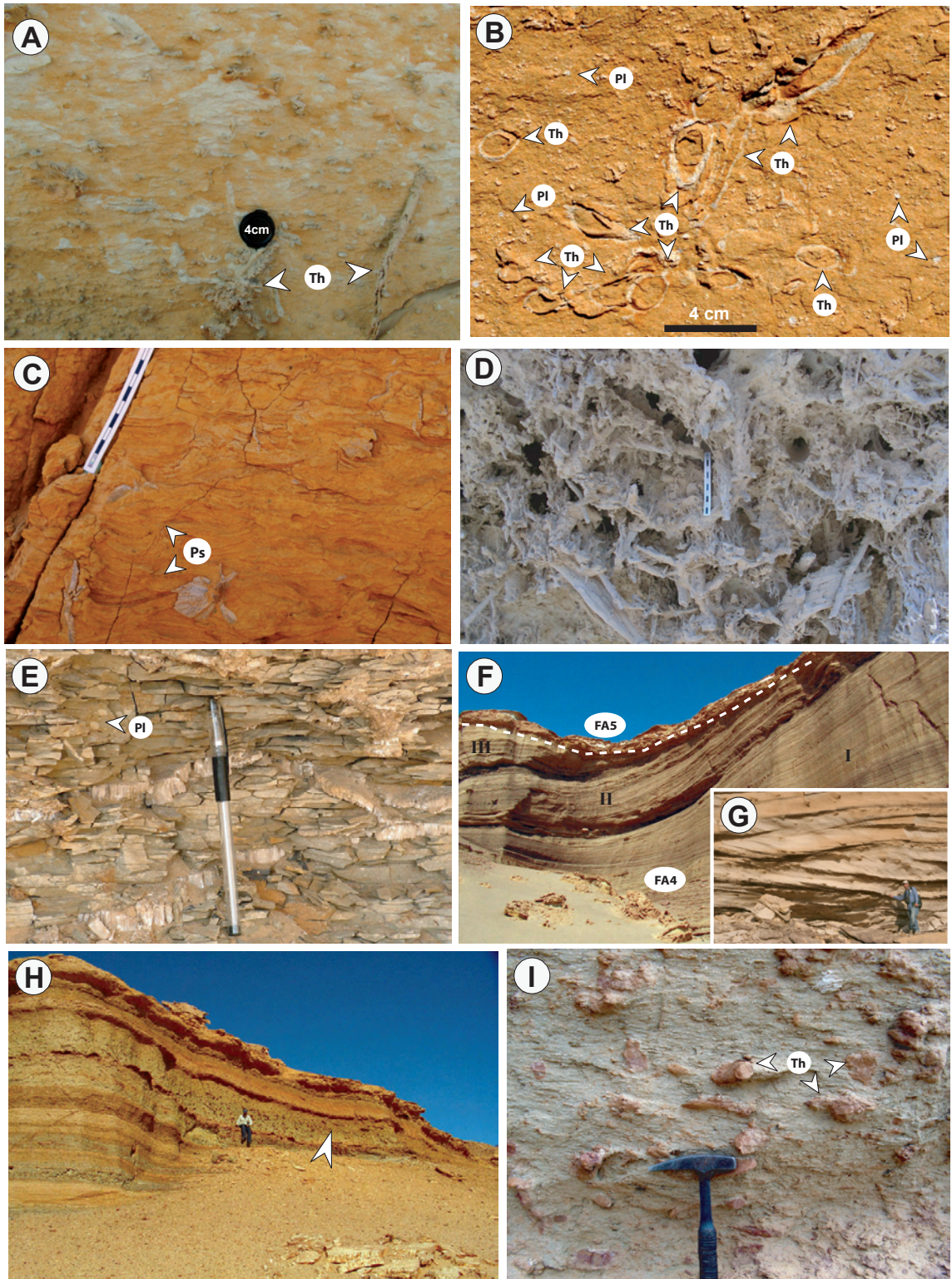
The characteristic ichnological and sedimentological features of the identified facies associations are shown in Fig. 5.3.

The Middle Eocene Gehannam Formation comprises highly bioturbated fine-grained sandstone (FA1— low-energy marine-bay deposits) and bedded mudstone/sandstone (FA2— bay-margin/coastal swamp deposits) (Table 5.1, Figs. 5.3A,C,D). Thoroughly bioturbated fine- to medium-grained sandstones (FA1— low-energy marine-bay deposits) define the entire Upper Eocene Birket Qarun Formation (Table 5.1; Fig. 5.3B). The upper Birket Qarun Formation displays several wave ravinement (TSE) surfaces, with associated sandstone/coquina beds. The intensive bioturbation and high ichnogenera diversities, coupled with the characteristic paucity of physical sedimentary structures in the Gehannam and Birket Qarun formations to indicate low-energy fully-marine depositional environment. Weak bioturbation and ichnological diversities of mudstone/sandstone deposits of FA2, along with rare wave-generated sedimentary structures and occurrences of gypsum veins and carbonaceous detritus, indicate a physico-chemically fluctuating, stressed quiescent bay-margin setting. Upwards, a complex paleoecologic horizon (Fig. 5.3D) within FA2 signifies the boundary between the Gehannam and Birket Qarun formations.

The lower Umm Rigl and Temple members of the Upper Eocene Qasr El-Sagha Formation are composed mainly of stacked parasequences consisting of carbonaceous shale and siltstone (FA3: lagoonal deposits) (Table 5.1, Fig. 5.3E). Wave and/or tidal ravinement (TSE) surfaces, as well their associated sandstones/coquina beds define the parasequence boundaries of FA3. The lower part of the upper Dir Abu Lifa Member of the Qasr El-Sagha Formation comprises weakly bioturbated (brackish trace-fossil suites) inclined heterolithic stratification (IHS) (FA4: deltaic distributary channels deposits) (Table 5.1, Figs. 5.3F-G). The lower parts of these distributary channels are characterized by abundant tidal/wave generated sedimentary structures (Figs. 5.3F-G). A general

paucity of physical sedimentary structures and the presence of weak bioturbation define the upper and middle estuarine sandstones/mudstones (FA5: estuarine deposits) of the upper Dir Abu Lifa Member. Moderate to high bioturbation intensities, low ichnogenera diversities, and large-scale tabular-planar cross-bedding are recorded in the distal middle estuary green sandstone and the lower estuary sandstone deposits of FA5, respectively (Figs. 5.3H-I).

FIGURE 5.3. Selected photographs showing the ichnological/sedimentologic characters of the identified facies associations (FA1 - FA5). **A-** *Thalassinoides* (Th) and complex burrow mottled ichnofabric in the bioturbated sandstone of FA1, base of Gehannam Formation, Sandouk El-Borneta section. **B-** Ichnological suite of *Thalassinoides* (Th) and *Planolites* (Pl), attributed to the *Cruziana* Ichnofacies in the sandstone (FA1) of the Birket Qarun Formation, Old Camp site. **C-** Monospecific suite of *Psilonichnus* (Ps) in the sandy siltstone (FA2), Minqar El-Hut section. **D-** Complex ichnofabric of rhizolith-bearing sandstone of the FA2, Sandouk El-Borneta section. **E-** Fissile sandy shale (FA3), with white gypsum streaks, *Planolites* (Pl) and dark spots of carbonaceous debris, Qasr El-Sagha Temple Mbr. **F-** Outcrop view of the laterally N- and NNW-ward migrating deltaic distributary channels I, II and III (FA4), truncated upwards by the transgressive estuarine deposits of the FA5 in the cliff behind Qasr El-Sagha Temple section (height is ~20 m from the sandy foreground). **G-** The characteristic large-sized sigmoidal cross-bedding at the base the deltaic distributary channels (FA4) in the Qasr El-Sagha Temple section. **H-** The estuarine deposits of the FA5. The cliff-forming green sandstone, underlying the slope-forming gypsiferous sandstone, and truncated upward by the sandstone/coquina deposits in Dir Abu Lifa. **I-** Close up of the green sandstone in H, showing monospecific ichnological suite of the reddish (ferruginous) large-sized *Thalassinoides* (Th).



GLOSSIFUNGITES ICHNOFACIES AND DISCONTINUITIES

Like other ichnofacies, the distribution of the *Glossifungites* Ichnofacies can not be separated from abiotic- (physical and chemical) and biotic-limiting factors. Unlike the softground ichnofacies, the occurrences of the *Glossifungites* Ichnofacies are strongly related to a hiatal event that is associated with and/or followed by transgression under marine influence (Fig. 5.4). Consequently, the occurrences of *Glossifungites* Ichnofacies can also be related to additional limiting and controlling factors such as eustatic sea level changes and tectonics. Therefore, the *Glossifungites* Ichnofacies is useful in sequence and genetic stratigraphic analyses. The occurrences of the *Glossifungites* Ichnofacies are common in both time and space throughout the rock record (Table 5.2).

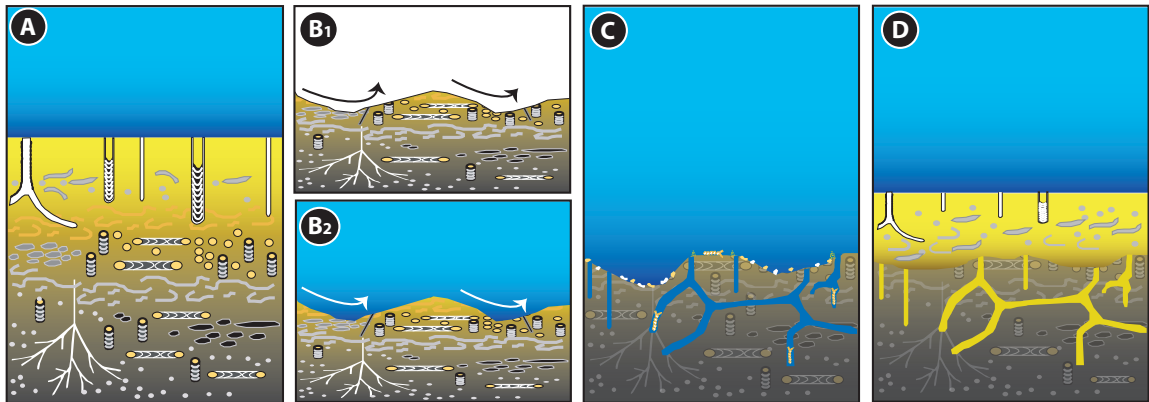


FIGURE 5.4. Schematic diagram, showing the development of a *Glossifungites* Ichnofacies-demarcated discontinuity. **A-** The mudstone/very fine-grained sandstone substrates are buried, dewatered and compacted. **B-** Subaerial erosion (B1) or submarine (B2) exhumation. **C-** Colonization of the discontinuity surface by the firmground trace makers under marine conditions during a depositional hiatus. **D-** The passive filling of the burrows by the succeeding depositional episodes and burial of the ichnological suites of the *Glossifungites* Ichnofacies. Modified after Pemberton et al. (2001) and MacEachern et al. (2007).

Table 5.2. Examples of occurrences of *Glossifungites* Ichnofacies through time and space in the rock record.

Period	Rock units & basins	Geographic location	Author
Quaternary	<ul style="list-style-type: none"> - Modern examples. - Modern / Pleistocene, Willapa bay. - Pleistocene siliciclastic slope. 	<ul style="list-style-type: none"> - Georgia Coast, USA. - Washington, USA. - New Jersey Margin, USA. 	<ul style="list-style-type: none"> - Pemberton and Frey, 1985. - Gingras et al., 2000, 2001. - Savrda et al., 2001b.
Tertiary	<ul style="list-style-type: none"> - Pliocene Quinault Fm. - Miocene Pebas Fm, Amazon basin. - Miocene, Monterey Fm. - Miocene, Tirikohua Fm. - Eocene – Pliocene clinoform. - Lower Paleocene. 	<ul style="list-style-type: none"> - Washington, USA. - Peru. - California, USA. - New Zealand - New Jersey Margin, USA. - Alabama, USA. 	<ul style="list-style-type: none"> - Campbell and Nesbitt, 2000. - Gingras et al., 2002a. - Ozalas et al., 1994. - Hayward, 1976. - Savrda et al., 2001a. - Savrda, 1991.
Cretaceous	<ul style="list-style-type: none"> - Lower Cretaceous WCSB (Viking, Bluesky and Spinney Hill formations). - Upper Cretaceous WCSB (Cardium, Dunvegan and Kaskapau formations). - Mesaverde Group, Bighorn basin. 	<ul style="list-style-type: none"> - Alberta; NE British Colombia; Central and Western Saskatchewan, Canada. - NW Wyoming, USA. 	<ul style="list-style-type: none"> - MacEachern et al., 1992a, b, 1999, 2007; MacEachern and Hobbs, 2004; Pemberton et al., 2004. - Fitzsimmons and Johnson, 2000.
Jurassic	<ul style="list-style-type: none"> - Sahtan Group. - Kap Stewart/Neill Klintner formations 	<ul style="list-style-type: none"> - Oman, Middle East. - East Greenland. 	<ul style="list-style-type: none"> - Rousseau et al., 2005. - Dam, 1990.
Triassic	<ul style="list-style-type: none"> - German Muschelkalk. 	<ul style="list-style-type: none"> - East Germany, Europe. 	<ul style="list-style-type: none"> - Bertling, 1999.
Permian	<ul style="list-style-type: none"> - Parana intracratonic basin. - Pebbly Beach Fm, S. Sydney basin. 	<ul style="list-style-type: none"> - South Brazil. - Australia. 	<ul style="list-style-type: none"> - Holz, 2003. - Bann et al., 2004; Fielding et al., 2006.
Carbonif.	<ul style="list-style-type: none"> - Morrow Sandstone. - Itarare Group, Parama basin. 	<ul style="list-style-type: none"> - SW Kansas, USA. - Santa Catarina, Brazil. 	<ul style="list-style-type: none"> - Buatois et al., 2002. - Balistieri and Netto, 2002.
Devonian	<ul style="list-style-type: none"> - Shujiaping and Jiwozhai formations. - Rushford Fm, Canadaway Group. 	<ul style="list-style-type: none"> - Dushan, Guizhou, China. - W New York state, USA. 	<ul style="list-style-type: none"> - Wang et al., 1997. - Smith and Jacobi, 1998.
Ordovician	<ul style="list-style-type: none"> - Late Ordovician paleosol. 	<ul style="list-style-type: none"> - S Appalachian, USA. 	<ul style="list-style-type: none"> - Driese and Foreman, 1991.
Cambrian	<ul style="list-style-type: none"> - Scandinavian strata. - East European Craton. 	<ul style="list-style-type: none"> - Norway, Western Europe. - Polish part, Europe. 	<ul style="list-style-type: none"> - Bromley and Hanken, 1991. - Paczeńska, 2001.

The *Glossifungites* Ichnofacies was originally attributed to littoral, stable and cohesive substrates (Seilacher, 1964, 1967a,b), and later to firm but unlithified marine substrates (mostly in dewatered mud) (Frey and Seilacher, 1980). Tracemakers of suites attributable to *Glossifungites* Ichnofacies typically colonize exhumed firm but unlithified (dewatered and compacted) substrates. These substrates are mostly muddy but sandy

substrates hosting the *Glossifungites* Ichnofacies are also documented (e.g., Saunders and Pemberton, 1986). Exhumation may occur in terrestrial environments (e.g., meandering channels or incised valleys), in shallow-water environments (e.g., meandering tidal channels, tidal and wave ravinement surfaces), and in deep-marine environments (e.g., oceanic and turbidity currents).

The *Glossifungites* Ichnofacies is dominated by both vertical and sub-vertical dwelling burrows of inferred suspension-feeders (e.g., *Diplocraterion*, *Skolithos*, *Psilonichnus*, *Arenicolites*, *Conichnus*, *Bergaueria*, and *Gastrochaenolites*), and dwelling structures of deposit-feeding organisms (e.g., *Thalassinoides*, *Spongeliomorpha*, *Palaeophycus*, *Taenidium*, *Rhizocorallium*, *Planolites*, and *Chondrites*). *Zoophycos* also has been added to the firmground suites (MacEachern and Burton, 2000). Some terrestrial arthropod-constructed trace fossils (e.g., *Lunulichnus tuberosus*) represent the alluvial firmground ichnological suites of the *Glossifungites* Ichnofacies (*sensu*, Zonneveld et al., 2006). These firmground trace-fossil suites have the following four diagnostic features: (1) elements are sharp-walled and unlined, demonstrating the cohesive nature of the substrate during burrow excavation; (2) burrows are dominantly infilled passively, indicating that the burrows remained open until the post-omission depositional event; (3) colonization locally occurs in large numbers and densities; and (4) the firmground (omission) suite typically crosscuts the softground (pre-omission) suite (Fig. 5.4).

GLOSSIFUNGITES ICHNOFACIES— DEMARCATED SURFACES

A genetic approach—relating *Glossifungites* Ichnofacies-demarcated surfaces to key sequence-stratigraphic surfaces (e.g., SB, TS, MFS and FS)—is used to propose a classification of more than twenty-five *Glossifungites* Ichnofacies-demarcated surfaces in the Middle-Upper Eocene succession in the Fayum area (Figs. 5.5-10). The stratigraphic, sedimentological and ichnological characters of the key-stratigraphic/*Glossifungites* Ichnofacies-demarcated surfaces and their sequence stratigraphic implications are

Table 5.3. The diagnostic characters of the identified key-stratigraphic surfaces in the study area.

Surface Type	Stratigraphic Position	Facies Assoc.	Substrate Type	Ichnology					Sequence Stratigraphy
				Trace fossil Suite	B [*]	Diversity	Th Max. Diameter	Penetration cm	
Au-GS1	Dir Abu Lifa Mbr	FA4	silty Shale	<i>Th, Pl, Pa, and Sk</i>	1-2	Low	1-2	5-15	Autocyclic surfaces, late LST of sequence 4.
Au-GS2	Dir Abu Lifa Mbr	FA5	Mudstone	<i>Th, Pl, Sk, and Ps</i>	2	Low	1-2	5-15	Autocyclic surfaces, TST of sequence 4.
FS/SB1-GS	Gehannam / Birket Qarun formations	FA2 / FA1	Very fine-grained Sst.	<i>Th</i> , hard to see other firmground traces .	2-3	Low	2-4	15-30	Merged FS/SB1 surface separates HST of sequence 1 from the upper HST of sequence 2.
FS/SB2-GS	Birket Qarun Fm	FA1 / (shale)	Fine/Medium grained Sst.	<i>Th, Sk, Ar, Ps, and Pa</i>	2-3	Mod.	1-2	< 20	Merged FS/SB2 separates HST of sequence 2 from either the thin TST (shale) or the HST of sequence 3.
SB3	Temple / Dir Abu Lifa members	FA3/ FA4	None observed	None observed (covered)					Sequence boundary surface separates HST of sequence 3 from the LST of sequence 4.
MFS-GS	Birket Qarun Fm	FA1 / marker shale bed	Shale	<i>Th</i> , hard to see other firmground traces.	2-4	Low	2-4	~ 40	Maximum flooding surface separates the thin TST shale from HST in sequence 3.
TS-GS	Dir Abu Lifa Mbr	FA4 / FA5	Mudstone	<i>Th, Sk, Ar, and Pl</i>	5	Low	2-4	~ 100	Transgressive surface separates the LST from the TST in sequence 4.
S1-Fss	Gehannam Fm	FA1	Very fine-grained Sst.	Archetypal <i>Cruziana</i> (Softground Ichnofacies)					Flooding surfaces bound the HST parasequences of sequence 1.
S2-Fss	Birket Qarun Fm	FA1	Fine/Medium grained Sst.	Proximal <i>Cruziana</i> / Distal <i>Skolithos</i> (Softground Ichnofacies)					Flooding surfaces bound the HST parasequences of sequence 2.
S3-Fss-GS	Birket Qarun Fm	FA1	Very fine-grained Sst.	Giant structures, <i>Th, Sk, Ar, and Pl</i>	3-4	Mod.	2-5	~ 200	Flooding surfaces (TSE1) bound the HST parasequences of sequence 3.
S3-Fss-GS	Umm Rigl / Temple members	FA3	Mudstone	<i>Th, Sk, Ar, Di, and Pl</i>	3-5	Mod.	2-4	< 100	Flooding surfaces (TSE2) bound the parasequences of the HST in sequence 3.
S4-Fss-GS	Dir Abu Lifa Mbr	FA5	Mudstone / Muddy Sst.	<i>Th, Sk, Ar, and Pl</i>	3-5	Low	2-4	~ 50	Flooding surfaces (TSE2) bound the TST parasequences of sequence 4.

* *Biourbation index (BI)* represents the intensity of burrowing immediately below the discontinuity surface.

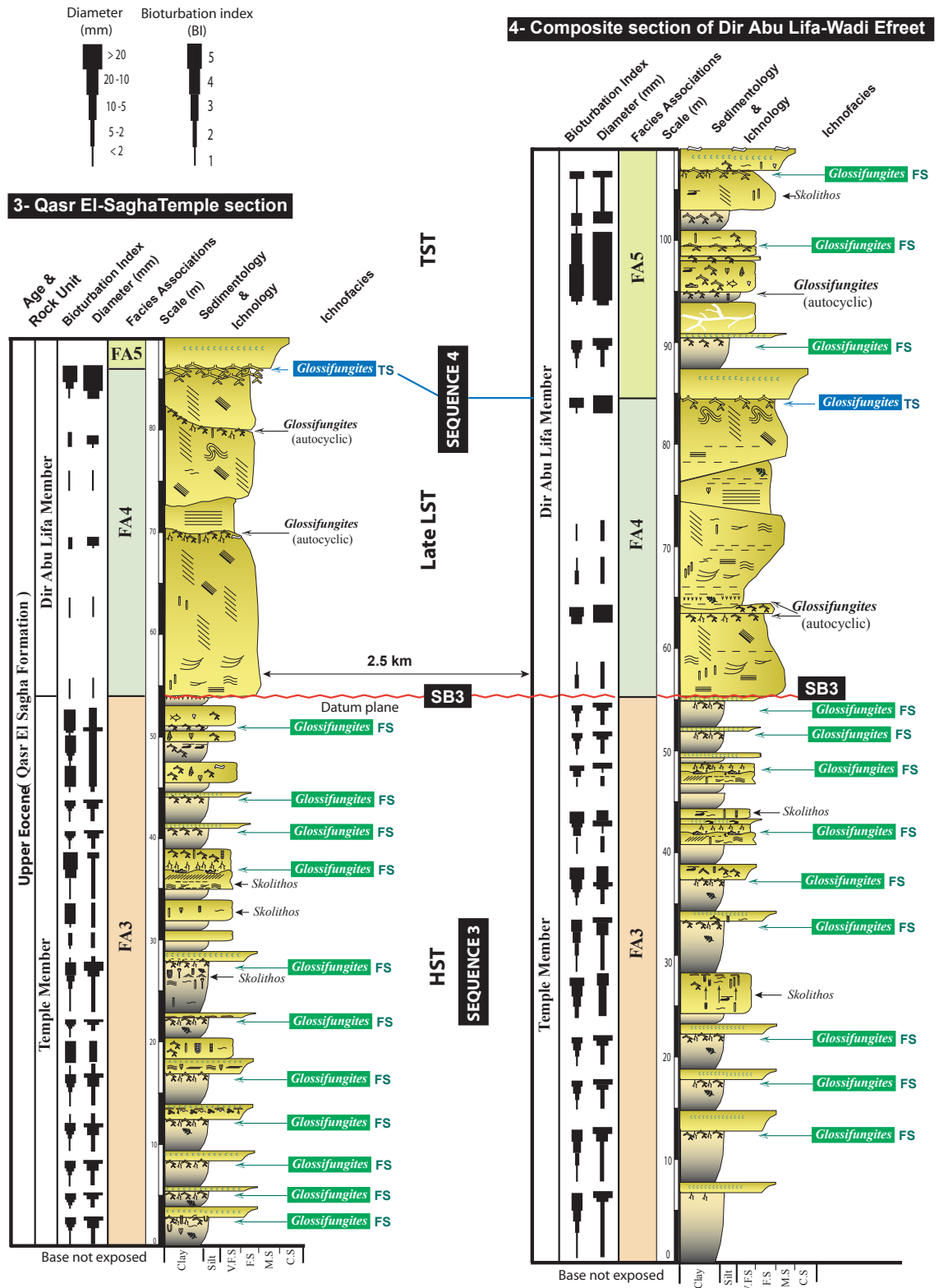


FIGURE 5.6. Correlation of the Upper Eocene succession of Qasr El-Sagha Temple section with Dir Abu Lifa – Wadi Efreet composite section, in the area of Qasr El-Sagha, NE Fayum.

summarized in Table 5.3.

Depending upon to the origin of the exhumation surfaces—whether they are originated as the result of autogenic or allogenic processes—these surfaces are grouped into two main types; those of autocyclic and those of allocyclic origin. Based on the integrated dataset, the occurrences of the allocyclic-originated *Glossifungites* Ichnofacies-demarcated surfaces are classified into three types (Figs. 5.5, 5.6): 1- sequence-bounding *Glossifungites* Ichnofacies-demarcated surfaces; 2-systems tract-bounding *Glossifungites* Ichnofacies-demarcated surfaces; and 3- parasequence-bounding *Glossifungites* Ichnofacies-demarcated surfaces.

AUTOCYCLIC *GLOSSIFUNGITES* ICHNOFACIES— DEMARCATED SURFACES

Autocyclic *Glossifungites* Ichnofacies-demarcated discontinuities are spatially limited and rarer in the studied sections (Figs. 5.5-5.7). These surfaces are formed as the result of scouring and exhumation associated with autogenic processes (e.g., laterally migrating distributary and estuarine channels). They are characterized by restricted geographic distributions, local lateral continuity, and show neither major lithofacies nor ichnofacies dislocations. The autocyclic surfaces are demarcated by impoverished firmground ichnological suites, attributed to the *Glossifungites* Ichnofacies. These autocyclic expressions of the *Glossifungites* Ichnofacies have very low bioturbation intensities and reduced ichnogenera diversities. Burrow-penetration depths are shallow. Some burrows are slightly deformed, showing evidence of compaction (e.g. Gingras et al., 2000). Based on the dominant style of the autogenic exhumation processes, two types of surfaces are documented.

Deltaic Distributary Channels: Autocyclic Glossifungites Ichnofacies-Demarcated Surfaces (AuGS1)

Two surfaces are encountered along the basal erosional discontinuities of

laterally migrating and prograding deltaic distributary channels (FA4) in Dir Abu Lifa Member of the Upper Eocene Qasr El-Sagha Formation. The firmground ichnoconos demarcate the upper muddier portions (carbonaceous shale and siltstone) of the fining-upward channels (Figs. 5.7A-B). Rhizoliths, terrestrial vertebrate bones, and sulphur nodules are observed along these surfaces. The *Glossifungites*-demarcated surfaces display only local lateral continuity and cannot be traced laterally for more than 10 m. In these examples, the suites of the *Glossifungites* Ichnofacies are impoverished, with low burrowing intensities (BI 1-2). The firmground trace-fossil suites are represented mainly by the dwelling structure *Thalassinoides* (1-2 cm in diameter), rare *Palaeophycus* and *Planolites*, and diminutive dwellings of inferred-suspension feeders (e.g., *Skolithos*) (Fig. 5.7B). The depth of burrow penetration below the surface is shallow (5-15 cm). Some *Thalassinoides* are slightly deformed, and show some evidence of compaction (Fig. 5.7B).

These surfaces coincide with the autocyclic erosion and scouring processes of laterally migrating deltaic distributary channels (FA4). The surfaces lie within the late-stage LST of sequence 4 (Figs. 5.6, 5.11).

Estuarine Channels: Autocyclic Glossifungites Ichnofacies-Demarcated Surfaces (AuGS2)

Surfaces associated with the autocyclic scouring and erosion of the estuarine channels (FA5) in the upper part of Dir Abu Lifa Member of the Upper Eocene Qasr El-Sagha Formation (Figs. 5.6, 5.7C-D) contain firmground trace fossil suites. The excavated substrates are silty to sandy mudstone. Rare to common rhizoliths are observed. The *Glossifungites*-demarcated surfaces are sporadically distributed, with limited lateral continuity. The maximum lateral continuity varies between a few meters and 10 m. The ichnological suites of the *Glossifungites* Ichnofacies are impoverished (Fig. 5.7D), with weak bioturbation intensities (BI 2). Trace-fossil suites are represented

mainly by the dwelling structure *Thalassinoides* (1-2 cm in diameter), rare *Planolites*, and rare to common, diminutive dwelling structures of *Skolithos* and *Psilonichnus*. The depth of burrow penetration below the discontinuity is shallow (5-15 cm).

These *Glossifungites*-demarcated surfaces coincide with the autocyclic erosion and scouring of estuarine channels (FA5) in the TST of sequence 4 (Figs. 5.6, 5.7C-D, 5.11).

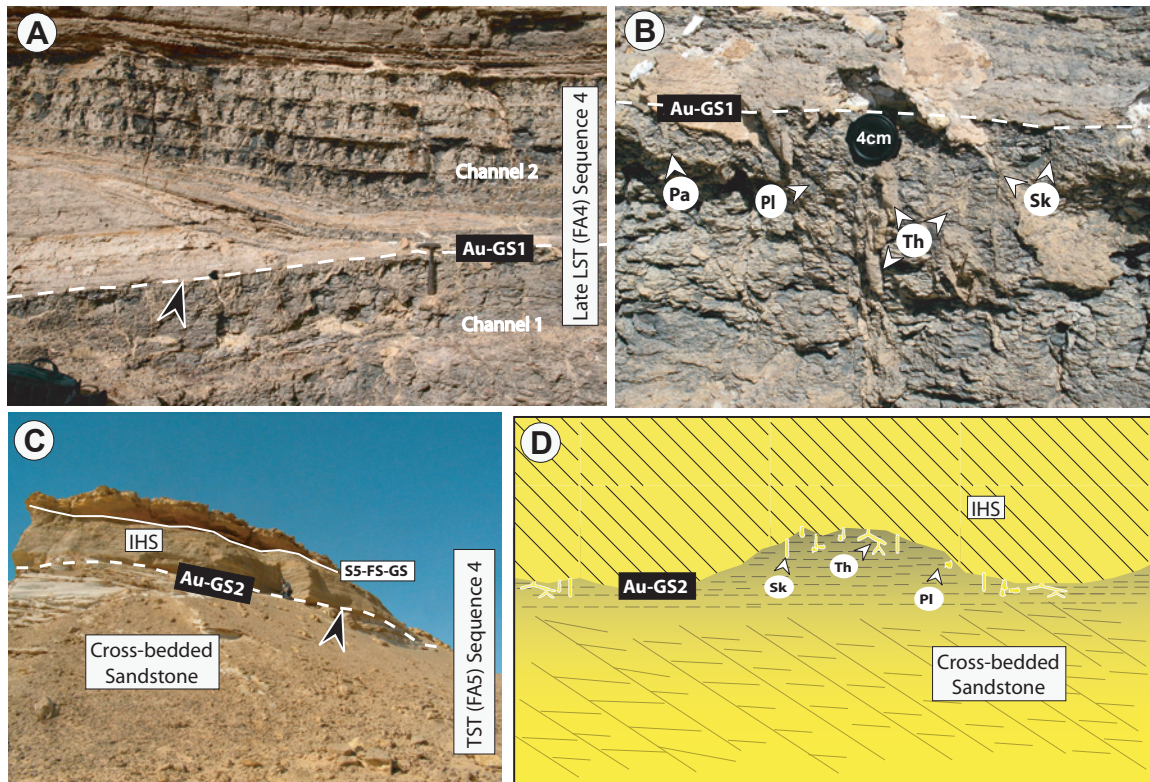


FIGURE 5.7. Autocyclic *Glossifungites* Ichnofacies-demarcated surfaces (Au-GS). **A-** The Au-GS1 surface lies at the contact between two superimposed deltaic distributary channels (FA4) in the Dir Abu Lifa Member, Qasr El-Sagha Temple section. **B-** Close-up view of (A) showing the impoverished ichnological suite of abundant *Thalassinoides* (Th), with rare *Skolithos* (Sk), *Planolites* (Pl) and *Palaeophycus* (Pa), attributed to the *Glossifungites* Ichnofacies. Note the shallow penetration depths and slight deformation and compaction of the burrows. **C-** The Au-GS2 surface at the contact between the cross-bedded sandstone and the IHS of the estuarine deposits (FA5) in the TST (sequence 4), Wadi Efreet section (man at the contact for scale). **D-** Schematic diagram (not to scale) illustrating the contact along the Au-GS2 surface of (C) and the ichnological firmground suite, mainly *Thalassinoides* (Th), *Skolithos* (Sk) and *Planolites* (Pl).

ALLOCYCLIC *Glossifungites* Ichnofacies– DEMARCATED SURFACES

The allocyclically generated *Glossifungites* Ichnofacies-demarcated surfaces are the most common surfaces in the studied succession (Figs. 5.5 and 5.6). In contrast with the autocyclically-generated *Glossifungites* Ichnofacies-demarcated surfaces, the allogenic discontinuities have the following characteristics: 1- relatively wide-geographic distributions; 2- demonstrative mappable lateral continuity; 3- show lithofacies and ichnofacies dislocation; 4- are demarcated by well-developed firmground ichnological suites, corresponding to the *Glossifungites* Ichnofacies; and 5- display moderate to high bioturbation densities as well as moderate to high ichnogenera diversities. Occurrences of allocyclically significant *Glossifungites* Ichnofacies can be subdivided into the following three types.

Sequence-bounding Glossifungites Ichnofacies-Demarcated Surfaces

The sequence-bounding discontinuity surfaces are fewer in number and represent major depositional omission. The sequence boundaries are either amalgamated with the flooding surfaces (e.g., FS/SB1 and FS/SB2) or overlain directly by late LST (e.g., SB3). The deposits of the transgressive systems tract (TST) and/or highstand systems tract (HST) directly overlie the earlier HST deposits, forming merged FS/SB surfaces. In coastal and shelfal settings (e.g., Middle - Upper Eocene Fayum (Gindi) sag basin), the sequence boundary may be overprinted by a well-developed ravinement (transgressive surface of erosion TSE) surface that removes the earlier LST and/or TST deposits. Ravinement (TSE) can erode up to 10-20 m of the substrate (e.g., Abbott, 1998) and up to 40 m in coastal settings characterized by high wave energy (see Leckie, 1994). Herein, three surfaces are identified (FS/SB1-GS, FS/SB2-GS and SB3) that divide the Middle-Upper Eocene succession (Figs. 5.5, 5.6, 5.8, 5.11, 5.12) into four third-order sequences (sequences 1 through 4).

FS/SB1-GS- *Glossifungites* Ichnofacies-demarcated surface:

The merged FS/SB1-GS surface marks a major discontinuity between Middle (Bartonian) and Late (Priabonian) Eocene. This coplanar surface has a characteristic facies dislocation from the underlying bay-margin (swampy/supratidal) deposits of the Middle Eocene Gehannam Formation (FA2) into the overlying low-energy open-marine bay sandstones (FA1) of the Upper Eocene Birket Qarun Formation (Figs. 5.5, 5.8A-B, 5.11). The exhumed and recolonized substrate is composed of siltstone and/or very fine-grained sandstone. The merged FS/SB1 surface emplaced a complex paleoecologic horizon (Figs. 5.8A-B), incorporating rhizoliths (root casts), marine or brackish-marine invertebrate fossils and trace fossils, and whale and/or marine vertebrate-bone fragments (Fig. 5.8B). Firmground ichnological suites are expressed mainly by the large-sized *Thalassinoides* (diameter > 2 cm). It is difficult to observe any other firmground ichnogenera. The burrows are passively filled with medium-grained sandstone from the overlying units of FA1. The bioturbation intensity is moderate (BI 2-3), whereas the ichnogenera diversity is very low. The depth of burrow penetration is moderate (ranging between 15 cm and 50 cm below the discontinuity).

The Bartonian/Priabonian discontinuity is represented, herein, by the coplanar FS/SB1 surface that separates the HST of the Middle Eocene sequence 1 below from the HST of Upper Eocene sequence 2 above (Figs. 5.5, 5.8A, 5.11).

FS/SB2-GS- *Glossifungites* Ichnofacies-demarcated surface:

This FS/SB2-GS discontinuity is marked by a major facies dislocation from the lower thick-bedded sandstone (FA1) to either a distinctive (locally eroded) transgressive shale bed (Fig. 5.8C) or to stacked progradational parasequences (Fig. 5.8D) of the Upper Eocene Birket Qarun Formation. The surface is excavated into either muddy fine-grained sandstone or mudstone. This surface demonstrates subaerial exposure, as evidenced by the occurrences of varicolored alluviated sandstone below the undulatory

erosional surface (Figs. 5.8C, 5.9A), and a local abundance of rhizoliths (Fig. 5.8E). Variable erosion of dark-grey shale marker bed (Fig. 5.8D) along with facies dislocations demonstrates a coplanar FS/SB surface. The firmground ichnological suites are expressed by *Thalassinoides* (diameter 1-2 cm), and rare to common (relatively small, 5-10 mm in diameter) *Skolithos*, *Arenicolites*, and *Psilonichnus*. These burrows are passively filled with medium-grained sandstone from the overlying FA1. The bioturbation intensity is low to moderate (BI 2-3), with moderate to low ichnogenera diversities. Locally, the *Glossifungites* Ichnofacies is difficult to observe. Burrows penetrate to shallow depths (< 20 cm) below the discontinuity.

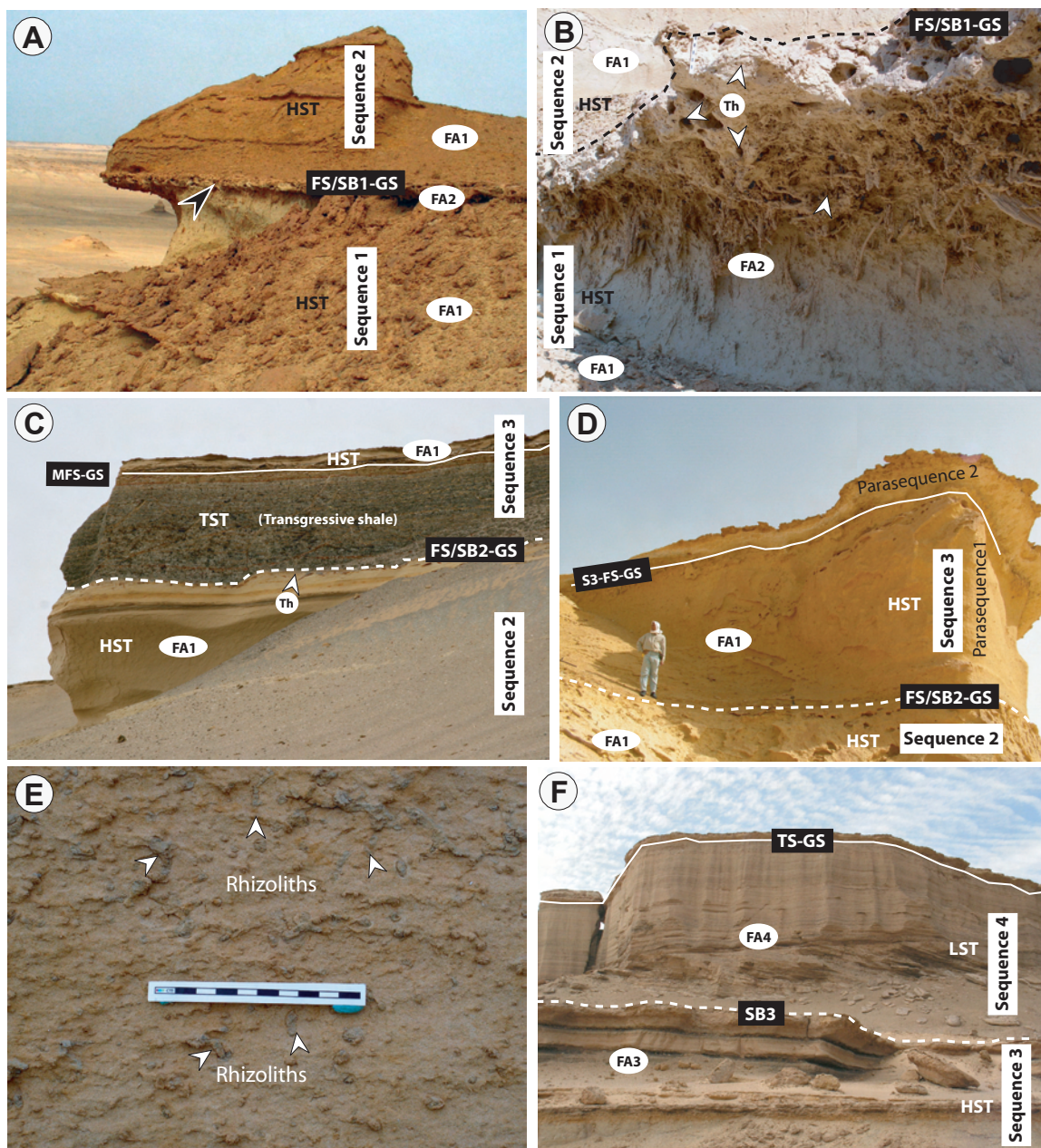
The coplanar FS/SB2-GS discontinuity surface separates the HST of sequence 2 below from either the thin TST or HST of sequence 3 in the Upper Eocene Birket Qarun Formation (Figs. 5.5, 5.8C-D, 5.11).

SB3- sequence boundary surface :

Sequence boundary 3 (SB3) is a major erosional unconformity (e.g., Bown and Kraus, 1988). The surface demarcates dislocation from the shallow lagoonal parasequences (FA3) of the lower Temple Member to the upper deltaic distributary channels (FA4) of the upper Dir Abu Lifa Member in the Upper Eocene Qasr El-Sagha Formation (Figs. 5.6, 5.8F). This surface is locally under cover in the study area.

The sequence boundary SB3 separates the HST of sequence 3 below from the late LST of the sequence 4 above in the Upper Eocene Qasr El-Sagha Formation (Figs. 5.6, 5.8F, 5.11).

FIGURE 5.8. Sequence-bounding *Glossifungites* Ichnofacies-demarcated surfaces (SB-GS). **A-** The merged FS/SB1–GS surface, juxtaposing 2 m-thick rhizolith-bearing facies of FA2 (black arrow), separate the HST of the Middle Eocene (Bartonian) sequence 1 below from the HST of the Upper Eocene (Priabonian) sequence 2 above, Sandouk El-Borneta section. **B-** Close-up view of (A), showing the large-sized *Thalassinoides* (Th) on top of rhizolith-bearing sandstone of FA2 (upper left scale is 10 cm long). **C-** Outcrop view of the dark-grey shale (~3 m thick) of a thin TST of sequence 3, onlapping the coplanar FS/SB2-GS surface (white broken line), and unconformably overlying the HST of sequence 2 in the area between Minqar El-Hut and Sandouk El-Borneta. **D-** The merged FS/SB2–GS surface (white broken line) between the HST (sequence 2) and the overlying parasequences of the HST (sequence 3) in the Old Camp site. Both of the LST and the thin TST (shale bed, shown in C) were either not deposited or have been eroded. **E-** Rhizobioturbation, marking the upper sandstone of the HST of sequence 2 below the FS/SB2-GS surface in Sandouk El-Borneta section. **F-** Outcrop view of the sequence boundary (SB3), showing a facies dislocation (with local erosional unconformity) from the lagoonal parasequences (FA3) of the HST (sequence 3) below to the deltaic distributary channels deposits (FA4) of the late LST (sequence 4) above, Qasr El-Sagha Temple section (Upper cliff is ~ 30 m high).



Systems Tract-bounding Glossifungites Ichnofacies-Demarcated Surfaces

The *Glossifungites* Ichnofacies-demarcated surfaces separate the four third-order sequences into systems tracts (Figs. 5.5, 5.6, 5.9, 5.11). Two documented stratigraphic surfaces—the maximum flooding surface (MFS) and the transgressive surface (TS)—are associated with moderate degrees of erosion, and display a marked facies dislocation. In paralic settings where the TST is thin, the transgressive surface (TS) may lie very close to the MFS (e.g., Shanley and McCabe, 1989). The maximum flooding surface represents the maximum transgression of the shelf, and separates the TST from the overlying HST (Posamentier and Allen, 1999). In this definition, the term “maximum transgression” refers to the maximum landward position of the coastline, rather than the maximum water depth on the shelf. Herein, the examined MFS and TS surfaces are mainly expressed as energetic wave and/or tidal ravinement (TSE) surfaces developed during flooding of the Fayum (Gindi)-Basin shelf.

Maximum flooding- *Glossifungites* Ichnofacies- demarcated surface (MFS-GS):

This surface separates the dark grey transgressive shale bed (marker horizon) from the overlying HST sandstone (FA1) in the Upper Eocene Birket Qarun Formation (Figs. 5.5, 5.9A,B). Wherever the transgressive shale bed is eroded, the MFS surface is coplanar with the sequence boundary, forming the FS/SB2 coplanar surface (Fig. 5.8D). The MFS surface is typically overlain by characteristic large, ovate concretionary sandstones with Mn/Fe staining (Fig. 5.9A). The firmground ichnogenera subtend from the top of the dark grey shale. The bioturbation intensity is moderate to high (BI 3-4) within the upper 20 cm of the surface. The ichnogenera diversity is very low. Abundant, large-sized (diameter > 2 cm) *Thalassinoides* comprise the only observed ichnogenus (Fig. 5.9B). They are passively filled with reddish (ferruginous) to yellow sandstones. The burrow-penetration depths reach 40 cm below discontinuity.

The MFS-GS surface separates the thin and discontinuous TST (marker shale bed)

from the overlying HST (sandstone) in sequence 3 of the Upper Eocene Birket Qarun Formation (Figs. 5.5, 5.9A-B, 5.11). Locally, the MFS is merged with SB2 (Fig. 5.8D).

Transgressive- *Glossifungites* Ichnofacies-demarcated surface (TS-GS):

This key-transgressive surface is well developed along the Qasr El-Sagha escarpment, forming a distinctive boundary between the lower deltaic distributary channels (FA 4) and the overlying estuarine deposits (FA5) of the Dir Abu Lifa Member (Figs. 5.6, 5.9C-E). Muddier substrates of the fining-upward (deltaic) distributary channels are extensively burrowed with firmground ichnological suites attributed to the *Glossifungites* Ichnofacies (Figs. 5.9D-E). Lag deposits and coquinas (e.g., bivalves, gastropods and echinoids) are associated with this surface. Reddish to golden-yellow robust *Thalassinoides* (diameter > 2 cm) are distinctive within the dark grey mudstone (Figs. 5.9D-E). Rare to common, relatively small (~ 5 mm in diameter) *Planolites*, *Palaeophycus*, *Arenicolites* and *Skolithos* are also present (Figs. 5.9D-E). Burrows are passively filled with medium- to coarse-grained sandstone and shell hash from the overlying transgressive deposits. The bioturbation intensity is high (BI 4-5; decreasing downward), whereas the ichnogenera diversities are moderate to low. Burrow penetration depths are relatively deep (up to 1m).

Taken together, the aforementioned characteristic point toward the presence of a transgressive surface (TS), which separates the late-stage LST from the subsequent TST in sequence 4 of the Dir Abu Lifa Member (Figs. 5.6, 5.9C-E, 5.11).

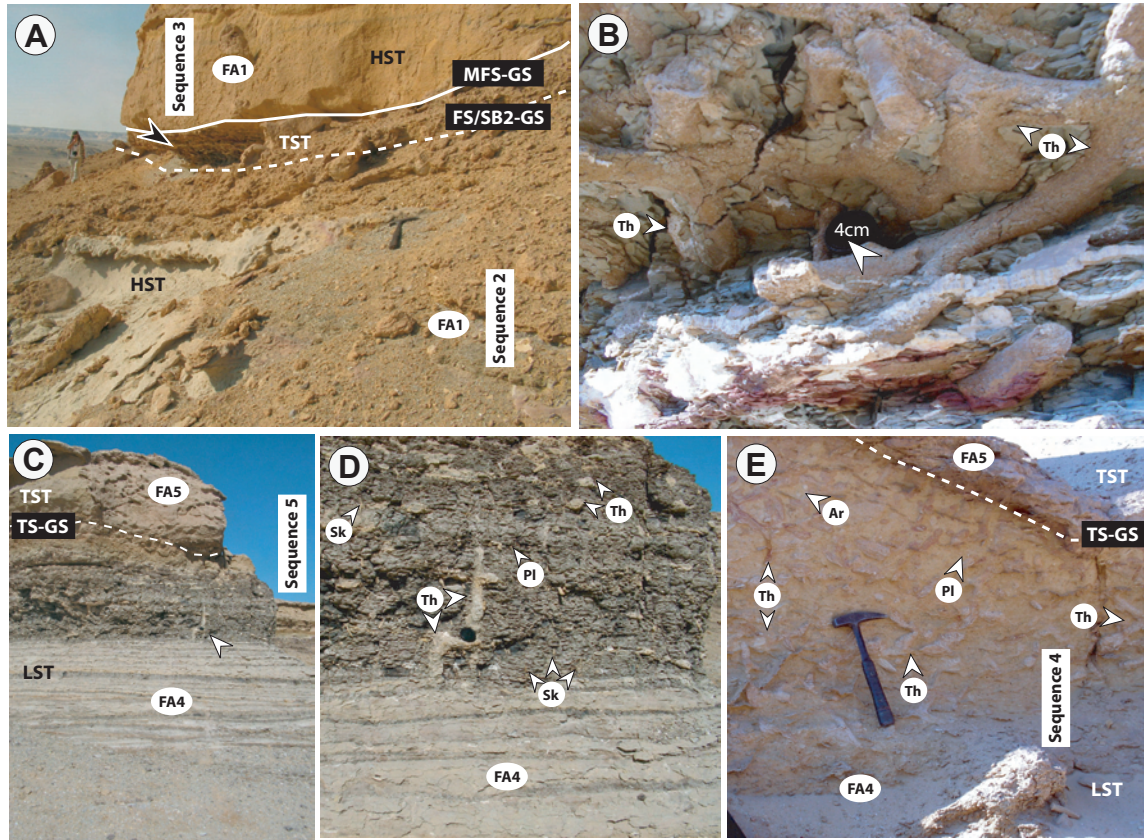


FIGURE 5.9. Systems tract-bounding *Glossifungites* Ichnofacies-demarcated surfaces (MFS-GS and TS-GS). **A-** Outcrop view of the MFS-GS (white solid line) separating the thin TST (shale bed) from the HST (sandstone) of sequence 3, Sandouk El-Borneta section. **B-** Close-up view of A (black arrow) showing reddish to yellow, passively filled robust *Thalassinoides* (Th), attributed to the *Glossifungites* Ichnofacies, in sandy shale. **C-** Transgressive surface (TS-GS) separating the deltaic distributary channel (FA4) of the late LST below from the basal transgressive estuarine deposits (FA5) of the TST above, in sequence 4, NE Dir Abu Lifa (White arrow points to lens cap, 4 cm in diameter). **D-** Close-up view of (C) showing an ichnological suite dominated by *Thalassinoides* (Th) and rare to common *Skolithos* (Sk) and *Planolites* (Pl), attributed to the *Glossifungites* Ichnofacies in a mudstone substrate. **E-** Ichnological suite of the *Glossifungites* Ichnofacies in a sandstone substrate, dominated by *Thalassinoides* (Th) with rare to common *Arenicolites* (Ar) and *Planolites* (Pl). This marks the TS-GS surface in the head of Wadi Efreet.

Parasequence-Bounding Surfaces (Flooding Surfaces FS)

The parasequence-bounding flooding surfaces (FS) comprise the most abundant allocyclically generated surfaces in the study area (Figs. 5.5 and 5.6). These flooding surfaces are associated with minor to moderate erosion and exhumation, which bound fourth- and fifth-order (parasequence) cycles. The parasequence-bounding flooding surfaces in sequence 1 (S1-FSs) and sequence 2 (S2-FSs) are not punctuated by the firmground suites of the *Glossifungites* Ichnofacies (see Table 5.3). Instead, they are identified via the juxtaposition of softground ichnofacies (e.g., archetypal *Cruziana*, proximal expressions of the *Cruziana* Ichnofacies, and distal expressions of the *Skolithos* Ichnofacies and their associated sedimentological features.

Conversely, more than twenty parasequence-bounding flooding surfaces (e.g., those of third-order sequences 3 and 4) are demarcated by well-developed ichnological suites attributed to the *Glossifungites* Ichnofacies. These *Glossifungites* Ichnofacies-demarcated surfaces are either expressed as wave ravinement (e.g., upper Birket Qarun S3-FSs-GS) or as wave and/or tidal (e.g., Qasr El-Sagha S3-FSs-GS and S4-FSs-GS) ravinement (TSE) surfaces, which demarcate the parasequence boundaries in sequences 3 and 4 (Figs. 5.5, 5.6, 5.10, 5.11).

Parasequence flooding (wave ravinement) surfaces (S3-FSs-GS):

Three well-developed parasequence-bounding flooding surfaces are identified in the upper part of the Upper Eocene Birket Qarun Formation (Figs. 5.5, 5.10A-D, 5.11). These flooding surfaces are expressed as wave-ravinement (TSE) surfaces that are associated with sandstone and coquina deposits (Fig. 5.10A). The firmground ichnological suites demarcate the yellow, fine-grained sandstone (FA1) substrate. Large conical concretionary sedimentary structures (up to 150 cm long and up to 15 cm in diameter) are constrained to these surfaces (see Chapter 4). The firmground ichnological suites of the *Glossifungites* Ichnofacies are composed mainly of the characteristic large

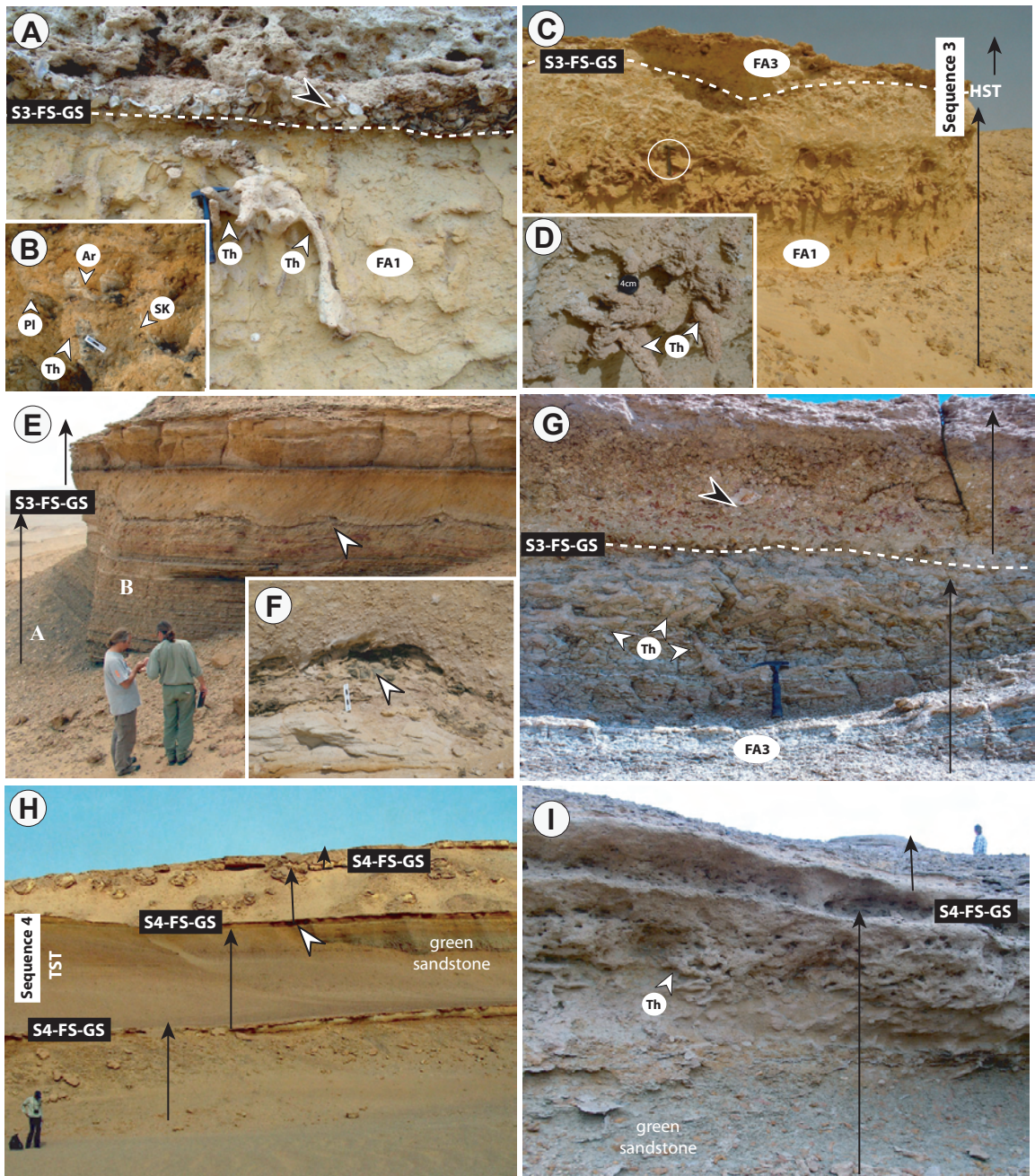
Thalassinoides (diameter >2 cm, up to 5 cm, Figs. 5.10A-D), rare to common small (diameter 5-20 mm) *Arenicolites* and *Skolithos*, and diminutive *Palaeophycus* and *Planolites* (Fig. 5.10B). Trace fossil suites are passively filled with the TSE-associated deposits (e.g., sandstone/shell hash/larger and benthic foraminifera) (Fig. 5.10D). The bioturbation intensity is high (BI 4) immediately below the discontinuity surface, but decreases downward. Ichnogenera diversities are moderate. Large *Thalassinoides* penetrate to an average depth of 50 cm below the surface. The upper flooding surface shows a burrow penetration depth up to 2 m below the surface (Fig. 5.10C).

These parasequence-bounding *Glossifungites* Ichnofacies-demarcated discontinuities are typically wave ravinement (TSE) surfaces (see Chapter 2). These TSE surfaces define the lower parasequences (upper Birket Qarun Formation) at the base of the HST in sequence 3 (Figs. 5.5, 5.10A-D, 5.11). The upper flooding surface separates the lower parasequences of the upper Birket Qarun Formation from those of Umm Rigl Member (base of Qasr El-Sagha Formation) (Figs. 5.5, 5.10D, 5.11).

Parasequence flooding (wave and/or tidal ravinement) surfaces (S3-FSS-GS and S4-FSS-GS):

The parasequence flooding surfaces delineate parasequence boundaries in the Umm Rigl and Temple members (S3-FSS-GS), and the upper part of Dir Abu Lifa Member (S4-FSS-GS) of the Upper Eocene Qasr El-Sagha Formation (Figs. 5.6, 5.8F, 5.10E-I). The S3-FSS-GS and S4-FSS-GS surfaces truncate carbonaceous shale/sandstone (FA3) (Figs. 5.10E-G) and mudstone/very fine-grained sandstone of FA5 (Figs. 5.10H-I), respectively. These short-lived discontinuity surfaces are considered to be wave and/or tidal TSE surfaces (detailed in Chapter 2) due to: 1- local occurrences of wavy and flaser bedding, and tidal rhythmite sedimentary structures (Fig. 5.10E); 2- characteristic associations of sandstone/lag deposits and discontinuous coquina beds (comprising *Carolia plucnoides*, *Terebra* sp., *Turritella* sp., and echinoids); and, 3- sporadic calcrete,

FIGURE 5.10. Parasequence-bounding *Glossifungites* Ichnofacies-demarcated surfaces (FSs-GS). **A-** Wave-ravinement surface (S3-FS-GS) bounding two parasequences of the HST in sequence 3, with passively filled, robust *Thalassinoides* (Th) and lag/coquina deposits (black arrow), Sandouk El-Borneta section. **B-** Ichnological suite of *Thalassinoides* (Th), *Arenicolites* (Ar), *Skolithos* (Sk) and *Planolites* (Pl), corresponding to the *Glossifungites* Ichnofacies along the S3/FS-GS surface, Old Camp site (scale is 3 cm long). **C-** Wave-ravinement surface (S3-FS-GS) bounding the upper open-marine bay parasequence and basal lagoonal parasequence in the HST of sequence 3. Note the deeply penetrating burrow (~ 2 m) in the very fine-grained sandstone substrate, Old Camp site (geologic hammer in the white circle for scale). **D-** Close-up view of (C), showing large-sized *Thalassinoides* (Th) passively filled with sandstone, large foraminifera (e.g., *Nummulites* sp.) and shell hash deposits. **E-** Tidal ravinement surface (S3-FS-GS) truncating the sandstone tidal rhythmites and wavy and flaser bedding at a parasequence boundary in the upper HST of sequence 3, Qasr El-Sagha Temple section. **F-** Close-up view of (E), showing the erosive and undulating nature of the S3-FS-GS surface, and associated coal and sulphur fragments. **G-** S3-FS-GS ravinement surface (Temple Member, at Wadi Efreet) marking the boundary between two parasequences of the HST (sequence 3), with well-developed suites of the *Glossifungites* Ichnofacies as well as shell hash/lag/sandstone deposits (black arrow). **H-** S4-FSs-GS ravinement surface bounding the TST parasequences of sequence 4 in the head of Wadi Efreet. **I-** Close-up view of H (white arrow), showing the demarcation of the green sandstone with a well-developed trace fossil suite of the *Glossifungites* Ichnofacies.



coal and sulfur fragments, as well as rhizoliths along the surface Fig. (5.10F). Firmground ichnological suites of the *Glossifungites* Ichnofacies are passively filled with ravinement deposits (sandstone, lag and shell hash). Directly below the discontinuity, the bioturbation intensity is moderate to high (BI 3-5) and ichnogenera diversity is low. Large-sized (diameter > 2 cm) *Thalassinoides* are abundant (Fig. 5.10). Rare to common diminutive (diameters 5-15 mm) ichnogenera are also observed (e.g., *Skolithos*, *Diplocraterion*, *Arenicolites* and *Planolites*). Depths of burrow penetration vary between 20 cm and 100 cm below the discontinuity.

The tidal and/or wave ravinement (TSE) S3-FSs-GS and S4-FSs-GS surfaces define the boundaries of the prograding parasequences of the HST (Umm Rigl and Temple members) in sequence 3, and the boundaries of the aggradational to retrogradational parasequences of the TST parasequences in sequence 4, respectively (Figs. 5.6, 5.10E-I, 5.11).

SEQUENCE STRATIGRAPHY AND SEA-LEVEL HISTORY

The *Glossifungites* Ichnofacies-demarcated discontinuities indicate that Middle-Late Eocene shoreline retreat and advance was both episodic and complex. These discontinuities (FS/SB1, FS/SB2 and SB3) divide the Middle-Upper Eocene successions into four third-order sequences (sequences 1 to 4) (Figs. 5.4, 5.5, 5.8, 5.11, 5.12). The depositional sequences are represented by thin, landward-stepping parasequences (i.e., TST) and well-developed progradational successions (i.e., HST) (see Fig. 5.11). Presumably, sediments of the LST dominantly reside basinward (e.g., Dolson et al., 2002). The systems tract- and parasequence-bounding *Glossifungites* Ichnofacies-demarcated surfaces display higher-order cycles that overprint these third-order cycles (see Figs. 5.12).

MIDDLE EOCENE (LATE BARTONIAN) SEQUENCE 1

Sequence 1 is represented by the Middle Eocene (upper Bartonian) Gehannam Formation (base not exposed). Progradationally stacked parasequences constitute the HST of sequence 1. Parasequences are composed mainly of highly bioturbated fine- to very fine-grained sandstones (FA1: open marine-bay deposits, Table 5.1). The parasequence-bounding flooding surfaces (S1-FSs) are not demarcated by suites of the *Glossifungites* Ichnofacies. These surfaces are identified through the vertical variations in ichnological softground suites of the archetypal *Cruziana* Ichnofacies and their associated sedimentological features. The Bartonian ended with a low stage of relative sea-level that was followed by relative sea-level rise (a transgressive phase) during the onset of the early Priabonian. These are well-expressed by the coplanar FS/SB1-GS surface that separates sequence 1 (Gehannam Formation) from the overlying sequence 2 (lower Birket Qarun Formation) (Figs. 5.11, 5.12). This surface is emplaced in a horizon of complex paleoecologic environments, including a complex association of rhizoliths, marine to brackish-water invertebrate fossils and trace fossils, and marine-vertebrate bones (Figs. 5.8A-B).

LATE EOCENE (EARLY PRIABONIAN) SEQUENCE 2

Relatively thick parasequences (~ 10 m thick) define the HST of sequence 2 (lower part of Birket Qarun Formation). These parasequences are composed mainly of fine- to medium-grained sandstones (e.g., FA1: proximal marine-bay deposits, resulting from the higher energy levels than observed in sequence 1; Table 5.1). The HST parasequences uncomfortably overlie the FS/SB1-GS surface, where the LST and TST were either not deposited or were subsequently eroded (Figs. 5.8A-B). The parasequence-bounding flooding surfaces (S2-FSs) are not demarcated with the suites of the *Glossifungites* Ichnofacies. The juxtaposition of suites attributable to proximal expressions of the *Cruziana* and distal expressions of the *Skolithos* ichnofacies, coupled

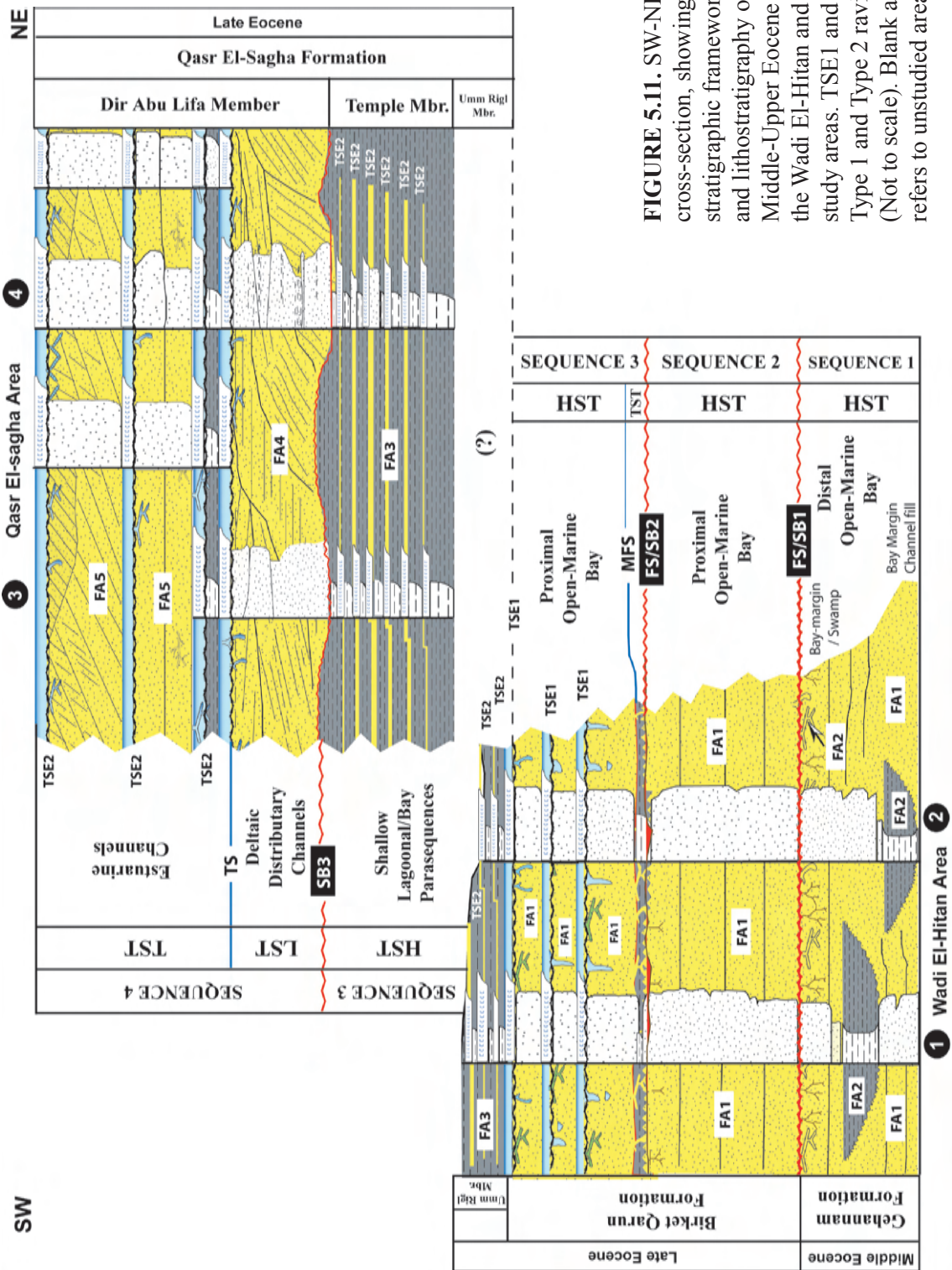


FIGURE 5.11. SW-NE diagrammatic cross-section, showing the sequence stratigraphic framework, sedimentology and lithostratigraphy of the compiled Middle-Upper Eocene succession in the Wadi El-Hitan and Qasr El-Sagha study areas. TSE1 and TSE2 refer to the Type 1 and Type 2 ravinement surfaces (Not to scale). Blank area marked by (?) refers to unstudied areas.

with the sedimentological features present, are used to detect these parasequence boundaries. The prograding HST parasequences shallow upwards to an undulating erosive surface with a distinctive rooted and alluviated horizon, marking subaerial exposure and low relative sea-level (Figs. 5.8C-E, 5.12). This horizon represents the merged FS/SB2-GS surface (Figs. 5.11, 5.12) that separates sequence 2 below from sequence 3 above (described below).

LATE EOCENE (PRIABONIAN) SEQUENCE 3

Sequence 3 constitutes the upper part of the Birket Qarun Formation and the lower two members (Umm Rigl and Temple members) of the Qasr El-Sagha Formation. In general, sequence 3 was deposited under shallow-water marginal-marine conditions during transgressive to highstand phases of a 3rd-order sea-level cycle, overprinted by abundant parasequences of higher-order cycles (Figs. 5.11, 5.12). Sea-level changes during the deposition of sequence 3 appear to have been rapid, and were possibly caused by a combination of local tectonic activity and eustasy.

The LST of sequence 3 has either not been deposited or was subsequently eroded during a transgressive phase that flooded the Fayum (Gindi) sag-basin shelf. The thin, TST shelf mudstone of sequence 3 was deposited unconformably on the coplanar FS/SB2 surface during a transgressive phase (Fig. 5.8C). The upper surface of the transgressive dark grey shale marks a MFS-GS that separates the thin TST below from the HST above in sequence 3 (Figs. 5.8C, 5.9A, 5.11). With continued transgression, the TSE (MFS) locally eroded this marker dark grey shale bed, and permitted the MFS and SB to merge (FS/SB2) (Figs. 5.6, 5.8D, 5.11).

The relatively thick (~ 100 m thick) HST of sequence 3 constitutes stacked and prograding parasequences of the upper Birket Qarun Formation, as well as the lower Umm Rigl and middle Temple members of the Qasr El-Sagha Formation (Fig. 5.11). Wave-ravinement surfaces (S3-FSs-GS) demarcate three parasequences of the upper

Birket Qarun Formation (Figs. 5.3, 5.10A-D). Upwards, these parasequences give way to the parasequences of the lower Umm Rigl and middle Temple members (Qasr El-Sagha Formation) (Fig. 5.10C). These parasequences are delineated by wave and/or tidal TSE (S3-FSS-GS and S4-FSS-GS) surfaces (Table 5.3, Figs. 5.6, 5.11). These shallow-marine parasequences (FA3) are incised upwards by the distributary channels (FA4) across a sequence boundary (SB3) (Fig. 5.8F).

Late Eocene (Late Priabonian) Sequence 4

The upper Dir Abu Lifa Member of the Upper Eocene Qasr El-Sagha Formation constitutes the third-order sequence 4 (Figs. 5.11, 5.12). The base of sequence 4 was the result of a lowered relative sea level (a regressive phase), as evidenced by the downward erosional unconformity SB3 (e.g., Bown and Kraus, 1988). The early-LST incision stage was followed by late-LST deposition of deltaic distributary-channel deposits (FA4; Table 5.1). The subsequent relative sea-level rise (transgressive phase) was initiated with the transgressive surface (TS-GS; Table 5.3) that separates the late LST below from the TST above in sequence 4 (Figs. 5.11, 5.12). Aggradational to retrogradational parasequences of the TST were deposited as estuarine deposits (FA5, Table 5.1). The parasequence-bounding surfaces (S4-FSS-GS, Table 5.3) are demarcated by wave and/or tidal TSE. The top of sequence 4 underlies the Oligocene continental to marginal-marine Gebel Qatrani Formation. The late LST and the TST of sequence 4 include many autogenic *Glossifungites* Ichnofacies-demarcated surfaces (AuGS1 and AuGS2; Table 5.3).

DISCUSSION AND CONCLUSIONS

***GLOSSIFUNGITES* ICHNOFACIES-DEMARCATED SURFACES**

Although firmground suites of the *Glossifungites* Ichnofacies have proven to

be a useful tool in sequence and genetic stratigraphic analyses, caution must be taken when assigning these surfaces to certain key sequence-stratigraphic discontinuities. The presence of the *Glossifungites* Ichnofacies may correspond to either autocyclic or allocyclic processes.

The autocyclically generated *Glossifungites* Ichnofacies-demarcated surfaces can be easily identified by their lack of lateral continuity, an absence of major lithofacies and ichnofacies dislocations (not be accommodated by Walther's Law), the demarcation by impoverished ichnological suites, shallow burrow-penetration depths, and evidence of burrow deformation during compaction. The autocyclic *Glossifungites* ichnofacies-demarcated surfaces can be further subdivided according to the principal sedimentological exhumation processes (e.g., those associated with deltaic distributary channels or those occurred within the estuarine channels) (Table 5.3, Figs. 5.6 and 5.7).

The allocyclically produced *Glossifungites* Ichnofacies-demarcated surfaces are strongly related to relative sea-level changes (i.e., tectonics and eustasy), as well as physical, chemical and biological factors. Therefore, the characteristics of these surfaces are complex. The genetic subdivision of these allocyclic surfaces is based mainly on: 1- the stratigraphic setting and relation of these discontinuities to the key sequence stratigraphic surfaces (e.g., SB, FS/SB, TS, MFS, and FS); 2- the associated sedimentological features and characters; and 3- ichnological criteria (e.g., substrate type, trace-fossils suites, bioturbation intensities, ichnogenera diversities, maximum burrow diameters, and burrow-penetration depths).

The occurrences of allocyclic *Glossifungites* Ichnofacies-demarcated surfaces are subdivided into three main types: 1- sequence bounding-; 2- systems tract bounding-; and 3- parasequence-bounding *Glossifungites* Ichnofacies-demarcated surfaces. These allogenic surfaces coincide with wave and/or tidal ravinement (TSE) surfaces (Table 5.3; Figs. 5.5, 6, 5.11). Although the amalgamated FS/SB1-GS and FS/SB2-GS surfaces display subaerial exposure, rhizobioturbation, and facies dislocations, they are

demarcated by poorly developed suites of the *Glossifungites* Ichnofacies (Table 5.3; Figs. 5.8A-E). These are characterized by low bioturbation intensities, reduced ichnogenera diversities and shallow burrow-penetration depths (Table 5.3; Figs. 5.8A-E). On the other hand, the systems tract-bounding surfaces (MFS-GS and TS-GS; Table 5.3) and the parasequence-bounding surfaces (S3-FSs-GS and S4-FSs-GS; Table 5.3) display well-developed ichnofossil suites attributable to the *Glossifungites* Ichnofacies. These suites show high bioturbation intensities, moderate to low ichnogenera diversities, and moderate to deep burrow-penetration depths (up to 2 m) (Table 5.3; Figs. 5.9, 5.10).

The dominant feature of all the studied *Glossifungites* ichnofacies-demarcated surfaces is the abundance of the dwelling structures of inferred deposit-feeders assigned to the ichnogenus *Thalassinoides*. Moreover, these firmground suites have rarer occurrences of dwellings of inferred suspension-feeding and carnivore tracemakers (e.g., *Skolithos*, *Arenicolites*, and *Psilonichnus*), as well as the diminutive deposit-feeding structures assigned to *Planolites* and dwelling structures identified as *Palaeophycus* (Table 5.3). The absence of relatively deep-marine expressions (e.g., *Zoophycos*), and the impoverished high-energy and shallow-water suites (e.g., *Skolithos* and *Arenicolites*) support generation in low- to moderate-energy conditions in a marginal-marine setting. Moreover, the common occurrence of robust *Thalassinoides* burrows (> 2 cm in diameter) may indicate low- to moderate-energy, and well-oxygenated nutrient-rich niches. Mudstone is the most common substrate for the suites of the *Glossifungites* Ichnofacies, but the present study shows the importance of very fine- to fine-grained sandstone as a firmground substrate. Some firmground suites in the study area show burrow penetrations reaching to 2 m below the discontinuity surface (Fig. 5.10C). Burial duration is hard to assess in both the modern and rock record. In modern settings, it is accepted that mappable *Glossifungites*-demarcated surfaces represent a minimum of 1 m of exhumation and burial durations that exceed about 1000 years (e.g., Pemberton and Frey, 1985; Gingras et al., 2000, 2001).

SEQUENCES' HIERARCHY

Based on the previous high-resolution biostratigraphic data (see Zalat, 1995; Haggag and Bolli, 1996), the Middle-Upper Eocene succession in the study area can be calibrated with the global Eocene chronostratigraphic time scale of Gradstein et al. (2004) and biostratigraphic zonations of Berggren et al. (1995) and Martini (1971) (Fig. 5.12). However, the identified key-stratigraphic surfaces and sequences can be correlated also with the regional sequences of Hardenbol et al. (1998) from Europe basins and those of Haq et al. (1987) (Fig. 5.12).

The studied Middle–Upper Eocene succession accumulated over a period of c. 3–4 my. The depositional sequences (considering that the base of sequence 1 is unexposed, and upper part of sequence 4 is unstudied) display a third-order cycle durations (e.g., Vail et al., 1977). The overall northward retreat of the Tethys shoreline is considered, here, to represent the upper part of a 2nd-order cycle, extending from the Eocene to Oligocene (Fig. 5.12). This Tethys retreat was strongly controlled by regional tectonics.

The allocyclically generated *Glossifungites* Ichnofacies-demarcated surfaces of the Middle-Upper Eocene succession (Table 5.3, Fig. 5.12) indicate episodic and oscillating third- and higher-order (4th and 5th) cycles of relative sea level change. The active movements (SE-throwing) along the NW/SE-striking faults (e.g., EGPC, 1992) resulted in irregular subsidence, compaction, and uplift in the basin. The subsidence/uplift tectonics, combined with eustatic sea-level rise and fall, controlled the relative sea-level changes and accommodation space during the deposition of Middle-Upper Eocene succession in the study area.

Sequence 1 (base not exposed) was deposited in a HST during late Bartonian. The Middle-Late Eocene boundary is expressed herein by the coplanar FS/SB1-GS surface between the Gehannam (sequence 1) and lower Birket Qarun (sequence 2) formations. This surface can be correlated with the Bart2/Pr1 of Hardenbol et al. (1998) (Fig. 5.12). Both the LST and TST of sequence 2 were either not deposited or were subsequently

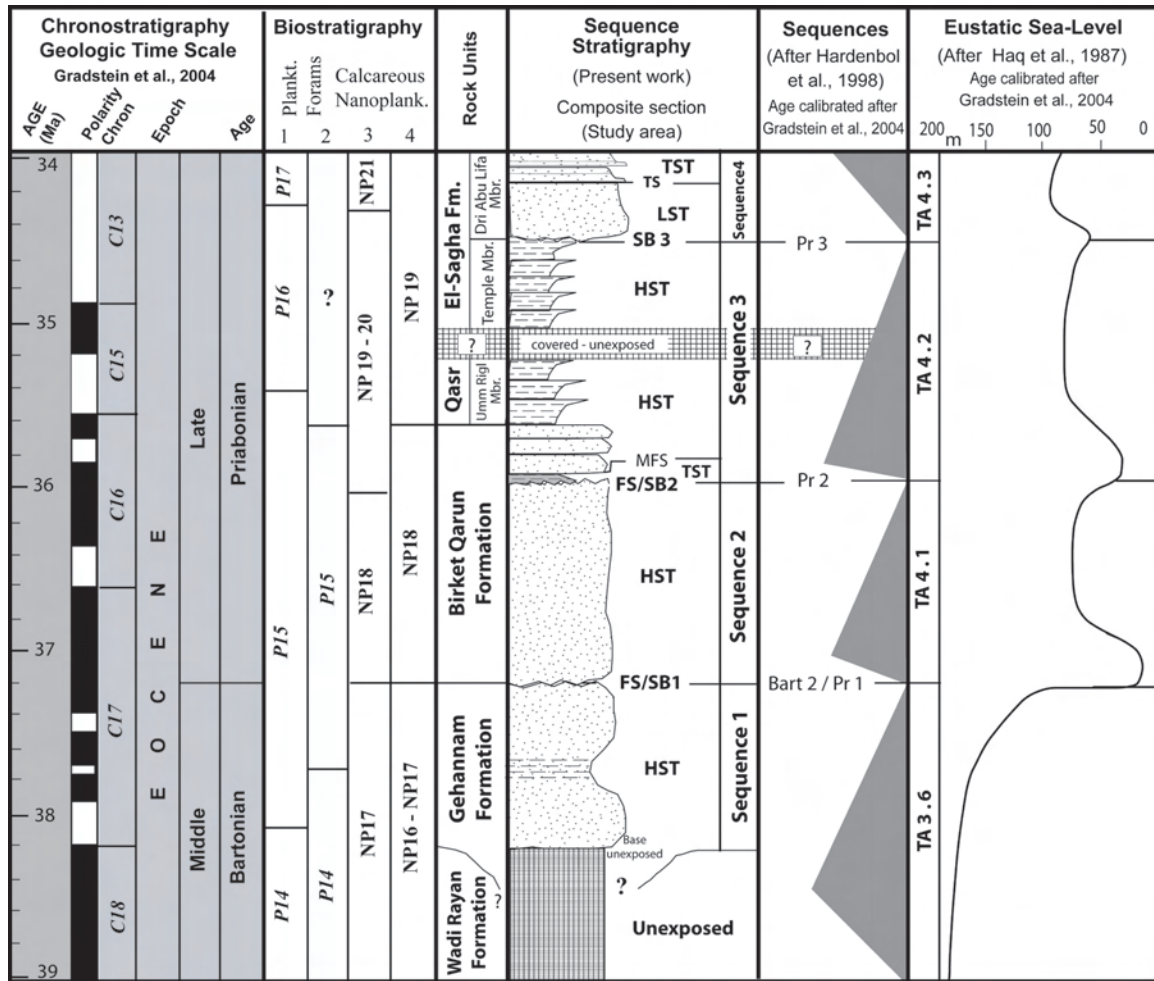


FIGURE 5.12. Correlation chart of the identified sequences and key-stratigraphic surfaces of the Middle-Upper Eocene succession in the study area with the regional sequences in European basins of Hardenbol et al. (1998) and the global eustatic sea-level curve of Haq et al. (1987). The age is calibrated after the global Eocene chronostratigraphic time scale (Gradstein et al., 2004), the planktonic foraminifera zonation of (1) Berggren et al. (1995) and (2) Haggag and Bolli (1996), and the nannoplanktonic zonation of (3) Martini (1971) and (4) Zalat (1995).

eroded. Upwards, the HST sandstone deposits of sequence 2 display highly rooted and alluviated horizons, indicating subaerial exposure during uplift and/or low relative sea level (Fig. 5.12). These horizons are truncated by an undulating erosional surface that marks the FS/SB2-GS. This coplanar surface separates sequences 2 and 3, and can be correlated with the Pr2 of Hardenbol et al. (1998) (Fig. 5.12). The LST of sequence 3 has been eroded or was not deposited. The thin TST (locally eroded) of sequence 3 was

deposited as shelf mudstone. The parasequences of the HST in sequence 3 were deposited during a HST that was overprinted by minor sea-level fluctuations (expressed by the abundant parasequences and TSE surfaces). Laterally migrating distributary channels (LST; base of sequence 4) incised into the lagoonal parasequences (HST; sequence 3), forming the sequence boundary SB3. SB3 matches well with Pr3 of Hardenbol et al. (1998) (Fig. 5.12). The upper estuarine deposits of sequence 4 were deposited during a transgressive pulse (TST), exhibiting inferably higher-order sea-level cycles (Fig. 5.12).

REFERENCES

- Abbott, S.T., 1998, Transgressive systems tracts and onlap shellbeds from mid-Pleistocene sequences, Wanganui Basin, New Zealand: *Journal of Sedimentary Research*, v. 68, p. 253-268.
- Balistieri, P.R.M.N. and Netto, R.G., 2002, A *Glossifungites* suite in deposits of the Itararé Group (Upper Carboniferous-Lower Permian of Paraná Basin) at Mafra region, north of Santa Catarina State, Brazil: Ichnotaxonomy, and paleoecological and stratigraphical constrains: *Acta Geologica Leopoldensia*, v. 55, p. 91-106.
- Beadnell, H.J.L., 1905, The topography and geology of the Fayum province of Egypt: Egyptian Survey Department, Cairo, 101 pp.
- Berggren, W.A., Kent, D.V., Swisher, C.C. and Aubry, M.-P., 1995, A revised Cenozoic geochronology and chronostratigraphy, *in* Berggren, W.A., Kent, D.V., Aubry, M.-P. and Hardenbol, J., eds., *Geochronology, time scales and global stratigraphic correlation*: Society of Economic Paleontologists and Mineralogists Special Publication, v. 54, p. 129–212.
- Bertling, M., 1999, Taphonomy of trace fossils at omission surfaces (Middle Triassic, East Germany): *Palaeogeography, palaeoclimatology, palaeoecology*, v. 149, p. 27-40.

- Bown, T.M. and Kraus, M.J., 1988, Geology and paleoenvironment of the Oligocene Jebel Qatrani Formation and adjacent rocks, Fayum depression, Egypt: U.S. Geological Survey Professional Paper, v. 1452, p. 1-60.
- Bromley R.G. and Hanken, N.-M., 1991, The growth vector in trace fossils: Examples from the Glossifungites ichnofacies, Lower Cambrian, Norway: *Ichnos*, v. 1, p. 261–276.
- Bromley, R.G., Pemberton, S.G. and Rahmani, R.A., 1984, A Cretaceous woodground: the Teredolites ichnofacies: *Journal of Paleontology*, v. 58, p. 488-498.
- Brown, L.F. and Fisher, W.L., 1977, Seismic-stratigraphic interpretation of depositional systems: Examples from Brazilian rift and pull-apart basins, *in* Payton, C.E. (ed.), *Seismic Stratigraphy-Applications to hydrocarbon exploration*: American Association of Petroleum Geologists Memoir, v. 26, p. 213-248.
- Buatois, L.A., Mángano, M. G., Alissa, A. and Carr, T.R., 2002, Sequence stratigraphic and sedimentologic significance of biogenic structures from a late Paleozoic marginal- to open-marine reservoir, Morrow Sandstone, subsurface of southwest Kansas, USA: *Sedimentary Geology*, v. 152, p. 99-132.
- Campbell, K.A. and Nesbitt, E.A., 2000, High-resolution architecture and paleoecology of an active margin, storm-flood influenced estuary, Quinault Formation (Pliocene), Washington: *Palaaios*, v. 15, p. 553–579.
- Cherif, O.H. and El Afifi, F.I., 1983, Remarks on the stratigraphy and tectonism of the main Oligocene exposures in Egypt: *Annals of the Geological Survey of Egypt*, v. 13, p. 247-255.
- Dam, G., 1990, Palaeoenvironmental significance of trace fossils from the shallow marine Lower Jurassic Neill Klintner Formation, East Greenland: *Palaeogeography, Palaeoclimatology, Palaeoecology*, v. 79, p. 221-248.

- Dames, W.B., 1894, Übere Zeuglodonten aus Aegypten und die Beziehungen der archaeouten zu den übrigen Cetacean: Géologique und Paläontologische Abhandlungen (Jena), v. 5, p. 189-222.
- De Gibert, J.M. and Robles, J.M., 2005, Firmground ichnofacies recording high-frequency marine flooding events (Langhian transgression, Vallès-Penedès Basin, Spain): *Geologica Acta: an international earth science journal*, v. 3, p. 295-305.
- Driese, S.G. and Foreman, J.L., 1991, Traces and related chemical changes in a Late Ordovician paleosol, Glossifungites ichnofacies, southern Appalachians, USA: *Ichnos*, v. 1, p. 207-219.
- EGPC, 1992, Western Desert, oil and gas fields (A comprehensive overview): The Egyptian General Petroleum Corporation, Cairo, 431 pp.
- El Hawat, A.S., 1997, Sedimentary basins of Egypt: An overview of dynamic stratigraphy, *in*, Selly, R.C., ed., African basins, *in*, Hsü, K.J. (series ed.), *Sedimentary Basin of the World*: Elsevier, Amsterdam, v. 3, p. 39-85.
- El Zarka, M.H., 1983, Mode of hydrocarbon generation and prospects of the northern part of the Western Desert, Egypt: *Journal of African Earth Science*, v. 1, p. 295-304.
- Fielding, C.R., Bann, K.L., MacEachern, J.A., Tye, S.C. and Jones, B.G., 2006, Cyclicity in the nearshore marine to coastal, Lower Permian, Pebbly Beach Formation, southern Sydney Basin, Australia: a record of relative sea-level fluctuations at the close of the Late Paleozoic Gondwanan ice age: *Sedimentology*, v. 53, p. 435-463.
- Fitzsimmons, R. and Johnson, S., 2000, Forced regressions: recognition, architecture and genesis in the Campanian of the Bighorn Basin, Wyoming, *in* Hunt, D. and Gawthorpe, R.L., eds., *Sedimentary Responses to Forced Regressions*: Geological Society Special Publication, v. 172, p. 113–139. London.
- Frey, R.W. and Goldring, R., 1992, Marine event beds and recolonization surfaces as revealed by trace fossil analysis: *Geological Magazine*, v. 129, p. 325–335.

- Frey, R.W., Pemberton, S.G. and Saunders, T.D.A., 1990, Ichnofacies and bathymetry: a passive relationship: *Journal of Paleontology*, v. 64, p. 155-158.
- Frey, R.W. and Seilacher, A., 1980, Uniformity in marine invertebrate Ichnology: *Lethaia* v. 13, p. 183-207.
- Geological Survey of Egypt 'GSE', 1981, Geological Map of Egypt, scale 1: 2,000,000: Egyptian Geological Survey and Mining Authority, Ministry of Industry and Mineral Resources, Cairo, 1 sheet.
- Geological Survey of Egypt 'GSE', 1983, Geological Map of Greater Cairo Area, scale 1: 100,000: Egyptian Geological Survey and Mining Authority, Ministry of Industry and Mineral Resources, Cairo, 1 sheet.
- Gingerich, P.D., 1992, Marine mammals (Cetacea and Sirenia) from the Eocene of Gebel Mokattam and Fayum, Egypt; stratigraphy, age and paleoenvironments: *University of Michigan Papers in Paleontology*, v. 30, p. 1-84.
- Gingras, M.K., Pemberton, S.G. and Saunders, T., 2000, Firmness profiles associated with tidal-creek deposits: The temporal significance of Glossifungites assemblages: *Journal of Sedimentary Research*, v. 70, p. 1017-1025.
- Gingras, M.K., Pemberton, S.G. and Saunders, T.D.A., 2001, Bathymetry, sediment texture, and substrate cohesiveness: their impact on Glossifungites trace assemblages at Willapa Bay, Washington: *Palaeogeography, Palaeoclimatology, Palaeoecology*, v. 169, p. 1-21.
- Gingras, M.K., Räsänen, M.E., Pemberton, S.G. and Romero, L.P., 2002a, Ichnology and sedimentology reveal depositional characteristics of bay-margin parasequences in Miocene Amazonian foreland basin: *Journal of Sedimentary Research*, v. 72, p. 871-883.
- Gingras, M.K., Räsänen, M.E. and Ranzi, A., 2002b, The significance of bioturbated inclined heterolithic stratification in the southern part of the Miocene Solimoes Formation, Rio Acre, Amazonia Brazil: *Palaios*, v. 17, p. 591-601.

- Gradstein, F.M., Ogg, J.G. and Smith, A.G., 2004, A Geologic Time Scale 2004: Cambridge University Press, London, 589 pp.
- Guiraud, R., Bosworth, W., Thierry, J. and Delplanque, A., 2005, Phanerozoic geological evolution of northern and central Africa: An overview: *Journal of African Earth Science*, v. 43, p. 83-143.
- Haggag, M.A. and Bolli, H.M., 1996, The origin of *Globigerina* *semiinvoluta* (Keijzer), Upper Eocene, Fayoum area, Egypt: *Neues Jahrbuch für Geologie und Paläontologie, Monatshefte*, v. 6, p. 365-374.
- Haq, B.U., Hardenbol, J. and Vail, P.R., 1987, Chronology of fluctuating sea level since the Triassic: *Science*, v. 235, p. 1156-1167.
- Hardenbol, J., Thierry, J., Farley, M.B., Jacquin, T., de Graciansky, P.C. and Vail, P.R., 1998, Mesozoic and Cenozoic sequence chronostratigraphic framework of European basins, *in* de Graciansky, P. C., Hardenbol, J., Jacquin, T., Vail, P.R., eds., *Mesozoic and Cenozoic Sequence Stratigraphy of European Basins*: Society of Economic Paleontologists and Mineralogists Special Publication, v. 60, p. 3-13.
- Hayward, B.W., 1976, Lower Miocene bathyal and submarine canyon ichnocoenoses from Northland, New Zealand: *Lethaia*, v. 9, p. 149-162.
- Holz, M., 2003, Sequence stratigraphy of a lagoonal estuarine system- an example from the lower Permian Rio Bonito Formation, Paraná Basin, Brazil: *Sedimentary Geology*, v. 162, p. 305-331.
- Leckie, D.A., 1994, Canterbury Plains, New Zealand- implications for sequence stratigraphic models: *American Association of Petroleum Geologists Bulletin*, v. 78, p. 1240-1256.

- MacEachern, J.A., Bechtel, D.J. and Pemberton, S.G., 1992a, Ichnology and sedimentology of transgressive deposits, transgressively-related deposits and transgressive systems tracts in the Viking Formation of Alberta, *in* Pemberton, S.G., ed., Applications of Ichnology to Petroleum Exploration: A Core Workshop: Society of Economic Paleontologists and Mineralogists, Core Workshop, v. 17, p. 251-290.
- MacEachern, J.A. and Burton, J.A., 2000, Firmground Zoophycos in the Lower Cretaceous Viking Formation, Alberta: A distal expression of the *Glossifungites* ichnofacies: *Palaios*, 15, 387-398.
- MacEachern, J.A., Gingras, M.K., Bann, K.L and Pemberton, S.G., Dafoe, L.T., 2007, Application of Ichnology to high-resolution genetic stratigraphic paradigms, *in*, MacEachern, J.A., Bann, K.L., Gingras, M.K. and Pemberton, S.G., eds., Applied Ichnology: Society of Economic Palaeontologists and Mineralogists, Short Course Notes, v. 52, p. 93-127.
- MacEachern, J.A. and Hobbs, T.W., 2004, The ichnological expression of marine and marginal marine conglomerates and conglomeratic intervals, Cretaceous Western Interior Seaway, Alberta and northeastern British Columbia, *in* Moslow, T. and Zonneveld, J.-P., eds., Marine Conglomerates: Bulletin of Canadian Society of Petroleum Geology, v. 52, p. 77-104.
- MacEachern, J.A. and Pemberton, S.G., 1994, Ichnological character of incised valley fill systems from the Viking Formation of the Western Canada Sedimentary basin, Alberta, Canada, *in* Dalrymple, R.W., Boyd, R. and Zaitlin, B.A., eds., Incised-Valley Systems: Origin and Sedimentary Sequences: Society of Economic Paleontologists and Mineralogists Special Publication, v. 51, p. 129-157.

- MacEachern, J.A., Raychaudhuri, I. and Pemberton, S.G., 1992b, Stratigraphic applications of the *Glossifungites* ichnofacies: delineating discontinuities in the rock record, *in* Pemberton, S.G., ed., Applications of Ichnology to Petroleum Exploration: A Core Workshop: Society of Economic Paleontologists and Mineralogists, Core Workshop, v. 17, p. 169-198.
- MacEachern, J.A., Zaitlin, B.A. and Pemberton, S.G., 1999, Coarse-grained, shoreline-attached, marginal marine parasequences of the Viking Formation, Joffre Field, Alberta Canada, *in* Bergman, K.M., Snedden, J.W., eds., Isolated Shallow Marine Sand Bodies: Sequence Stratigraphic and Sedimentologic Interpretation: Society of Economic Paleontologists and Mineralogists Special Publication, v. 64, p. 273–296.
- Martini, E., 1971, Standard Tertiary and Quaternary calcareous nannoplankton zonation, *in*, Farinacci, A., ed., Proceedings of the II Plankton Conference: Roma, p. 739–785.
- Mitchum, R.M., Vail, P.R. and Thompson, S., 1977, Seismic stratigraphy and global changes of sea level, Part 2: The depositional sequence as a basic unit for stratigraphic analysis, *in* Payton, C.E., ed., Seismic stratigraphy-Applications to hydrocarbon exploration: American Association of Petroleum Geologists Memoir, v. 26, p. 53-62.
- Morris, J.E., Hampson, G.J. and Johnson, H.D., 2006, A sequence stratigraphic model for an intensely bioturbated shallow-marine sandstone: the Bridport Sand Formation, Wessex Basin, UK: *Sedimentology*, v. 53, p. 1229-1263.
- Ozalas, K., Savrda, C.E. and Fullerton, R.R., 1994, Bioturbated oxygenation-event beds in siliceous facies: Monterey Formation (Miocene), California: *Palaeogeography, Palaeoclimatology, Palaeoecology*, v. 112, p. 63-83.
- Paczeńska, J., 2001, An application of trace fossils in the facies analysis and high-resolution sequence stratigraphy- an example from the Cambrian of the Polish part of the East European Craton: *Przegląd Geologiczny*, v. 49, p. 1137-1146. (in Polish with English abstract).

- Pemberton, S.G. and Frey, R.W., 1985, The *Glossifungites* ichnofacies: Modern examples from the Georgia coast, U.S.A., in Curran, H.A., ed., Biogenic structures: Their use in interpreting depositional environments: Society of Economic Paleontologists and Mineralogists Special Publications, v. 35, p. 237-259.
- Pemberton, S.G. and MacEachern, J.A., 1995, The sequence stratigraphic significance of trace fossils: examples from the Cretaceous foreland basin of Alberta, Canada, in Van Wagoner, J.C. and Bertram, G., eds., Sequence stratigraphy of foreland basins deposits: Outcrops and subsurface examples from the Cretaceous of North America: American Association of Petroleum Geologists Memoirs, v. 64, p. 429-475.
- Pemberton, S.G., MacEachern, J.A. and Frey, R.W., 1992a, Trace fossil facies models: Environmental and allostratigraphic significance, in Walker, R.G. and James, N., Eds., Facies models: Response to sea level change: Geological Association of Canada, St. John's, NF, p. 47-72.
- Pemberton, S.G., MacEachern, J.A. and Saunders, T., 2004, Stratigraphic applications of substrate-specific ichnofacies: delineating discontinuities in the rock record, in MacIlory, D., ed., The Application of Ichnology to Palaeoenvironmental and Stratigraphic Analysis: Geological Society of London Special Publications, v. 288, p. 29-62.
- Pemberton, S.G., Reinson, G.E. and MacEachern, J.A., 1992b, Comparative ichnological analysis of late Albian estuarine valley-fill and shelf-shoreface deposits, Crystal Viking field, Alberta, in Pemberton, S.G., ed., Applications of ichnology to petroleum exploration, a core workshop: Society of Economic Paleontologists and Mineralogists, Core Workshop, v. 17, p. 291-317.
- Pemberton, S.G., Spila, M., Pulham, A.J., Saunders, T., MacEachern, J.A., Robbins, D. and Sinclair, I., 2001, Ichnology and sedimentology of shallow and marginal marine systems: Ben Nevis and Avalon reservoirs, Jeanne D'Arc Basin: Geological Association of Canada, Short Course Notes, St. John's NF, v. 15, 343 pp.

- Posamentier, H.W. and Allen, G.P., 1999, Siliciclastic sequence stratigraphy- concepts and applications: Society of Economic Paleontologists and Mineralogists, Concepts in Sedimentology and Paleontology, v. 7, 210 pp.
- Posamentier, H.W., Jervey, M.T. and Vail, P.R., 1988, Eustatic controls on clastic deposition I-Conceptual framework, *in* Wilgus, C.K., Hastings, B.S., Kendall, C.G.St.C., Posamentier, H.W., Ross, C.A. and Van Wagoner, J.C., eds., Sea-level changes- an integrated approach: Society of Economic Paleontologists and Mineralogists Special publication, v. 42, p. 109-124.
- Raychaudhuri, I., Brekke, H.G., Pemberton, S.G. and MacEachern, J.A., 1992, Depositional facies and trace fossils of a low wave energy shoreface succession, Albian Viking Formation, Chigwell Field, Alberta, Canada, *in* Pemberton, S.G., ed., Applications of Ichnology to Petroleum Exploration, a Core Workshop: Society of Economic Paleontologists and Mineralogists, Core Workshop, v. 17, p. 319-337.
- Rousseau, M., Dromart, G., Garcia, J-P., Atrops, F. and Guillocheau, F., 2005, Jurassic evolution of the Arabian carbonate platform edge in the central Oman Mountains: Journal of the Geological Society, London, v. 162, p. 349-362.
- Said, R., 1962, The geology of Egypt: Elsevier, Amsterdam and New York, 377 pp.
- Said, R., 1990, The geology of Egypt: A. A. Balkema, Rotterdam, 734 pp.
- Salem, R., 1976, Evolution of Eocene-Miocene sedimentation patterns in parts of northern Egypt: American Association of Petroleum Geologists Bulletin, v. 60, p. 34-64.
- Saunders, T. and Pemberton, S.G., 1986, Trace fossils and sedimentology of the Appaloosa Sandstone: Bearpaw-Horseshoe Canyon Formation, Dorothy, Alberta: Canadian Society of Petroleum Geologists field trip guide book, 117 pp.
- Savrda, C.E., 1991a, Ichnology in sequence stratigraphic studies: An example from the lower Paleocene of Alabama: *Palaios*, v. 6, p. 39-53.

- Savrda, C.E., 1991b, Teredolites, wood substrates, and sea-level dynamics: *Geology*, v. 19, p. 905-908.
- Savrda, C.E., 1995, Ichnologic applications in paleoceanographic, paleoclimatic, and sea level studies: *Palaios*, v. 10, p. 565-577.
- Savrda, C.E., Browning, J.V., Krawinkle, H. and Hesselbo, S.P., 2001a, Firmground ichnofabrics in deep-water sequence stratigraphy, Tertiary clinoform-toe deposits, New Jersey slope: *Palaios*, v. 16, p. 294-305.
- Savrda, C.E., Krawinkle, H., McCarthy, F.M.G., McHugh, C.M.G., Olson, H.C. and Mountain, G., 2001b, Ichnofabrics of a Pleistocene slope succession, New Jersey margin: relations to climate and sea-level dynamics: *Palaeogeography, Palaeoclimatology, Palaeoecology*, v. 171, p. 41-61.
- Seilacher, A., 1964, Biogenic sedimentary structures. In: Imbrie, J. and Newell, N.D., eds., *Approaches to Paleoecology*: Wiley & Sons, New York, p. 296-316.
- Seilacher, A., 1967a, Bathymetry of trace fossils: *Marine Geology*, v. 5, p. 413-428.
- Seilacher, A., 1967b, Fossil behavior: *Scientific American* 217, 72-80.
- Sestini, G., 1984, Tectonic and sedimentary history of NE African margin (Egypt/Libya), in Dixon, J.E. and Robertson, A.H.F., eds., *Geological evolution of the eastern Mediterranean*: Geological Society of London Special Publication, v. 17, p. 161-175.
- Shanley, K.W. and McCabe, P.J., 1989, Sequence stratigraphic relationships and facies architecture of Turonian-Campanian strata, Kaiparowits Plateau, south-central Utah: *American Association of Petroleum Geologists Bulletin*, v. 73, p. 410-411.
- Smith, A.G., 1971, Alpine deformation and the oceanic areas of the Tethys, Mediterranean, and Atlantic: *Bulletin of the Geological Society of America*, v. 82, p. 2039-2070.

- Smith, G.J. and Jacobi, R.D., 1998, Fault-induced transgressive incised shoreface model for the Canadaway Group, Catskill delta complex: *Journal of Sedimentary Research*, v. 68, p. 668–683.
- Strougo, A. and Haggag, M.A.Y., 1984, Contribution to the age determination of the Gehannam Formation in the Fayum Province, Egypt: *Neues Jahrbuch für Geologie und Paläeontologie, Monatshefte*, v. 1, p. 46-52.
- Vail, P.R., Mitchum, R.M.Jr. and Thompson, S., III, 1977, Seismic stratigraphy and global changes of sea level, part 3: Relative changes of sea level from coastal onlap, *in* Payton, C.E. (ed.), *Seismic stratigraphic- Applications to hydrocarbon exploration: American Association of Petroleum Geologists Memoir*, v. 26, p. 63-98.
- Van Wagoner, J.C., Mitchum, R.M., Campion, K.M. and Rahmanian, V.D., 1990, Siliciclastic sequence stratigraphy in well logs, cores, and outcrops: Concepts for high-resolution correlation of time and facies: *American Association of Petroleum Geologists, Methods in Exploration Series*, v.7, p. 1-55.
- Van Wagoner, J.C., Posamentier, H.W., Mitchum, R.M., Vail, P.R., Sarg, J.F., Loutit, T.S. and Hardenbol, J., 1988, An overview of the fundamentals of sequence stratigraphy and key definitions, *in* Wilgus, C.K., Hastings, B.S., Kendall, C.G.St. C., Posamentier, H.W., Ross, C.A. and Van Wagoner, J.C. (Eds.), *Sea-level changes- an integrated approach: Society of Economic Paleontologists and Mineralogists Special publication*, v. 42, p. 39-45.
- Vossler, S.M. and Pemberton, S.G., 1988, Ichnology of the Cardium Formation (Pembina oilfield): Implications for depositional and sequence stratigraphic interpretations, *in* James, D.P. and Leckie, D.A., eds., *Sequences, Stratigraphy, Sedimentology: surface and subsurface: Canadian Society of Petroleum Geologists Memoir*, v. 15, p. 237-253.

- Wang, Y., Shen, J. and Zhou, Z., 1997, Ichnofacies and sequence stratigraphy of the Lower-Middle Devonian in Dushan County, southern Guizhou: *Acta Micropalaeontologica Sinica*, v. 14, p. 203-213. (in Chinese).
- Zalat, A.A., 1995, Calcareous nanoplankton and diatoms from the Eocene / Pliocene sediments, Fayoum depression, Egypt: *Journal of African Earth Sciences*, v. 20, p. 227-244.
- Zonneveld, J.P., Lavigne, J.M., Bartels, W.S., and Gunnell, G.F., 2006, *Lunulichnus tuberosus* ichogen. and ichnosp. nov. from the early Eocene Wasatch Formation, Fossil Butte National Monument, Wyoming: an arthropod-constructed trace fossil associated with alluvial firmground: *Ichnos*, v. 13, p. 87-94.

CHAPTER 6: SUMMARY AND CONCLUSIONS

The current study integrates applied ichnology with sedimentologic and sequence stratigraphic analyses of the Middle-Upper Eocene successions in the Fayum depression. Excellent outcrop exposure affords the dataset for developing sedimentologic, stratigraphic and paleoenvironmental models.

The pertinent results of the current thesis can be summarized under the following four main themes. Firstly, the sedimentary environments and depositional characteristics of Middle-Upper Eocene strata in the Fayum depression are established in Chapter 2. Secondly, the facies architectures, trace fossils and paleoenvironments of the whale-bearing Gehannam and Birket Qarun formations in the area of Wadi El-Hitan are assessed in Chapter 3. Thirdly, establishment of a bio-sedimentologic model reveals the origin and development of the unusual, large-sized sedimentary structures of the Birket Qarun Formation (Wadi El-Hitan area) in Chapter 4. Finally, the application of the *Glossifungites* Ichnofacies in sequence stratigraphic analysis is presented in Chapter 5, using the Middle-Upper Eocene succession in the Fayum depression as an outstanding case study.

Based on sedimentological and ichnological data, five facies associations (FA1 - FA5) are identified (Table 2.3). Facies Association 1 (FA1) is characterized by thoroughly bioturbated sandstone and diverse trace-fossil suites that reflect the *Cruziana* Ichnofacies (BI 5) (Fig. 2.5). Facies Association 2 (FA2) is heterolithic, and contains sporadically distributed trace fossils attributable to the *Psilonichnus* Ichnofacies and a restricted, proximal expression of the *Cruziana* Ichnofacies locally (Fig. 2.6). Facies Association 3 (FA3) comprises weakly and sporadically burrowed sandy shales interbedded with mudstones (Fig. 2.8). Therein, bioturbation is generally reduced in intensity, and the ichnological suites are representative of distal expressions of the *Skolithos* Ichnofacies. Facies association 4 (FA4) comprises sporadically burrowed inclined heterolithic

stratification (IHS) with a brackish-water trace fossil suite (Fig. 2.9). Facies Association 5 (FA5) comprises weakly burrowed sandstones and mudstones containing restricted ichnological suites that correspond to impoverished expressions of the *Skolithos* and *Psilonichnus* ichnofacies (Fig. 2.11).

Depositional models (Figs. 2.12, 2.13) show that the facies associations and their corresponding depositional environments record a gradual shallowing-upward succession. The general stratigraphic evolution resulted from a regional, tectonically controlled second-order cycle, associated with northward regression of the Tethys. Subordinate cycles (i.e., third- and higher-order cycles) are delineated by several *Glossifungites* Ichnofacies- demarcated discontinuities, which were emplaced at the base of flooding surfaces.

The Middle Eocene (Bartonian) Gehannam Formation is interpreted to have deposited in a low-energy broad bay or gulf (FA1), locally interrupted by the deposits of FA2 under low-energy bay margin, which abruptly shallowed upward to marginal-marine swamps. The Birket Qarun Formation reflects a proximal, low-energy bay or gulf setting (FA1), with an intercalated thin, transgressive, dark-grey shale unit. The upper Birket Qarun Formation displays repeated wave ravinement and coastal margin transgressive sediments that accumulated in a bay margin setting. The lower Temple Member of the Upper Eocene (Priabonian) Qasr El-Sagha Formation is represented by shallow lagoonal or bay parasequences (FA3) in arid to semi-arid (tropical to subtropical) climates. Facies Association 3 is truncated upward by a sequence boundary (SB3) overlain by deltaic distributary channels (FA4) of the upper Dir Abu Lifa Member. The upper part of Dir Abu Lifa is represented by stacked estuarine channels (FA5), recording a return to relative sea-level rise and transgressive conditions within the study area.

Many of the studied intervals display unusual ichnological-sedimentological associations. The highly bioturbated sandstones (FA1) differ markedly from the

shallowing-upwards profiles of shoreface and delta complexes, and those normally associated with embayed nearshore settings. The large-scale IHS of FA4 (up to 28 m thick) provide an important example of heterolithic tidally influenced fluvial channel deposits. These may assist in the interpretation of the stratigraphic record elsewhere. The Eocene Fayum whales are restricted to the strata highstand systems tracts. They appear to have thrived under conditions of low depositional energy, moderate sedimentation rates in fully marine waters and an environment, characterized by a high biomass. The residence of the Fayum Middle-Upper Eocene whales in fully open-marine environments within the highstand systems tracts adds additional evidence strengthening the interpretation that the Early-Middle Eocene whales show a transition from land/shallow sea margins (e.g., those found in Pakistan) to a fully marine environment.

Special attention is paid to the paleoenvironment and source of sediments, as well as the preservation of the fossil whales of the Middle-Upper Eocene Gehannam and Birket Qarun formations in the area of Wadi El-Hitan (Chapter 3). The deposits of the whale-bearing Gehannam and Birket Qarun formations are divided into two main facies associations (Table 3.1; Fig. 3.3). Facies Association 1 (FA1) is represented by two genetically related bioturbated sandstones facies (Facies 1 and 2) (Figs. 3.4, 3.5). Facies Association 2 (FA2) is represented by gypsiferous shale, sandy siltstone, and fine-grained sandstone (F3-5) (Fig. 3.6). Within these facies associations, seventeen ichnospecies belonging to thirteen ichnogenera (Tables 3.2, 3.3 and Figs. 3.7, 3.8) are identified. Additionally, fossil-plant roots (rhizoliths) are recognized at a number of discrete stratigraphic levels (Figs. 3.9).

The biological and sedimentological characteristics of the facies associations suggest that FA1 accumulated in an open, low-energy, fully marine bay (Figs. 3.10, 3.11). Facies Association 2 marks shallowing episodes, and represents landward sedimentation in low energy, bay-margin locales, possibly in a poorly drained intertidal to supratidal paleoenvironment. The notable absence of hydraulic reworking (i.e., oscillation ripples,

current ripples, and hummocky cross stratification) in FA1 and FA2 suggests that clastic point-sources were dominantly hypopycnal and were deposited from suspension, nominally suggesting flashy point-source discharge. These sediments were redistributed and transported along the bay by low-energy wave and current processes. Locally and occasionally in the basin, eolian sand may represent an important source of sediment supply.

The quiescent marine bay covering the area of Wadi El-Hitan (Figs. 3.10, 3.11) appears to have represented an important biome for the celebrated Middle-Late Eocene whales. The aquatic fully marine habitat of these large whales resulted in their global paleogeographic distribution, extending from Southeast Asia to North America. Moreover, the preservation of the whale fossils is somewhat paradoxical with respect to depositional conditions, in that the sedimentation rates must be: (1) sufficiently rapid to inter the whales and discourage scavenging boring or encrustation; and, (2) adequately slow that sediment-dwelling endobenthos were afforded the time necessary to eradicate essentially all the physical sedimentary structures.

The integrated sedimentologic, ichnological and stratigraphic data of chapters 2 and 3 are coupled with petrography, diagenesis, and stable-isotope analyses in order to propose a bio-sedimentological model interpreting the origin and development of unusual large-sized structures in the Birket Qarun Formation (Chapter 4). These structures are massive appearing, and of variable size and morphology. Structures vary from a boxwork or branched pillar morphology (up to dm-scale) in Sandouk El-Borneta and along Wadi El-Hitan, to a perpendicular amphora-like morphology (up to 180 cm height) in the Old Camp site (Figs. 4.2 - 4.4).

Firmground *Thalassinoides*, belonging to the *Glossifungites* Ichnofacies mediated and modified the physical and chemical microenvironments during early diagenesis. Eodiagenesis led to the precipitation of pervasive authigenic calcite-dominated cement in and around the burrows, forming large concretionary sedimentary structures. The

sequential order of the authigenic carbonate cement types (Figs. 4.5-4.9) combined with the negative (light) biasing carbon and oxygen stable isotopic values of the bulk calcite ($\delta^{13}\text{C}_{\text{PDB}}$ from -0.94 to -4.98‰ and $\delta^{18}\text{O}_{\text{PDB}}$ from -4.63 to -7.22‰) and bulk dolomite ($\delta^{13}\text{C}_{\text{PDB}}$ from -2.05 to -8.23‰ and $\delta^{18}\text{O}_{\text{PDB}}$ from -1.41 to -11.20‰) (Fig. 4.10) imply that the pore-water carbon was derived directly from seawater and dissolution of metastable carbonate that was highly influenced by bacterial decomposition of organic carbon and the mixing of meteoric ground water. As a result, the authigenic carbonate cement precipitated mostly under eodiagenetic conditions at the sediment/water interface (< ~3m in depth).

The distribution of the concretionary sedimentary structures is mappable and confined to parasequence-bounding flooding surfaces (generally expressed as transgressive surfaces of erosion) (Figs. 4.2, 4.13, 4.14). Parasequences were initiated by the deposition of the highly bioturbated, fine-grained sandstones in a tropical, low-energy, open-marine bay. The sandstones reflect shoaling, and were truncated upward by wave ravinements (TSE), which mark the parasequence boundaries. Ravinement surfaces are overlain and associated with weakly bioturbated, sandstone/lag/coquina deposits (structure-passive fills) developed under medium- to high-energy condition in a tropical bay margin to coastal setting.

Finally, a genetic classification of an extraordinary occurrences of more than twenty-five *Glossifungites* Ichnofacies- demarcated surfaces is established within a sequence stratigraphic framework and relative sea-level history of the compiled Middle-Upper Eocene strata in the Fayum depression (Chapter 5). Based on the origin of the discontinuity surfaces (i.e., whether they originated as the result of autocyclic processes such as deltaic distributary channels or estuarine channels or by allocyclic processes such as eustatic sea-level changes and tectonics), these surfaces are grouped into two main types those of autocyclic and those of allocyclic origins.

The autocyclically produced *Glossifungites* Ichnofacies– demarcated

discontinuities (Fig. 5.7) are spatially limited and relatively uncommon. They are characterized by restricted geographic distributions, localized lateral continuities, are generally not mappable, and show no major lithofacies or ichnofacies dislocations. These autocyclic surfaces are demarcated by impoverished firmground ichnological suites that are attributed to the *Glossifungites* Ichnofacies.

Allocyclically generated *Glossifungites* Ichnofacies- demarcated surfaces corresponding to key-stratigraphic discontinuities are common in the succession (Figs. 5.8-5.10). They are characterized by a relatively wide geographic distributions, demonstrate extensive lateral continuity, display diagnostic lithofacies and ichnofacies dislocations that can not be explained using Walther's law, and have well developed and diverse firmground ichnological suites. Occurrences of allocyclically significant suites of the *Glossifungites* Ichnofacies can be classified into the following three types: (1) sequence-bounding *Glossifungites* Ichnofacies-demarcated surfaces (e.g., amalgamated flooding surfaces and sequence boundaries or FS/SB) (Fig. 5.8); (2) systems tract-bounding *Glossifungites* Ichnofacies-demarcated surfaces (maximum flooding surface (MFS) and transgressive surface (TS)) (Fig. 5.9); and (3) parasequence-bounding surfaces (Flooding surfaces or FS) (Fig. 5.10).

Both regional (i.e., Cretaceous-Eocene Syrian Arc Orogeny) and local subsidence/uplift tectonics occurred in combination with the eustatic sea-level rise and fall, resulting in the adjustment of accommodation space during the deposition of Middle-Upper Eocene succession in the study area. Using high-resolution biostratigraphic data, the identified key stratigraphic surfaces and sequences can be correlated with global Eocene sequence stratigraphic data (e.g., Figs. 5.11, 5.12). The nature and distribution of the identified key stratigraphic surfaces indicate episodic and oscillating third-order cycles that are overprinted by higher-order cycles of relative sea-level changes (Fig. 5.12). The sequence-bounding *Glossifungites* Ichnofacies-demarcated surfaces (FS/SB1, FS/SB2) and the SB3 surface divide the Middle-Upper Eocene successions into four third-order

sequences (sequences 1 to 4) (Figs. 5.11, 5.12). Systems tract-bounding *Glossifungites* Ichnofacies-demarcated surfaces (MFS and TS) and parasequence-bounding surfaces (FS) display higher-order cycles that overprint the identified third-order cycles.

APPENDIX

Description of the stratigraphic, sedimentologic and ichnological field data, collected through detailed outcrop logging in the measured sections of the Middle-Upper Eocene succession in the areas of Wadi El-Hitan and Qasr El-Sagha, Fayum-Egypt.

1. Minqar El-Hut Composite Section (Wadi El-Hitan):

Sample No.	Description	Thickness (m)
Top:		
Top	Quaternary: subaerial talus and weathered debris covering the top of the section.	1.00
Upper Eocene: Qasr El Sagha Formation		20.0
Mh29	Shale ; gray, fissile, silty, sandy and gypsiferous, grading to siltstone and fine-grained sandstone upward, and topped by highly weathered coquina bed	2.00
Mh28	Sandstone/coquina ; yellow, medium to coarse-grained sandstone, with coquina and shell hash of <i>Ostrea</i> sp., <i>Carolia plucnoides</i> and <i>Turritella</i> sp.	2.00
Mh27	Shale ; gray, gypsiferous, silty and sandy upward, demarcated on top by ichnological suites attributable to the <i>Glossifungites</i> Ichnofacies	3.00
Mh26	Sandstone/coquina ; yellow, medium to coarse-grained sandstone, with oysters and <i>Carolia plucnoides</i> coquina, and shell hash deposits	2.00
Mh25	Shale ; brownish gray, gypsiferous, silty and sandy upward, demarcated on top by ichnological suites attributable to the <i>Glossifungites</i> Ichnofacies	3.00
Mh24	Sandstone ; yellow, silty to fine-grained size, with bivalves and fish remains, highly bioturbated (locally), with grayish-white concretions around burrows and burrow mottles, ichnological suites including <i>Thalassinoides</i> , <i>Skolithos</i> , <i>Planolites</i> and <i>Teichichnus</i>	2.00
MH23	Sandstone/coquina ; yellow, medium to coarse-grained sandstone, embracing oysters, <i>Carolia</i> sp., <i>Turritella</i> sp. and shell hash coquina.	1.00
Mh22	Shale ; gray, sandy and gypsiferous, grading to siltstone and very fine-grained sandstone upwards, fissile, with ferruginous <i>Lithophaga</i> sp., demarcated on top by ichnological suites, corresponding to the <i>Glossifungites</i> Ichnofacies.	2.00
Mh21	Sandstone/coquina ; yellow, medium- to coarse-grained sandstone, including <i>Ostrea</i> sp., <i>Carolia plucnoides</i> and <i>Turritella boghosi</i> coquina, and shell hash deposits.	1.00
Mh20	Shale ; grayish, silty to sandy, ferruginous, gypsiferous, with barite mineralization, grading to siltstone and very fine-grained sandstone upward, fissile, demarcated on top by ichnological suite of <i>Thalassinoides</i> , corresponding to the <i>Glossifungites</i> Ichnofacies.	2.00
Upper Eocene: Birket Qarun Formation		56.5
Mh19	Sandstone/coquina ; yellow, medium- to very coarse-grained sandstones, with oysters and Nummulitic coquina layers.	1.00

Mh18	Sandstone ; yellow, fine to medium grained, highly bioturbated (BI 5), ichnological suites including <i>Arenicolites</i> , <i>Planolites</i> and <i>Rhizocorallium</i> , demarcated upwards by large-sized passively-filled (with <i>Nummulites</i> sp. and molluscan shell hash) <i>Thalassinoides</i> suite, attributed to the <i>Glossifungites</i> Ichnofacies.	3.00
Mh17	Sandstone/coquina ; yellow, medium- to very coarse-grained sandstones, fossiliferous, with basal oyster/large foraminifera coquina layer, and an uppermost <i>Carolia</i> sp.-dominated coquina layer.	1.50
Mh16	Sandstone ; grayish yellow, medium-grained size, fossil content including task shells, scallops and sea pens, intensively bioturbated (BI 5) with ichnological suites of <i>Thalassinoides</i> , <i>Skolithos</i> , <i>Planolites</i> and burrow mottles, demarcated upwards by passively-filled ichnological suites, attributable to the <i>Glossifungites</i> Ichnofacies and a characteristic giant conical sedimentary structures (up to 150 cm long and > 20 cm in diameter).	3.00
Mh15	Sandstone/coquina ; yellow and white composite bed, lower medium-grained sandstones (25 cm thick) rich in bivalve/gastropod shells, grading upward to a 25 cm thick large foraminifera/ <i>Turritella</i> sp./ <i>Carolia</i> sp.-dominated coquina layer, followed by another 50 cm thick large foraminifera-dominated coquina layer, and topped by 25-50 cm thick oyster-dominated coquina layer.	1.50
Mh14	Sandstone ; yellow, medium grain size, cliff forming, fossiliferous (rich in <i>Turritella</i> sp., oysters, thin-shelled pectinids and irregular echinoids), highly bioturbated (BI 5) with burrow mottles, demarcated upward by passively-filled <i>Thalassinoides</i> , <i>Arenicolites</i> and <i>Skolithos</i> ichnological suites, attributed to the <i>Glossifungites</i> Ichnofacies, and a diagnostic large conical sedimentary structures (up to 1 m long and 20 cm in diameter).	7.00
Mh13	Shale ; grayish black shale, gypsiferous, silty and sandy, fissile, basal surface comprising rhizoliths, demarcated upward with ichnofossil suites including <i>Thalassinoides</i> , <i>Ptilonichnus</i> , iron-cemented <i>Skolithos</i> and <i>Arenicolites</i> , corresponding to the <i>Glossifungites</i> Ichnofacies.	0.50
Mh12	Sandstone ; yellowish to grayish white, saliferous, medium grain size, highly bioturbated (BI 5), showing alluviation and rhizobioturbation upwards.	3.00
Mh11	Sandstone ; yellow, medium-grained size, cliff forming, highly bioturbated (BI 5), comprising the following three horizons from top to base. C: Upper horizon rich in oysters, ichnological suites including abundant large-sized <i>Thalassinoides</i> , and small-sized <i>Skolithos</i> , <i>Teichichnus</i> , <i>Planolites</i> , <i>Cylindrichnus</i> , <i>Asterosoma</i> and burrow mottles. (7 m thick). B: Middle horizon including thin-shelled bivalves, gastropods and large foraminifera, ichnological suite of large-sized <i>Thalassinoides</i> (up to 60 cm long), <i>Ophiomorpha</i> (up to 12 cm long) and <i>Skolithos</i> . (4 m thick). A: Lower horizon comprising trace-fossil suites of burrow mottles, large-sized <i>Thalassinoides</i> , <i>Skolithos</i> and <i>Planolites</i> . (3 m thick).	14.0
Mh10	Sandstone ; grayish white, medium-grained size, cliff forming, friable, intensive bioturbation (BI 5), ichnofossils including <i>Thalassinoides</i> , <i>Skolithos</i> , rare <i>Teichichnus</i> and <i>Asterosoma</i> ?, and abundant small thread-worm burrows.	10.0
Mh9	Sandstone ; fine to medium grained, yellow, saliferous, highly bioturbated (BI 5), ichnofossil suites comprising burrow mottle, <i>Thalassinoides</i> , <i>Planolites</i> and abundant small-sized <i>Skolithos</i>	2.00

Mh8	Sandstone; yellow, silty, fine- to medium-grained size, cliff forming, fossils reported including articulated bivalves of <i>Lucina</i> sp. and gastropods in their life position at the basal part, high bioturbation (BI 5) expressed by trace-fossils suites of abundant <i>Thalassinoides</i> , <i>Skolithos</i> (abundant upward) and <i>Planolites</i> , and rare <i>Teichichnus</i> , <i>Palaeophycus</i> and <i>Asterosoma</i>	10.0
-----	---	------

***The Middle Eocene: Gehannam Formation* 30.0**

Mh7	Sandstone; slope forming, mostly covered, underlying cliff-forming sandstones of Birket Qarun Formation.	8.00
Mh6	Siltstone; brownish yellow, sandy, grading to very fine-grained sandstone upward, thick gypsum streaks, wave ripple and low angle cross-lamination marking the contact with the underlying shale bed, the lower part including rare <i>Teichichnus</i> , the upper part comprising abundant ichnological suites of <i>Thalassinoides</i> , <i>Psilonichnus</i> , <i>Planolites</i> and <i>Teichichnus</i>	2.00
Mh5	Shale; grayish green, gypsiferous, sandy and silty, fissile, locally ferruginous, with Mn micro veins and possible carbonaceous dark spots, with rare <i>Teichichnus</i> and <i>Planolites</i> ichnogenera.	8.00
Mh4	Sandstone; grayish yellow, fine-grained size, fossil content including shell debris, task sells, echinoid spines and shells, and upward large shark teeth and badly preserved whale skeletons of <i>Basilosaurus isis</i> , highly bioturbated (BI 5), with ichnological suites of abundant <i>Thalassinoides</i> , <i>Teichichnus</i> , <i>Ophiomorpha</i> and <i>Planolites</i> , and rare <i>Skolithos</i> and <i>Scolicia</i>	2.00
Mh3	Sandstone; yellowish white, fine grained, rich in irregular echinoids, task shells and fossil whale-bones, intensive bioturbation (BI 5), ichnological suites comprising <i>Scolicia</i> , <i>Planolites</i> , <i>Thalassinoides</i> , <i>Ophiomorpha</i> and rare <i>Skolithos</i>	3.00
Mh2	Sandstone; pale yellow, silty- to fine-grained size, rich in echinoids and larger foraminifera (e.g., <i>Nummulites</i> sp.), thoroughly bioturbated (BI5), ichnogenera reported comprising <i>Thalassinoides</i> , <i>Planolites</i> , <i>Ophiomorpha</i> , <i>Teichichnus</i> and rare <i>Skolithos</i>	1.00
Mh1	Sandstone; grayish white (yellow-weathering color), fine to medium grain size, rare cross-lamination upwards, highly bioturbated (BI 5), ichnological suites including <i>Planolites</i> (ferruginous at the base), <i>Thalassinoides</i> , <i>Ophiomorpha</i> , <i>Teichichnus</i> and rare <i>Skolithos</i>	6.00

Base: Not exposed

Total thickness = 107.5 m

2. Sandouk El-Borneta Section (Wadi El-Hitan):

Sample No.	Description	Thickness (m)
Top:		
Top	Quaternary: subaerial veneer deposits of pebbles and cobbles.	2.00
Upper Eocene: Qasr El Sagha Formation		6.50
B25	Sandstone/coquina ; yellow, medium- to coarse-grained sandstone, intercalating thin and discrete coquina layers of gastropods and oysters.	1.00
B22	Shale ; grayish green, gypsiferous, silty and sandy upward, demarcated on top by ichnological suites of passively-filled <i>Thalassinoides</i> and <i>Teichichnus</i> , attributable to the <i>Glossifungites</i> Ichnofacies.	3.00
B21	Sandstone/coquina ; yellowish brown, coarse-grained sandstone, intercalating a coquina layer of gastropods and bivalves (oysters and <i>Carolia</i> sp.).	0.50
B20	Shale ; grayish green, gypsiferous, silty and sandy upward, demarcated upwards by firmground ichnofossil suites of the passively-filled <i>Thalassinoides</i> , attributed to the <i>Glossifungites</i> Ichnofacies.	2.00
Upper Eocene: Birket Qarun Formation		51.0
B19	Sandstone and coquina ; grayish yellow, medium to coarse-grained sandstone, embracing a thin (20-30 cm thick) oysters/bivalves/gastropods/large-foraminifera coquina layer.	2.00
B18	Sandstone ; yellow, fine grained, highly bioturbated (BI 5), demarcated upwards by giant box-work (passively filled with shell hash) <i>Thalassinoides</i> , corresponding to the <i>Glossifungites</i> Ichnofacies.	4.00
B17	Sandstone and coquina ; the lower one meter including coquina layer, full of bivalves (large oysters, <i>Carolia plucnoides</i>), gastropods (<i>Turritella</i> sp.) and large foraminifera (<i>Nummulites</i> sp.) in a sandstone matrix, the upper meter comprising fossiliferous sandstone, moderately bioturbated, with thin discrete coquina band (mainly <i>Carolia plucnoides</i>).	2.0
B16	Sandstone ; grayish yellow, fine-grained size, highly bioturbated (BI 5), demarcated upwards by passively-filled ichnological suites of <i>Thalassinoides</i> , <i>Psilonichnus</i> , <i>Skolithos</i> and <i>Planolites</i> , attributed to the <i>Glossifungites</i> Ichnofacies.	4.00
B15	Sandstone and coquina ; the lower one meter comprising yellow, coarse-grained sandstone, fossiliferous (rich in gastropods, <i>Carolia</i> sp. and oysters), the upper meter including grayish white to yellow coquina layers of oyster and large foraminifera.	2.00
B14	Sandstone ; yellow, fine grained, basal part defining oval to circular (20-50 cm in diameter) concretionary sandstones with Mn staining, highly bioturbated (BI 5), with a characteristic burrow mottle ichnofabric, demarcated upwards by large vertical burrows (passively filled with oysters, bivalves, gastropods, large foraminifera and shell hash), attributable to the <i>Glossifungites</i> Ichnofacies.	13.0
B13	Shale ; grayish black, sandy and silty, fissile, with dark rhizoliths (root and rootlet casts), well-developed ichnological suites (mainly <i>Thalassinoides</i>) demarcating the upper sandy part, these suites having yellow and ferruginous color, passively filled and defining a <i>Glossifungites</i> Ichnofacies.	1.00

B12	Sandstone ; grayish white, fine to medium grain size, slope forming, highly bioturbated downwards, upper horizon suffering an alluviation (reddish to varicolored) and rhizobioturbation.	3.00
B11	Sandstone ; grayish yellow, fine to medium grain size, highly bioturbated (BI5), with ichnological suites of abundant <i>Teichichnus</i> , <i>Skolithos</i> , <i>Planolites</i> and <i>Thalassinoides</i> . . .	10.0
B10	Sandstone ; yellow, silty to fine-grained size, thick, cliff forming, with thin-shelled bivalves, highly bioturbated (BI 5), ichnological suites including burrow mottles, abundant large-sized <i>Thalassinoides</i> , <i>Skolithos</i> , <i>Planolites</i> , <i>Teichichnus</i> and laminated-infill <i>Psilonichnus</i>	10.0

Middle Eocene: Gehannam Formation **34.0**

B9	Sandstone ; grayish white, fine-grained size, fossil content including dispersed shell fragments of bivalves, barnacles, fish spines and teeth, task shells, crab shells, highly bioturbated (BI 5), ichnological suite including <i>Ophiomorpha</i> , <i>Thalassinoides</i> , <i>Skolithos</i> , rare <i>Planolites</i> and <i>Psilonichnus</i> , demarcated upwards by large-sized root casts (rhizoliths), defining a complex paleoecologic horizon including invertebrate trace-fossil suites of <i>Thalassinoides</i> , <i>Psilonichnus</i> and <i>Ophiomorpha</i> , invertebrate fossils and marine vertebrate fossils (whale skeletons, fish spines and teeth), upper surface heralding large-sized passively-filled <i>Thalassinoides</i> , attributed to the <i>Glossifungites</i> Ichnofacies.	2.0
B8	Sandstone ; grayish white, silty to fine-grained size, intensive bioturbation (BI 5), with ichnological suites of <i>Skolithos</i> (large-sized upward), <i>Teichichnus</i> , <i>Thalassinoides</i> and <i>Ophiomorpha</i>	5.0
B7	Sandstone ; grayish white, silty to fine grained, highly bioturbated (BI 5), ichnological suites as described in B8.	5.0
B6	Sandstone ; grayish white, silty, with thin-shelled fossils, task shells, intensively bioturbated (BI 5), trace-fossil suites comprising abundant small-sized <i>Thalassinoides</i> , <i>Planolites</i> , <i>Skolithos</i> and <i>Psilonichnus</i> , with large-sized <i>Thalassinoides</i> upwards, displaying couplets tidal filling.	2.0
B5	Sandstone ; grayish white, fine-grained size, highly bioturbated (BI 5), with ichnological suites of <i>Thalassinoides</i> and <i>Planolites</i> , and <i>Skolithos</i> (abundant upward).	3.0
B4	Sandstone ; grayish yellow, fine- to very fine-grained, thorough bioturbation (BI 5), ichnofossil suites including <i>Thalassinoides</i> , <i>Planolites</i> , <i>Ophiomorpha</i> , <i>Teichichnus</i> , <i>Skolithos</i> , <i>Psilonichnus</i> , <i>Cylindrichnus</i> , <i>Arenicolites</i> , <i>Skolithos</i> and <i>Thalassinoides</i>	5.0
B3	Sandstone ; yellow, silty to very fine-grained size, high bioturbation intensity (BI 5), ichnofossil suites comprising <i>Thalassinoides</i> , <i>Teichichnus</i> , <i>Planolites</i> , <i>Ophiomorpha</i> , <i>Rhizocorallium</i> , <i>Asterosoma</i> , <i>Cylindrichnus</i> and small-sized <i>Skolithos</i>	3.0
B2	Siltstone ; yellowish to reddish purple weathering color, sandy and ferruginous.	1.0
B1	Shale ; grayish green, gypsiferous, sandy, coarsening upward into siltstone, fissile, with black spots of possible rhizoliths and plant imprints.	8.0

Base: Not exposed.

Total thickness = 91.5 m

3. Qasr El-Sagha Temple Section (Qasr El Sagha):

Sample No.	Description	Thickness (m)
Top:		
<i>Upper Eocene: Qasr El Sagha Formation (Dir Abu Lifa Member)</i>		45.0
Top:	The remaining 10 m of Upper Dir Abu Lifa forming small dome-shaped hills on the top of the sandstone cliff behind Qasr El-Sagha Temple (hard to be accessed).	10.0
Qs 35	Sandstone and coquina; yellow, medium to coarse-grained sandstone, richly fossiliferous, grading upward to white sandy coquina layer, dominated by <i>Ostrea</i> sp. and <i>Carolia</i> sp. . .	3.00
Qs 34	Sandstone/mudstone; three to four N and NNW laterally prograding fining-upward channels, each channel composed mainly of basal white (yellow and gray black weathering color) fine- to medium-grained sandstone, fining upward to dark gray siltstone and mudstone, dominated by inclined stratification (IS) and inclined heterolithic stratification (IHS), lower channels including small tabular planar cross-bedding, trough cross-bedding, large sigmoidal cross-bedding and mudstone drapes, with local small-scale wavy/flaser bedding and large convoluting bedding structures, very weak bioturbation intensity characterizing these channel deposits (expressed by rare occurrences of <i>Planolites</i> and <i>Protovirgularia</i>), the channel boundaries defining an association of sulphur/coal fragments, rhizoliths, terrestrial vertebrate bone fragments, and poorly impoverished ichnological suites (dominated by <i>Thalassinoides</i> , <i>Skolithos</i> , <i>Planolites</i> and <i>Palaeophycus</i>) attributed to autocyclic <i>Glossifungites</i> Ichnofacies.	32.0
<i>Upper Eocene: Qasr El Sagha Formation (Temple member)</i>		54.0
Qs 33	Shale; gray, gypsiferous, covered by thin layer (20 cm thick) of gypsum.	1.00
Qs32	Sandstone; yellow, argillaceous, with bivalves and fish (rays) teeth, moderate bioturbation intensity (BI 3), dominated by ferruginous large-sized <i>Thalassinoides</i> burrows.	2.00
Qs 31	Shale; gray, sandy and silty, gypsiferous, demarcated by large-sized passively-filled <i>Thalassinoides</i> , attributable to the <i>Glossifungites</i> Ichnofacies.	0.50
Qs 30	Sandstone; grayish yellow, argillaceous, with small-sized (dwarfed) bivalves and gastropods, and local monospecific ichnological suites of <i>Thalassinoides</i>	1.00
Qs 29	Shale; gray, silty and gypsiferous, fissile, with local ichnological suites of <i>Thalassinoides</i> and <i>Psilonichnus</i>	2.00
Qs 28	Sandstone; grayish yellow, calcareous and fossiliferous, with small dwarfed gastropods and vertebrate-bone fragments, with abundant monospecific suites of <i>Thalassinoides</i> . . .	2.00
Qs 27	Shale; gray, gypsiferous and silty.	1.00
Qs 26	Sandstone and coquina; yellow, coarse-grained sandstone, fossiliferous, intercalating a coquina layer of oysters, bivalves and gastropods.	0.50
B 25	Shale; gray, gypsiferous, sandy upwards, demarcated on top by ichnological suites of the passively-filled <i>Thalassinoides</i> , attributed to the <i>Glossifungites</i> Ichnofacies.	2.50
Qs 24	Sandstone and coquina; pale yellow, coarse-grained sandstone, fossiliferous, with discrete thin coquina layers of small-sized oysters, bivalves and gastropods.	0.50

Qs 23	Shale ; brownish gray, sandy and gypsiferous, fissile, demarcated upward by ichnofossil suites of the passively-filled <i>Thalassinoides</i> , attributed to the <i>Glossifungites</i> Ichnofacies.	2.00
Qs 22	Sandstone ; lower yellowish white sandstone (1 m thick), with abundant irregular rhizoliths ichnofabric, topped by the upper (1 m thick) yellow medium-grained sandstone, with moderate (local high) bioturbation intensities (BI 3-4), ichnological suites including <i>Thalassinoides</i> , <i>Teichichnus</i> and <i>Skolithos</i>	2.00
Qs 21	Sandstone ; yellow, argillaceous and silty to fine grained, sedimentary structures including tidal rhythmites, wavy/flaser bedding and wave-ripple laminations, truncated upward by undulating erosive surface, associating rip up clasts, lag deposits, coal/sulphur fragments and rhizoliths	2.00
Qs 20	Shale ; grayish black, sandy to silty, and gypsiferous.	1.00
Qs 19	Sandstone ; yellow, fine grained, calcareous, fossiliferous, with articulated clams, highly bioturbated (BI 4), with ichnological suites of burrow mottles, <i>Skolithos</i> , <i>Planolites</i> and <i>Teichichnus</i>	2.00
Qs 18	Shale ; grayish yellow, sandy and silty, with massive appearance.	1.00
Qs 17	Sandstone ; yellow, silty to fine grained, relatively hard and compact.	1.00
Qs 16	Shale ; gray, sandy, gypsiferous, and fissile.	1.00
Qs15	Sandstone and coquina ; grayish to pinkish yellow, coarse-grained sandstone, fossiliferous, grading upward to a veneer coquina layer of large oysters, large <i>Carolia</i> sp., <i>Turritella</i> sp., and echinoid shells and spines.	1.00
Qs 14	Shale ; gray, gypsiferous, silty and sandy upwards, upper sandier part comprising wavy and cross-lamination structure, bioturbation intensities and ichnological diversities increasing upward, lower muddier portion defining local ichnological suites of <i>Skolithos</i> and <i>Planolites</i> , upper sandy portion including highly diversified ichnological suites of <i>Monocraterion</i> , <i>Diplocraterion</i> , <i>Planolites</i> , <i>Skolithos</i> and rhizoliths, followed upward by well-developed ichnological suites dominated by the passively-filled <i>Thalassinoides</i> , corresponding to <i>Glossifungites</i> Ichnofacies, in association with shell hash and lag deposits.	5.00
Qs 13	Sandstone ; grayish yellow, fine to medium grained, coquinal, full of oysters, <i>Carolia</i> sp. and <i>Turritella</i> sp., with a characteristic alluviation horizon at the base.	0.50
Qs12	Shale ; greenish gray, gypsiferous, sandy and silty upward, fissile, with black spots of possible plant imprints.	2.00
Qs 11	Sandstone ; yellow, silty to very fine grained, highly bioturbated (BI 4), ichnological suites including <i>Thalassinoides</i> , <i>Diplocraterion</i> , <i>Skolithos</i> , <i>Planolites</i> , and <i>Teichichnus</i>	2.00
Qs 10	Sandstone and coquina ; grayish green, fine- to very fine-grained sandstone, with wavy- and parallel-lamination structure, fossiliferous, grading upward to a coquina layer of abundant oysters, <i>Carolia</i> sp., <i>Turritella</i> sp., and irregular echinoid shells and spines . . .	1.50
Qs 9	Shale ; brownish to purple yellow, gypsiferous, silty and sandy upward, fissile, demarcated upward by ichnological suites of ferruginous passively-filled <i>Thalassinoides</i> , corresponding to the <i>Glossifungites</i> Ichnofacies.	3.00

Qs 8	Sandstone and coquina ; composite bed comprising from top to base: C- reddish alluviated sandstone horizon (50 cm thick), topped by coquina layer of bivalves (mainly <i>Carolia</i> sp. and <i>Ostrea</i> sp.); B- middle green sandstone horizon (50 cm thick), with white calcrete and small-scaled convolute bedding, locally bioturbated with bivalves traces and irregular ichnofabric of rhizoliths; and, A- lower grayish yellow, silty and laminated fossiliferous sandstone horizon (50 cm thick).	1.50
Qs 7	Shale ; gray, gypsiferous, fissile, silty and sandy upward, with thin-shelled bivalves, demarcated upward by firmground ichnological suites, dominated by the passively-filled <i>Thalassinoides</i> , attributable to the <i>Glossifungites</i> Ichnofacies	3.00
Qs 6	Sandstone and coquina ; grayish white, fine- to coarse-grained sandstone, intercalating a discrete coquina layer of full-articulated and in-articulated bivalves and shell debris, dominated by oysters and <i>Carolia</i> sp.	1.00
Qs 5	Shale ; grayish black (with brownish weathering color in its lower part), grayish white and sandy upward, gypsiferous, the upper part is intensively burrowed by ichnological suites (mainly passively-filled <i>Thalassinoides</i>) of the <i>Glossifungites</i> Ichnofacies.	2.50
Qs 4	Sandstone and coquina ; pinkish yellow, medium- to coarse-grained sandstone, fossiliferous, intercalating coquina bands of lag deposits and shall hash of thin-shelled bivalves.	0.50
Qs 3	Shale ; greenish gray, gypsiferous, very weak bioturbation, with rhizoliths and dispersed dark plant imprints, demarcated upwards by monospecific ichnological suites of <i>Thalassinoides</i> , attributed to the <i>Glossifungites</i> Ichnofacies.	1.50
Qs 2	Sandstone and coquina ; grayish yellow, medium- to coarse-grained sandstone, ferruginous, calcareous, with local ichnological suites of <i>Teichichnus</i> , <i>Planolites</i> and <i>Arenicolites</i>	1.00
Qs1	Shale ; gray, gypsiferous, fissile, sandy and silty upward, the bioturbation intensities increasing upward (BI 0-3), ichnological suites including <i>Planolites</i> and <i>Arenicolites</i> , demarcated upwards by poorly-developed ichnological suites of the passively-filled <i>Thalassinoides</i> , attributable to the <i>Glossifungites</i> ichnofacies.	3.00

Base: Not exposed

Total thickness = 99.00 m

4. Wadi Efreet-Dir Abu Lifa Section (Qasr El-Sagha):

Sample No.	Description	Thickness (m)
Top:		
Upper Eocene: Qasr El Sagha Formation (Dir Abu Lifa Member)		32.0
Top:	Sandstone and coquina; yellow, fine- to coarse-grained sandstone, white and shelly upwards, topped by a distinctive coquina bed of oysters (e.g., <i>Ostrea</i> sp., <i>Carolia</i> sp.) and gastropods (e.g., <i>Turritella</i>).	3.00
EA34	Sandstone; white (grayish black weathering color), fine to medium grain size, friable, fining upward to siltstone and mudstone, rare body fossils, very weak bioturbation, NNW-dipping inclined heterolithic stratification (IHS), with local tidal rhythmites and mudstone drapes, large-scale convolute bedding and slumping structures defining the middle and upper part, the upper muddier portion topped by undulating erosive surface, associating lag deposits, shell hash, and well-developed ichnological suites (e.g., passively-filled <i>Thalassinoides</i>), attributed to the <i>Glossifungites</i> Ichnofacies.	8.00
EA33	Sandstone; yellow to brownish gray (with blue and black staining upward), silty and argillaceous, gypsiferous, locally fossiliferous with small thin-shelled bivalves and pectinids, muddier portion including dark carbonaceous materials and leaf imprints.	2.00
EA32	Sandstone; white, fine to medium grained, friable, NNW-dipping inclined heterolithic stratification (IHS), as well as small tabular-planar cross-bedding, mudstone drapes, cross-laminations and wavy/flaser bedding, with local ichnological suites of <i>Skolithos</i> and <i>Planolites</i> occurring downwards.	8.00
EA31	Mudstone; gray to purplish gray, silty and sandy, gypsiferous, with dark carbonaceous spots and leaf imprints.	2.00
EA30	Sandstone; yellow, fine grained, locally bioturbated with burrow mottles.	1.00
EA29	Sandstone; white, friable, fine to medium grained, fining (silty and argillaceous) upwards, NNW-dipping inclined heterolithic stratification (IHS), with mudstone drapes, rhythmites structures, trough- and tabular-planar cross-bedding structures defining the lower part, weak to very weak bioturbation, with local monospecific ichnological suites of <i>Skolithos</i> , upper muddier portion including ferruginous concretions, rhizoliths ichnofabric and abundant passively-filled <i>Thalassinoides</i> ichnological suites, attributable to the autocyclic <i>Glossifungites</i> Ichnofacies.	8.00
Upper Eocene: Qasr El Sagha Formation (Temple Member)		55.5
EA28	Sandstone; brownish yellow, medium grained, ferruginous, fossiliferous, grading upward to a highly weathered coquina bed including abraded shell fragments.	0.50
EA27	Shale; brownish gray, gypsiferous, sandy upwards, intensively demarcated upward by abundant ichnological suites of passively-filled <i>Thalassinoides</i> , corresponding to the <i>Glossifungites</i> Ichnofacies	2.50
EA26	Sandstone; yellow, fine to medium grained, ferruginous, topped by thin discrete coquina band of bivalves and gastropods.	0.50

EA25	Shale ; gray, gypsiferous, silty and sandy upwards, demarcated upward with trace-fossil suites of <i>Thalassinoides</i> , corresponding to the <i>Glossifungites</i> Ichnofacies.	2.00
EA24	Sandstone ; yellow, silty to fine grained, fossiliferous, dominated by <i>Turritella</i> sp.	0.50
EA23	Shale ; gray, gypsiferous, silty and sandy, and fissile.	0.50
EA 22	Sandstone ; white fine- to medium-grained sandstone, with tidal rhythmmites, wave ripples and flaser bedding, locally bioturbated with ichnological suites of abundant <i>Teichichnus</i> , <i>Skolithos</i> and <i>Planolites</i> , truncated by undulated erosive surface, associating rip-up clasts, with coal/sulphur fragments and ferruginous reddish concretions, followed by yellowish white, silty to fine-grained sandstone, with irregular rhizoliths ichnofabric and upward ichnological suites of <i>Thalassinoides</i> , and topped by 25 cm thick bivalves/gastropods coquina layer.	2.00
EA21	Shale ; gray, silty and sandy, gypsiferous and fissile.	1.00
EA20	Shale ; brownish gray, silty, highly gypsiferous, topped by 30 cm thick oyster-dominated coquina bed.	1.50
EA19	Sandstone ; yellow, silty to fine grained, argillaceous, highly bioturbated, with abundant ichnological suites of <i>Psilonichnus</i> , <i>Thalassinoides</i> , <i>Skolithos</i> , <i>Planolites</i> and <i>Teichichnus</i>	1.00
EA18	Sandstone and coquina ; yellow, fine- to coarse-grained sandstone, highly bioturbated, with ichnological suite of the large-sized <i>Thalassinoides</i> , topped by a thin coquina layer.	0.50
EA17	Sandstone ; yellowish to grayish white, fine grained, with root-mottled ichnofabric.	1.00
EA16	Sandstone ; white, clean, friable, fine to medium grained, with tidal rhythmmites and wavy/flaser bedding, truncated by erosive undulated surface, associating black coal/bright yellow sulphur fragments and rip-up clasts, weakly bioturbated, with local ichnological suites of <i>Skolithos</i> and <i>Planolites</i>	1.00
EA15	Shale ; brownish gray, silty and sandy, gypsiferous and fissile.	2.00
EA14	Sandstone ; yellow, fine grained, characterized by sharp basal contact and ferruginous concretions, highly burrowed upward (BI 4-5), ichnological suites comprising <i>Thalassinoides</i> , <i>Ophiomorpha</i> , <i>Planolites</i> , <i>Teichichnus</i> and ? <i>Psilonichnus</i>	1.50
EA13	Shale ; gray, silty and gypsiferous, sandy and bioturbated upward, ichnological suites of the passively-filled <i>Thalassinoides</i> demarcating the upper sandier part.	3.00
EA12	Sandstone and coquina ; yellow, fine- to coarse-grained sandstone, saliferous, fossiliferous with task shells, lower fine-grained part locally bioturbated with ichnological suites of <i>Skolithos</i> , <i>Thalassinoides</i> , <i>Planolites</i> , <i>Teichichnus</i> and <i>Psilonichnus</i> , fossiliferous upward and grading to a coquina layer, dominated by the gastropod <i>Turritella</i> sp. and <i>Carolia</i> sp., as well as oysters.	1.00
EA11	Shale ; gray (brownish upward), silty and gypsiferous, sandy and cliff forming upward, weakly bioturbated (BI 0-2), demarcated upward by the firmground ichnological suites (dominated by <i>Thalassinoides</i>), corresponding to the <i>Glossifungites</i> Ichnofacies.	5.00
EA10	Sandstone ; yellow, silty to fine grained, fossiliferous (mainly bivalves), bioturbation intensities increasing upward (BI 3-5), with abundant ichnofossil suites of <i>Thalassinoides</i> , <i>Teichichnus</i> , <i>Skolithos</i> , <i>Planolites</i> and ? <i>Psilonichnus</i> , upper horizon displaying varicolored alluviation and rhizoliths ichnofabric.	4.00
EA 9	Shale ; brownish gray, silty and gypsiferous.	1.00

EA8	Sandstone and coquina ; yellow, medium- to coarse-grained sandstone, intercalating lag deposits and a coquina layer of bivalves (mainly <i>Ostrea</i> sp. and <i>Carolia</i> sp.).	1.00
EA7	Shale ; brownish gray, silty, gypsiferous and sandy upward, ichnological suites (dominated by the passively-filled <i>Thalassinoides</i>) demarcating the upper sandier part and attributed to the <i>Glossifungites</i> Ichnofacies.	3.50
EA6	Sandstone and coquina ; yellow, medium- to coarse-grained sandstone, fossiliferous, grading upward to a coquina layer (20 cm thick) of oysters and gastropods.	1.00
EA5	Shale ; brownish gray, gypsiferous, silty and sandy upward, demarcated upward by ichnological suites (mainly passively-filled <i>Thalassinoides</i>), attributed to the <i>Glossifungites</i> Ichnofacies.	3.00
EA4	Sandstone ; yellow, medium to coarse grained, fossiliferous, intercalating discrete and thin coquina layers of bivalves.	2.00
EA3	Shale ; grayish yellow, sandy, gypsiferous and fissile	5.00
EA2	Sandstone and coquina ; yellow, fine- to coarse-grained sandstone, fossiliferous, with thin and discrete coquina layers.	1.00
EA1	Shale ; gray, sandy, forming the base of the outcrop exposure, with possible rhizoliths ichnofabric	7.00

Base: Not exposed

Total thickness = 87.50

5. Upper Part of Dir Abu Lifa Member (Qasr El-Sagha Fm) in the Four Measured Sections Between Dir Abu Lifa and West Wadi Efreet (Qasr El-Sagha):

Sample No.	Description	Thickness (meters)
Top:		
1- North-East Dir Abu Lifa:		32.0
A10	Sandstone; lower yellow fine- to medium-grained sandstone (1 m thick), intensively burrowed at base with ichnological suites of large <i>Ophiomorpha</i> and <i>Skolithos</i> , middle white coarse sandstone (1m thick), shelly and fossiliferous, intercalating discrete coquina layers, upper yellowish white highly weathered sandstone (1 m thick) forming the top-plateau surface and underlying the Oligocene Gebel Qatrani Formation.	3.00
A9	Sandstone/mudstone; yellowish white, fine- to medium-grained and mudstone, friable, displaying NNW-dipping inclined heterolithic stratification (IHS), with tabular planar and trough cross-beddings, and local abundance of ichnological suites of <i>Skolithos</i> and rare <i>Planolites</i> , finning upward muddier horizon demarcated by firmground suites (mainly <i>Thalassinoides</i> and rare <i>Skolithos</i>), attributable to the <i>Glossifungites</i> Ichnofacies	10.0
A8	Sandstone; greenish yellow, fine grained and slope forming.	2.00
A7	Sandstone; yellow, fine grained, capping the greenish sandstone cliff, fossiliferous, associating shell hash / lag deposits at its basal part.	1.00
A6	Sandstone; greenish yellow, fine grained, silty and argillaceous, fossiliferous, demarcated upward by firmground suites (mainly <i>Thalassinoides</i>) attributable to the <i>Glossifungites</i> Ichnofacies.	1.00
A5	Sandstone; green, fine grained, fossils including fish teeth, bivalves and gastropods, highly bioturbated (BI 4-5), with characteristic reddish and ferruginous monospecific suites of large-sized <i>Thalassinoides</i>	2.00
A4	Sandstone; yellow and green, fine grained, with iron concretionary bands, fossils including fish remains and gastropods, moderately bioturbated (BI 3), with monospecific ichnofossil suites of the reddish large-sized <i>Thalassinoides</i>	2.50
A3	Sandstone; yellow, fine grained, with a characteristic thick gypsum veins.	3.00
A2	Sandstone and coquina; yellow, fine- to coarse-grained sandstone, fossiliferous, grading upward to a coquina layer of bivalves (mainly oysters) and gastropods.	0.50
A1	Sandstone/siltstone; yellow to yellowish green, sandy siltstone to very fine-grained sandstone, gypsiferous, demarcated upward by ichnological suites of <i>Thalassinoides</i> , corresponding to the <i>Glossifungites</i> Ichnofacies	7.00
2- Head and Eastern Cliff of Wadi Efreet:		21.5
WE11	Sandstone; yellow, medium to coarse grained, calcareous, fossiliferous with shell fragments and shark teeth, with local ichnological suites of small-sized <i>Skolithos</i> and <i>Planolites</i> , the topmost surface comprising mammalian-vertebrate bones of dungeons (sea cow).	2.00

WE10	Sandstone/mudstone ; greenish white, fine- to medium-grained sandstone and mudstone, displaying inclined heterolithic stratification (IHS), fining upward to siltstone and mudstone, with pedogenic alteration and rhizoliths ichnofabric, demarcated upward by firmground ichnological suites of <i>Thalassinoides</i> , <i>Skolithos</i> and <i>Psilonichnus</i> , attributable to the <i>Glossifungites</i> Ichnofacies.	4.00
WE9	Shale ; grayish green, sandy, saliferous and gypsiferous, slope forming, with ferruginous and monospecific ichnological suites of the large-sized <i>Thalassinoides</i>	2.00
WE8	Sandstone and coquina ; golden yellow, fine- to medium-grained sandstone, locally high bioturbation (BI 4), ichnological suites comprising <i>Thalassinoides</i> , <i>Skolithos</i> and <i>Planolites</i> , fossiliferous, rich in bivalves, grading upward to a coquina layer,	1.50
WE7	Sandstone ; greenish yellow, silty and gypsiferous, horizontally stratified, highly bioturbated (BI 4-5) with ichnological suites of <i>Thalassinoides</i> , <i>Skolithos</i> , <i>Planolites</i> and <i>Psilonichnus</i> , demarcated upward by firmground ichnological suites, attributable to the <i>Glossifungites</i> Ichnofacies.	1.00
WE6	Sandstone ; yellow, fine grained, highly bioturbated (BI 4-5), with monospecific ichnological suites of <i>Thalassinoides</i>	0.50
WE5	Sandstone ; green, fine grained, fossils content comprising bivalves (articulated long clams), gastropods (<i>Turritella</i> sp.), shark teeth, fish teeth, crab shell fragments, and sporadic wood fragments, highly bioturbated (BI 4-5), ichnological suites including abundant monospecific ichnofossil suite of the ferruginous large-sized <i>Thalassinoides</i> , with rare <i>Psilonichnus</i>	3.00
WE4	Siltstone ; greenish gray, sandy, gypsiferous, weak to moderate bioturbation (BI 1-3), ichnological suites including rare <i>Teichichnus</i> and upward abundant <i>Thalassinoides</i>	1.00
WE3	Sandstone ; greenish yellow, fine to very fine grained, with diagnostic thick gypsum veins and streaks.	3.00
WE3	Sandstone ; greenish yellow, fine to medium grained, calcareous, fossiliferous, rich in shell hash and lag deposits, and grading upward to discrete and thin coquina layer.	0.50
WE1	Shale ; greenish gray, sandy and silty upward, gypsiferous, fissile, demarcated upwards by firmground ichnological suites (mainly <i>Thalassinoides</i> and <i>Skolithos</i>), attributable to the <i>Glossifungites</i> Ichnofacies.	3.00

3- North-West Wadi Efreet:

34.0

WW11	Sandstone and coquina ; yellow, medium- to coarse-grained sandstone, calcareous, fossiliferous, and grading upward to coquina (shells/shell hashes/shark teeth) deposits. . .	2.00
WW10	Sandstone ; white, fine to medium grained, fining upward to siltstone and very fine-grained sandstone, tabular-planar cross-bedded, bedsets ranging between 20-50 cm, with dip angles of (20 NNE, 31 NNE, 30 NNE, 28 NNE, 27 NNE, 41 NNE, 82 NNE, 63 NNE, and 68 NNE), weakly bioturbated (BI 0-2), with local abundance of monospecific suites of <i>Skolithos</i> , and sporadic termite burrows, demarcated upward by large-sized passively-filled <i>Thalassinoides</i> , <i>Skolithos</i> and <i>Planolites</i> , corresponding to the <i>Glossifungites</i> Ichnofacies.	9.00
WW9	Shale ; grayish green, sandy, gypsiferous, slope forming, moderately bioturbated (BI 3), with ichnological suites of the ferruginous large-sized <i>Thalassinoides</i>	2.00






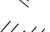





WW8	Sandstone and coquina ; golden yellow, fine- to coarse-grained sandstone, fossiliferous, rich in molluscan shells, grading upward to discontinuous coquina layer, locally bioturbated by ichnological suites of <i>Thalassinoides</i> , <i>Skolithos</i> and <i>Planolites</i>	1.50
WW7	Sandstone ; greenish yellow, silty and gypsiferous, horizontally stratified, demarcated upward by ichnological suites of <i>Thalassinoides</i> , <i>Skolithos</i> , <i>Planolites</i> and <i>Psilonichnus</i> , corresponding to the <i>Glossifungites</i> Ichnofacies.	1.00
WW6	Sandstone ; yellow, fine grained, highly bioturbated (BI 3), with abundant ichnological suites of <i>Thalassinoides</i>	0.50
WW5	Sandstone ; green, fine grained, body fossils including bivalves (articulated long clams), gastropods (e.g., <i>Turritella</i> sp.), shark teeth, ray teeth, crab shell fragments and dispersed wood fragments, moderate to high bioturbation (BI 3-5), trace-fossil suites comprising large-sized ferruginous <i>Thalassinoides</i> and rare <i>Psilonichnus</i>	4.00
WW4	Siltstone ; greenish gray, sandy and gypsiferous, moderately bioturbated (BI 3), ichnological suites including mainly <i>Thalassinoides</i> and rare <i>Teichichnus</i>	1.00
WW3	Sandstone ; greenish yellow, fine grained, with diagnostic thick gypsum radial veins. . .	3.00
WW2	Sandstone ; greenish yellow, fine grained, calcareous, fossiliferous, rich in bivalves shells and lag deposits at the base, associating thin and discrete coquina layers upwards	0.50
WW1	Shale ; greenish gray, sandy and gypsiferous, fissile, demarcated upward by ichnological suites (dominated by passively-filled large-sized <i>Thalassinoides</i>), attributed to the <i>Glossifungites</i> Ichnofacies.	5.00

4- South-West Wadi Efreet: 36.5


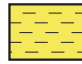



WS11	Sandstone and coquina ; yellow, medium-grained sandstone, grading upward to white calcareous sandstone and a coquina layer of bivalve and gastropod shells.	2.00
WS10	Sandstone/mudstone ; greenish white, fine- to medium-grained sandstone and mudstone, showing IHS structures, fining upward rhizolths-bearing horizon demarcated with firmground ichnological suites of the large-sized <i>Thalassinoides</i> and small-sized <i>Skolithos</i> , attributable to the <i>Glossifungites</i> Ichnofacies	4.00
WS9	Sandstone ; white, fine to medium grained, with tabular-planar cross-bedding, bedsets ranging between 20-50 cm, weakly bioturbated (BI 0-2), with abundant ichnological suites of <i>Skolithos</i> and termite trace-fossil nests.	10.0
WS9	Sandstone ; yellow, silty, fine grained and gypsiferous.	2.00
WS8	Sandstone and coquina ; yellow, fine-grained sandstone, fossiliferous, grading upward to a discontinuous coquina layer (mainly bivalve/gastropod shells).	2.00
WS7	Sandstone ; green, fine grained, body fossils including ferruginous articulated clams, the gastropod <i>Turritella</i> sp. and shark/ray teeth, highly bioturbated (BI 4-5), ichnological suites comprising mainly large-sized ferruginous <i>Thalassinoides</i> and rare <i>Psilonichnus</i> , <i>Skolithos</i> and <i>Planolites</i>	4.00
WS6	Siltstone ; greenish gray, sandy and gypsiferous, moderately bioturbated (BI 3) with trace-fossil suites of <i>Thalassinoides</i> and rare <i>Teichichnus</i>	1.00
WS5	Sandstone ; greenish yellow, fine grained, with diagnostic thick gypsum veins.	3.00

WS4	Sandstone and coquina ; greenish yellow, fine- to medium-grained sandstone, rich in bivalves/gastropod shells, locally grading to thin and discrete coquina bands.	0.50
WS3	Sandstone ; yellow, silty to very fine grained, demarcated upward by ichnological suites of passively-filled <i>Thalassinoides</i> , attributed to the <i>Glossifungites</i> Ichnofacies.	2.50
WS2	Shale ; gray black, silty, gypsiferous and ferruginous, brownish lag deposits at the base, demarcated on top by firmground suites, attributable to the <i>Glossifungites</i> Ichnofacies. . .	0.50
WS1	Sandstone/siltstone ; yellow, silty to very fine-grained sandstone and siltstone, locally cliff forming, weakly bioturbated and unfossiliferous.	5.00






Physical Sedimentary Structures

	Convolute lamination
	Wavy bedding
	Flaser bedding
	Ripple laminations (wave)
	Low-angle cross-stratification
	Cross-bedding
	Trough cross-stratification
	Lamination
	Sigmoidal bedding
	Tidal bundles and rhythmites
	Mud drapes

Lithology

	Sandstone
	Silty sandstone
	Cross-bedded sandstone & IHS
	Siltstone
	Shale










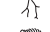







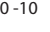
Maximum diameter
(mm)

	> 20
	20-10
	10-5
	5-2
	< 2











Bioturbation index
(BI)

	5
	4
	3
	2
	1














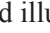
Ichnofossils

	<i>Arenicolites</i> (Ar)
	<i>Astrosoma</i> (As)
	<i>Chondrites</i> (Ch)
	<i>Cylindrichnus</i> (Cy)
	<i>Diplocraterion</i> (Di)
	<i>Monocraterion</i> (Mo)
	<i>Ophiomorpha</i> (Op)
	<i>Palaeophycus</i> (Pa)
	<i>Planolites</i> (Pl)
	<i>Psilonichnus</i> (Ps)
	<i>Rhizocorallium</i> (Rh)
	Root Traces/Casts
	<i>Scolicia</i> (Sc)
	<i>Skolithos</i> (Sk)
	<i>Teichichnus</i> (Te)
	<i>Thalassinoides</i> (Th)
	<i>Termites</i> (Ter)
	(Insect-ant traces)

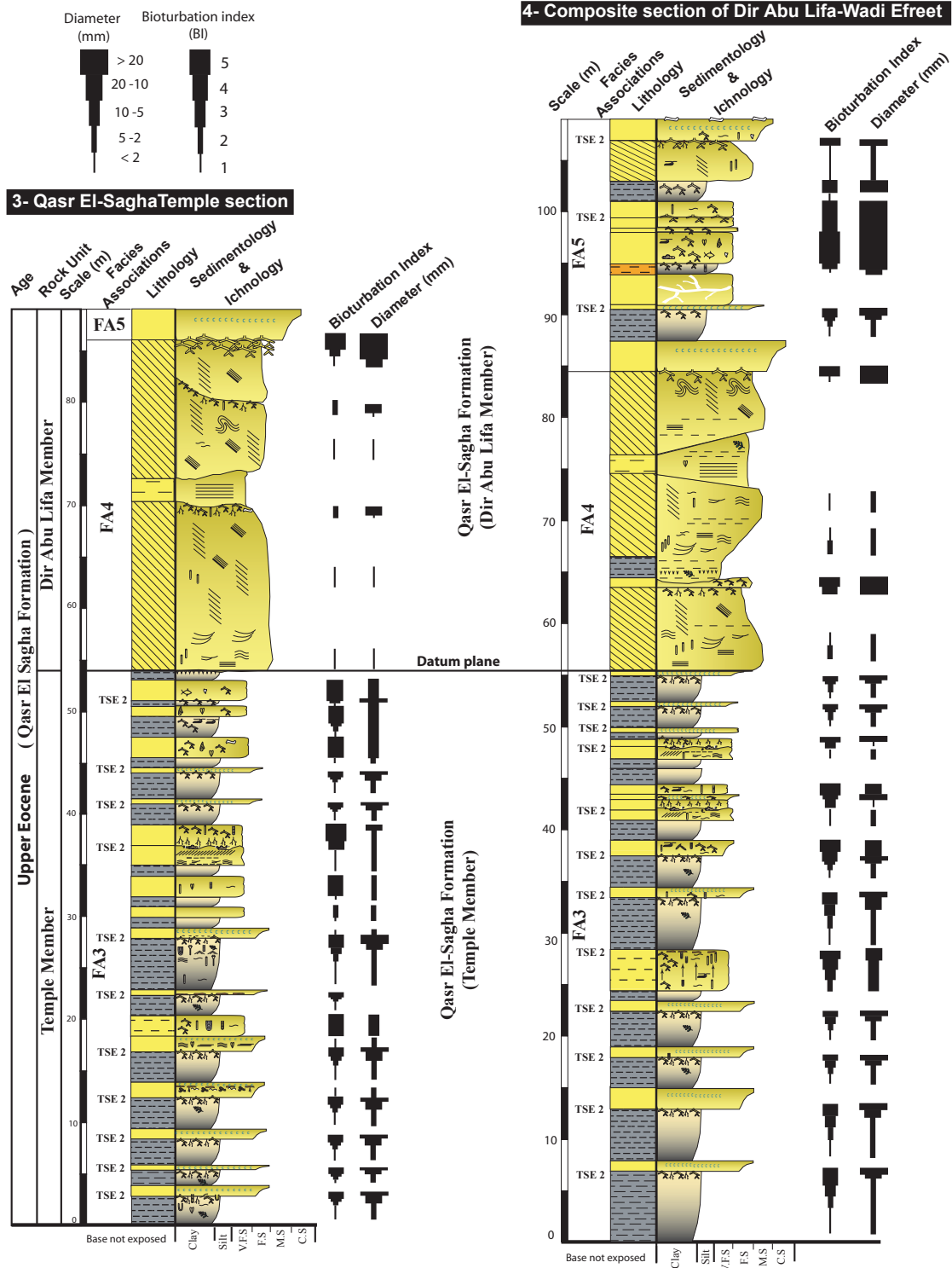
Fossils

	Bivalves
	Gastropods
	Echinoids
	Foraminifers, in general
	Large foraminifers
	Fish remains
	Vertebrates & bones
	Teeth
	Plant remains, leaf imprints
	Wood

Others

	Coal fragment
	Sulphur fragment
	Concretionary sandstone
	Alluviation
	Shale lamina
	Gypsum streak
	Thick gypsum veins
	Coquina
	Calcrete
	Discontinuity
	Unconformity
	Th
	Giant structures
	Glossifungites Ichnofacies

Legend and key to symbols used in figures and illustrations.



Correlation of the Upper Eocene Qasr El-Sagha Formation in the two composite sections; Qasr El-Sagha Temple and Dir Abu Lifa – Wadi Efreet in the area of Qasr El-Sagha, NE Fayum.

